



**STRUCTURAL RESPONSE  
OF STEEL AND COMPOSITE BUILDING  
FRAMES FURTHER TO AN IMPACT LEADING  
TO THE LOSS OF A COLUMN**

**Luu Nguyễn Nam Hải**

A thesis submitted in fulfilment  
of the requirements for  
the degree of Doctor of Philosophy

**Academic year 2008 – 2009**

Université de Liège  
Faculté des Sciences Appliquées

**STRUCTURAL RESPONSE  
OF STEEL AND COMPOSITE BUILDING  
FRAMES FURTHER TO AN IMPACT LEADING  
TO THE LOSS OF A COLUMN**

**Luu Nguyễn Nam Hải**

A thesis submitted in fulfilment  
of the requirements for  
the degree of Doctor of Philosophy

**Academic year 2008 – 2009**

## Members of the Jury

Prof. **André PLUMIER** (President of the Jury)

University of Liège, Department Argenco

Chemin des Chevreuils, 1 B52

4000 Liège – Belgium

Prof. **Jean-Pierre JASPART** (Promoter of the thesis)

University of Liège, Department Argenco

Chemin des Chevreuils, 1 B52

4000 Liège – Belgium

Ad. Prof. **Cong Thanh BUI** (Co-Promoter of the thesis)

Ho Chi Minh University of Polytechnich

167 Ly Thuong Kiet Str

Ho Chi Minh city –Vietnam

Prof. **René MAQUOI**

University of Liège, Department Argenco

Chemin des Chevreuils, 1 B52

4000 Liège – Belgium

Dr.-Ing. **Klaus WEYNAND**

Feldmann + Weynand GmbH

Pauwelsstr. 19

52074 Aachen – Germany

Prof. **Dan DUBINA**

“Politehnica” University of Timisoara

1, Ioan Curea

300224 Timisoara – Romania

## Acknowledgments

This thesis would not have been possible without the support of many people. I am deeply indebted to my advisor, Professor Jean-Pierre Jaspard, his patient guidance, encouragement and excellent advice throughout this research. Without his help, this work would not have been possible.

My sincere thanks to Professor Bui Cong Thanh, as my co-promoter, for his continuous guidance, advice, encouragement throughout the master's course EMMC 3 and especially in the year 2006.

I would also like to thank my colleagues: Jean-Francois Demonceau and Ly Dong Phuong Lam. Their advice and patience has been greatly appreciated. Especially for Jean-Francois Demonceau, it has been a pleasure to collaborate with him.

Next, I would like to express my gratitude to my scholarship sponsor from the Vietnamese Government, the Ministry of Education and Training, for financing my study. My gratitude goes to Professor Nguyen Dang Hung, Professor Pham Khac Hung and Professor Le Xuan Huynh for their contributions as coordinators.

Words fail me to express my appreciation to my beloved parents, Luu Van Quan and Nguyen Thi Thuan, for their moral support and patience during my study overseas in Liege. My father's presence at my graduation was deeply missed.

I would like to take this opportunity to express my profound gratitude to my wife Huyen whose dedication, love and persistent confidence in me has taken the load off my shoulder. I owe her for unselfishly letting her intelligence, passions, and ambitions unite with my own.

Furthermore, I am very grateful to Tinh, Long, Cuong, Binh, Huynh and Dung, my Vietnamese teammates, for the stimulating scientific discussions we had and their impressions of the student life we share in Belgium. I am thankful to Mrs Ellen Harry for her assistance in editing my thesis writing.

Finally, I would like to thank everybody who was involved in the successful realization of this thesis, as well as to express my apologies that I could not mention each one personally.

## Table of contents

|   |    |
|---|----|
| <b>Members of the Jury</b> .....  | 3  |
| <b>Acknowledgments</b> .....  | 4  |
| <b>Table of contents</b> .....  | 5  |
| <b>List of figures</b> .....  | 16 |
| <b>Notations</b> .....  | 26 |
| <b>CHAPTER 1: GENERAL INTRODUCTION</b> .....  | 33 |
| <b>1.1. INTRODUCTION</b> .....  | 33 |
| <b>1.2. ORGANIZATION OF THE PRESENT DOCUMENT</b> .....  | 34 |
| <b>CHAPTER 2: STATE-OF-THE-ART WITH PARTICULAR EMPHASIS TO THE<br/>ALTERNATIVE LOAD PATH METHOD</b> ..... | 36 |
| <b>2.1. REVIEWS OF CATASTROPHIC EVENTS</b> .....  | 37 |
| <b>2.1.1. Ronan point</b> .....   | 37 |
| <b>2.1.2. Alfhred P. Murrah federal building 19 April 1995</b> .....                                      | 38 |
| <b>2.1.3. World Trade Center 11 September 2001</b> .....  | 38 |
| <b>2.2. GLOBAL CONCEPTS AND DEFINITIONS</b> .....   | 41 |
| <b>2.3. REVIEW ON AVAILABLE CODES AND STANDARDS</b> .....   | 44 |
| <b>2.4. RESEARCHES ON THE ALTERNATIVE LOAD PATH METHOD AND<br/>CATENARY ACTION</b> .....                  | 48 |
| <b>2.4.1. Alternative load path</b> .....   | 48 |

|  |    |
|--|----|
| <b>2.4.2. Catenary action</b> .....  | 50 |
| <b>2.5. SUMMARY AND CONCLUSIONS</b> .....  | 54 |
| <b>CHAPTER 3: GLOBAL CONCEPTS FOR THE STRUCTURAL ROBUSTNESS<br/>ASSESSMENT</b> .....   | 57 |
| <b>3.1. INTRODUCTION</b> .....   | 58 |
| <b>3.2. DEFINITIONS AND ASSUMPTIONS</b> .....  | 58 |
| <b>3.2.1. Frame response under “normal” loading</b> .....                              | 58 |
| <b>3.3. COLUMN LOSS SIMULATION</b> .....   | 60 |
| <b>3.4. SUMMARY AND CONCLUSIONS</b> .....  | 62 |
| <b>CHAPTER 4: ADOPTED RESEARCH STRATEGY</b> .....                                      | 63 |
| <b>4.1. INTRODUCTION</b> .....   | 64 |
| <b>4.2. RESEARCH METHODOLOGY</b> .....   | 64 |
| <b>4.2.1. Objectives – Requirements</b> .....  | 64 |
| <b>4.2.2. Investigations along the loading process</b> .....                           | 66 |
| <i>4.2.2.a. Investigation of Phase 1 and 2</i> .....                                   | 66 |
| <i>4.2.2.b. Investigation of Phase 3</i> .....   | 67 |
| <b>4.3. TYPES OF STRUCTURAL FRAME SYSTEM</b> .....                                     | 71 |
| <b>4.4. IDENTIFICATION OF THE FRAME ZONES AND THEIR RESPECTIVE<br/>BEHAVIOUR</b> ..... | 72 |
| <b>4.4.1. Directly affected part</b> .....   | 73 |
| <b>4.4.2. Damage level</b> .....   | 74 |
| <b>4.4.3. Neighbour columns</b> .....  | 75 |
| <b>4.4.4. Lower level and outside blocks</b> .....                                     | 76 |

|  |    |
|--|----|
| <b>4.5. NUMERICAL TOOLS USED FOR FURTHER VALIDATIONS</b> .....   | 76 |
| <b>4.5.1. Multilevel validation method</b> .....   | 77 |
| <b>4.5.2. Numerical tools</b> .....  | 78 |
| <b>4.6. SUMMARY AND CONCLUSIONS</b> .....  | 80 |
| <br>   |    |
| <b>CHAPTER 5: IMPLIMENTATION OF THE ALTERNATIVE LOAD PATHS<br/>METHOD</b> .....                                  | 81 |
| <br>   |    |
| <b>5.1. INTRODUCTION</b> .....   | 82 |
| <br>   |    |
| <b>5.2. ADDITIONAL LOADS RESPECT TO THE EVENT “LOSS OF A<br/>COLUMN”</b> .....                                   | 83 |
| <b>5.2.2. Definition of the initial and residual states</b> .....  | 83 |
| <b>5.2.2. Definition of extension of the localized damage</b> .....  | 85 |
| <br>   |    |
| <b>5.3. ALTERNATIVE LOAD PATHS</b> .....   | 86 |
| <b>5.3.1. Damage columns positions</b> .....   | 86 |
| <b>5.3.2. Alternative load path and elements chain</b> .....   | 87 |
| <br>   |    |
| <b>5.4. YIELDING OF THE DIRECTLY AFFECTED PART</b> .....   | 89 |
| <br>   |    |
| <b>5.5. DEVELOPMENT OF THE CATENARY ACTION</b> .....   | 90 |
| <b>5.5.1. Conditions to be respected to develop catenary actions within the<br/>directly affected part</b> ..... | 91 |
| <b>5.5.2. Extended alternative load path and element’s chain</b> .....   | 92 |
| <br>   |    |
| <b>5.6. POSSIBLE DESIGN SITUATIONS</b> .....   | 92 |
| <br>   |    |
| <b>5.6. SUMMARY AND CONCLUSIONS</b> .....  | 94 |
| <br>   |    |
| <b>CHAPTER 6: ANALYTICAL MODEL FOR THE DIRECTLY AFFECTED PART</b> ..   | 95 |
| <br>   |    |
| <b>6.1. INTRODUCTION</b> .....   | 96 |

|  |            |
|--|------------|
| <b>6.2. INTERNAL FORCES DISTRIBUTION IN DIRECTLY AFFECTED PART</b>                 | <b>97</b>  |
| <b>6.2.1. Distribution of internal forces</b>                                      | <b>97</b>  |
| <b>6.2.2. Key members and sections</b>   | <b>100</b> |
| <i>6.2.2.a. The ends sections of the equivalent beams</i>                          | 100        |
| <i>6.2.2.b. The axial force in the beams</i>                                       | 101        |
| <i>6.2.2.c. Middle columns</i>   | 102        |
| <b>6.3. SUB-MODEL TO SUBSTITUTE TO THE WHOLE DIRECTLY AFFECTED PART</b>            | <b>103</b> |
| <b>6.3.1. Equivalent beam model</b>  | <b>104</b> |
| <i>6.3.1.a. Partially restrained ends</i>  | 104        |
| <i>6.3.1.b. Restraint at beam middle point</i>                                     | 105        |
| <i>6.3.1.c. Semi-rigid beam-to-column connection</i>                               | 105        |
| <b>6.3.2. Column in tension</b>  | <b>106</b> |
| <b>6.3.3. Substructure model</b>   | <b>106</b> |
| <b>6.3.4. Conclusion</b>   | <b>107</b> |
| <b>6.4. PARTIAL RESTRAINT COEFFICIENT <math>K_S</math></b>                         | <b>107</b> |
| <b>6.4.1. Adjacent members and continuity</b>                                      | <b>108</b> |
| <b>6.4.2. Influence of the position of the impacted column on <math>K_S</math></b> | <b>108</b> |
| <b>6.4.3. Simplified model</b>   | <b>109</b> |
| <b>6.4.4. Semi-rigid connections</b>   | <b>111</b> |
| <b>6.4.5. Validation</b>   | <b>113</b> |
| <b>6.4.6. Conclusion</b>   | <b>116</b> |
| <b>6.5. ANALYTICAL MODEL OF EQUIVALENT BEAM – 3-SPRINGS MODEL</b>                  | <b>116</b> |
| <b>6.5.1. Evaluation of the equivalent beam stiffness</b>                          | <b>117</b> |
| <i>6.5.1.a. Damage of the internal column</i>                                      | 117        |



|   |         |
|---|---------|
| 6.5.1.b. <i>Damage of the external column</i> .....   | 118     |
| <b>6.5.2. Simplification the equivalent beam stiffness for practical use</b> .....  | 118     |
| 6.5.2.a. <i>The case of constancy EI</i> .....  | 118     |
| 6.5.2.b. <i>Using the value of <math>\alpha=0.5</math></i> .....  | 119     |
| 6.5.2.c. <i>Using same <math>K_S</math> for both ends rotational stiffness</i> .....                                      | 119     |
| <b>6.5.3. Validation</b> .....  | 120     |
| 6.5.3.a. <i>Validation of the model and the substructure</i> .....  | 120     |
| 6.5.3.b. <i>Tests organization</i> .....  | 120     |
| 6.5.3.d. <i>Results</i> .....   | 122     |
| <b>6.5.4. Conclusion</b> .....  | 123     |
| <b>6.6. RESISTANCE OF THE DIRECTLY AFFECTED PART</b> .....  | 124     |
| <b>6.6.1. Simple example and collapse scenarios</b> .....   | 124     |
| 6.6.1.a. <i>First scenario:</i> .....   | 126     |
| 6.6.1.b. <i>Second scenario:</i> .....  | 127     |
| 6.6.1.c. <i>Last scenario:</i> .....  | 128     |
| <b>6.6.2. Individual equivalent beam load carrying curve – 1<sup>st</sup> order plastic hinge by hinge analysis</b> ..... | 129     |
| <b>6.6.3. Assembly of the components curves</b> .....   | 131     |
| <b>6.6.4. Quick-estimation method for</b> .....   | 132     |
| <b>6.6.3. Validation</b> .....  | 134     |
| <b>6.6.4. Conclusion</b> .....  | 135     |
| <b>6.7. SUMMARY AND CONCLUSIONS</b> .....   | 136     |
| <br><b>CHAPTER 7: ANALYTICAL MODEL TO INVESTIGATE THE NEXT COLUMNS AND “ARCH” EFFECT</b> .....                            | <br>138 |
| <br><b>7.1. INTRODUCTION</b> .....  | <br>139 |

|   |     |
|---|-----|
| <b>7.2. DISTRIBUTION OF INTERNAL FORCES AND DISPLACEMENT OF THE SPECIFIC POINTS</b> ..... | 140 |
| <b>7.2.1. Loading phases and the additional load</b> .....                                | 141 |
| <b>7.2.2. The “arch effect” and the axial force in the beams</b> .....                    | 142 |
| <b>7.2.3. The compression on the next columns</b> .....                                   | 143 |
| <b>7.2.3. Conclusion</b> .....  | 144 |
| <b>7.3. DEVELOPMENT OF THE SUBSTRUCTURE MODEL</b> .....                                   | 144 |
| <b>7.3.1. Requirements for “extraction”</b> .....   | 145 |
| <b>7.3.2. Beams/columns partial end restraints</b> .....                                  | 146 |
| <b>7.3.3. Horizontal restraint</b> .....  | 147 |
| 7.3.3.a. <i>Un-braced part</i> .....  | 147 |
| 7.3.3.b. <i>Braced part</i> .....   | 148 |
| 7.3.3.c. <i>Equivalent next span beam</i> .....   | 149 |
| <b>7.3.4. Extended substructure</b> .....   | 149 |
| <b>7.3.5. Conclusion</b> .....  | 151 |
| <b>7.4. SIMPLIFICATION OF THE MODEL FOR TYPICAL BUILDING FRAMES</b> .....                 | 151 |
| <b>7.4.1. Major properties of the model for typical frames</b> .....                      | 152 |
| <b>7.4.2. Half-model and the definition of the “weaker half”</b> .....                    | 153 |
| <b>7.4.3. Validation</b> .....  | 156 |
| <b>7.4.4. Conclusion</b> .....  | 158 |
| <b>7.5. “NEXT COLUMNS” KEY ELEMENT AND RESISTANCE</b> .....                               | 159 |
| <b>7.5.1. Key elements and the loading status</b> .....                                   | 159 |
| <b>7.5.2. Element stability check</b> .....   | 161 |
| <b>7.5.4. Conclusion</b> .....  | 162 |

|   |            |
|---|------------|
| <b>7.6. SUMMARY AND CONCLUSIONS .....</b>   | <b>162</b> |
| <b>CHAPTER 8: PARAMETERS INFLUENCING THE DEVELOPMENT OF A<br/>CATENARY ACTION FUTHER TO THE LOSS OF A COLUMN.....</b> | <b>164</b> |
| <b>8.1. INTRODUCTION.....</b>   | <b>165</b> |
| <b>8.2. CATENARY ACTION IN BEAMS AND INFLUENCING PARAMETERS .</b>   | <b>166</b> |
| <b>8.2.1. Why only the bottom equivalent beam goes to the catenary action .....</b>                                   | <b>166</b> |
| <b>8.2.2. Load-carrying behaviour of the bottom equivalent beam.....</b>  | <b>167</b> |
| <b>8.2.3. Lateral translation stiffness <math>K</math> .....</b>  | <b>168</b> |
| <b>8.2.4. Limit of the restraint at the end of catenary beam - <math>F_{Rd}</math> .....</b>                          | <b>169</b> |
| <b>8.2.5. Hanging force and the <math>Q</math> value.....</b>   | <b>169</b> |
| <b>8.2.6. Conclusion.....</b>   | <b>171</b> |
| <b>8.3. BEHAVIOUR OF THE ADJACENT MEMBERS TO THE DAMAGED<br/>COLUMN .....</b>   | <b>171</b> |
| <b>8.3.1. Extra compression and bending in the columns.....</b>   | <b>171</b> |
| <i>8.3.1.a. Initial loading phase .....</i>   | <i>171</i> |
| <i>8.3.1.b. Load phase 2.....</i>   | <i>172</i> |
| <i>8.3.1.c. Load phase3.....</i>  | <i>173</i> |
| <b>8.3.2. Axial forces in the beams .....</b>   | <b>174</b> |
| <b>8.3.3. Conclusion.....</b>   | <b>175</b> |
| <b>8.4. ANALYTICAL MODEL TO SIMULATE THE DAMAGED LEVEL .....</b>  | <b>176</b> |
| <b>8.4.1. Individual columns.....</b>   | <b>176</b> |
| <i>8.4.1.a. Partial restraint at the column's ends .....</i>  | <i>177</i> |
| <i>8.4.1.b. Boundary condition at column top .....</i>  | <i>177</i> |
| <b>8.4.2. Beam in tension.....</b>  | <b>178</b> |

|   |     |
|---|-----|
| <b>8.4.3. Assembly of the members</b> .....   | 179 |
| <b>8.4.4. Conclusion</b> .....  | 179 |
| <b>8.5. LATERAL STIFFNES COEFFICIENT K</b> .....  | 179 |
| <b>8.5.1. Column model and stiffness matrix with 2<sup>nd</sup> order effects</b> ..... | 180 |
| <i>8.5.1.a. First order full stiffness matrix.</i> .....                                | 180 |
| <i>8.5.1.b. Second order effect.</i> .....  | 182 |
| <b>8.5.2. Specific column shear stiffness with 2<sup>nd</sup> order effects</b> .....   | 183 |
| <i>8.5.2.a. External column</i> .....   | 183 |
| <i>8.5.2.b. Intermediate column</i> .....   | 183 |
| <i>8.5.2.c. Beside/next column</i> .....  | 184 |
| <b>8.5.3. Stiffness assembly principle</b> .....  | 185 |
| <b>8.5.4. Simplification <i>K</i> formula by summing the individual columns</b> .....   | 186 |
| <b>8.5.5. Validation</b> .....  | 186 |
| <b>8.5.6. Conclusion</b> .....  | 188 |
| <b>8.6. LATERAL RESISTANCE OF DAMAGED LEVEL</b> .....                                   | 188 |
| <b>8.6.1. Column instability</b> .....  | 189 |
| <i>8.6.1.a. Plastic resistance of the individual column</i> .....                       | 189 |
| <i>8.6.1.b. Columns instability</i> .....   | 190 |
| <b>8.6.2. Weakest column and the simplification of the resistance formula</b> .....     | 190 |
| <b>8.6.3. Validation</b> .....  | 191 |
| <b>8.6.4. Conclusion</b> .....  | 192 |
| <b>8.7. SUMMARY AND CONCLUSIONS</b> .....   | 192 |
| <b>CHAPTER 9: MULTILEVEL ROBUSTNESS ASSESSMENT OF A FRAME</b> .....                     | 194 |
| <b>9.1. INTRODUCTION</b> .....  | 195 |

|   |            |
|---|------------|
| <b>9.2. MULTI-LEVELS ROBUSTNESS ASSESSMENT FRAMEWORK .....</b>                | <b>196</b> |
| <b>9.2.1. Critical value.....</b>   | <b>199</b> |
| 9.2.1.a. <i>Objective</i> .....   | 199        |
| 9.2.1.b. <i>Input data</i> .....  | 199        |
| 9.2.1.c. <i>Methodology</i> .....   | 199        |
| 9.2.1.d. <i>Formulae</i> .....  | 199        |
| 9.2.1.e. <i>Expected results</i> .....  | 201        |
| 9.2.1.f. <i>Remarks – Decisions</i> .....                                     | 201        |
| <b>9.2.2. First alternative load path integrity and continuity.....</b>       | <b>201</b> |
| 9.2.2.a. <i>Objective</i> .....   | 201        |
| 9.2.2.b. <i>Input data</i> .....  | 201        |
| 9.2.2.c. <i>Methodology</i> .....   | 201        |
| 9.2.2.d. <i>Formulae</i> .....  | 202        |
| 9.2.2.e. <i>Expected results</i> .....  | 206        |
| 9.2.2.f. <i>Remarks – Decisions</i> .....                                     | 206        |
| <b>9.2.3. Achieves the values of <math>K</math>, <math>F_{Rd}</math>.....</b> | <b>207</b> |
| 9.2.3.a. <i>Objective</i> .....   | 207        |
| 9.2.3.b. <i>Input data</i> .....  | 207        |
| 9.2.3.c. <i>Methodology</i> .....   | 207        |
| 9.2.3.d. <i>Formulae</i> .....  | 207        |
| 9.2.3.e. <i>Expected results</i> .....  | 209        |
| 9.2.3.f. <i>Remarks – Decisions</i> .....                                     | 210        |
| <b>9.3. EXAMPLE.....</b>  | <b>211</b> |
| <b>9.3.1. Input data.....</b>   | <b>211</b> |
| <b>9.3.2. Internal forces.....</b>  | <b>212</b> |
| <b>9.3.3. Full assessment flow chart.....</b>                                 | <b>213</b> |

|   |     |
|---|-----|
| <b>9.3.4. Step 1.</b> .....   | 214 |
| <b>9.3.5. Step 2</b> .....  | 216 |
| <b>9.3.6. Step 3</b> .....  | 228 |
| <b>9.4. CONCLUSION</b> .....  | 232 |
| <b>CHAPTER 10: DISCUSSIONS AND CONCLUSIONS</b> .....  | 234 |
| <b>10.1. INTRODUCTION</b> .....   | 235 |
| <b>10.2. CONCLUSION OF THE THESIS</b> .....   | 235 |
| <b>10.2.1. Main achievements related to the global behaviour of the frame<br/>    further to the lost of a column</b> .....   | 236 |
| <i>10.2.1.a. Prediction of the two activated alternative load paths in the frame</i> .....  | 236 |
| <i>10.2.2.b. Investigation on the redistribution of the internal forces within the<br/>      frame after the accidental event through the simplified analytical model</i> ..... | 236 |
| <i>10.2.2.c. Development of the analytical method to predict the behaviour of the<br/>      frame further to the lost of a column</i> .....                                     | 237 |
| <i>10.2.2.d. Development of the analytical method to assess the influences of the<br/>      surrounding structural member to the activation of the catenary action</i> .....    | 237 |
| <b>10.2.2. Accuracy and tolerance</b> .....   | 238 |
| <i>10.2.2.a. Error on the analytical method</i> .....   | 238 |
| <i>10.2.2.b. Error on the selected analytical model</i> .....   | 238 |
| <i>10.2.2.c. Error on the <math>K</math> an <math>F_{Rd}</math> value</i> .....   | 239 |
| <b>10.2.3. Necessities of development</b> .....   | 239 |
| <i>10.2.3.a. Simplify practical oriented analytical method for the typical and<br/>      general building</i> .....   | 239 |
| <i>10.2.3.b. Development on the expanded analytical model</i> .....   | 239 |
| <b>10.3. DISCUSSIONS</b> .....  | 240 |

|   |            |
|---|------------|
| <b>10.3.1. Determining structural risks .....</b>   | <b>240</b> |
| <b>10.3.2. Energy absorption .....</b>  | <b>240</b> |
| <b>10.3.3. Design process.....</b>  | <b>241</b> |
| <b>10.3.4. Damage assessment .....</b>  | <b>241</b> |
| <b>10.3.5. Monitoring and protection .....</b>  | <b>242</b> |
| <b>10.4. FUTURE RESEARCH RECOMMENDATIONS.....</b>   | <b>242</b> |
| <b>10.4.1. Extend the analytical approaches to composite steel-concrete structure.....</b>                              | <b>242</b> |
| <b>10.4.2. Extend the solution to the 3D problem.....</b>   | <b>243</b> |
| <b>10.4.3. Automatically tool programmed for frame robustness assessment.....</b>                                       | <b>243</b> |
| <b>10.4.4. Energy absorption comparison between the catenary phenomenon<br/>and the full alternative load path.....</b> | <b>243</b> |
| <b>References .....</b>   | <b>244</b> |

---

## List of figures

|  |    |
|--|----|
| Figure 2.1. Ronan Point building after the accident [ <i>NISTIR 7396, 2005</i> ] .....   | 38 |
| Figure 2.2.a. Murrah Building showing the damage after the debris was removed.....   | 38 |
| Figure 2.3. WTC 2 main structures and damage .....   | 39 |
| Figure 2.4. A FEMA diagram depicting debris distribution from the collapses of WTC 1 and 2. Dotted, darker and light orange areas denote heaviest, heavy and lighter debris distribution respectively. Red 'X' marks denote isolated perimeter columns ejected farther than in average debris distribution [ <i>FEMA, 2002</i> ] ..... | 39 |
| Figure 2.5. Photograph showing mild debris damage to WFC 2 and WFC 3, with the heaviest debris falling perpendicular to the west face of WTC 1 onto the Winter Garden [ <i>FEMA, 2002</i> ].....   | 40 |
| Figure 2.6. North face of Bankers Trust Building with impact damage .....  | 41 |
| between floors 8 and 23 (Smilowitz – FEMA, 2004) .....   | 41 |
| Figure 2.7. The guideline in EUROCODE.....   | 46 |
| Figure 2.8. The basic ring and round in the Agarwal method (Agarwal, 2008).....  | 49 |
| Figure 2.9. A 3D frame and its hierarchical representation (Agarwal, 2008) .....   | 50 |
| Figure 2.10. (a) Catenary illustration .....   | 51 |
| Figure 2.11. (a) Loss of one and 2 columns models.....   | 51 |
| Figure 2.13. a. Representation of a frame losing a column;.....  | 52 |
| Figure 2.14. Izzuddin and Vlassis’s (2007) reduction process.....  | 53 |



## List of figures

---

|  |    |
|--|----|
| Figure 2.15.(a) The member and axial force generated.....                                      | 54 |
| Figure 3.1. Definitions of zones within the investigated frame .....                           | 59 |
| Figure 3.2. Definition of directly and indirectly affected part.....                           | 60 |
| Figure 3.3: Representation of a frame losing a column.....                                     | 60 |
| Figure 3.4. Column axial force and Y displacement of the top of a collapsed column.....        | 62 |
| Figure 4.1. Loss of a column in the frame [ <i>Demonceau, 2008</i> ].....                      | 64 |
| Figure 3.4. Column axial force and Y displacement of the top of a collapsed column.....        | 66 |
| Figure 4.2. Division of the frame loading (when a column is lost) in 2 load phases .....       | 67 |
| Figure 4.3. Distribution of the membrane forces developing in the directly affected part ..... | 68 |
| Figure 4.4. The 3-levels extraction.....   | 69 |
| Figure 4.5. Simplified subsystem .....   | 70 |
| Figure 4.6. The types of frames: (a) Side braced frame (b) Middle braced frame .....           | 71 |
| (c) Sway frame (d) Fully braced frame .....  | 71 |
| Figure 4.7. The single and middle braced frames simplified to a one braced side model.....     | 72 |
| Figure 4.8. The fully braced frame becomes a two braced side model .....                       | 72 |
| Figure 4.9. A typical frame with a lost column.....  | 72 |
| Figure 4.10. Separating the frame zones .....  | 73 |
| Figure 4.11. Directly affected zone (a) and its components (b) .....                           | 74 |

## List of figures

---

|   |    |
|---|----|
| Figure 4.12. The frame and zone border investigated (a) and member's names and positions (b) .....  | 75 |
| Figure 4.13: Neighboring column zones (a) and the members on the left (b).....  | 76 |
| Figure 4.14: Lower level (a) and outside blocks (b) .....   | 76 |
| Figure 4.4. The 3-levels extraction.....  | 77 |
| Figure 4.15. The procedures for building the analytical substructure model.....   | 78 |
| Figure 4.16. Classic beam element used in FINELG and OSSA2D [ <i>Finelg manual</i> ] .....  | 79 |
| Figure 4.17. Linear and bi-linear behavior laws applied to the calculation .....  | 79 |
| Figure 4.4. The 3 levels of extraction.....   | 82 |
| Figure 4.15. The procedures for building the analytical substructure model.....   | 83 |
| Figure 3.4. Column axial force and Y displacement of the top of a collapsed column.....   | 84 |
| Figure 5.1. Frame in the initial state.....   | 84 |
| Figure 5.2. Identification of two loading sequences.....  | 85 |
| Figure 5.3. Identification of the position of the columns .....   | 86 |
| Figure 5.4. Distribution of internal forces in an investigated frame when only additional load applied and in elastic 1 <sup>st</sup> order range ..... | 87 |
| Figure 5.5. The alternative load path and the influenced frame zones.....   | 88 |
| Figure 5.6. Activated alternative load paths in a frame losing a column .....   | 88 |
| Figure 5.7. Axial load in the lost column vs. deflection at the top of the lost column.....   | 89 |

## List of figures

---

|   |     |
|---|-----|
| Figure 5.8. Membrane phenomenon when $N_{lost}^{Pl.Rd} < N_{design}$ .....                  | 91  |
| Figure 5.9. Structural members within the extended alternative load path .....              | 92  |
| Figure 5.10. Full alternative load paths and their conditions .....                         | 93  |
| Figure 6.1. The procedures for building the analytical substructure model .....             | 96  |
| Figure 6.2: Directly affected zone (a) and the members (b).....                             | 97  |
| Figure 6.3. Axial load in the lost column vs. deflection at the top of the lost column..... | 98  |
| Figure 6.4. Distribution of the internal forces in the initial state.....                   | 98  |
| Figure 6.5: Distribution of the internal forces in the residual state .....                 | 99  |
| Figure 6.6. Internal force distribution in Phase 3; catenary forces increase.....           | 100 |
| Figure 6.7. Isolated membrane beam.....   | 101 |
| Figure 6.8. Bending moment diagram of equivalent beam in Phase 2.....                       | 101 |
| Figure 6.9. Axial forces in the directly affected beams.....                                | 102 |
| Figure 6.10: Axial forces of the middle columns (Phase 2).....                              | 103 |
| Figure 6.11.(a) The directly affected part AGIC .....                                       | 103 |
| Figure 6.12.(a) The equivalent beam ABC (b) Analytical model .....                          | 105 |
| Figure 6.13. (a) Middle beam in the frame.....  | 106 |
| Figure 6.14. The analytical substructure model .....  | 107 |
| Figure 6.15.a. Transfer of equivalent beam ends' bending moment in the frame.....           | 108 |

List of figures

---

Figure 6.16. Different equivalent beam end positions ..... 109

Figure 6.17. Three levels development of  $K_S$  at point C ..... 111

Figure 6.18. The  $K_S$  in different positions within the frame..... 111

Figure 6.19: Semi-rigid beam segment. .... 112

Figure 6.20. The partially restrained stiffness of point C with semi-rigid connections ..... 113

Figure 6.21. a. 3 positions in fully rigid frames ..... 114

Chart 6.1. The error percentages of analytical results ..... 115

Chart 6.2. Error distribution for  $S_C/S_B$ ..... 115

Figure 6.22. The simplified analytical model of the equivalent beam ..... 116

Figure 6.23. The FEM model to develop the analytical formula for the equivalent beam..... 117

Figure 6.24. The analytical model of the side beam..... 118

Figure 6.25. The 3-spring model ..... 120

Figure 6.26. Tested frame configuration ..... 121

Chart 6.3. Distribution of  $K$  errors..... 123

Chart 6.4.  $K$  Error distribution for  $S_C/S_B$ ..... 123

Figure 6.27. Substructure and the internal force distribution ..... 124

Figure 6.28. Resistance of the single equivalent beam..... 125

Figure 6.29. Resistance of the fully yielded beams..... 125

## List of figures

---

|  |     |
|--|-----|
| Figure 6.30. Loading process in the first scenario.....  | 127 |
| Figure 6.31. Loading process in the second scenario .....  | 128 |
| Figure 6.32: Loading process in the third scenario .....   | 129 |
| Figure 6.33. Critical sections on the model .....  | 130 |
| Figure 6.34.a. Bending diagram of the model .....  | 131 |
| Figure 6.35. Assembly of parallel spring groups [ <i>SSEDTA, 2000</i> ].....                         | 132 |
| Figure 6.36. Assembly of serial spring groups [ <i>SSEDTA, 2000</i> ] .....                          | 132 |
| Figure 6.37. The individual beam's resistance .....  | 133 |
| Figure 6.38. The frame configuration under investigation.....  | 134 |
| Chart 6.5. The resistances of the directly affected part for different damaged column positions..... | 135 |
| Figure 5.7. The axial force and deflection of top point of damaged column .....                      | 136 |
| Figure 5.5. The alternative load path and the influenced zones .....                                 | 139 |
| Figure 7.1. The investigated zone in the residual frame.....   | 141 |
| Figure 7.2. The distribution of internal forces in the residual frame in Load Phase 2 .....          | 141 |
| Figure 7.3. The distribution of axial forces in the equivalent beam due to the arch effect ....      | 143 |
| Figure 7.4. Adjacent column's internal forces .....  | 144 |
| Figure 7.5. Two alternative load paths .....   | 145 |
| Figure 7.6. Specific identified zones .....  | 146 |

## List of figures

---

|   |     |
|---|-----|
| Figure 7.7. Repeat of the development of the formula for $K_S$ .....                      | 147 |
| Figure 7.8. Horizontal restraint definition.....  | 147 |
| Figure 7.9. The development of the model and its stiffness.....                           | 148 |
| Figure 7.10. The braced part.....   | 149 |
| Figure 7.11. The original residual frame and the full model (internal damage).....        | 150 |
| Figure 7.12. The original residual frame and the full model (external damage).....        | 151 |
| Figure 7.13. Resembling a symmetrical geometrical substructure.....                       | 152 |
| Figure 7.14. The bending stiffness of different beam units.....                           | 153 |
| Figure 7.15. The simplified half model.....   | 153 |
| Figure 7.16. Equilibrium at a node.....   | 154 |
| Figure 7.17. Calculating the axial forces in the equivalent beam (arch effect).....       | 155 |
| Figure 7.18. Simplified half model.....   | 155 |
| Figure 7.19. The first and second frames and models for validation.....                   | 157 |
| Figure 7.20. The third, fourth and fifth frames.....                                      | 157 |
| Figure 7.21. Moment where frame could collapse due to the loss of second key element .... | 159 |
| Figure 7.22. Axial forces in the key elements.....  | 160 |
| Figure 7.23. General model and the key elements.....                                      | 160 |
| Figure 7.24. Frame member section stability check.....                                    | 161 |

## List of figures

---

|  |     |
|--|-----|
| Figure 8.1. The full loading process where the catenary action take effect .....   | 165 |
| Figure 8.2. Only the bottom equivalent beam undergoes catenary action .....  | 167 |
| Figure 8.3. Simplified substructure simulating the behavior of the frame during Phase 3<br>[Demonceau, 2008] .....                               | 168 |
| Figure 8.4. Different scenarios of the bottom beam depending on $K$ values. ....   | 168 |
| Figure 8.5. Behavior when $Q$ reaches $Q_K^{F.Rd}$ .....   | 169 |
| Figure 8.6. The hanging force $N_{up}$ and the additional load $N_{lost}$ .....  | 170 |
| Figure 8.7. Axial forces of the middle columns and evolution of $N_{up}$ .....   | 170 |
| Figure 8.8.a. The frame and identification of the zone investigated .....  | 171 |
| Figure 8.9. Evolution of the bending moment $M$ and axial force $N$ within the columns of<br>the damaged level at the collapsed floor level..... | 173 |
| Figure 8.10. Diagrams of the bending moment $M$ and axial force $N$ within the columns .....   | 174 |
| Figure 8.11: The beams at column top .....   | 174 |
| Figure 8.12: Distribution of axial forces in the beams as a function of the membrane force   | 175 |
| Figure 8.13: Left part of damaged level .....  | 176 |
| Figure 8.14: The members' influence on the column's restrained end rotation.....   | 177 |
| Figure 8.15. Analytical individual model.....  | 178 |
| Figure 8.16. Horizontal and vertical components of the membrane force .....  | 178 |
| Figure 8.17. Top beams and their analytical models.....  | 178 |

## List of figures

---

|   |     |
|---|-----|
| Figure 8.18. The left side damaged level model.....   | 179 |
| Figure 8.19. Semi-rigid frame member. ....  | 180 |
| Figure 8.20. Axial forces in the three column positions.....                                    | 183 |
| Figure 8.21. Frame investigated. ....   | 186 |
| Figure 8.22. Single analytical model validation.....  | 187 |
| Figure 8.23. Individual column in frame and model result.....                                   | 187 |
| Figure 8.24. Left side of damaged level behavior and analytical results.....                    | 188 |
| Figure 8.25: The resistance of the first floor column.....                                      | 189 |
| Figure 8.26.a. Extracted column's behavior.....   | 191 |
| Figure 9.1. The multi-level frame robustness assessment.....                                    | 198 |
| Figure 9.2. The model and required data.....  | 199 |
| Figure 9.3. The individual beam's resistance.....   | 200 |
| Figure 9.4. The reduction process to simulate the partially restrained stiffness of point C ... | 202 |
| Figure 9.5. $K_S$ in different positions within the frame.....                                  | 202 |
| Figure 9.6. Bending diagram on the model.....   | 203 |
| Figure 9.7. Load-carrying curve in the case where hinges appear in order (31-32-1-2).....       | 204 |
| Figure 9.8. The original residual frame and the full model.....                                 | 204 |
| Figure 9.9. The simplified half model.....  | 205 |



## List of figures

---

|  |     |
|--|-----|
| Figure 9.10. Horizontal restraint definition .....                                   | 205 |
| Figure 9.11. The relation between members in the group .....                         | 205 |
| Figure 9.12. Calculating the axial forces in the equivalent beam (arch effect) ..... | 206 |
| Figure 9.13. General model and the key elements .....                                | 206 |
| Figure 9.14: The resistance of the one floor column .....                            | 207 |
| Figure 9.15. Model of the left side of the damaged level .....                       | 209 |
| Figure 10.1. The tolerance of analytical results .....                               | 238 |

## Notations

### Chapter 3

|                    |  |
|--------------------|--|
| $N_{UP}$           | Axial force in the column just above the damaged column (upper column).    |
| $N_{LO}$           | Axial force in the damaged column (lower column).                          |
| $V_1, V_2$         | Shear forces on the two beam's section on both side of the damaged column. |
| $N_{AB}$           | Axial force in column AB.  |
| $\Delta_A$         | Displacement of the damaged column top point.                              |
| $N_{lost}^{Pl.Rd}$ | Additional load when the directly affected part fully yielded.             |
| $N_{design}$       | Axial force of the damaged column associates to the initial state.         |
| $N_{ABdesign}$     | Axial force of the damaged column AB associates to the initial state.      |

### Chapter 4

|                           |   |
|---------------------------|---|
| $N_{top.beam}^-$          | Negative normal force of the top beam in the directly affected part.                      |
| $N_{inter.beam}^{zerror}$ | Very small normal force of the intermediate beams in the directly affected part.          |
| $N_{bottom.beam}^+$       | Positive normal force of the bottom beam in the directly affected part.                   |
| $N_{membranar.beam}^+$    | Membranar force of the bottom beam in the directly affected part.                         |
| $Q$                       | Resultal vertical force acting on the middle point of membranar beam.                     |
| $K$                       | Lateral stiffness coefficient represents the horizontal restrains to the catenary action. |
| $F_{Rd}$                  | Resistance of the lateral stiffness coefficient.  |
| $u$                       | Horizontal degree of freedom.   |
| $v$                       | Vertical degree of freedom.   |
| $\theta$                  | Rotational degree of freedom.   |

Chapter 6

|                                |   |
|--------------------------------|---|
| $M_A, M_B, M_C$                | Bending moment of section A,B,C through loading phases.   |
| $M_P^i$                        | Beam section plastic resistance ( $i = A, B, C$ ).  |
| $K_{Model}$                    | is the directly affected part model stiffness under $N_{lost}$ .  |
| $S_{Bi}$                       | Beam bending stiffnes   |
| $S_{Ci}$                       | Column bending stiffness.   |
| $E_B, E_C$                     | Elastic modulus of the beam and column.   |
| $I_B, I_C$                     | Inertia of the beam and column sections.  |
| $L_B, L_C$                     | Beam, column lengths.   |
| $k_C$                          | End rotation stiffness of the columns.  |
| $k_B$                          | End rotation stiffness of the beam.   |
| $S_{C1}, S_{B1}$               | Bending stiffness of the column, beam with rotation string end.   |
| $K_S$                          | Partial restrain's coefficient.   |
| $\theta_A$                     | Rotation of point A.  |
| $\theta_B$                     | Rotation of point B.  |
| $\theta_{rA}$                  | Relative rotation of point A associates to the semi-rigid spring.   |
| $\theta_{rB}$                  | Relative rotation of point B associates to the semi-rigid spring.   |
| $S_{C1}^{semi}, S_{B1}^{semi}$ | Bending stiffness of the column, beam with rotation string end taking into account the semi-rigid connection. |
| $K_S^{semi}$                   | Semi-rigid partial restrain's coefficient.  |
| $S_{jA}$                       | Initial stiffness of the beam-to-column connection at point A.  |
| $r_{ib}, r_{ij}, r_{jj}$       | Intermediate stiffness ratio.   |
| $C, D, H$                      | Intermediate scalar to predict $K$ value.   |
| $\alpha$                       | Beam's lengths ratio.   |
| $\beta_i$                      | Partial restrain stiffness/column stiffness ratio   |
| $\gamma$                       | Two segment of beam/column's stiffness ratio.   |
| $L_1, L_2$                     | Lengths of left and right part of beam.   |
| $L$                            | Whole equivalent beam length.   |
| $E_{B1}, E_{B2}$               | Elastic modulus of left and right part of beam.   |

|                     |   |
|---------------------|---|
| $I_{B1}, I_{B2}$    | Inertia moments of left and right part of beam.         |
| $M_{max}$           | Maximum bending moment values.                          |
| $N_{max}$           | Maximum axial forces values.                            |
| $n$                 | Number of the storey within the directly affected part. |
| $N_{max}$           | Maximum axial force values.                             |
| $N_{lost}^{C.Rd}$   | Individual middle column resistance.                    |
| $K_{nB}$            | Directly affected part stiffness conclude $n$ beams.    |
| $N_{lost}^{nB.Rd}$  | All $n$ equivalent beams resistance.                    |
| $\Delta_1$          | Displacement of the loaded point.                       |
| $\Delta_2$          | Displacement of the loaded point.                       |
| $M_p^B$             | Plastic bending moment of beam section.                 |
| $K_B$               | Single equivalent beam stiffness.                       |
| $N_{lost}^{B.Rd}$   | Single column resistance.                               |
| $E_B I_B$           | Elastically modulus and inertia moment of the beam.     |
| $N_{lost,i}^{B.Rd}$ | Resistance of beam number $i$ .                         |

### Chapter 7

|                             |   |
|-----------------------------|---|
| $N_{Phase2}, M_{Phase2}$    | Axial force and bending moment in load phase 2.                 |
| $N_{design}$                | Designed axial force.   |
| $M_{Add.load}$              | Bending moment associates to additional load.                   |
| $N_{Add.load}$              | Axial force associates to additional load.                      |
| $K_{(3columns)}^{UnBraced}$ | Horizontal restrained coefficient of the point C.               |
| $k_i$                       | Beam or column stiffness.                                       |
| $K_{(3columns)}^{Braced}$   | Horizontal restrained coefficient of the point C in the braced  |
| $A_{equ3.right}$            | Equivalent next span beam cross section area on the right side. |
| $L_B$                       | Next span beam length.  |
| $E_B$                       | Elastic modulus of beam.  |

|               |   |
|---------------|---|
| $K_B^i$       | Equivalent beam number i.   |
| $n$           | Number of storey within the model.  |
| $F_i$         | Vertical force applied to the equivalent beam number i.   |
| $N_{Ed}$      | Design normal force   |
| $N_{pl,Rd}$   | Design plastic resistance to normal forces of the gross cross-section                             |
| $A_w$         | Area of a web   |
| $A$           | Area of a cross section   |
| $M_{N,y,Rd}$  | Characteristic value of resistance to bending moments about y-y axis associates to axial force N. |
| $M_{Pl,y,Rd}$ | Characteristic value of plastic resistance to bending moments about y-y axis                      |
| $t_f$         | Flange thickness  |
| $b$           | Width of a cross section  |
| $h$           | Depth of a cross section  |

### Chapter 8

|                            |   |
|----------------------------|---|
| $K_{bottom.beam}$          | Individual bottom beam stiffness.   |
| $K_{Bi}$                   | Individual equivalent beam stiffness included bottom beam.  |
| $N_{up.design}$            | Design value of axial force in the upper column.  |
| $M_{design}$               | Designed bending moment of the columns at the end of Phase 1.   |
| $N_{design}$               | Designed axial force within the columns at the end of Phase 1.  |
| $\Delta_X$                 | Horizontal displacement of at the top of the considered columns.  |
| $M_{Elastic}^{Max}$        | Maximum bending moment within the considered columns at the end of Phase 2  |
| $N_{Elastic}^{Max}$        | Maximum axial force values within the considered columns at the end of Phase 2  |
| $\alpha$                   | Coefficient linking the bending moment and the axial load within the considered columns during Phase 2 ( $\Delta N_2$ ) |
| $n_1$                      | Coefficient linking $\Delta N_2$ and $N_{lost}^{Pl.Rd}$   |
| $M_{Failure}, N_{Failure}$ | Maximum internal forces values associated to the collapse of the  |

|                      |  |
|----------------------|--|
|                      | damage's level.  |
| $\beta$              | Coefficient linking the bending moment and the horizontal load associated to the membranar forces.         |
| $n_2$                | Coefficient linking $\Delta N_3$ and the membranar forces $H_{memb}$ .                                     |
| $S_{Ci}$             | Stiffness of column number $i$   |
| $m$                  | Number of columns in the investigated zone.  |
| $K_C^{1st}$          | is the shear stiffness of column included the second order effect and the initial rotation at column ends. |
| $k_{s1}, k_{s2}$     | Semi-rigid rotational stiffness of both column ends.   |
| $E_C I_C$            | Elastic modulus and inertia moment of column section.  |
| $\alpha$             | Linear coefficient of end rotation to the horizontal force $H_{memb}$ .                                    |
| $\gamma$             | Ratio between 2 initial rotations of both column ends (normal case, $\gamma = 2$ )                         |
|                      | .  |
| $K_C^{2nd}$          | Shear stiffness of column included the second order effect and the initial rotation at column ends.        |
| $K_C^{side}$         | Shear stiffness of outside column included the second order effect.  |
| $K_{C.1st}^{side}$   | First order shear stiffness of outside column.   |
| $N_{design}^{exter}$ | Compression force applied to the column top.   |
| $L_C$                | Column's length.   |
| $K_C^{Inter}$        | Shear stiffness of intermediate column included the second order effect                                    |
| $K_{C.1st}^{Inter}$  | First order shear stiffness of intermediate column   |
| $N_{design}^{inter}$ | Compression force applied to the column top  |
| $N^{Beside}$         | Full axial force applied to the adjacent column in load phase 3.   |
| $K_{C.1st}^{Beside}$ | First order shear stiffness of next/beside column.   |
| $N_{additional}^1$   | Additional axial force applied to the adjacent column at point (4).  |
| $N_{additional}^2$   | Additional axial force applied to the adjacent column after point (4).                                     |
| $H_{memb}$           | Horizontal component of the membranar force.   |
| $\Delta_X$           | Horizontal displacement of the adjacent column top point.  |

## Notations

---

|                           |   |
|---------------------------|---|
| $n_2$                     | Scalar of the secondary additional axial force due to the horizontal component of the membranar force.    |
| $K_C^{Beside}$            | Shear stiffness of beside column included the second order effect and the initial rotation at column ends |
| $F_C^{dangerous}$         | Dangerous applied force.  |
| $F_C^i$                   | Applied force on column number $i$ .  |
| $K_C^{dangerous}$         | Weakest columns stiffness.  |
| $K_C^i$                   | Stiffness of the column number $i$ .  |
| $F_C^{Rd}$                | Weakest column resistance.  |
| $K_{DamageLevel}^{Left}$  | $K$ value on the left part of the zone damage's level.  |
| $K_{DamageLevel}^{Right}$ | $K$ value on the right part of the zone damage's level.   |

**CHAPTER 1: GENERAL INTRODUCTION**



## 1.1. INTRODUCTION

Throughout history, catastrophic events such as the accident of the Ronan Point building in 1968, the terrorist act at the Alfred P. Murrah Federal Building in 1995 or the disaster of the World Trade Center on September 11, 2001 have horrified the population by their damages and deadly consequences. These collapses, associated with events not considered in the design process, show the necessity of ensuring the protection of inhabitants of residential and industrial building structures subjected to an exceptional event. Following the Ronan Point event, the UK authorities drew up requirements for progressive collapse prevention which have been introduced in their building code. Moreover, the behavior of building structures subjected to exceptional events and the specificity of the associated collapse, i.e. the progressiveness/disproportion of the collapse, have become a topic of interest for the worldwide scientific and engineering communities.

In 2004, the European RFCS project called “Robust structures by joint ductility” was set up with the objective of providing requirements and practical guidelines to ensure the structural integrity of steel and composite structures through appropriate robustness, taking into account joints’ behavior and, especially, their ductility.

As part of the project, the University of Liège’s investigations were mainly dedicated to the exceptional event of a *loss of a column in steel and steel-concrete composite buildings* with the objective of developing analytical procedures to forecast building behavior following such damage. Two PhD theses have been created from the activities of this project. The first thesis, presented by Jean-François Demonceau (2008), describes the *local response of a frame* when membrane effects associated with the development of significant second order effects appear within the beams directly above the damaged column. The present thesis is dedicated to the investigation of the *global behavior of a frame* following a column loss, taking account of the redistribution of the internal forces. The different failure modes which could appear within a damaged structure will be investigated and the influence of the structure’s properties on the development of catenary actions will also be studied. With these two complementary theses, a general model for predicting the response of a steel and composite frame following a column loss is developed and validated.

The following briefly presents the organization of the present document by introducing the contents of each chapter.

## 1.2. ORGANIZATION OF THE PRESENT DOCUMENT

The first chapter of this thesis provides a brief introduction to the research conducted on the first section. The outline and organization of the thesis are given.

Chapter 2 presents a general overview of the information available in the literature about the topic studied. This chapter begins with a short review of three famous catastrophic events: the Ronan Point building collapse in the UK, the Murrah Federal Building bombing in Oklahoma, USA, and the attack on the Twin Towers of the World Trade Center in New York. From this review, the global concepts related to building response following such catastrophic events are presented. Then, a brief description on available codes, standards and provisions and on the state of the art of the thesis topics investigated is given; in particular, two major aspects dealt with in the thesis are presented: the frame redundancy associated with the development of alternative load paths and the conditions required to develop and to maintain a membrane effect. For the membrane effect, the literature review is mainly dedicated to the influence of the structure on these effects and not to these effects themselves.

Chapter 3 introduces key definitions and assumptions to be investigated later on in this work. This chapter is divided into 3 parts. The first part provides the definitions and assumptions associated with the frame in its initial state. The second part describes the loading sequence associated with the investigated event. Finally, the third part explains how the loading sequence is divided in order to highlight the investigation methods which will be used later on.

Next, Chapter 4 presents the methodologies followed during the investigations conducted throughout the thesis. The essential objectives associated with each investigation method are listed. In particular, the building frames are separated according to different zones, representing parts of the frame which are influenced by the column loss. The general procedure, which will be used for the validation of the results obtained, is described afterwards.

Chapter 5 then discusses the development of the alternative load paths within the damaged structure after the event of the *loss of a column*. In particular, numerical simulations of the frame under the load sequence described in Chapter 3 are carried out on the building frames. Based on these results, structural elements, which transfer the load to the foundation, are isolated. These elements form the alternative load paths. Two possible load

paths in the event investigated are described.

Next, Chapter 6 concentrates on a part of the frame which is directly affected by the loss of column event. This chapter describes the distribution of the internal forces within the part above the damaged column. This part is extracted from the frame. An analytical model of the part, representing its behaviour, is developed and validated.

Chapter 7 analyzes behavior of the column in the alternative load path. Two columns, which are placed on both sides of the damaged column, support an extreme load. This chapter describes the development of an analytical model to predict the compression on these columns. Based on this model, a critical element, which undergoes a high combination of compression and bending, is extracted as a key element.

Chapter 8 presents the alternative load path when the beams above the damaged column fully yield. A membrane effect develops in the beams directly above that column. So, the previous load path extends to maintain the stability of the frame thanks to such a phenomenon. Thus, the behavior of the structural members within the storey where a column is lost is investigated. Additionally, the influence of the structure's properties on the development of catenary action is studied.

Chapter 9 then provides a demonstration of a robustness assessment procedure. The formulae from the three previous chapters are systematized and placed in order. Next, the essential objectives of the robustness assessment procedure are presented in detail. Finally, an existing frame structure example was solved to clarify the necessary details.

Chapter 10 concludes the content of this thesis and discusses the topics which are not covered in previous chapters. Parametric analyses on the way a frame is supposed to behave after the loss of a column event are demonstrated in order to assist future engineers in accident prevention design. To conclude, perspectives on future research and activities are also proposed.

**CHAPTER 2: STATE-OF-THE-ART WITH PARTICULAR  
EMPHASIS ON THE ALTERNATIVE LOAD PATH METHOD**

## 2.1. INTRODUCTION

Chapter 2 presents a general overview of the available information in the literature about the topic studied. The chapter begins with a short review of three famous catastrophic events: the Ronan Point building collapse in the UK, the Murrah Federal Building bombing in Oklahoma, USA, and the attack on the World Trade Center Twin Towers in New York.

From this review, the global concepts related to building response following such catastrophic events are presented.

Then, a brief description on available codes, standards and provisions and on the state of the art of the topics investigated in this work is given; in particular, two major aspects dealt with in this thesis are presented: the frame redundancy associated with the development of alternative load paths and the conditions required to develop and to maintain a membrane effect.

For the membrane effect, the literature review is mainly dedicated to the influence of the structure on these effects and not to these effects themselves.

## 2.1. REVIEWS OF CATASTROPHIC EVENTS

### 2.1.1. Ronan Point

On the day of 16 May 1968 in East London, a small gas explosion happened on the 18<sup>th</sup> floor of the 22-story building Ronan Point. The explosion threw out the load bearing pre-cast concrete panel near the corner of the building. Without a support, the floors above collapsed. Then, the impact of the debris on lower floors led to a chain of collapses going down to the ground floor of the building as present in Figure 2.1. As a result, the corner rooms of all floors were destroyed. Four persons died but, surprisingly, the woman who was closest to the gas explosion survived.

This event is not a major historical accident, but it is a clear example of the problem called *progressive collapse*. As a process begins from the failure of small localized member, a chain of failures develops and grows disproportionately.



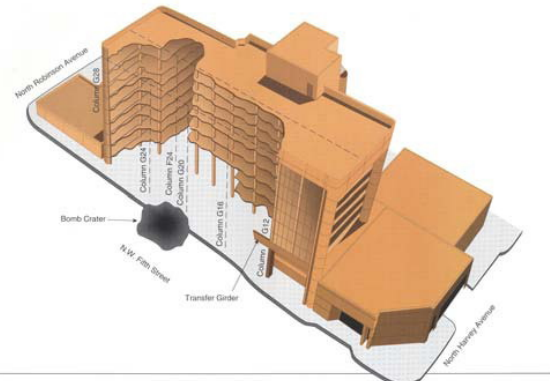
Figure 2.1. Ronan Point building after the accident [NISTIR 7396, 2005]

### 2.1.2. Alfred P. Murrah Federal Building 19 April 1995

The Alfred P. Murrah Federal Building, a government office building in Oklahoma City, was completed in 1976. On 19 April 1995, it was attacked on the east side close to the middle point by a car bomb. The explosion destroyed three columns of the ground floor. The transfer girders then lost their support due to the collapse of the columns. The damage developed and extended to the final collapse as appears in the image below.



Figure 2.2.a. Murrah Building showing the damage after the debris was removed



b. The simulation model [NISTIR 7396, 2005]

### 2.1.3. World Trade Center 11 September 2001

World history was changed after this infamous terrorist attack. Both of the World Trade Center twin towers were crashed into by Boeing 767 jet airplanes traveling at high speed.

According to FEMA reports, a part of the floors including columns and beams was destroyed by the combination of the impact and fire. Figure 2.3 presents a model of WTC 2 and the damage on the floor at the site of the crash. The structures around the impact zone lost their support capacity, causing the floors above to fall down and leading to an overloading and an impact on the lower structures. The damage developed in both vertical and horizontal directions. As a result both towers were fully annihilated.

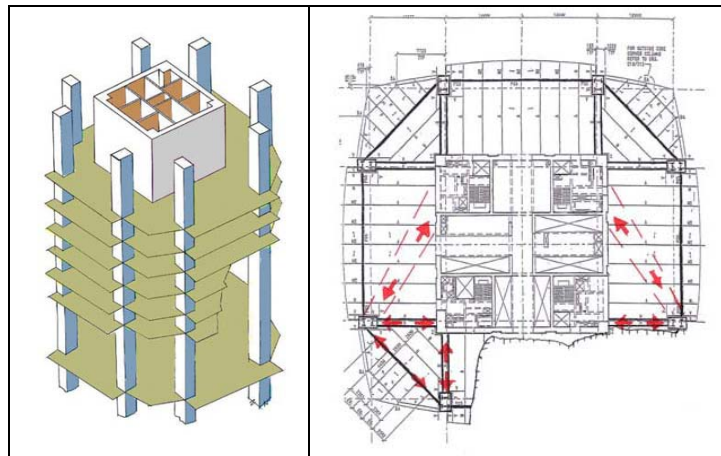


Figure 2.3. WTC 2 main structures and damage



Figure 2.4. A FEMA diagram depicting debris distribution from the collapses of WTC 1 and 2. Dotted, darker and light orange areas denote heaviest, heavy and lighter debris distribution respectively. Red 'X' marks denote isolated perimeter columns ejected farther than in average debris distribution [FEMA, 2002].

According to professional opinions, this event is famous in that it proves that the magnitude and probability of abnormal loads are unpredictable. However, the damage was

not limited to the twin towers: the debris from the collapse of these twin towers also impacted and damaged or destroyed neighboring buildings. Some of the secondary collapses are actually the most interesting examples because they illustrate the transfer capacity of the girders which kept the structures stable despite the loss of one or more columns.

The first such example is the World Financial Center 3 – the American Express Building. During the event, sections of the corner columns were destroyed by the debris from WTC 1 as seen in Figure 2.5. Unlike the Ronan Point building, the injured part of WFC 3 was limited to localized damage. As a result, the whole building remained stable and was repaired for reuse afterwards.



Figure 2.5. Photograph showing mild debris damage to WFC 2 and WFC 3, with the heaviest debris falling perpendicular to the west face of WTC 1 onto the Winter Garden [FEMA, 2002].

The second most interesting building is the Bankers Trust Building. Several columns on the front of the building were impacted by the debris from WTC 2. However, the upper structural members still functioned and, in the end, the building survived.





Figure 2.6. North face of Bankers Trust Building with impact damage  
between floors 8 and 23 (Smilowitz – FEMA, 2004)

Although the ranges and natures of the previous incidents are different, they have a similar property, namely that the cause of the accident was unpredictable. In other words, they had to support an abnormal or extreme load. Progressive and disproportionate collapse can therefore occur. In some cases, progressive collapse develops while in other cases, the building manages to maintain its stability.

Regarding these possibilities, the investigations, surveys and studies on these accidents reach the same conclusion: if the buildings are designed with an appropriate level of integrity or have the necessary robustness, they can survive and any damage is limited.

## **2.2. GLOBAL CONCEPTS AND DEFINITIONS**

Buildings and structures are designed for certain loads and hazards. All normal loads and hazards are defined by codes and standards as the requirements for the engineers or designers that depend on the objective and position of the building. Direct contact between the structural designer, architects, building owner and building officer has to be carried out in order to determine all of the loads involved.

However, the engineering design procedure cannot cover every extreme type of hazard which may occur during the structure's life. In commercial buildings, hazards such as meteorite impacts, accidental events or military attacks are not considered in the design.

Normally, the design procedure considers four major known types of hazards which must be well defined: gravity, wind, earthquake and fire. Using these definitions, in each case, a performance and thus a conformance objective are ensured.

Nevertheless, throughout a building's life, it may support *extreme loads* which go beyond the design specifications – this is an *exceptional event*. Usually, the magnitude and probability of extreme loads are not predictable. In many cases, the buildings are mostly or totally destroyed due to hazards beyond the design value. However, there are cases where the building can survive. The differences between these cases may reveal a way to diminish an accident's repercussions and to increase the probability of saving lives.

Extreme loads can affect a structure to many different degrees. In some situations, damage to a building is the direct result of an accident. In other cases, most or all of a structure is destroyed indirectly from initial damage. Three situations are therefore to be distinguished: proportionate, progressive and disproportionate collapses.

A *proportionate collapse* happens when an accidental event leads to proportionate damage, e.g. a nuclear blast totally blows out a building or a car's impact destroys only one column of a building but does not lead to wider damage.

On the contrary, a *disproportionate collapse* defines a situation where a consequence is disproportionate to its cause. The Ronan Point event in 1968 is the most famous example where the small gas explosion led to a chain of damage.

A *progressive collapse* denotes an extensive structural failure initiated by local structural damage, or a chain reaction of failures following damage to a relatively small portion of a structure. This occurs when, due to damage sustained, a loading pattern or a structural configuration changes and leads to a residual structure seeking an alternative load path in order to redistribute the abnormally applied load. Then, another structural member fails due to this load redistribution. The evolution of the damage continues until a global collapse occurs.

There is a distinction between *disproportionate* and *progressive* collapses concerning the final extent of damage. However, the definitions become similar when the ultimate damage is major and leads to a dangerous situation. Consequently, the term *progressive collapse* will be used throughout this thesis to refer to progressive and disproportionate events. This is the term employed today worldwide.

To avoid the development of progressive collapse, there are two guidelines which

construction engineers are advised to follow. The first guideline points to an *identification of risks* which aims to decrease the vulnerability of the structure based on a maximum understanding of the risks. In the present thesis, this is not taken into consideration.

The second guideline is to create the design so as to prevent progressive collapse. Section 1.4 of ASCE Standard 7-05 describes protection through “an arrangement of the structural elements that provides stability to the entire structural system by transferring loads from any locally damaged region to adjacent regions capable of resisting these loads without collapse.”

There are two approaches used for providing resistance against progressive collapse, namely, by indirect or direct methods. The indirect method is a prescriptive approach providing a minimum level of connectivity between various structural components so that little additional structural analysis is required by the designer. This method is associated with an implicit design approach that incorporates measures to increase the overall robustness of the structure. [NISTIR 7396]

The direct methods, on the other hand, rely heavily on structural analysis. The designer explicitly considers the ability of the structure to withstand the effects of an abnormal load event. In general, there are three alternative approaches towards increasing the strength of a structure in the building design process. Engineers are advised to ensure the following:

- *Redundancy or alternative load path.*
- *Local resistance.*
- *Interconnection or continuity.*

Ensuring redundancy or an alternative load path is the simplest and most direct method. In this approach, the structure is designed to transfer the load to the new alternate path when the critical structural component is destroyed. The next consideration, local resistance, involves the process of increasing the strength of the critical component to add to its ability to withstand attacks. Obviously, this approach requires an understanding of the nature of the attack. Therefore it is difficult to codify a general approach in this case.

In the last approach, the designer has to consider increasing the interconnection within or the continuity of the structures. In fact, this involves a combination of the two previous approaches. The increase in continuity will enhance the resistance of the structural part, that is to say, by bridging the load over the local damage in the case of accidental events.

All three approaches are considered an improvement in *structural integrity*. In other words,

to avoid the global instability of the structure due to an exceptional/extreme event, the building should be designed so that it could remain stable for a given time to evacuate or rescue victims when one area is damaged. Once damaged, the structure is called a *residual structure*.

Integrity will enhance the probability of global stability in the residual structure. That property of the building is called the *robustness* of the structure. According to Eurocodes, BS, designers are advised to increase structural integrity in order to prevent progressive collapses but these codes lack practical guidelines.

In the present thesis, an exceptional event which is investigated is the loss of a column in commercial and residential buildings. In such a catastrophic event, a so-called *catenary effect* describes a phenomenon where two connected beams lose their middle support column. Nonlinear behavior develops and the high axial forces which appear within the beams are called the *membrane forces*. This phenomenon helps in extending the structure's ability to maintain stability. According to Hamburger and Whitaker (2002), this is the key to ensuring robustness.

In the next sections, the available codes and standards are briefly presented showing not only the existing guidelines for ensuring structural integrity but also the lack of detail in those guidelines.

### **2.3. REVIEW ON AVAILABLE CODES AND STANDARDS**

Ensuring an alternative load path is one of the three approaches in the direct design method. It is taken into account when the basic design of the building frame is completed or applied to an existing structure. In fact, it constitutes a review of the influence of structural key elements on the whole structure. The method consists in estimating whether a building can bridge over the initial localized damage. During the design process, this approach involves the notional removal of key structural elements, one at a time, to assess the local and overall structural stability without them. Once accomplished, modifications of the design are incorporated if necessary. [NISTIR 7396, 2005]

So, using an alternative load path is a direct design approach which is applied to the frame under stipulated damage. However, the cause of the threat is unknown. The advantage of this method is the structural improvement in ductility, continuity and energy absorbing properties, preventing progressive collapse.

The British Standards were the first codes to propose recommendations to avoid the progressive collapse of buildings, strongly motivated by the catastrophic event of Ronan Point in 1968 (Figure 2.1). According to the British Standards [*BS 5950-1:2000*], it is required that, in the event of an accident, the building will not suffer collapse to an extent disproportionate to the cause, i.e. the progressive collapse of the structure is avoided following a limited collapse.

Three main methods are proposed to ensure that structures have a minimum level of strength to withstand accidental loading. They are briefly described here below [*Moore, 2002*]:

- The “tying” method: this first design option consists in providing effective horizontal and vertical ties in accordance with the structural Codes of Practice.

The provision of ties increases structural continuity creating a structure with a high degree of redundancy; providing the building with alternative load paths should part of the structure be removed by an accidental action. Generally, the ties are steel members or steel rebars; also, the beam-to-column joints have to be able to transfer the tying forces. The recommended minimum value for the tying force is equal to 75 kN.

- The “bridging” method: where “tying” is not feasible, it is recommended that the structure should be designed to bridge over a loss of an untied member and that the area of collapse be limited and localised. This is usually achieved by notionally removing each untied element (including load bearing vertical members and beams supporting one or more columns), one at a time, and checking that on its removal the affected zone does not extend further than the immediate adjacent stories and that the area of structure at risk of collapse is limited to the smaller of the following areas:

- o 15 % of the area of the considered storey or,
- o 70 m<sup>2</sup>

The loads to be considered are one third of the characteristic imposed and wind loads and the full dead loads, except if the imposed load can be considered as a permanent one (mainly for storage buildings) where its full value has to be used in the computations.

- The “key element” method: if it is not possible to bridge over the missing member, such a member should be designed as a protected (or key) element capable of sustaining additional loads related to a pressure of 34 kN/m<sup>2</sup>. The value of 34 kN/m<sup>2</sup> was chosen with reference to a rounded estimated failure load of the load bearing flank wall at Ronan Point. This estimation was based on observational evidence. In practice, the 34 kN/m<sup>2</sup> is used to determine a notional load that is applied sequentially to key elements and is not a specific overpressure that would result from a gas explosion. Such accidental design loading is assumed to act simultaneously with one third of all the normal characteristic loading.

The above requirements are considered to produce more robust structures which are more resistant to disproportionate failure due to various causes, such as impact as well as gas explosions (Demonceau, 2008).

Compared to the other conventions, EUROCODE appears to be a general systematized set of guidelines for accidental design situations. Two strategies are provided: 1) the strategy based on identified accidental action and 2) treatment based on limiting the extent of localized failure. The advice on this second strategy is to ensure redundancy and to find the key element. Concerning the key element, the codes are concerned with giving advice on directions, but lack any specific guidelines, such as how to decide what the key element is.

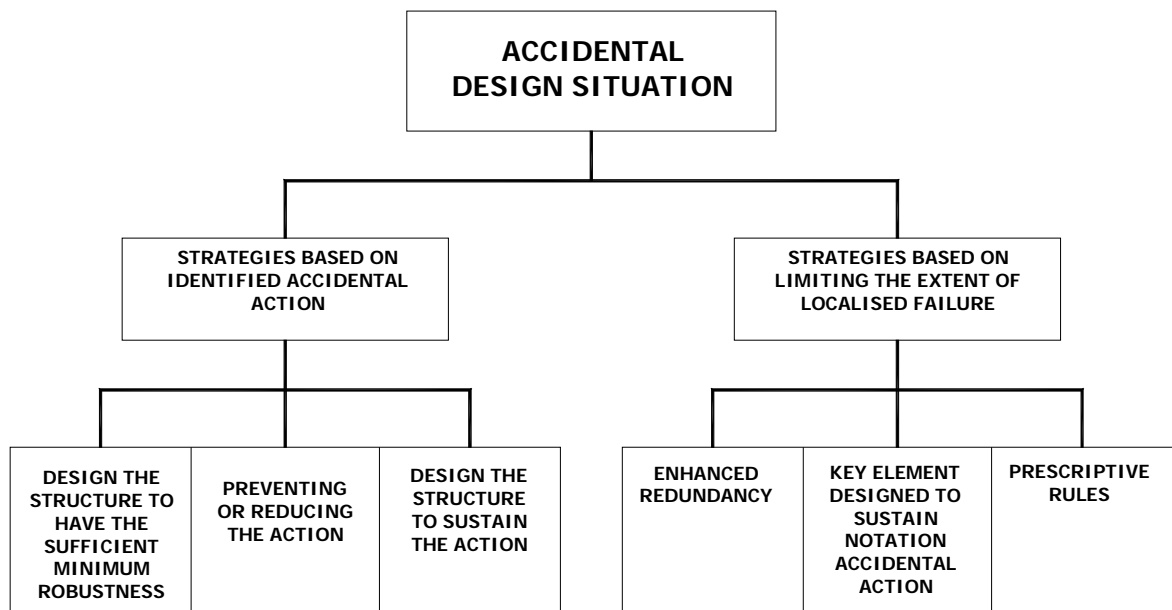


Figure 2.7. The guideline in EUROCODE

Specified by the General Service Administration (GSA 2003) and afterwards in the Department of Defense – Unified Facilities Criteria (DoD – UFC 4-023-03 2005), this

method is interpreted as the removal of one load-bearing element. In this way, an individual structural component, such as a critical column, is destroyed. This assumption does not take into consideration the other damage on the surrounding components as may occur in reality. The processing from the original structural configuration to the damaged one is instantaneous; exposing the progressive collapse is a dynamic phenomenon. Depending on the method of analysis, the dynamic effect will be taken into account or not. Four analytical procedures can be applied here:

- Elastic static. The GSA (2003) progressive design guideline proposes the “equivalent” elastic static method to simulate the dynamic and inelastic behavior of the frame response during the event. The dead load plus 25% of the live load with a dynamic load factor equal to 2 is applied to the residual frame. The formula can also include a demand-capacity ratio larger than 1 to account for inelastic deformation development. The DoD UFC consider the same analysis procedure with a load of 90% - 100% dead load plus 50% live load and 20% wind load. The elastic analysis iteration method is applied.

This method is suitable to simple structures and predictable behavior. It cannot, however, account for nonlinear behavior, P-Delta instability and force redistribution. Still, the simplification of the analytical procedure and the ability to provide member resistance, while defining necessary criteria and evaluating the potential of progressive collapse, prove its usefulness.

- Inelastic static. To take into account such effects as illustrated in the previous paragraph, inelastic analysis is applied. The nonlinear geometry resulting from the large deformation and nonlinear physics, such as the non-linear behavior of the material, are considered. Thus this is called the non-linear equivalent static method. This method simulates the dynamic response of the frame through the dynamic load factor and in addition applies the load reaction of the damaged column to generate the push-down curve of the structural behavior.
- Elastic dynamic. This method incorporates the linear elastic and dynamic methods to analyze the frame’s reaction to the sudden loss of column but does not take into account force redistribution or the P-Delta behavior of the frame.
- Inelastic dynamic. This method, which is the most complex, covers all the difficulties of structural analysis of progressive collapse evaluated by inelastic

finite element programs. It provides the most accurate behavior but requires experience and knowledge of the full frame behavior.

The GSA permits the use of this full analysis, but cautions that it should only be used by someone with experience in structural dynamics. The DoD UFC also provide the step-by-step procedure for this type of analysis. Also, both sets of guidelines give the performance criteria for structures in term of deformation limits.

## **2.4. RESEARCH ON THE ALTERNATIVE LOAD PATH METHOD AND CATENARY ACTION**

### **2.4.1. Alternative load path**

Officially provided worldwide in codes and many other provisions, the direct design method using the “alternative load path” approach is usually addressed in official documents on progressive collapse prevention. However, this method, according to Smilowitz (2007), can only be applied to individual constructions. The next paragraph examines studies on the same aspect associated with this method.

From a different standpoint, the alternative load path method can be described as the search for a structure’s defense against the propagation of failure. According to Ettouney (2004) and Smilowitz (2007), the initial damage propagates through the building structure and forms a “failure front”. The failure front spreads outwards from the initial damaged region. Therefore, at a given instant during the propagation process, only a small portion of the structure needs to be investigated because the outer structural properties do not affect the current damaged region. And because the column’s axial stiffness is typically greater than the beam’s bending stiffness, the vertical propagation of the failure front is faster than the horizontal one. In normal structural geometry, the horizontal failure front goes through the beam-to-column points and causes flexural yield in the beam end-section but not across the column line. In the region adjoining the damaged one, the beam may form a flexural hinge, fail in shear or undergo axial failure due to a catenary action.

In many articles, alternative load path assessment has been discussed. Examples of these articles are case studies such as Powell (2004), proposals for an alternative load path analysis method as in Elvira et al. (2005) or designs to prevent progressive collapse by increasing frame redundancy, proved by an efficient alternative load path and taking into



account the flexural and axial deformations, as in Hamburger and Whittaker (2002). However, they only described general guidelines for solving the problem of the assessment of a structure's capacity.

Recently, the intriguing method described in J. Agarwal et al. (2003) and in England, Agarwal, and Blockley (2008) provides a mathematical solution to the automatic estimation of the alternative load path within the existing building frame. Agarwal's work presents a method for enumerating the structure members and creates a hierarchical description of the frame configuration. Through structural hierarchy, different vulnerability scenarios are predicted. In this way, the alternative load paths and the key elements are pointed out based on the connectivity of the structural elements.

In particular, in this method, as demonstrated in Figure 2.8, three elements are connected in the basic ring defined as "well deformed". Depending on the connectivity between the elements, a basic ring is built up. The basic ring connects to the other element or another ring incorporates the higher level ring. The rings connect to the round. The procedure is repeated until the full frame is described. When the hierarchical description is compiled, the scenario of building behavior without any structural member can be clearly predicted.

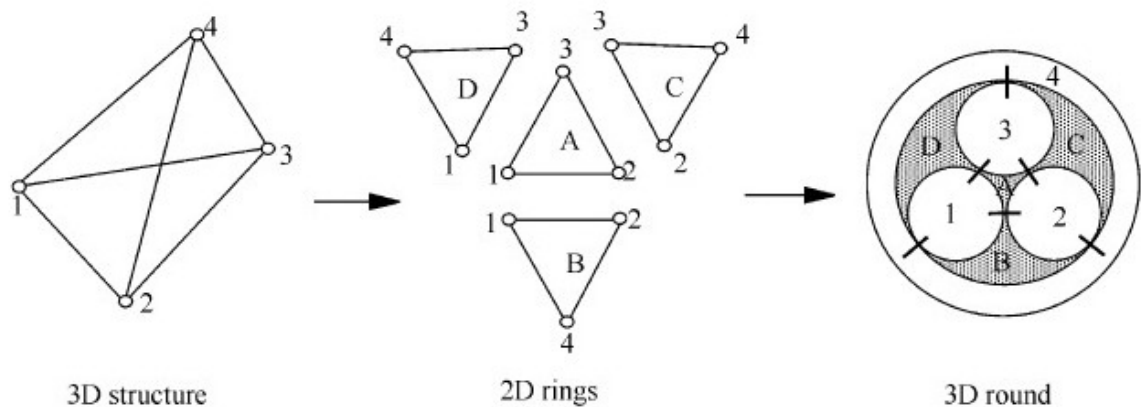


Figure 2.8. The basic ring and round in the Agarwal method (Agarwal, 2008)

Agarwal's method has the advantage of automatically predicting the "failure front" within any arbitrary structure. It is general and already developed in 2D and 3D. However, as shown in the figure above, even a simple structure will be described by a complex hierarchy. This is because the process requires complex calculations and is solved by PC programming.

With the exception of this article, even though the alternative load path method has been widely proposed on provisions and in other articles, no diaphragm solution had been

provided until this time.

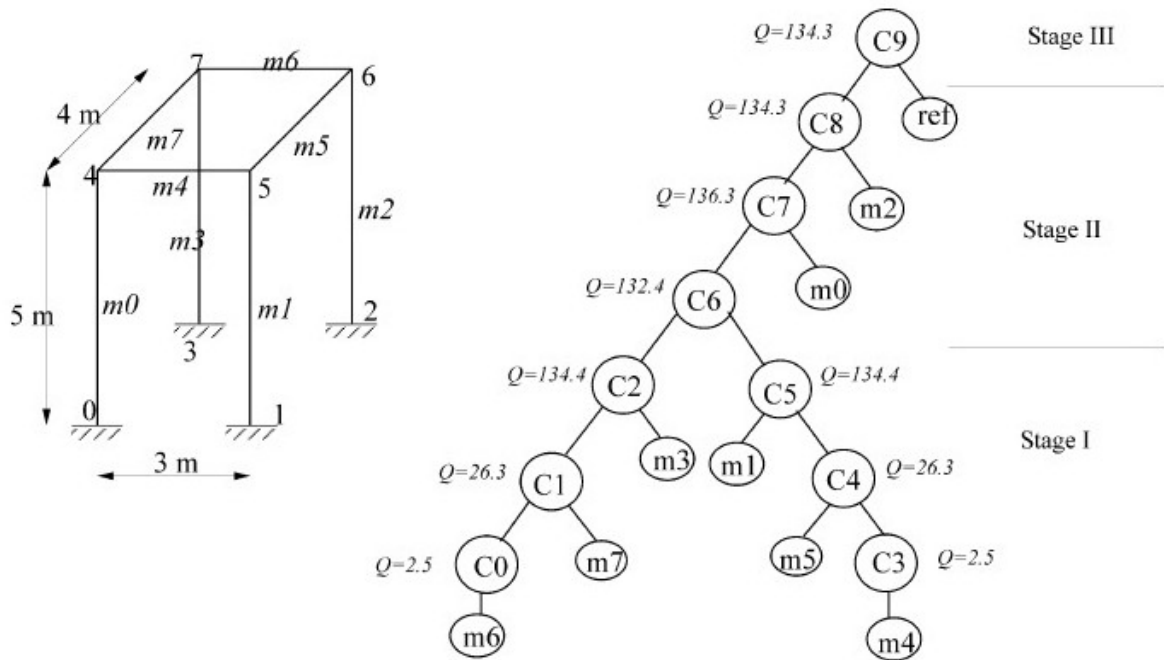
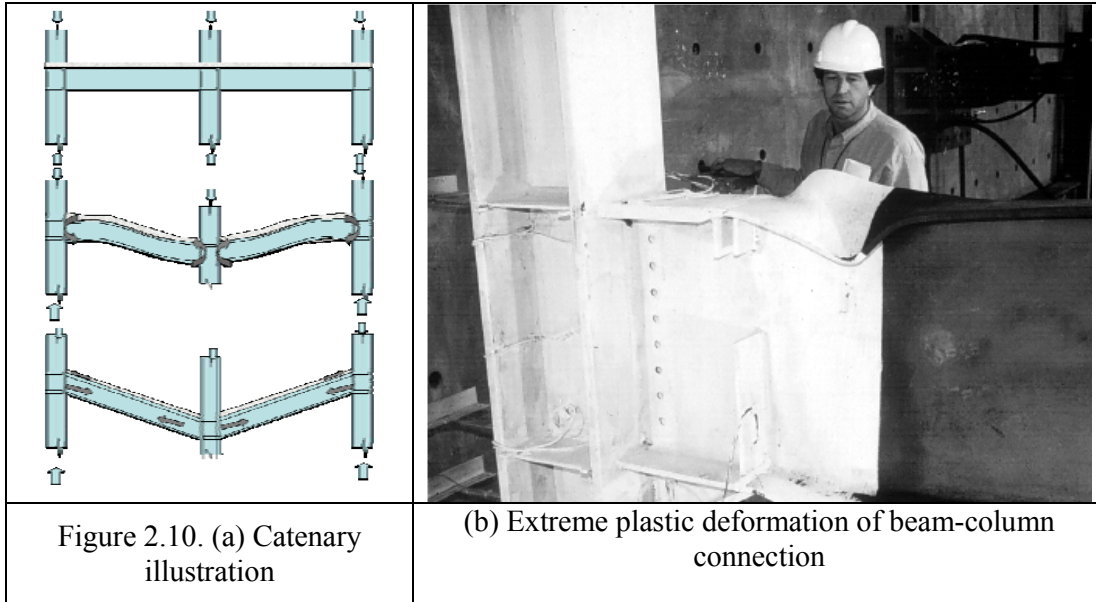


Figure 2.9. A 3D frame and its hierarchical representation (Agarwal, 2008)

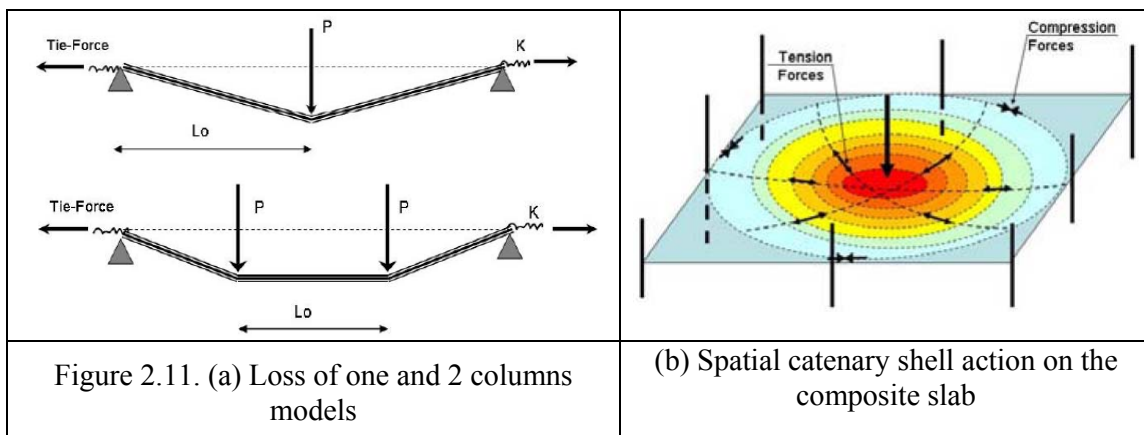
### 2.4.2. Catenary action

As discussed before, the membrane effect or catenary action is accepted as the solution to the increase in frame redundancy in an abnormal situation. However, as in the case of the alternative load path method, this solution appeared many times in general guidelines and in experts' reports but there was a lack of information on processing and analytical solutions. In this section, some reviews associated with studies on the same phenomenon are reassessed. In addition, studies on a different aspect, but one with similar structural behavior, are presented in order to note the position of earlier studies.

According to Hamburger and Whitaker (2002), in a catastrophic situation, a steel frame should be designed in order to have the capacity to withstand the large tensile demand simultaneously applied with large inelastic flexural deformations. However, the article is limited to design strategies and the idea of design applications. No analytical model or detailed prediction of catenary phenomena is presented. Figure 2.10 presents the catenary phenomena and a photo of the experiment of the investigated joint which are presented in the article.



In the same proceedings of the National Workshop on Prevention of Progressive Collapse, held on July 10-12, 2002, Ahmad Rahimian and Kamran Moazami (2002) proposed a method to increase frame integrity by expanding the alternative load path with the catenary action. The case study of a 35-story composite building, with full-scale numerical simulations, was carried out to investigate the structural behavior and to provide integrity criteria. A restrained spring was placed at the beam end and it is defined as  $K$ . According to the authors, the value  $K$  comes from the adjacent columns close to the damaged one. Figure 2.11 presents the catenary model in 2D and 3D.



The next article performed research on a different aspect. Yin and Wang (2005) developed the analytical model of the catenary action in steel beams under different temperature conditions. They provide the nonlinear model seen in Figure 2.12. The two inelastic and plastic interactions between the axial force and bending moment in the catenary beams are

covered. Of course, the model behavior is entirely different from the case of this thesis. The initial condition and the hinges' appearance on their model before the catenary action are not taken into consideration here or in Demonceau's work.

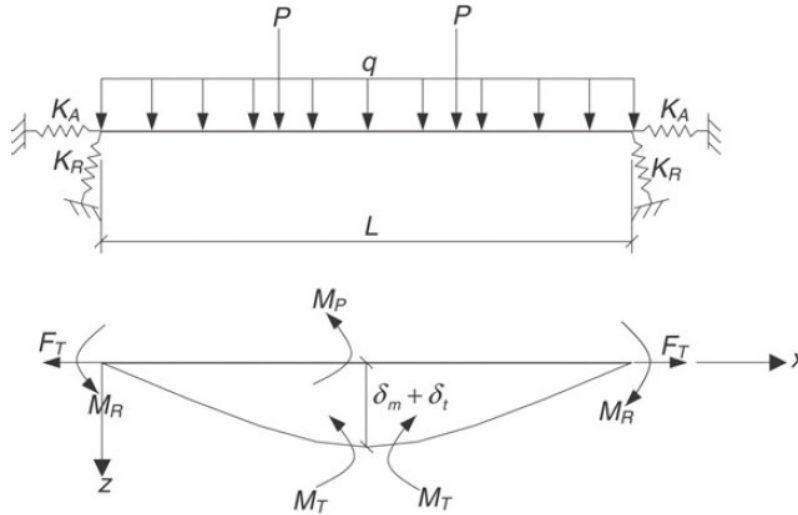
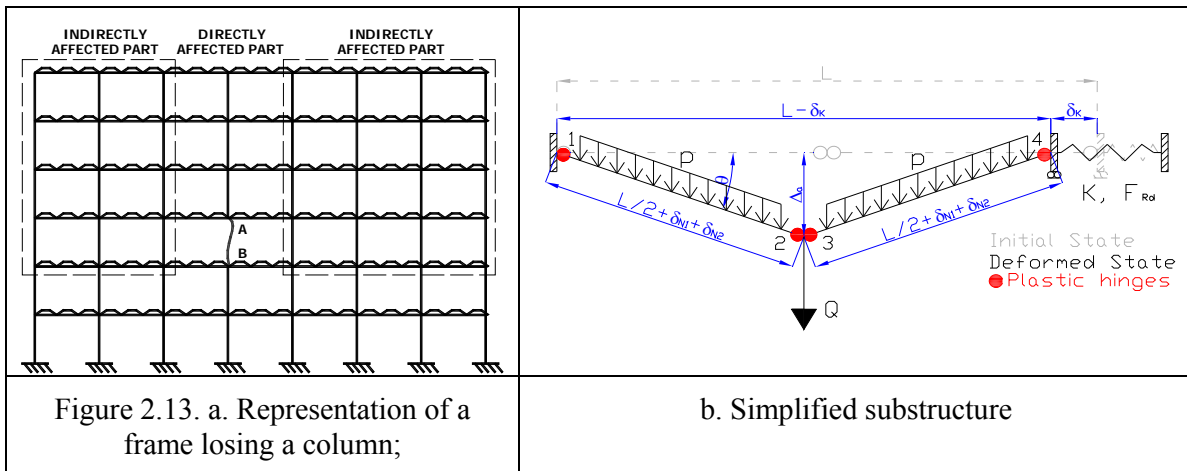


Figure 2.12. Yin and Wang's model [Yin and Wang, 2005]

In this article, the axial restraint translation  $K_A$  and the rotational stiffness  $K_R$  are proposed. There is a lack of information on how to derive  $K_A$ ,  $K_R$ , except in some proofs, where the value of  $K_A$  varies from  $0.05EA/L$  to  $EA/L$ .

In the introductory chapter, both Jean-François Demonceau and the author's complementary works are briefly introduced. In fact, the majority of the research presented in this thesis was carried out as the continuation of Demonceau's work.



Demonceau predicted the behavior of the beams directly above the damaged column when plastic hinges appeared. A simplified substructure model was extracted from the frame as

shown in Figure 2.13.b. To define this simplified substructure, some parameters had to be predicted. In particular, the characteristics of the horizontal spring  $K$  and  $F_{Rd}$ , which simulate the behavior of the indirectly affected part (see Figure 2.13.a) subjected to membrane forces, had to be determined. The analytical models developed in [Demonceau,2008] to predict the latter are presented in the following sections.

Parallel to Demonceau's research, an investigation and development of the same aspect were performed at Imperial University in the UK by Izzuddin and Vlassis (2007). In this thesis, only a part of their analytical theory is considered. In order to develop the multi-level assessment of a building's robustness due to the sudden loss of a column, the 3-step reduction procedure is applied. The first step is to consider the directly affected part as demonstrated in Figure 2.14.a. This part was extracted from the building as a substructure. The appropriate value for boundary conditions is applied to the spring which is represented by the elongated stiffness of the beam next to the directly affected part. The second reduction reduces the substructure from full dimensions to one level only above the damaged column. This is explained by the neighboring column's capacity to withstand the load redistribution. The columns in the same line with the damaged one are not taken into account. The last step separates the double span beam and the orthogonal one to obtain the 2D simplified model. The full process is presented in Figure 2.14.

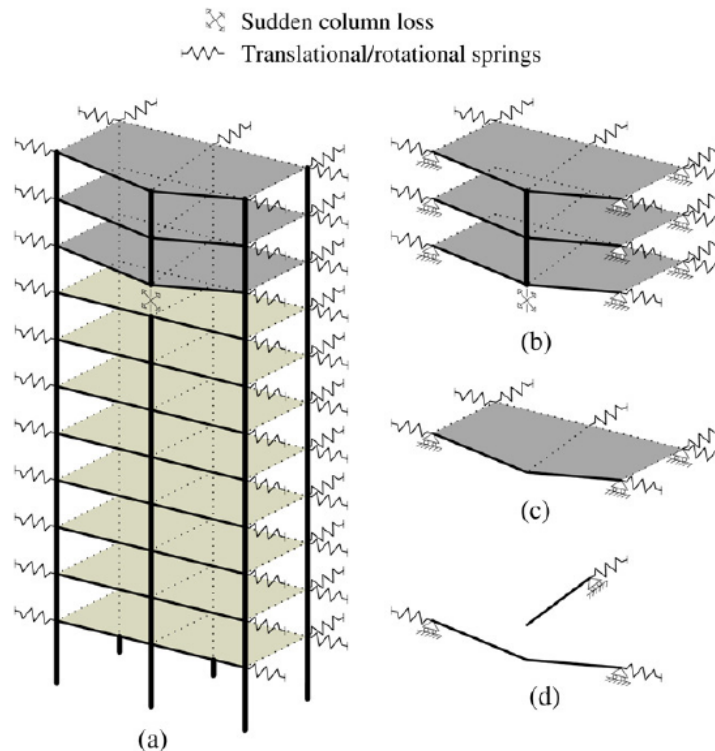
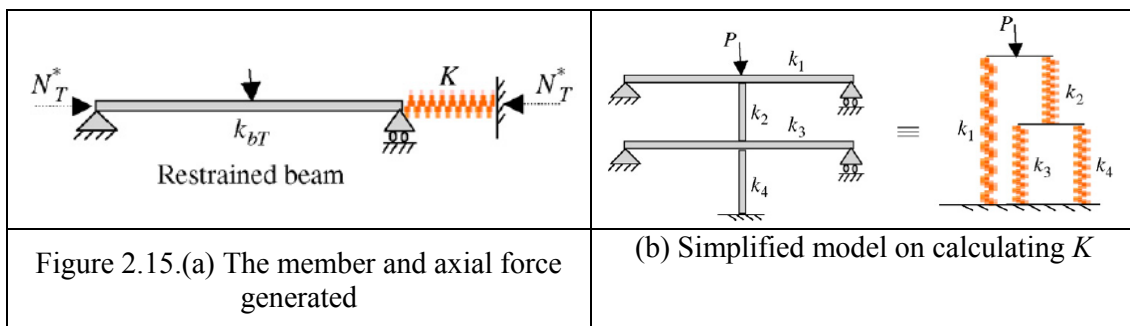


Figure 2.14. Izzuddin and Vlassis's (2007) reduction process

The additional details in catenary behavior and the numerical validations are commented on in Demonceau’s thesis, where he writes: “The developed method is very easy to apply; the accuracy of the method is linked to the accuracy of the load-deflection response curve which is used within the method. In [Izzuddin and al, 2007] and Vlassis’s thesis, the models which are presented to compute this curve are based on rough assumptions, in particular for the computation of the parameters to be used within the models.”

Last but not least, the specific study of Wong (2005) is presented below. After examining the reviews of the investigations and studies above, the author has demonstrated the lack of knowledge on the axial and the rotational restraint stiffness. Still, investigations have shown the important influence of such a parameter on the catenary action. In fact, this type of coefficient has already been studied in an entirely different domain which was explored by Wong (2005): frame works in fire conditions.

This study proposes a method for modeling the axial elongation of a beam in a fire. According to the article, when the beam is subjected to a fire, a high axial force is generated and is exerted on the neighboring members which are linked to its restraints. The maximum temperature which the beam could support is predicted according to the stiffness of that restraint. In particular, the stiffness  $K$  is predicted by a combination of the associated beams’ and columns’ stiffness. The figure below demonstrates a procedure to obtain the stiffness which will be improved on in the present thesis. The relationship between the stiffness in the different parts is seen in Figure 2.15.b.



## 2.5. SUMMARY AND CONCLUSIONS

Two extracts from official documents are reproduced here to conclude this chapter as they effectively summarize unresolved structural requirements. The first extract is from Section 8 of the article “Facts for Steel Buildings: Blast and progressive collapse – AISC” (2005).

## **“SECTION 8: RESEARCH AND FUTURE NEEDS**

### **8.2. What are the main steel structure response issues that are still undetermined?**

Key issues that remain unresolved concerning progressive collapse mitigation and the performance of steel connections under high blast demands include:

- *The specific mechanics by which a moment resisting frame devolves from a flexure dominant system to a tensile membrane or catenary dominant system, and what are the rotation demands on connections at this devolution point.*
- *The reserve axial tension capacity of steel beam-to-column connections (i.e., “simple” and moment-resisting) after reaching significant inelastic rotations.*
- *The importance and impact of analysis approaches chosen; e.g., is a static linear alternate path analysis predictably conservative or unreliable?*

[...]

### **8.3. What kind of research is ongoing or planned for the near future?**

Several current research initiatives are progressing [sponsored by the Defense Threat Reduction Agency (DTRA), the GSA, and the Technical Support Working Group (TSWG)] to investigate “key” issues related to the response of steel structures to blast loads and progressive collapse mitigation in steel structures. These include:

[...]

- *Determination of post-blast gravity load-carrying capacity of a double span beam following column removal. ”*

**“Facts for Steel Buildings: Blast and progressive collapse – AISC” (2005)**

Next, the second article is taken from NISTIR 7396 – session 5.3.3.5, “Best Practices for Reducing the Potential for Progressive Collapse in Buildings” (2007).

### **“5) Allow catenary action to develop**

*Within this general category are means to provide catenary action within existing element of a structural frame. The concept involves engagement of tensile forces in members that are draped or that deform into configurations that allow cable action to be engaged. In catenary action, engineers generally expect that elements (e.g., beams and slabs) that are intended to support load in flexure will deform enough and have sufficiently stiff and strong anchorages that they will take on load as tension members. In this case, adjacent structure needs to be able to resist the high horizontal loads that are necessarily associated with the resolution of the forces in the flexural members that must work while deforming to*

*relatively small angles to the horizontal.”*

**“Best Practices for Reducing the Potential for Progressive Collapse in Buildings – NISTIR 7396” (2007)**

These excerpts, which come from two professional organization’s official documents, illustrate the lack of knowledge not only regarding the frame’s response to an exceptional event but also more specifically on the catenary action. Thus, in order to reveal a small part of this larger problem, this thesis will carry out investigations into exceptional event response and the catenary action.



**CHAPTER 3: GLOBAL CONCEPTS FOR STRUCTURAL  
ROBUSTNESS ASSESSMENT**

### 3.1. INTRODUCTION

This chapter introduces key definitions and assumptions necessary for later discussions. The first part of this chapter provides the definitions and assumptions associated with the frame in its initial state. More specifically, this part describes a change of the loads acting on the frame in the transition from a “normal” to an “abnormal” state. Assumptions used to clarify further investigations are also discussed, e.g. in progressively removing a column or when investigating an event as a static problem.

The second part describes the loading sequence corresponding to the event being investigated. The sequence is applied to a specific point on the frame to represent its behavior in a given event. The third part describes how the loading sequence is divided in order to highlight the investigation methods which will be used later on.

### 3.2. DEFINITIONS AND ASSUMPTIONS

#### 3.2.1. Frame response under normal loading

The structures under investigation here are typical urban structures such as residential or office frames. The applied loads to be considered when the frame is used in a proper way include:

- the weight of the structure itself;
- permanent loads;
- variable (or live) loads;
- wind loads;
- snow weight;
- ...

These loads are defined in standards and codes and, when they correspond to the appropriate safety factor, they are referred to as the *design loads*. These design loads are then combined to check the ultimate limit states. The application of these loads (and their combination) to the frame under investigation are defined as the *normal loading* of the frame, i.e., the set of loads to be considered when the frame is used under usual conditions.

### 3.2.2. Frame response under exceptional loading

In the present work, the loss of a column is considered to be an exceptional case, i.e., an event which is not explicitly taken into account in the design process. The lost column can be at different positions in the frame; therefore, two specific positions of the damaged column are identified, as illustrated in Figure 3.1. The internal columns are in red while the external columns are in blue.

Also, if the frame being examined is braced, two sides are identified: the braced side, where the bracing system is placed, and the unbraced side (or free side) on the opposite side (as illustrated in Figure 3.1).

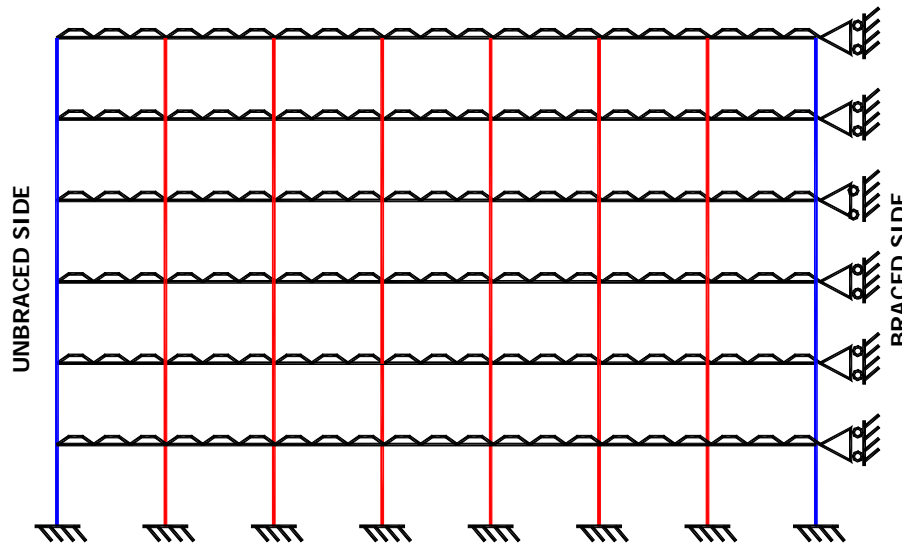


Figure 3.1. Definitions of zones within the investigated frame

The loss of a column can be explained by different types of exceptional events, such as explosions or vehicle impacts. In some of these exceptional events, dynamic effects may play an important role; within the present work, however, it is assumed that the event associated with the column loss does not induce significant dynamic effects. So, the investigations performed are based on static approaches.

Accordingly, the column is assumed to be progressively removed from the frame and the normal load within this column varies progressively from one appearing under the “normal” design loads to 0 (when the column is completely removed from the frame).

When a column is lost in a frame, the frame can be divided into two parts (illustrated in Figure 3.2, where a column on the 2<sup>nd</sup> floor is lost):

- the directly affected part, which represents the part of the building which is directly affected by the loss of the column, i.e., the beams and the columns which are just above the lost column (in red in Figure 3.2);
- the indirectly affected part, which represents the part of the building which is affected by the forces developing within and influenced by the directly affected part (in blue in Figure 3.2).

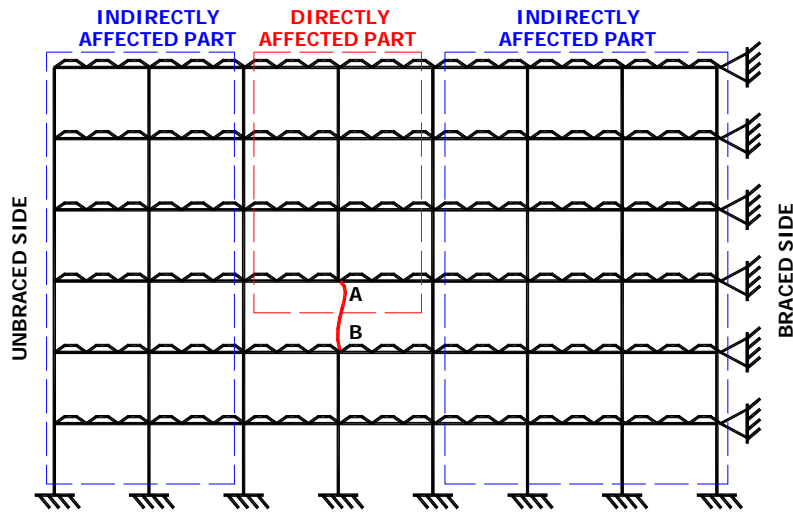


Figure 3.2. Definition of directly and indirectly affected part

### 3.3. COLUMN LOSS SIMULATION

Figure 3.3 represents a frame where the damaged column is column **AB**. Uniformly distributed loads are applied to each beam and column (to simulate design loads such as self-weight, permanent loads, and live loads - see Section 3.2.1 for more). For simplicity's sake, the wind loads are not represented in Figure 3.3.

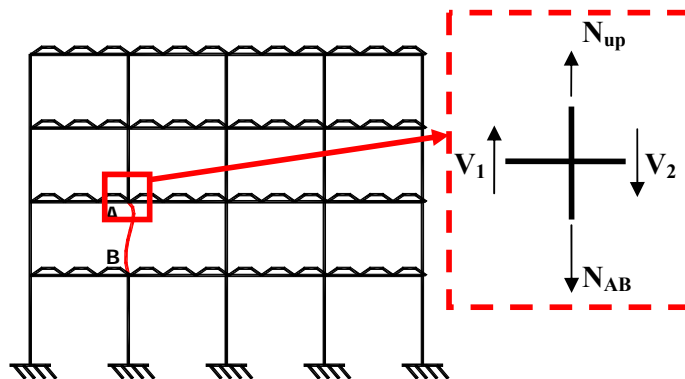


Figure 3.3: Representation of a frame losing a column

In Figure 3.4, the curve representing the evolution of the normal load in column **AB** ( $N_{AB}$ ) according to the vertical displacement at point A is illustrated:

- At point (1), the frame is not loaded; hence,  $N_{AB}$  and  $\Delta_A$  are equal to 0.
- From point (1) to (2) (*Phase 1*), the design loads are progressively applied, i.e. normal loading is applied to the structure; hence,  $N_{AB}$  progressively decreases (as column **AB** is subjected to compression) while  $\Delta_A$  can be assumed to be equal to 0 during this phase. (In reality, there is a small vertical displacement at point A attributable to the compression of the columns below point A.) It is assumed that no yielding appears in the investigated frame during this phase, i.e., the frame remains fully elastic.
- From point (2) to (5), the column progressively disappears. Indeed, from point (2) on, the compression  $N_{AB}$  in column **AB** decreases until it reaches a value equal to 0 (i.e., no more axial loads in the lost column) at point (5) which means that the column can be considered fully destroyed. So, in this zone, the value of  $N_{AB}$  progressively decreases while the value of  $\Delta_A$  increases. This part of the graph is divided into two phases as represented in Figure 3.4:
  - From point (2) to (4) (*Phase 2*): during this phase, the directly affected part passes from fully elastic behavior (from point (2) to (3)) to a plastic mechanism (beam mechanism on each floor of the directly affected part) (at point (4)). At point (3), the first plastic hinges appear in the directly affected part.
  - From point (4) to (5) (*Phase 3*): during this phase, high deformations of the directly affected part are observed and second order effects play an important role. In particular, significant catenary actions develop in the bottom beams of the directly affected part.

It is only possible to pass from point (1) to (5) if:

- the loads which are transferred from the directly affected part to the indirectly affected part do not induce the collapse of elements in the latter (for instance, buckling of the columns or formation of a global plastic mechanism in the indirectly affected part);

- the compression loads appearing in the upper beams of the directly affected part (corresponding to an “arch” effect) do not lead to the buckling of the latter;
- the different structural elements have a sufficient level of ductility to reach the vertical displacement corresponding to point (5).

Also, it is possible that the complete removal of the column is reached (i.e.,  $N_{AB} = 0$ ) before reaching Phase 3.

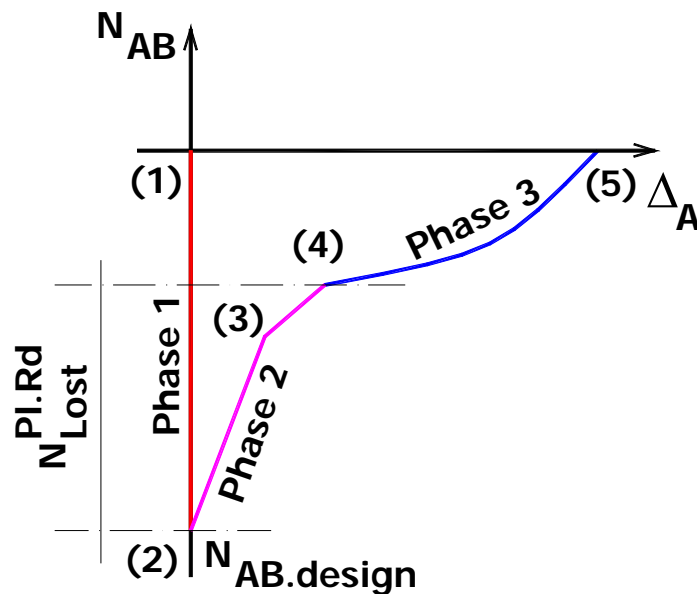


Figure 3.4. Column axial force and Y displacement of the top of a collapsed column

### 3.4. SUMMARY AND CONCLUSIONS

After having examined the descriptions above, the structural nature of the exceptional loss of a column has been highlighted. The nature is described by the loading sequence at a specific point on the frame. From this, a load-carrying curve has been simulated in Figure 3.4. This curve is separated into three phases representing the frame’s behavior: before the loss of a column, removing the column and the catenary action’s development. In fact, as presented in Section 3.3, the behavior of a frame depends on the axial force designed for the damaged column. It is possible, therefore, that the loss of a column does not lead to the catenary action. In the next chapters, this load-carrying curve will be reproduced to clarify future analyses.

**CHAPTER 4: ADOPTED RESEARCH STRATEGY**

## 4.1. INTRODUCTION

This chapter presents a global view of the methodology used in the investigations carried out for this thesis. As such, the chapter begins with an explanation of the research objectives. Specifically, two objectives are presented: understanding a frame's behavior further to the loss of a column and understanding the influence of different parameters on the catenary action. Each objective is briefly discussed to clarify its respective meaning and research requirements. Based on these requirements, a simple flowchart illustrates the plan of investigation, simulation and analytical development discussed in later chapters.

After the description of methodology, a typical frame undergoing the loss of a column is broken down into geometrical zones, with each zone representing a specific part of the frame influenced by this event. The members within each extracted zone are then identified for later investigations. In addition, the frames are categorized according to their structural properties.

The last section provides a general description of the validation procedure which will be used in later chapters to verify the analytical formulae. In fact, the analytical model will be validated by comparing it to numerical simulations. In this case, two FEM tools are used: FINELG and OSSA2D. Thus, a short description of these two programs along with the details of their corresponding finite elements is given in the third section.

## 4.2. RESEARCH METHODOLOGY

### 4.2.1. Objectives – Requirements

The present discussion focuses on two targets for this study, as just introduced. The first target is to understand the frame's behavior in the event of the loss of a column. The second target concentrates on different parameters' influence on the catenary action.

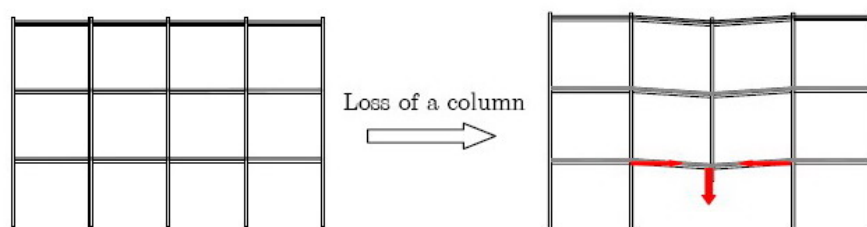


Figure 4.1. Loss of a column in the frame [Demonceau, 2008]



In order to understand the frame's behavior following the loss of a column, the author has divided the problem into three specific points. These three essential points provide the answers to the following questions:

- What defines an external load and how much of one is applied to the frame in such an abnormal event? This question requires a deeper understanding of the exceptional event, in which the nature of its unique physical cause is known. Based on this knowledge, a clear simulation of the extreme load and its impact on the frame can be carried out.
- How are the internal forces distributed within a frame that is lacking a damaged column? The response of any frame, in such an exceptional event, depends strictly on the cause. Many parameters influence the possible scenarios following the event. A general demonstration of the frame's behavior, which includes systematized parameters, is represented by the internal forces' flow within the frame. The alternative load path, which is obtained from this flow, will render the frame capable of surviving.
- Where are the most dangerous positions/members on the frame? Also, how much force is to be withstood by those positions/members? To maintain the alternative load path, the members which compose it have to have the ability to support the additional load and to bridge over the damage. The details of this path's working state provide the information necessary to the engineer for making appropriate decisions.

The second objective relates to Demonceau's investigations on the catenary action. According to Hamburger and Whitaker (2002), designing a structure in which the catenary action could function is a key to the building's survival in an abnormal situation.

As mentioned before, the catenary action is defined as the nonlinear behavior of two connected beams losing a middle support. The displacement of the un-supported point rapidly increases. Then, a second-order effect develops and a significant axial force appears in the beam section.

Obviously, the catenary behavior of the beam is influenced by surrounding structures. Thus the second objective of this thesis is to estimate the nature and degree of these influences.

### 4.2.2. Investigations during the loading process

This section describes the investigative process used to examine a frame which has undergone the loss of a column. The phases in this event are listed along the load-carrying curve which has been shown earlier in Figure 3.4. For simplicity's sake, this figure is reproduced below.

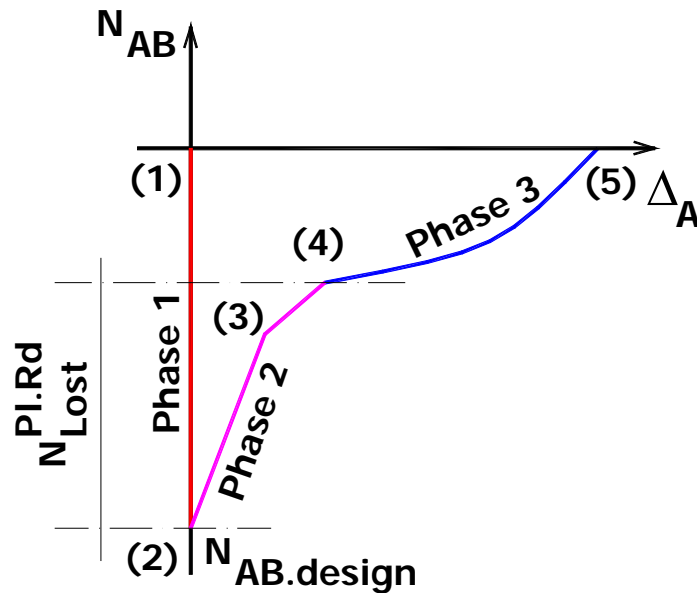


Figure 3.4. Column axial force and Y displacement of the top of a collapsed column

#### 4.2.2.a. Investigation of Phase 1 and 2

As previously mentioned, Phase 1 represents the application of the normal design loads (such as self weight, permanent loads, live loads, or snow) to the frame under investigation. During this phase, the column to be lost is replaced by a pair of loads, as illustrated in Figure 4.2, which are equal to the normal loads  $N_{AB,design}$  appearing in the column under the normal design loads; this is only possible because, as said in the previous section, the frame is assumed to remain fully elastic during this phase. So, this phase can be divided into two loading phases: one where the design loads are applied to the frame and the column to be lost is removed (case 1 in Figure 4.2) and one where the pair of loads corresponding to the column to be lost are applied to the frame at points A and B (phase 2 in Figure 4.2).

As illustrated in Figure 4.2, Phase 2 is divided into two parts: one part where the frame remains fully elastic (from point (2) to (3)) and one part where plastic hinges develop in

the directly affected part (from point (3) to (4)). At the end of Phase 2, a fully plastic mechanism is formed in the directly affected part. During Phase 2, a pair of concentrated loads called  $N_{lost}$  (case 3 in Figure 4.2) are applied at points **A** and **B** in the opposite direction to the ones defined in the previous phase (case 2 in Figure 4.2); so, these loads are increased from zero to the value of normal load  $N_{AB,design}$  appearing under the normal design loads. Thus, during Phase 2,

$$N_{AB} = N_{AB,design} - N_{lost}. \quad (4.1)$$

Physically, this process simulates the removal of the column. When this column disappears, the pairs of beams on each side of the lost column work as one beam with a span equal to the sum of their own span and a beam plastic mechanism forms in the so-defined beam when point (4) is reached.

To investigate this behavior during Phases 1 and 2, elastic – perfectly plastic analyses taking account of the second order effects are performed; the loading of the frame considered is the one presented in Figure 4.2, i.e. the sum of the two load phases previously described.

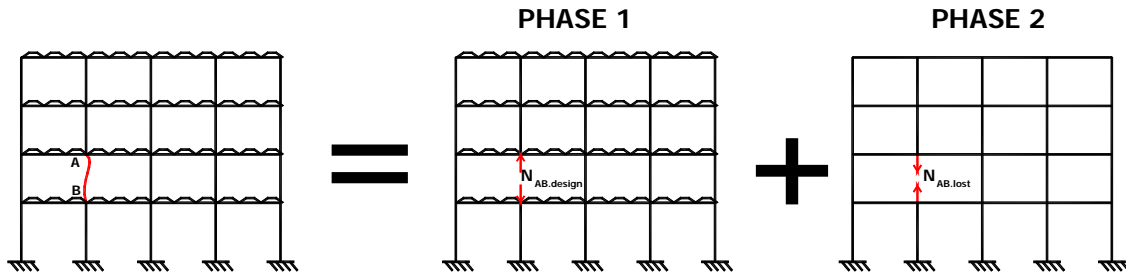


Figure 4.2. Division of the frame loading (when a column is lost) in 2 load phases

#### 4.2.2.b. Investigation of Phase 3

In this phase, a plastic mechanism is created in the directly affected part and the vertical displacement at point **A** rapidly increases. The consequence of this is that the second-order effects developing in the directly affected part become significant. In particular, membrane forces develop in the bottom beams of the directly affected part.

Through parametrical studies performed on thousands of frames, it has been shown that the membrane forces developing in the beams of the floor just above the column lost are significantly higher than the ones developing in the other beams, as illustrated in Figure

4.3. The columns, which are on both sides of the directly affected part, bend and produce compression on the top beams.

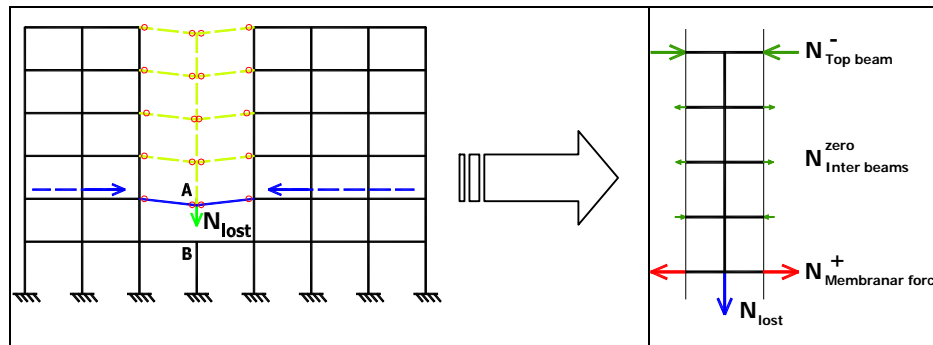


Figure 4.3. Distribution of the membrane forces developing in the directly affected part. Consequently, it was decided to investigate the behavior of this floor which represents the response of the frame in such a load phase. In order to investigate the extension of frame capacity by activating the catenary action, the bottom beams are extracted from the frame in the three following levels of extraction: frame level, substructure level and isolated membrane beam level. This section presents only a brief description of the three-level simulation which was carried out. In the next chapters, this simulation will be discussed more in depth.

At the frame level, the frame's response to an unusual loss of a column is simulated by the reduction of the whole building to the 2D frame and the definition of the abnormal load as presented in Figure 4.2. This external load breakdown will be demonstrated in Chapter 5. From the investigation results done at this level, the full scale distribution of the internal forces is obtained. Along with the internal forces' flow within the frame, it can be pointed out that the directly affected part mainly represents the response of the frame, especially in Load Phase 3.

The second level, which is called the substructure/subsystem level, involves the extraction of the directly affected part to create a substructure model. The extraction includes two procedures: simplifying the part members and creating the equivalent boundary conditions. Once this appropriate substructure is developed, its behavior will represent the response of the frame to the exceptional event.

Especially in load Phase 3, after the directly affected part fully yields, catenary action is activated in the bottom beams. Since the other members of the part cannot support the load, this beam's behavior represents the behavior of the part, and likewise, of the frame. So, in load Phase 3, the investigation is done at the isolated equivalent beam's level.

The full 3-level extraction procedure is demonstrated in Figure 4.4

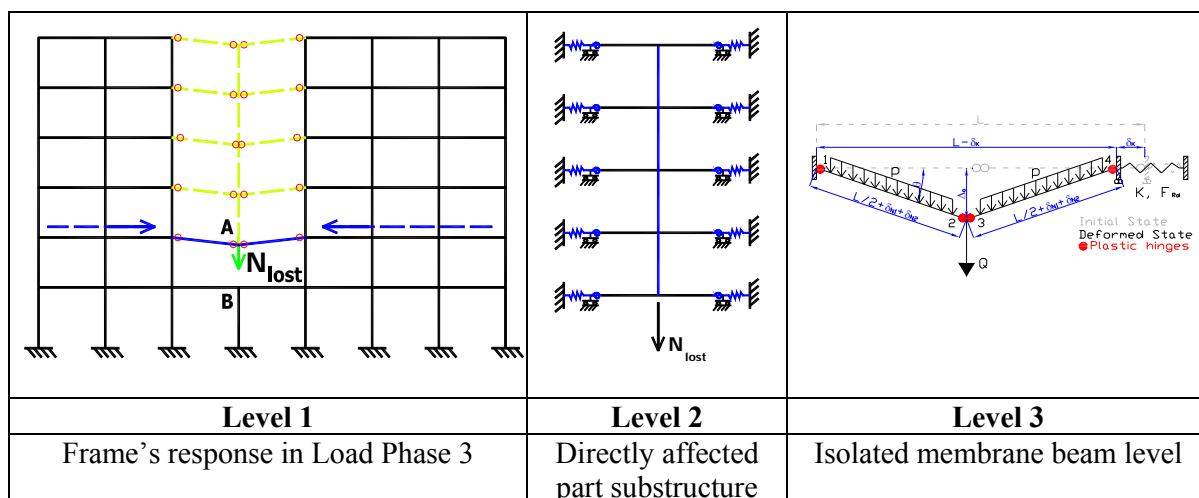


Figure 4.4. The 3-levels extraction

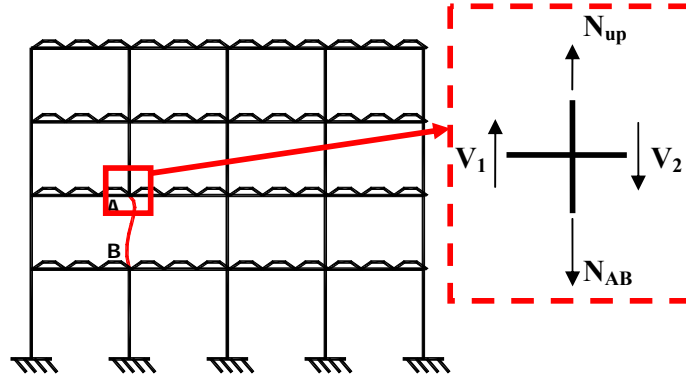
As presented in Chapter 2, the investigation of this level was performed by Demonceau in his companion study at the University of Liege. As a complement to his work, this thesis investigates the frame's behavior and substructure model in order to provide the parameters necessary for Demonceau's study. The resulting analytical model is demonstrated in Figure 4.5.b.

The validity of the simplified subsystem and isolated beam modeling has been illustrated through numerical investigations showing that the answer obtained by this simulation is in good agreement with the one obtained by the full frame modeling [Demonceau, 2008].

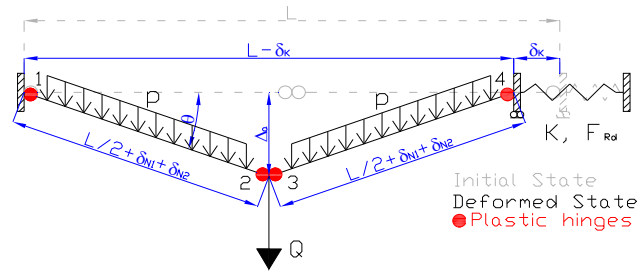
To be able to isolate the subsystem represented in Figure 4.5, certain parameters have to be defined:

- the lateral restraint  $K$ , which represents the lateral stiffness of the indirectly affected part when the membrane forces develop in the directly affected part;
- the resistance  $F_{Rd}$  of the indirectly affected part, i.e. the maximum horizontal load coming from the directly affected part that the indirectly affected part can sustain;
- the load  $Q$  that the system has to support.

Thus, the parameters  $K$  and  $F_{Rd}$  are properties of the indirectly affected part which will influence the development of the membrane forces in the beams.



a) Equilibrium of forces at damaged column's top point



b) Simplified substructure simulating the behavior of the frame during Phase 3

Figure 4.5. Simplified subsystem

In Figure 4.5, it can be observed that the only load transferred to the subsystem is a concentrated load  $Q$ . Indeed, when the beam's plastic mechanism is formed, the only additional load to be supported is a concentrated one owing to the column loss which can be defined according to the internal loads defined in Figure 4.5.a. This concentrated load  $Q$  is equal to the difference between the axial load appearing in the upper column ( $N_{up}$ ) and the axial load in the lower column ( $N_{AB}$ ), i.e. in the lost column. When the column is fully removed, the value of  $Q$  to be supported is equal to the normal load coming from the upper column,  $N_{up}$ .

$$Q = N_{up} - N_{AB} \quad (4.2)$$

To investigate the behavior of the subsystem, a second-order rigid-plastic analysis has been performed. The effect of the development of the membrane forces on the plastic hinges is included in the procedure. This model investigation was performed by Demonceau, whose thesis was successfully defended in 2008.

### 4.3. TYPES OF STRUCTURAL FRAME SYSTEMS

This section presents a demonstration of building frame categories. The full 3-D frame is investigated through the 2-D frame according to the principle in Eurocode 4. In fact, there are many types of regular building frames. They include the sway frame, the middle braced frames, the single-side braced frames, and the fully braced frames. As concerns the methodology of this investigation, the frame is categorized according to the position of the damaged column and the part of the frame which includes that damage.

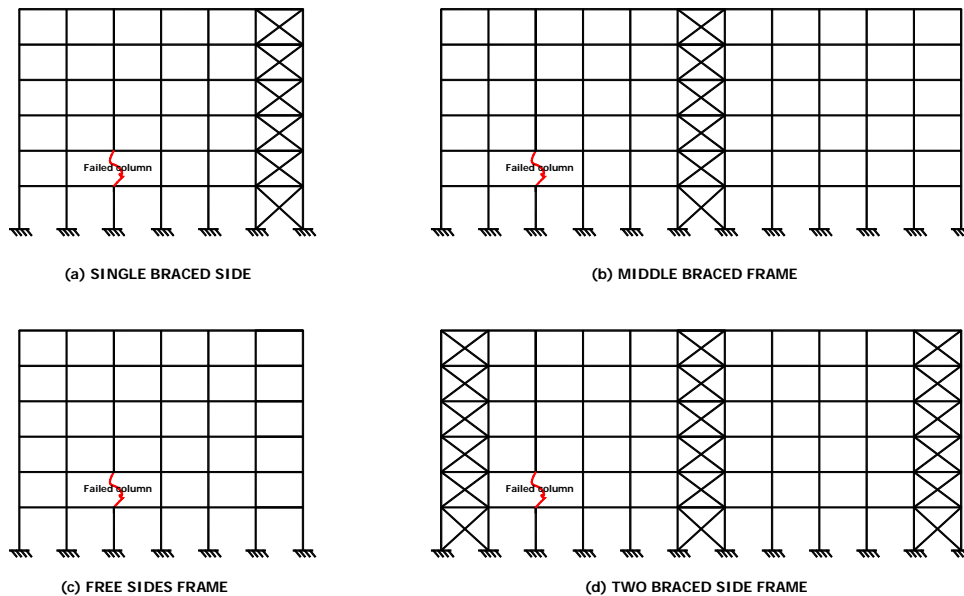


Figure 4.6. The types of frames: (a) Side braced frame (b) Middle braced frame  
(c) Sway frame (d) Fully braced frame

In fact, when the brace is within the frame, the internal forces cannot transfer through it. Thus, the frame being investigated is simplified to only the injured part, while the undamaged part is not taken into account. The brace is replaced by fixed hinges at the end of the beams. To illustrate this, the investigated models are shown below. For obvious reasons, the sway frame is modeled as is.

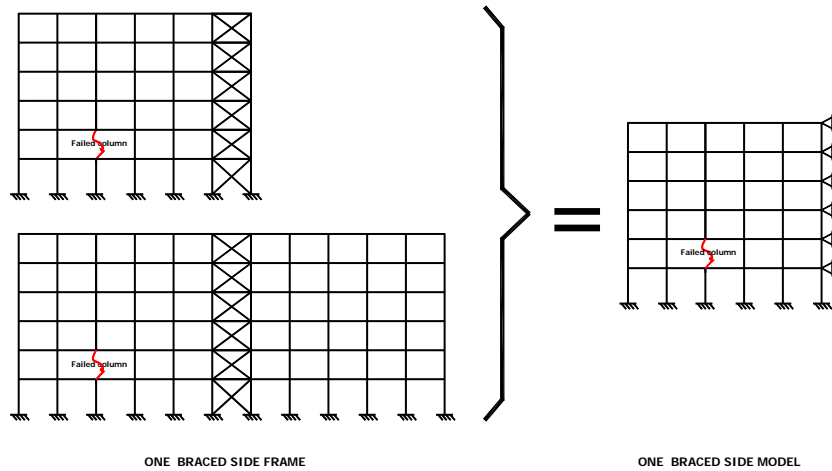


Figure 4.7. The single and middle braced frames simplified to a one braced side model

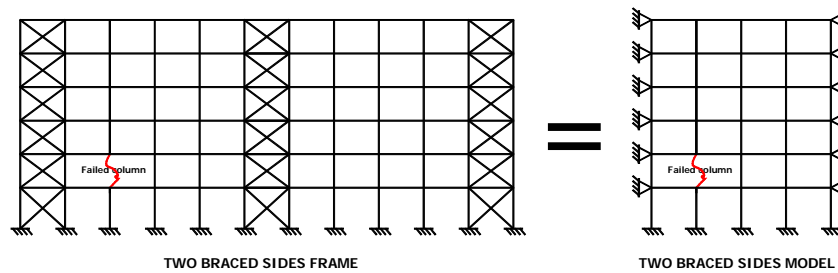


Figure 4.8. The fully braced frame becomes a two braced side model

#### 4.4. IDENTIFICATION OF THE FRAME ZONES AND THEIR RESPECTIVE BEHAVIOR

The present section describes the zones of a typical frame identified in relation to the position of the damaged column. To illustrate this division, Figure 4.9 presents a sway frame in which the 3<sup>rd</sup> column on the 2<sup>nd</sup> floor is destroyed.

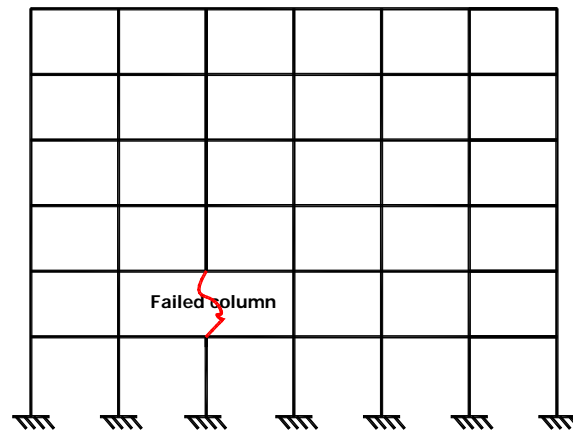


Figure 4.9. A typical frame with a lost column

The frame is divided into five separate parts: the directly affected zone, the two



neighboring column zones, the damaged levels on the left and right, the outside blocks, and the lower level. The zones are identified by their behavior. Obviously, the frame's components' behavior is influenced by the damage's position. As such, some components are simultaneously included in different zones due to their specific behavior. These zones are demonstrated in Figure 4.10.

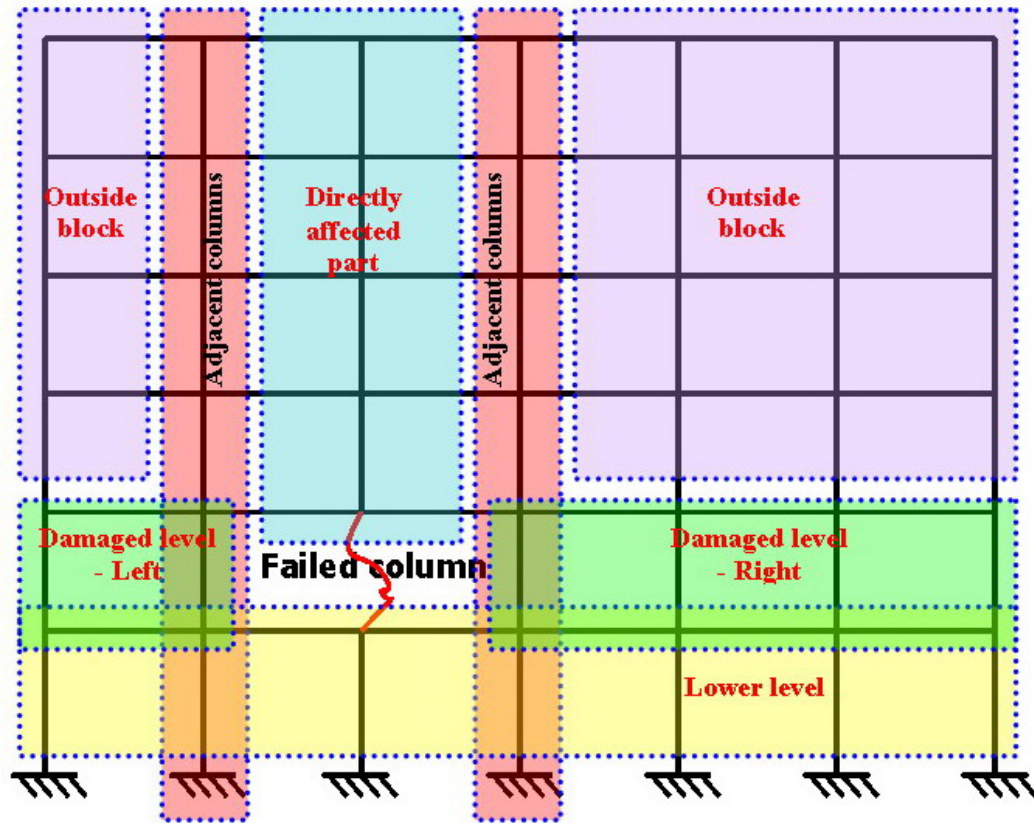


Figure 4.10. Separating the frame zones

#### 4.4.1. Directly affected part

The first zone to be investigated below is the zone within the blue rectangle. As the name suggests, this zone's behavior is directly affected by the loss of the column. The components in this zone are separated into two groups: beam group and column group.

The *beam group* includes the beams which are above the damaged column. Therefore, those beams lose their supports following the event. Instead of each beam working in the normal condition, on each floor, two beams are connected to combine one larger beam whose length is equal to the length of two beams. It will be referred to as the *equivalent beam* from now on.

Based on the position and level of the equivalent beams in relation to the damaged column, each beam is identified as the *bottom beam*, the *intermediate beam* and the *top beam*. The membrane effect develops at the beams directly above the damaged column; thus, the bottom beam is called the membrane beam.

The *column group* includes the columns which connect equivalent beams at the middle point. These are called the middle columns and are numbered from bottom to top. The lowest one is called the bottom column, and the highest one is the top column. With these connections provided by the columns, all equivalent beams work together. This zone is colored as the dashed green line in Figure 4.11.

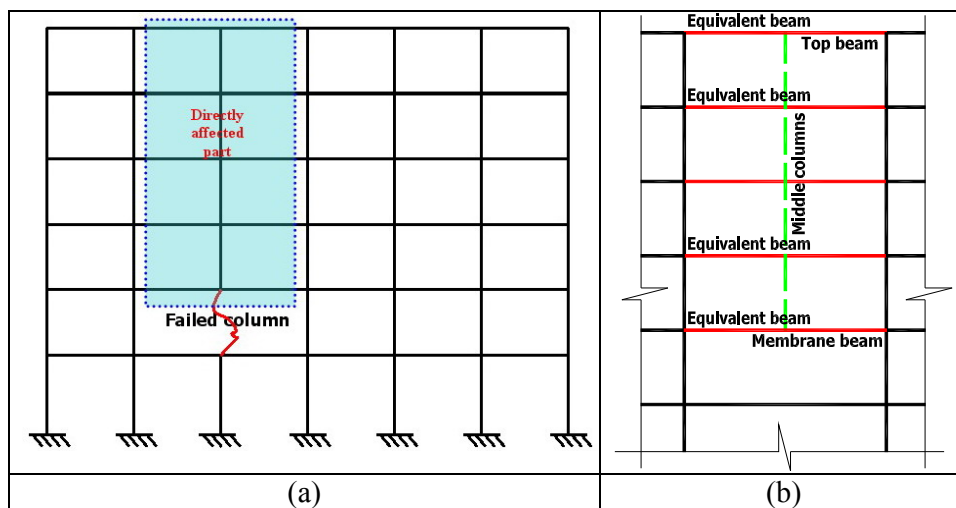


Figure 4.11. Directly affected zone (a) and its components (b)

#### 4.4.2. Damaged level

This zone is defined by a light green rectangle in Figures 4.10 and 4.12.a. It has been divided into two parts: the left side and the right side. The members' names and positions on the right side are represented in Figure 4.12.b. (The right side's members are identified in the same way as the left side's members.) The damaged level includes columns on the same floor as the destroyed column, as well as the beams above and below the column.

With regards to the columns, they are identified by their positions in relation to the damaged column. From the external to internal positions, they are named the *outside column* (or *side column*), the *inner column* and the column next to the destroyed column – the *column beside*. The inner columns are numbered from right to left, as illustrated in Figure 4.12.b.

In addition, the beams connecting the columns' top points are called Top Beam 1, Top Beam 2, etc, from right to left. The bottom beams are identified in the same way.

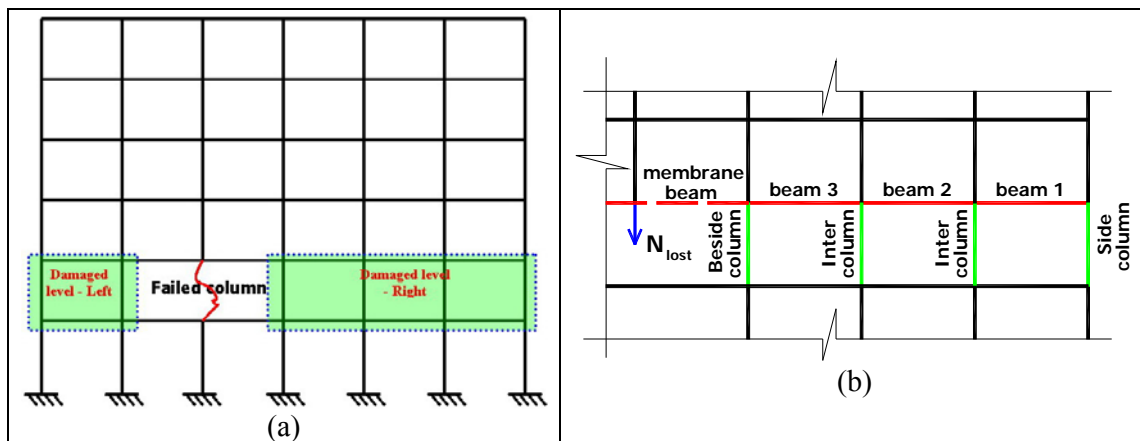


Figure 4.12. The frame and zone border investigated (a) and member's names and positions (b)

#### 4.4.3. Neighboring columns

Neighboring or adjacent column zones include the columns which are placed at the end of the equivalent beams on both sides. In fact, the directly affected part supporting the load transfers this load to the columns at the ends of the beams. These columns are represented by two red rectangles in Figure 4.13. This zone is the principal part of the alternative load path, which will be discussed in further detail in Chapter 5.

Figure 4.13.b illustrates the position of columns and their names. The special column position – the *beside column* – is identified at the end of the membrane beam. This column is also included in the damaged level zone. It has been proved as the most important key element on both Load Phases 2 and 3.

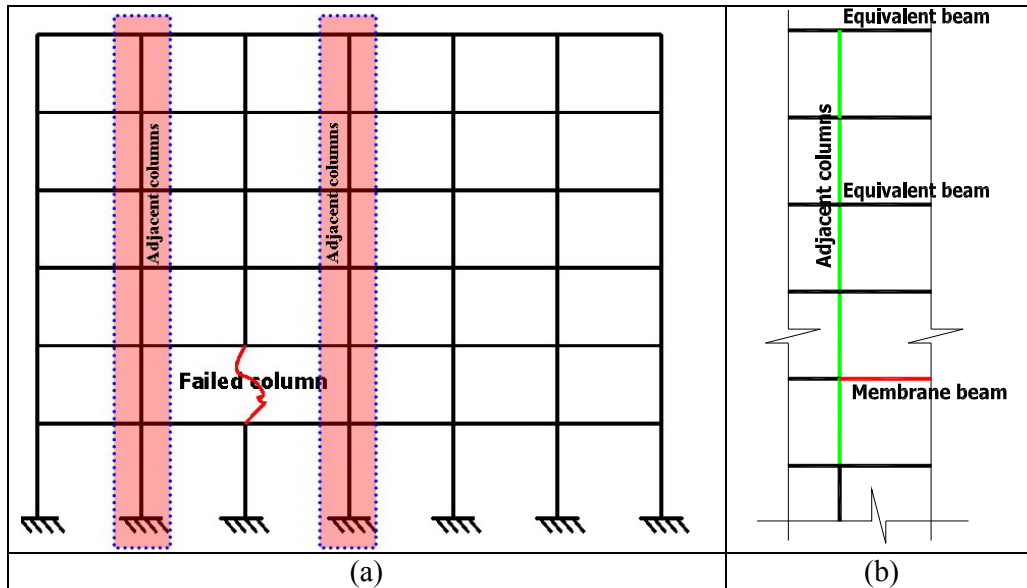


Figure 4.13: Neighboring column zones (a) and the members on the left (b)

#### 4.4.4. Lower level and outside blocks

Next, the remaining two zones – *lower level* and *outside blocks* – are described in this section. The former includes the elements which are situated lower than the damaged column. They are drawn within the yellow rectangle in Figure 4.14.a.

The latter is the *outside block*. It is defined in Figure 4.14.b by the violet rectangle. In fact, this zone is virtually unaffected by the loss of the column.

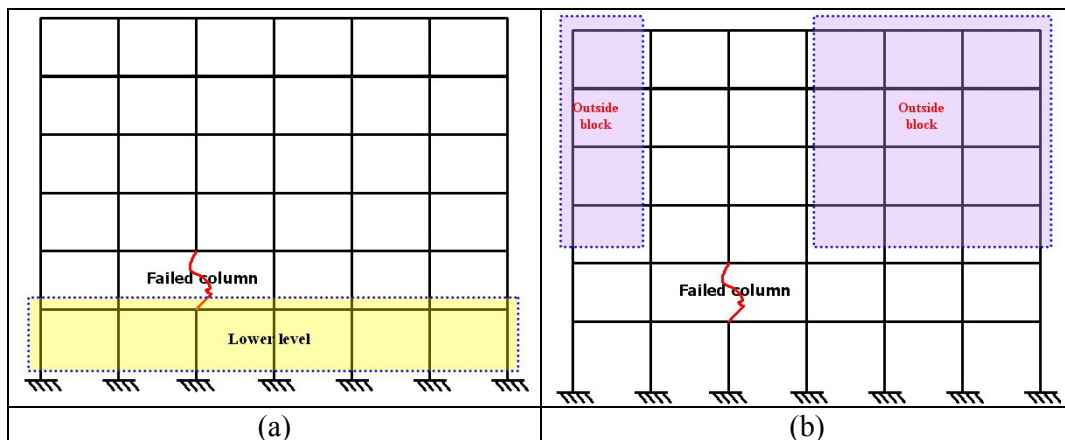


Figure 4.14: Lower level (a) and outside blocks (b)

### 4.5. NUMERICAL TOOLS USED FOR FURTHER VALIDATIONS

This section introduces the validation approaches for later analytical simulations and the

numerical tools used. Also, Level 1 and Level 2 are described in systematic detail, namely regarding the validation procedures which correspond to the simulation steps.

#### 4.5.1. Multilevel validation method

The full 3-level extraction procedure, which is demonstrated in Figure 4.4, is repeated below to illustrate the creation of the substructure model and its validation approaches.

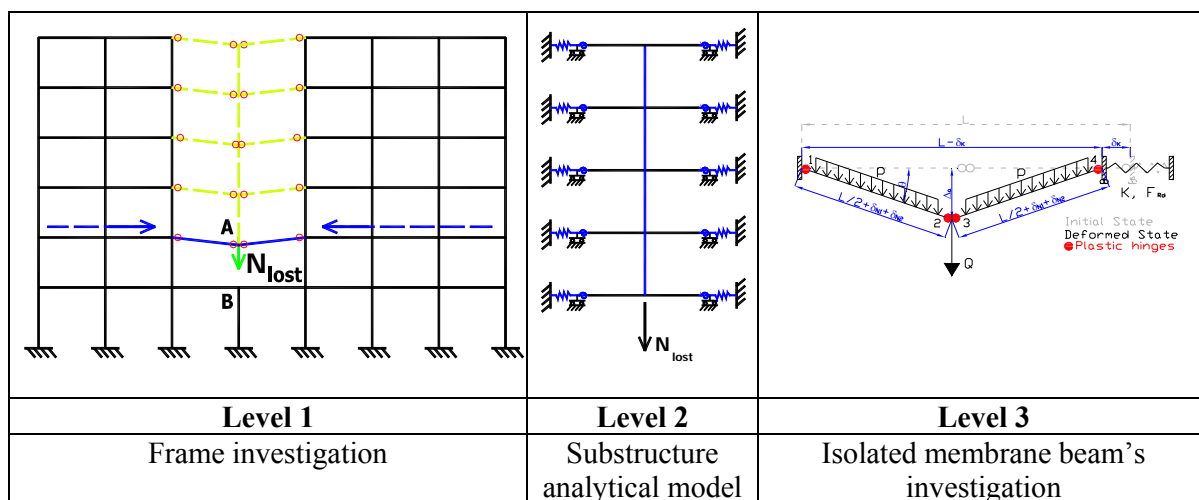


Figure 4.4. The 3-levels extraction

As discussed in Section 4.2.2.b, Demonceau's research and that of the author were performed as a three-level extraction. Levels 1 and 2 are covered in the present work, while Level 3 was examined by Demonceau. So, this section describes the procedure for investigating the frame response in Levels 1 and 2 at the frame level and the substructure level.

In the *frame level*, according to the loading process defined in Chapter 3, the frame was first simulated using numerical tools. The tools used are two finite element programs: OSSA2D and FINELG. They will be presented in the next section. Then, full-scale linear and nonlinear investigations were carried out on the frame supporting normal and abnormal loads. Next, parametrical investigations were performed which focused on the distribution of internal forces within the frame throughout the accidental event. Finally, the load transfer flow was drawn out, which defined the alternative load path developed in such an abnormal situation. Thus, the structural members which influence the frame's behavior were identified.

In the *substructure level*, the extracted substructure was simulated by a simplified analytical model. Firstly, from the parametrical investigation, the influences of the surrounding structure on the isolated member were recorded. They have been defined by the boundary conditions of the individual member and by the specific load applied to it.

Next, in the second step, the analytical behavior of the individual member was simulated and simplified in order to create a more manageable analytical formula.

In the last step, the individual members were assembled according to conditions of continuity. These conditions were also simplified, forming the practical model.

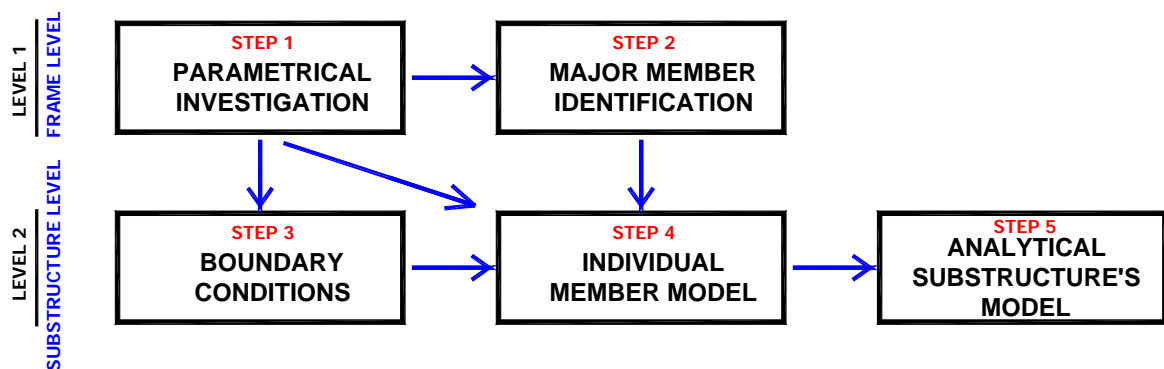


Figure 4.15. The procedures for building the analytical substructure model

Then, three separate validations were performed:

- The validation of the single member boundary condition.
- The validation of the single model simulation.
- Last, but most importantly, the validation of the simplified zone model.

The validation process has been applied to each step of the analytical simulation according to the procedure demonstrated above. So, the next section provides a short description of two numerical tools which were used in the validation process.

#### 4.5.2. Numerical tools

The first software used for this purpose was FINELG, a non-linear finite element program that has been developed for decades at the MS<sup>2</sup>F Department, ArGenCo, University of Liege. The computer program FINELG is a finite element program used to solve

- geometrically and materially nonlinear solid or structural problems under static dead loads;

- linear and nonlinear instability problems, leading to buckling loads and instability modes by an eigenvalue computation;
- dynamic problems, leading to eigen frequencies and vibration modes taking account, or not, of the internal stresses.

The 2-node classic plane beam element number 33 was used to model the 2-D frames investigated. Each node has 3 degrees of freedom ( $u$ ,  $v$  and  $\theta$  - see Figure 4.16). Plasticity and residual stress could be considered for any cross section. However, residual stress was not included in this work in light of the author's aim of understanding the global behavior of the frame, not local problems. Non-linear bending springs could be applied to the node along the  $\theta$  direction.

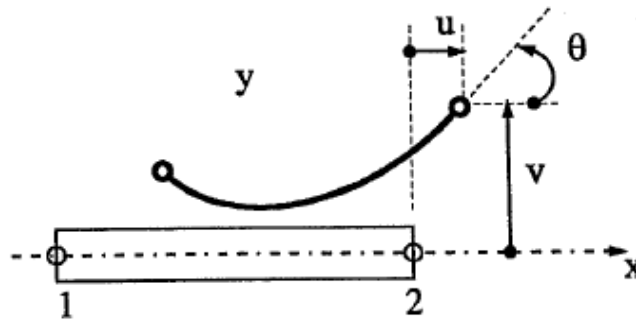


Figure 4.16. Classic beam element used in FINELG and OSSA2D [*Finelg manual*]  
 With this type of element, a linear law (Hooke's law) is used for elastic analyses and a bilinear one for non-linear analyses (Figure 4.17).

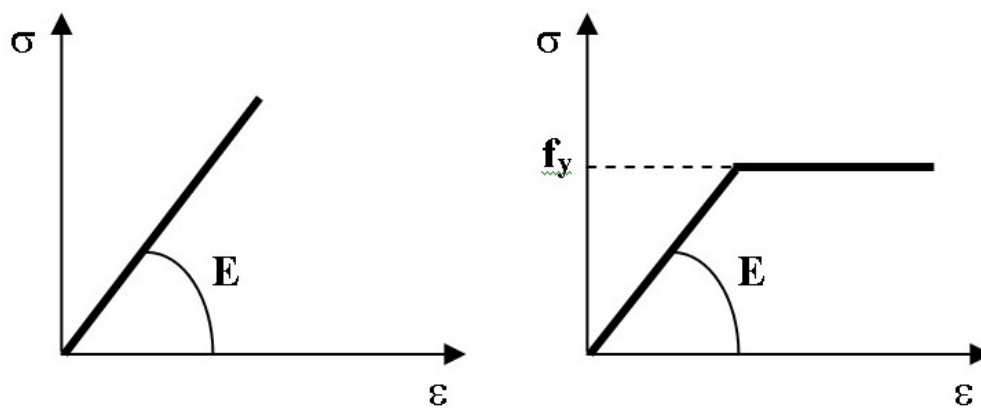


Figure 4.17. Linear and bi-linear behavior laws applied to the calculation  
 For simpler numerical simulations, such as single member validation or frame response in elastic ranges, the other FEM software, OSSA2D, is used.

OSSA2D is a program for linear elastic analysis using the method of displacements applied to plane structures formed by beams and bars. Those members are connected by rigid, hinge or semi-rigid connections, and many types of loads can be applied to the structure. The program's objective is to predict a frame's mechanical behavior quickly to engineers.

Unlike the FINELG program described above, OSSA2D's limits in elastic and geometric second-order analyses of plane frames are well suited to our purposes. The main element used in OSSA2D is the 2D classic beam element.

#### **4.6. SUMMARY AND CONCLUSIONS**

The current chapter focuses on an overview of the methodology employed in this work. For the sake of simplification, and since processing details will be described in the next chapters, each section has been limited only to brief descriptions of these methods.

Based on the geometrical identifications in Section 4.4, the next chapters will describe the investigation and the development of the physical aspect to ensure the validity of final analytical models. Continuity and compatibility between frame zones will also be compared in the related chapters.



**CHAPTER 5: IMPLEMENTATION OF  
THE ALTERNATIVE LOAD PATHS METHOD**

5.1. INTRODUCTION

The previous chapter presented the strategy adopted to develop an assessment of a building’s structural robustness. The capacity of the frame was studied through the investigation of the substructure and, moreover, by isolating the key membrane beam. The full 3-level extraction of the research has been discussed and is repeated below in Figure 4.4. These levels consist of the frame investigation, substructure model and isolated beam model. In this thesis, Levels 1 and 2 are analyzed to develop the substructure model as described in Section 4.2.

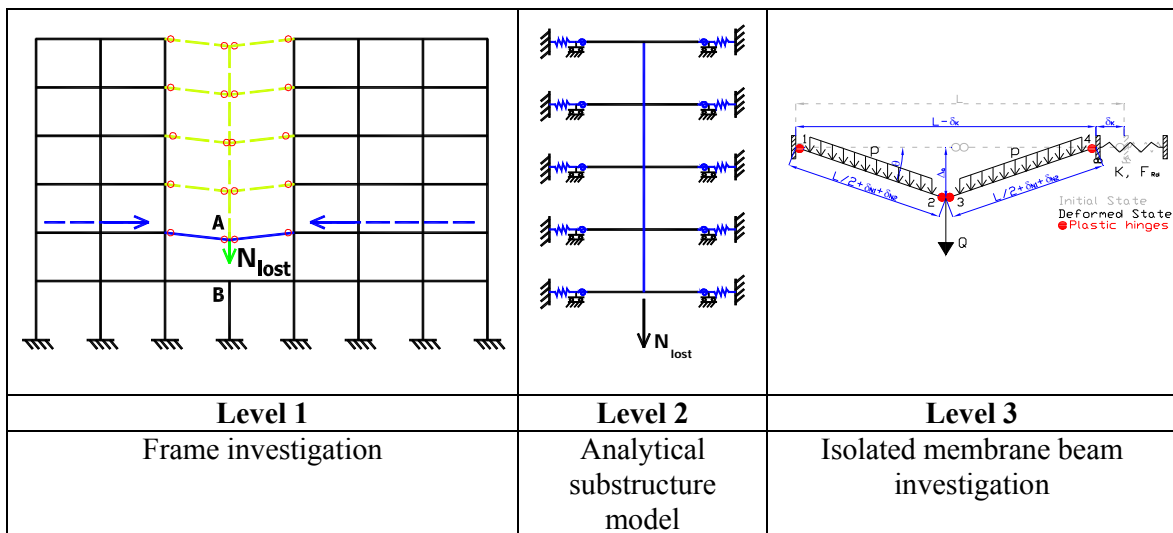


Figure 4.4. The 3 levels of extraction

This chapter concentrates on Level 1 (the *frame investigation*), seen here in Figure 4.4. To be exact, the frame investigation refers to the study of a frame undergoing the exceptional loss of a column. These results have been parameterized to isolate the flow of internal forces within the frame. The substructure will be developed based on that knowledge in Level 2, which involves the development of the *substructure model*. With this aim in mind, Level 1 is divided into two parts: parametrical analyses of the frame’s behavior and identification of the principal member. This level has been broadly discussed in Section 4.5.1 and reviewed in more detail in Figure 4.15 (reproduced below).

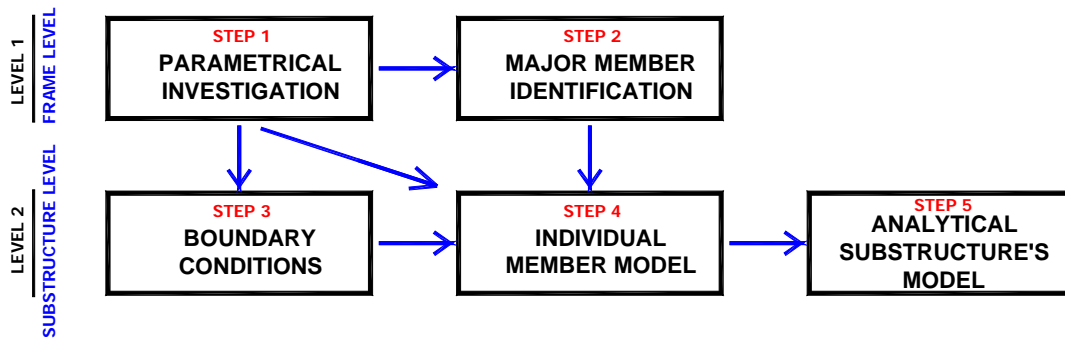


Figure 4.15. The procedures for building the analytical substructure model

In this chapter, the numerical analyses conducted on frames to simulate the loss of a column are presented. The results obtained are then used to predict the redundancy of the investigated frames. In particular, the following aspects are studied in detail: definition of the loads, distribution of internal forces, identification of the alternative load path and identification of critical zones.

The definition of loads concerns the detection of additional loads that the frame has to support when the column loss occurs. The knowledge of the internal force distribution helps to understand how these additional loads to be supported are transferred to the foundation within the structure. The members activated in this way constitute the alternative load path. Through the identification of the alternative load path, it is finally possible to identify the critical zones; in particular, continuity between the structural elements involved in the alternative load path has to be ensured.

In Sections 5.2 and 5.3, the investigations conducted on these aspects are presented.

## 5.2. ADDITIONAL LOADS RELATED TO THE LOSS OF A COLUMN

### 5.2.2. Definition of the initial and residual states

The exceptional event is illustrated in Figure 3.4, representing the evolution of the axial load within the lost column according to the vertical displacement at the top of this column; this figure is reproduced below.

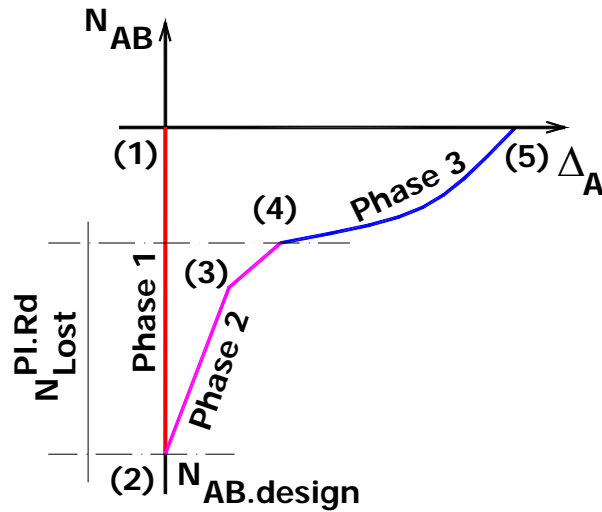


Figure 3.4. Column axial force and Y displacement of the top of a collapsed column

This section describes in greater detail the difference between two states: the initial state, i.e. the state of the structure before the loss of the column, and the residual state, i.e. the state of the structure when the column is lost. In this way, this chapter's investigation of the frame level aims to identify the alternative load path which appears in the frame after the damage is sustained.

In the frame's initial state, the loads to be supported are the conventional ones as defined in the codes and standards. When combined with appropriate safety factors, they are used to check serviceability and the ultimate limit states. In the analyses carried out, the column to be lost is replaced by equivalent loads reflecting the internal forces found within the lost column when the structure is subjected to conventional loads, as illustrated in Figure 5.1. For simplicity's sake, only the equivalent axial loads will be reported in the following figures.

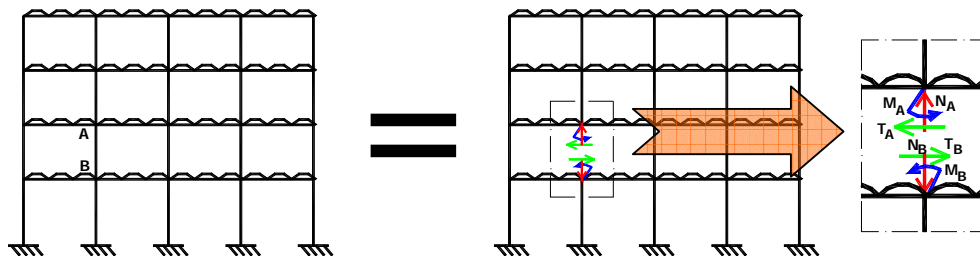


Figure 5.1. Frame in the initial state

After the column loss due to an exceptional event, the remaining structure is in its *residual* state. To pass from the initial to the residual state, the applied loads are assumed to constant, i.e. only the structural system is modified to pass from the initial to the residual

state. With the assumption of a progressive removal of the column, the axial load in the lost column is progressively reduced from the design value, i.e. its value in the initial state, to zero. As illustrated in Figure 5.2, two loading sequences have been defined to pass from the initial to the residual state.

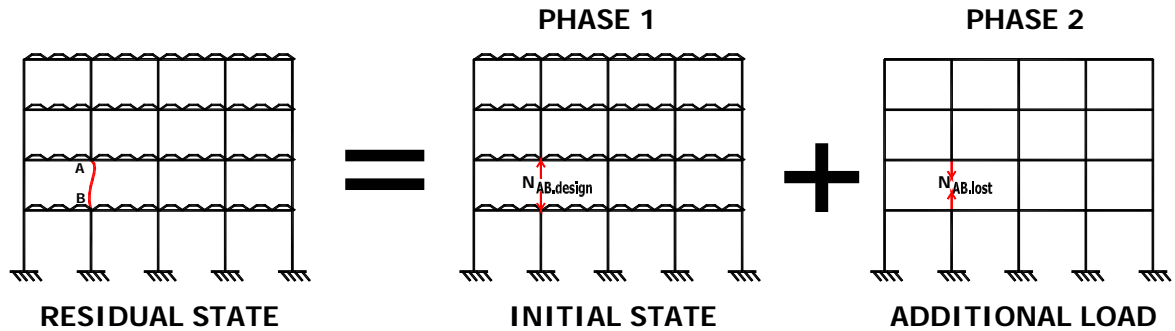


Figure 5.2. Identification of two loading sequences

Accordingly, the evolution of the loads when passing from the initial state to the residual state is linked to the evolution of the loads associated with the column loss. These loads are concentrated forces applied at the top and at the bottom of the lost column in the direction opposite to the column’s internal forces in the initial state, named  $N_{AB,design}$ . The value of the loads associated with the column loss, named  $N_{AB,lost}$ , is as follows:

$$0 \leq N_{AB,lost} \leq N_{AB,design} \quad (5.1)$$

(For clarity’s sake, the load  $N_{AB,lost}$  will be referred to simply as  $N_{lost}$  in the following paragraphs.) Within the structure, the alternative load path is activated by the onset of  $N_{lost}$ .

### 5.2.2. Definition of extension of the localized damage

As previously defined, *progressive collapse* denotes an extensive structural failure initiated by local structural damage, or a chain reaction of failures following damage to a relatively small portion of a structure. It occurs when, because of damage sustained, a loading pattern or a structural configuration changes and leads to a residual structure seeking an *alternative load path* in order to redistribute the *abnormal* load applied. Then, another structural member fails due to this load redistribution. Finally, the evolution of the damage continues until a global collapse occurs.

According to this definition, a progressive collapse starts from the initial localized failure and then extends to a secondary one. The scale of damage spreads until most of the structural members collapse. In this section, the term “extension of the localized damage” defines this spreading. Therefore, in the following discussions, after a column is lost, the

progressive collapse is *confirmed* when another structural member fails.

With this reduction of the definition of progressive collapse, the objective of the present thesis is likewise narrowed to identifying the first alternative load path which appears in the frame immediately after the event. This means that this study does not investigate the possible case where the frame could find a new load path after the first alternative load path has failed. In that case, the frame collapses.

### 5.3. ALTERNATIVE LOAD PATHS

When the exceptional event occurs, the structure looks for an alternative load path to transfer the additional loads to the foundation. The alternative load path exists so long as the structure is able to withstand the additional loads acting on it.

#### 5.3.1. Damaged column positions

In the present thesis, the exceptional event resulting in the loss of a column is under investigation; logically, the frame response following this event is a function of the position of the damaged column. For classification purposes, the position of the damaged column considered in the present analyses is identified as follows: the columns are numbered from left to right with Arabic numerals and from bottom to top (according to the floor under consideration) with Roman numerals. Consequently, the position of the damaged column is identified by a pair of numbers; for instance, column II-4 is the fourth column from the left and on the second floor of the structure studied, as illustrated in Figure 5.3.

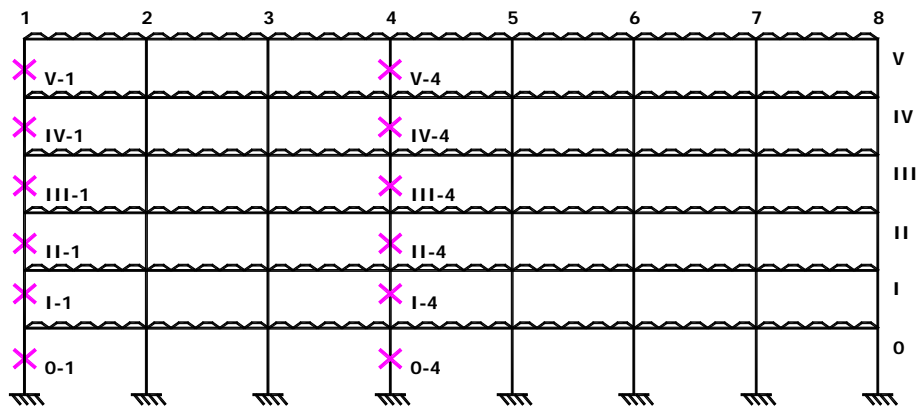


Figure 5.3. Identification of the position of the columns

The columns within the frame can also be divided into two groups: external and internal ones. In Figure 5.3, the series of columns with the second position number equal to 1 are the external columns while the series of columns with the second position number equal to 4 are internal ones. It is important that these two specific groups be identified, as the development of alternative load paths differs strongly according to whether the damaged column is part of one group or another.

### 5.3.2. Alternative load path and chain of elements

According to Section 5.2.2, the study of a frame losing a column is mainly linked to the investigation of the structure subjected to the additional loads associated with that column loss,  $N_{lost}$  (see Figure 5.2). The alternative load path provides a way to transfer these additional loads to the foundation. This section briefly describes the behavior of the structure subjected to these additional loads.

Through roughly a hundred numerical simulations of steel frames performed with OSSA2D and FINELG, the global behavior of these frames was investigated when a column is fully removed and when the frame is subjected to the additional loads  $N_{lost}$  only. In Figure 5.4, diagrams of typical distributions of internal forces within an investigated frame are given.

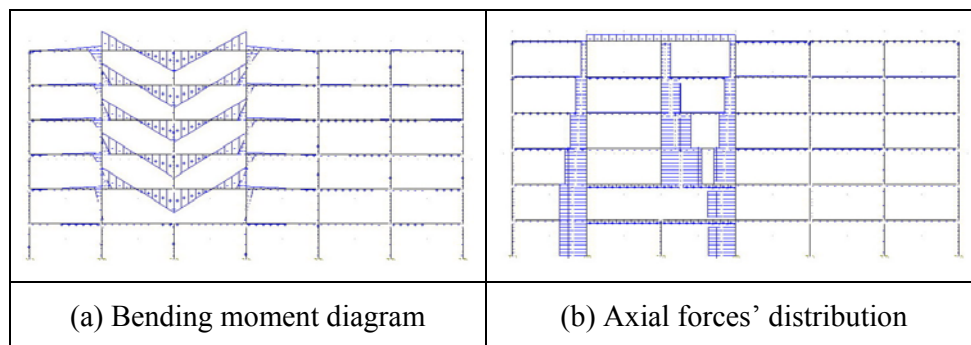


Figure 5.4. Distribution of internal forces in an investigated frame when only additional load applied and in elastic 1<sup>st</sup> order range

Figure 5.5 presents the path followed by the internal forces when the additional forces  $N_{lost}$  are applied. In this situation, the directly affected part supports the loads as a hanging system. Recall that the directly affected part is composed of the columns just above the lost column and the beams linking these columns to the indirectly affected part. The columns above the lost column work as tension members and the supported tensile loads are transmitted to the indirectly affected part through the beams of the directly affected part.

Thanks to the numerical analyses performed, it can be observed that the greater part of the loads travels vertically toward the foundation through the columns next to the directly affected part, as illustrated in Figure 5.5.

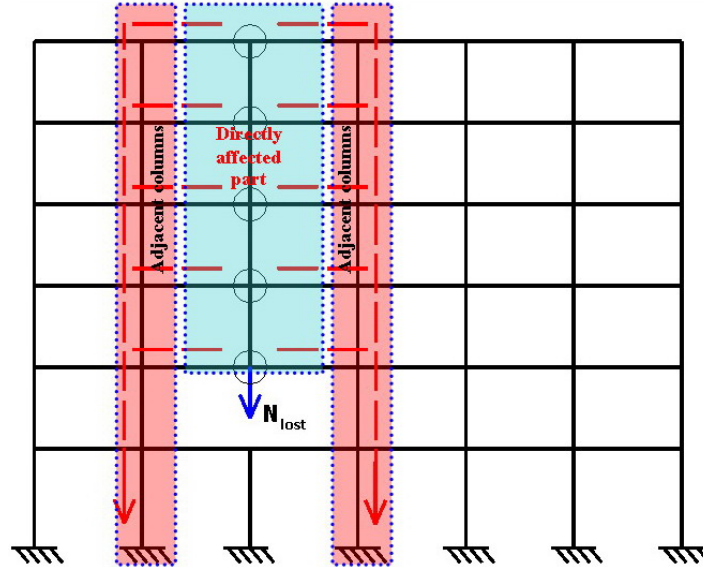


Figure 5.5. The alternative load path and the influenced frame zones

If the column lost is external, only one span is involved in the directly affected part instead of two, as in the case of an internal column being lost (see Figure 5.6). The external columns and the outside span beams involved in the directly affected part work together to transfer the load to the columns next to the lost column. So, for this situation, there is only one column zone included in the path. The two possible alternative load paths described are demonstrated in Figure 5.6.

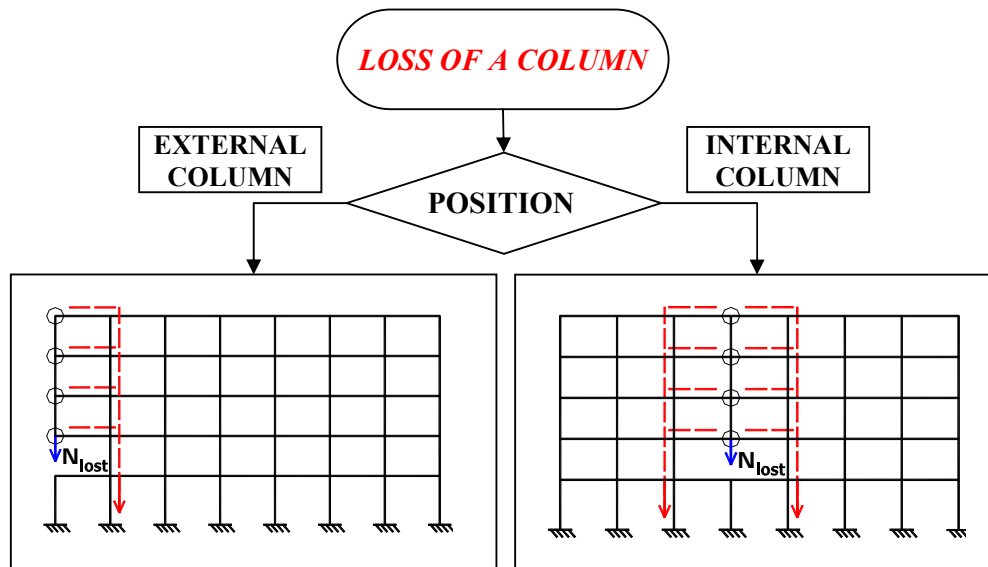


Figure 5.6. Activated alternative load paths in a frame losing a column



Given the definition of the alternative load paths, there are 2 critical zones to be investigated: the directly affected part, which has to transfer the loads to the indirectly affected part, and the indirectly affected part, which has to support the additional loads resulting from the column loss. The studies carried out on the directly affected part are presented in Chapter 6 while Chapter 7 deals with the indirectly affected part.

#### 5.4. YIELDING OF THE DIRECTLY AFFECTED PART

As presented in Chapter 3, the frame's behavior when subjected to the exceptional loss of a column can be represented through a curve plotting the deflection at the top of the lost column vs. axial load in the lost column. The shape of this curve is shown again below in Figure 5.7:

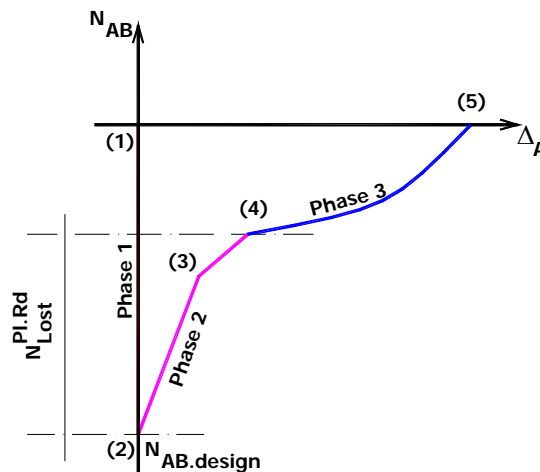


Figure 5.7. Axial load in the lost column vs. deflection at the top of the lost column

The force  $N_{lost}^{Pl.Rd}$  illustrated in Figure 5.7 represents the plastic resistance of the directly affected part, i.e. the axial load which has to be lost in order to develop a plastic mechanism within the directly affected part, and the axial load which is lost during Phase 2. At the end of Phase 2, the sections at the extremities of the beams included in the directly affected part yield, and, at that moment, significant catenary actions begin to develop within the directly affected part.

The value of  $N_{lost}^{Pl.Rd}$  depends mainly on the properties of the beams included in the directly affected part. As presented in Figure 5.2,  $N_{lost}$  represents the reduction of the value of  $N_{AB.design}$  (which is the load within the lost column before its removal and corresponding to the conventional loading applied) due to the column loss. The value of  $N_{lost}^{Pl.Rd}$  can only be

reached if:

$$N_{lost}^{Pl.Rd} < N_{design} \cdot \quad (5.2)$$

If this is not the case, it means that the plastic mechanism within the directly affected part is not generated when the loss column is fully removed from the structure and the directly affected part remains stable.

At the end of Phase 2, regardless of whether the indirectly affected part collapses when the plastic mechanism is formed within the directly affected part or the indirectly affected part remains stable, the additional loads transferred to the indirectly affected part (mainly resulting in additional vertical loads and bending moments in the columns on each side of the lost column) have to be supported by the latter.

In fact, the loads to be supported by the indirectly affected part result from two load cases: the initial state and the additional loads coming from the column loss, as illustrated in Figure 5.2. So, when  $N_{lost} < N_{lost}^{Pl.Rd}$ , the frame still functions within the elastic range. Consequently, the compression found within the columns of the indirectly affected part stems from a combination of 2 processes: the compression from the initial state and the compression from the additional loads due to the column loss. The bending moment applied to the column can be approached in the same manner.

If the indirectly affected part remains stable, catenary action may develop within the directly affected part during Phase 3 and, so, additional loads are transferred to the indirectly affected part. Accordingly, other alternative load paths are activated during Phase 3, which is demonstrated in detail in Section 5.5.

### 5.5. DEVELOPMENT OF CATENARY ACTION

After point (4) shown in Figure 5.7, a plastic mechanism is formed in the directly affected part and the vertical displacement at point A rapidly increases. The consequence of this is that the second order effects develop significantly in the directly affected part. Specifically, membrane forces develop in the bottom beams of the directly affected part. This catenary action is illustrated in Figure 5.8

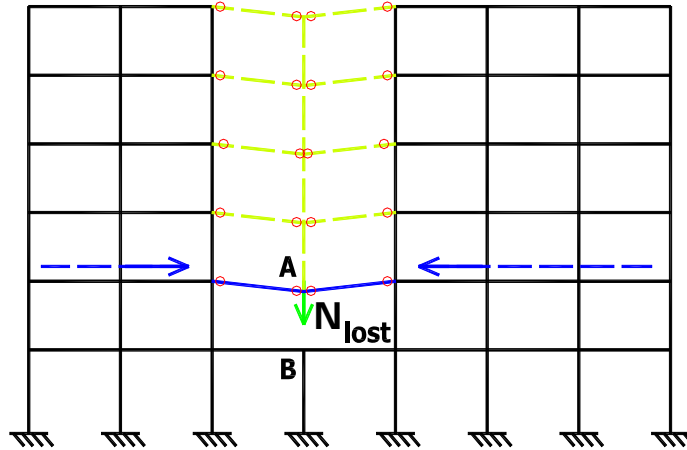


Figure 5.8. Membrane phenomenon when  $N_{lost}^{Pl.Rd} < N_{design}$

### 5.5.1. Conditions to be respected to develop catenary actions within the directly affected part

As stated in Section 5.2, progressive collapse occurs when the alternative load path cannot be maintained, i.e. when the additional loads coming from the directly affected part and to be supported by the indirectly affected part exceed the resistance of the latter.

For that reason, the first condition for the development of significant catenary actions within the directly affected part is to be able to reach point (4) in Figure 5.7, which means that the directly affected part has to be able to support the additional loads coming from the directly affected part to pass from point (2) to point (4). In other words, the columns just around the lost column have to remain stable when subjected to the additional compression loads coming from the directly affected part.

The second condition is linked to the possibility of forming a plastic mechanism within the directly affected part. Specifically, the joints (in the case of partial-strength joints) or the beam extremities included in the directly affected part have to possess sufficient ductility to develop plastic hinges (which means that for the beam extremities, they have to be Class 1, according to the Eurocodes).

The development of catenary actions has been further investigated in Jean-Francois Demonceau's thesis. In the present thesis, however, only the requirements necessary for the indirectly affected part to maintain the membrane effects are investigated. This will be studied in Chapter 8.

### 5.5.2. Extended alternative load path and element chain

When catenary actions develop within the structure, tying forces increase in the bottom beam of the directly affected part only. As a result, when the plastic mechanism is formed in the directly affected part, the response of the latter is mainly governed by the response of the bottom beam. The tying forces appearing in the bottom beam have to be supported by the indirectly affected part. These loads are in addition to the loads to be supported by the indirectly affected part in order to pass from point (2) to point (4) of Figure 5.7.

The new distribution of internal forces defines an extended alternative load path.

Figure 5.9 illustrates the zones included in the extended alternative load path. As seen below, membrane forces develop in the bottom beams, producing an additional load on the structure on both sides of the frame. There are three zones which transfer the additional load to the foundation: the directly affected part, the adjacent columns and damaged level.

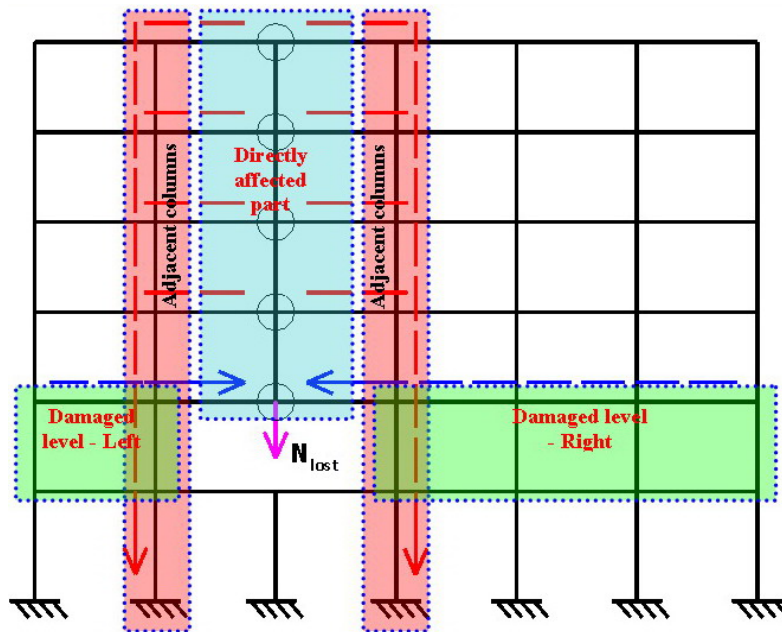


Figure 5.9. Structural members within the extended alternative load path

### 5.6. POSSIBLE DESIGN SITUATIONS

Figure 5.10 recapitulates the outcome scenarios possible when the frame loses a column. As described in Sections 5.4 and 5.5, the frame's behavior depends significantly not only on the position of the damaged column but also on the configuration of the specific element in the applied alternative load path. In particular, the capacity of the directly

affected part, which is represented by  $N_{lost}^{PL.Rd}$ , and the surrounding elements' parameters are critical points in showing the frame's behavior.

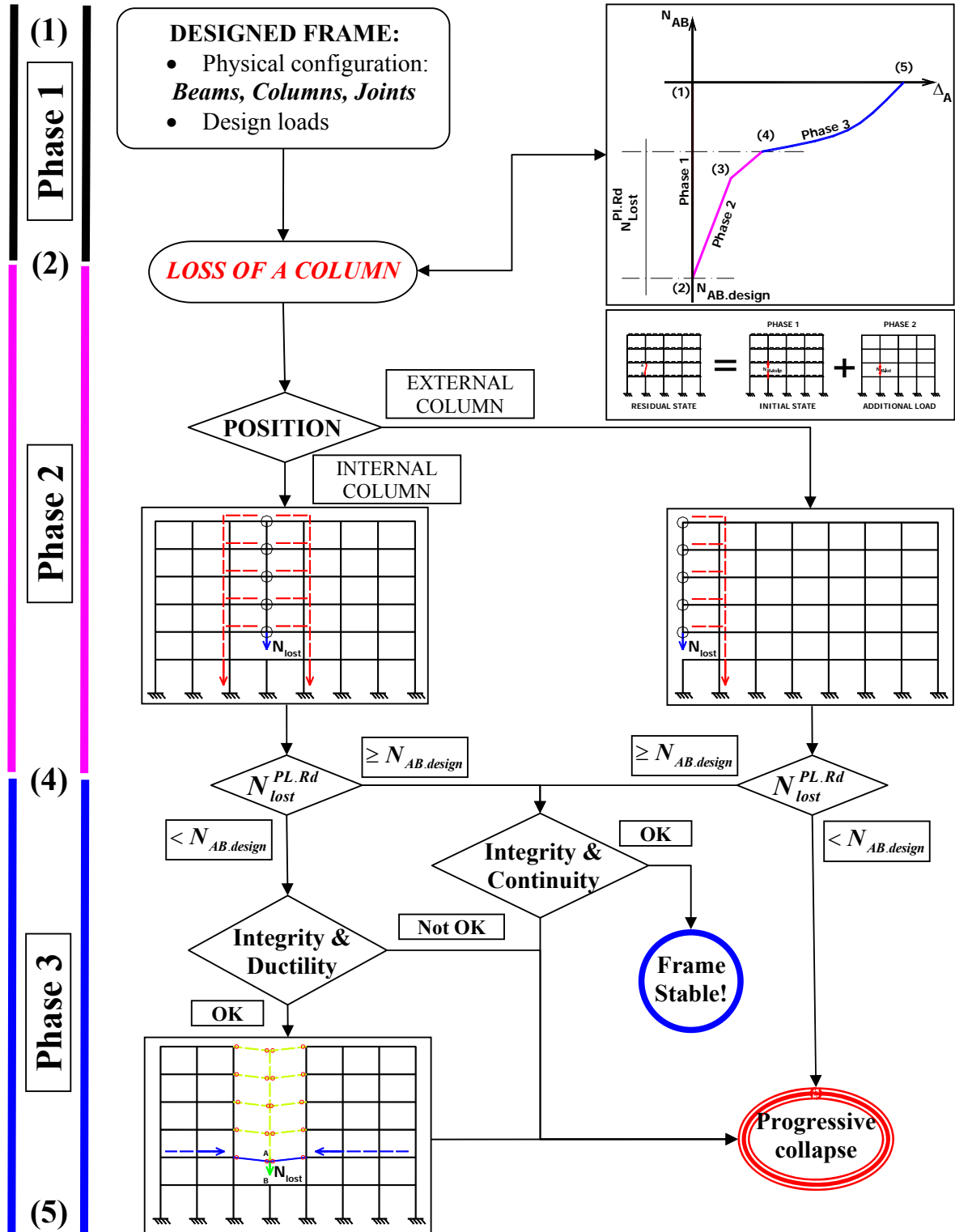


Figure 5.10. Full alternative load paths and their conditions

## 5.7. SUMMARY AND CONCLUSIONS

Chapter 5 describes the systematized analyses concerning the response of the frame in the event of the loss of a column. In Chapter 2, the global concepts associated with an exceptional event have been presented. This chapter continues that discussion then in order to provide more details on the frame's response to such an event.

After the introduction, Section 5.2 examines the additional load associated with column loss. The first part differentiates the two states of the frame before and after the event, i.e. the initial state and the residual state. An additional load associated with the residual state is defined. The limit of the additional load lower than the value of  $N_{design}$  is also provided. The second part looks into the definition of the *extension of localized damage*. This definition is the key to confirming the occurrence of progressive collapse.

Next, Section 5.3 presents the alternative load path that appears in the frame after the loss of a column. A description of the structural components and their position in the load path is given. In this section, two possible outcome scenarios are identified depending on the position of the lost column. An illustration of internal force distribution within the frame in the residual state is then presented.

Section 5.4 explains the behavior of the directly affected part in Load Phase 2. The axial force  $N_{lost}^{Pl.Rd}$  in the damaged column is achieved based on the yield limit of this part. This value is the critical point as it represents the point at which the directly affected part can no longer support the additional load. At this point, Load Phase 2 ends.

Section 5.5 goes on to describe the development of the catenary action. If the previous alternative load path fails, the catenary action could be produced if certain conditions are fulfilled. In this case, the bottom beams take on membrane behavior and keep the frame stable. This action extends the alternative load path in Load Phase 3.

Finally, Section 5.6 summarizes the frame's behavior in the event of the loss of a column in a detailed flowchart, in which possible outcome scenarios are illustrated. Future investigations will be performed based on this overview of possible outcomes.

**CHAPTER 6: ANALYTICAL MODEL FOR THE DIRECTLY  
AFFECTED PART**

## 6.1. INTRODUCTION

This chapter aims to develop an analytical substructure model which would represent the directly affected part's behavior. More precisely, it provides further detail on Levels 1 and 2, discussed in Chapter 4, specifically in the case of the directly affected part. A flowchart describing this procedure is reproduced below in Figure 6.1.

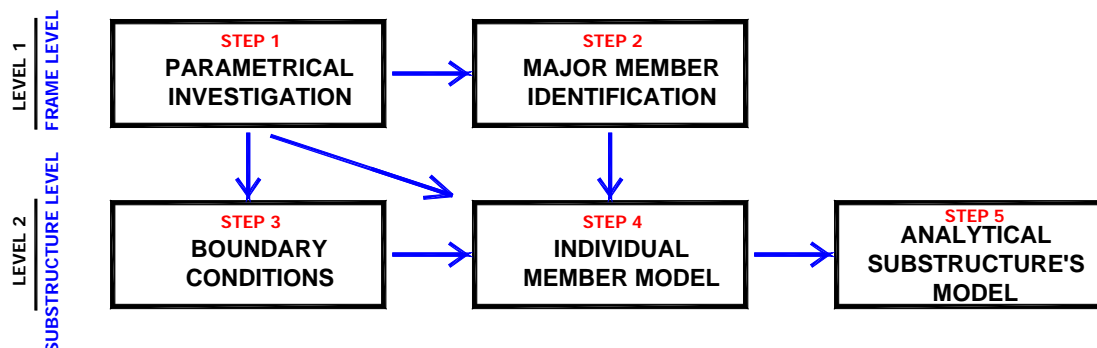


Figure 6.1. The procedures for building the analytical substructure model

Based on the numerical results, Section 6.2 describes the distribution of internal forces within the part. Then, the principal flow of internal forces is identified. Its properties are also listed for use in later simulations. Section 6.3 describes three steps for developing an analytical model of the part.

Section 6.4 then concentrates on partially restrained stiffness. This stiffness stems from the continuity of the part and the surrounding structures. It is the factor which influences the behavior of the equivalent beams the most. An analytical formula to predict its value is given, accompanied by a comparison with numerical results in order to validate the formula.

The individual equivalent beam's analytical model is built in Section 6.5. Once this model was obtained, an elastic—perfectly plastic analysis was performed to calculate its resistance. An analytical substructure model was obtained by assembling the individual models, i.e., the equivalent beam's models and the middle column's model. The displacement of the damaged column's top point was verified according to the substructure's stiffness.

The last section concerns the moment when the directly affected part fully yields. It is represented by the critical point (4) in the loading process in Figure 5.7. Finally, a quick method for estimating the value of  $N_{lost}^{Pl.Rd}$  is developed in this section.



## 6.2. INTERNAL FORCE DISTRIBUTION IN THE DIRECTLY AFFECTED PART

Before going into the details of the analyses, it is necessary to illustrate the identification of the directly affected zone within the frame (see Figure 6.2).

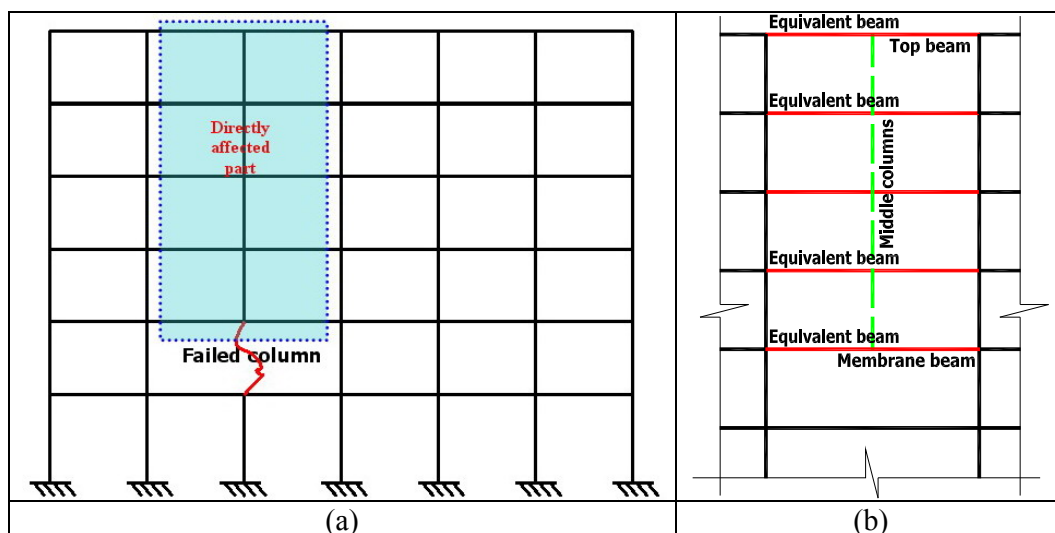


Figure 6.2: Directly affected zone (a) and the members (b)

Consequently, this section presents the evolution of the internal forces within the directly affected part, which must support the design load and the additional load simultaneously. They are demonstrated separately with diagrams. To highlight the major evolution of the internal forces within the components, only the diagram of axial force on the middle columns, the bending moment and the shear force on the equivalent beams are illustrated.

### 6.2.1. Distribution of internal forces

As presented in Chapter 3, the load sequence applied to the frame is demonstrated by a load-carrying curve. This curve, repeated below, will be referred to for the following discussion. Next, the distribution of internal forces is demonstrated along that curve, with a brief description of each load phase.

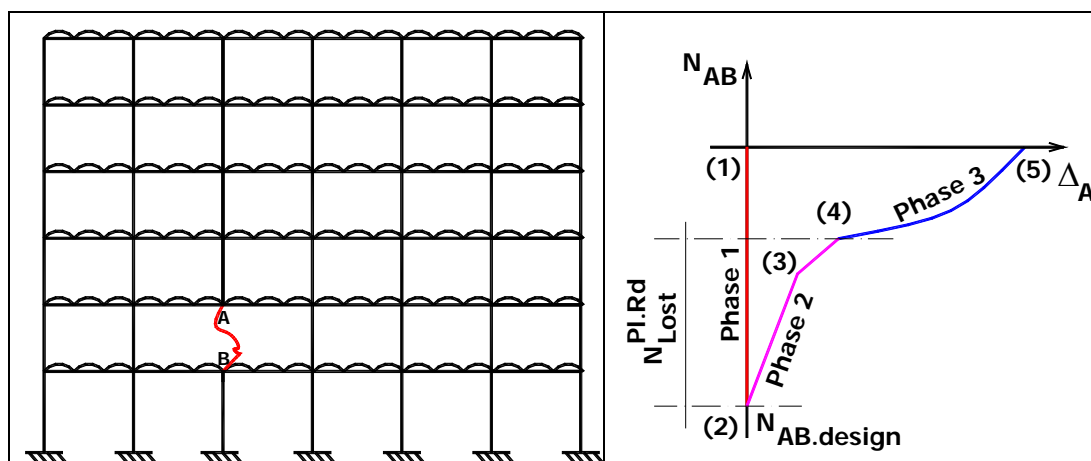


Figure 6.3. Axial load in the lost column vs. deflection at the top of the lost column

**Phase one:** From point (1) to point (2), the design load is applied to the frame. It is in its *initial state*. The frame is illustrated with one modification to its physical configuration: the damaged column is replaced by its normal force. At point (1), the frame is not loaded. From point (1) to (2), the design loads are applied progressively. A compression force appears in the middle columns and progressively increases due to the applied load. Then, a bending moment and shear force appear in the equivalent beams as demonstrated in Figure 6.4.

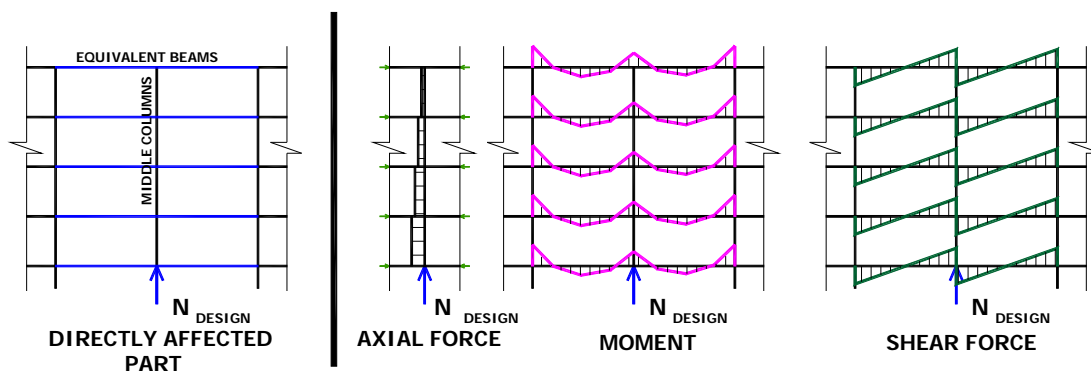


Figure 6.4. Distribution of the internal forces in the initial state

**Phase 2:** From point (2) to point (4), the column progressively disappears. The frame goes from its initial state to a *residual state*. The axial force  $N_{AB}$  of the damaged column progressively increases. Figure 6.3.b illustrates the Load Phase 2 from point (2) to point (4). Point (3) corresponds to the first plastic hinge's appearance in the directly affected part. While the frame goes from point (2) to point (3), its behavior is fully elastic. As soon as the first plastic hinge is formed within the directly affected part, the frame's behavior is no longer elastic.

Accordingly, the evolution of the loads when passing from the initial to the residual state is

linked to the evolution of the loads due to the column loss. These loads are concentrated forces applied at the top and bottom of the lost column in the direction opposite to the column's internal forces in its initial state, called  $N_{design}$ . The value of the loads due to the column loss is named  $N_{lost}$ . Thus, the internal forces' form and magnitude within the directly affected part change, as seen in Figure 6.5. Here, the bending moments in the section next to the middle columns increase while the values at both ends of the section closest to the adjacent columns decrease. Likewise, the shear forces change according to the variation in the bending moment. Their evolution is described in the next paragraph to highlight the danger inherent in this part's position.

However, the disappearance of the damaged column produces a special phenomenon within the directly affected part. This part acts as an "arch", bridging over the damaged position. The *arch effect* describes the special behavior of the directly affected part and surrounding members resulting in the development of a fictitious arch over the damaged column. This is achieved by the distribution of the beam's normal forces. The axial forces appearing within the equivalent beams are distributed as demonstrated in Figure 6.5. The top beams are compressed, while the bottom beams are under tension. This phenomenon will be discussed and simulated in Chapter 7.

The axial force within the middle columns is directly linked to the progressive disappearance of the damaged column. Its distribution does not change, but its magnitude decreases. This is also discussed in the next paragraph on Phase 3.

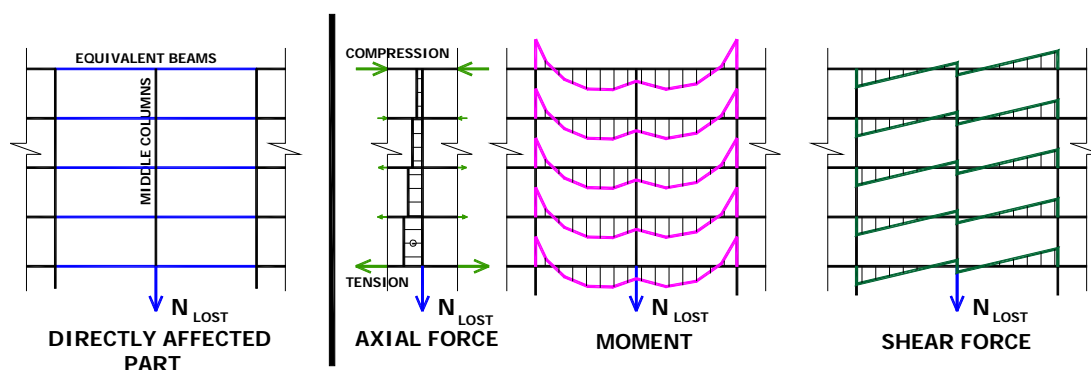


Figure 6.5: Distribution of the internal forces in the residual state

**Phase 3:** In the case where the maximum value of  $N_{design}$  is higher than the directly affected part's resistance  $N_{lost}^{Pl.Rd}$ , and where a catenary action could arise, the frame can go from point (4) to point (5) in Figure 6.3. When point (4) is reached, the equivalent beam's end sections fully yield. Each equivalent beam then becomes a mechanism. In this case, the

bending moment's values at the yield positions are equal to that section's plastic resistances. In other words, the bending moment diagram does not change in this segment. Depending on the bending moment's values, the shear force's distribution remains at point (4).

Without the suspension of the upper structures, the damaged column's top point falls rapidly. Thus, the second-order phenomenon is activated in the bottom beams of the directly affected part. Membrane forces develop in that beam, as demonstrated in Figure 6.6. The middle columns are attached to the catenary beam and so follow its deflection. Its axial forces remain constant between points (4) and (5).

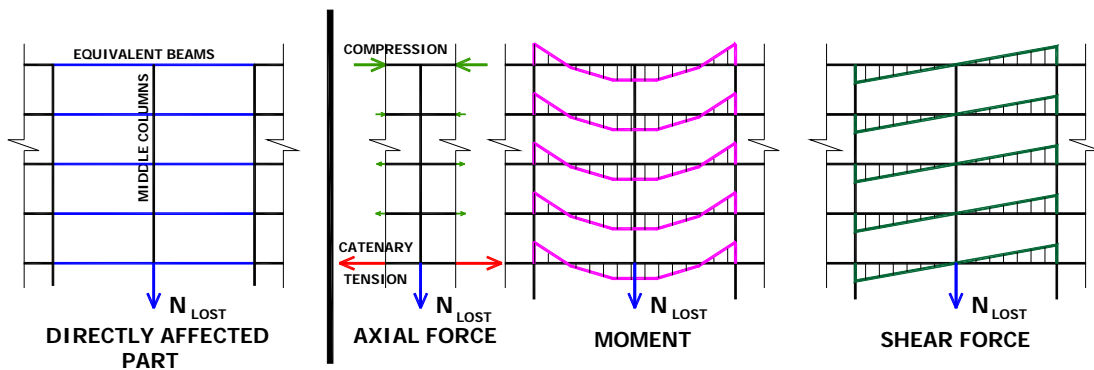


Figure 6.6. Internal force distribution in Phase 3; catenary forces increase

The next section concentrates on the individual members' behavior in this zone of the frame.

### 6.2.2. Key members and sections

#### 6.2.2.a. The end sections of the equivalent beams

In the investigation of the directly affected part, the equivalent beam appeared to be the most precarious member due to the sudden increase in its length and load. Indeed, the highest bending moment appears at that beam's end sections.

Figure 6.7 presents the bottom beam, which connects points A, B, and C, more closely.

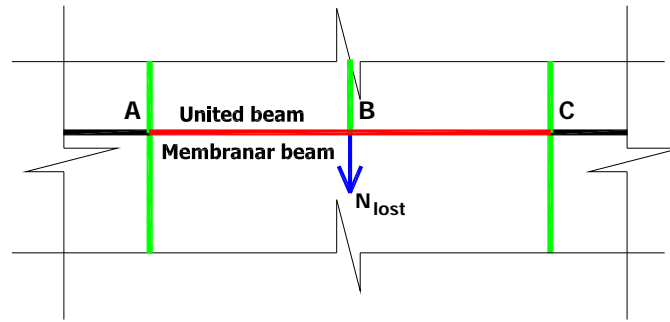


Figure 6.7. Isolated membrane beam

Figure 6.8.a demonstrates the bending moment diagram of the equivalent beam at point (2). At that moment, i.e., the initial state, the bending moment correlates to the initial state and so is called  $M_{design}^{+,-}$ . From point (2) to point (4), the additional load is gradually transferred to the beam as a result of the progressive disappearance of the column. This load produces additional internal forces within the frame. In the beam being studied, this load is called  $M_{lost}^{+,-}$ .

After that, Figure 6.8.b presents the bending moment of the *additional state*. Before point (3), the frame's behavior is still within the elastic range. At this point, the bending moment's distribution is composed of both initial and additional states and behaves as seen below in Figure 6.8.c.

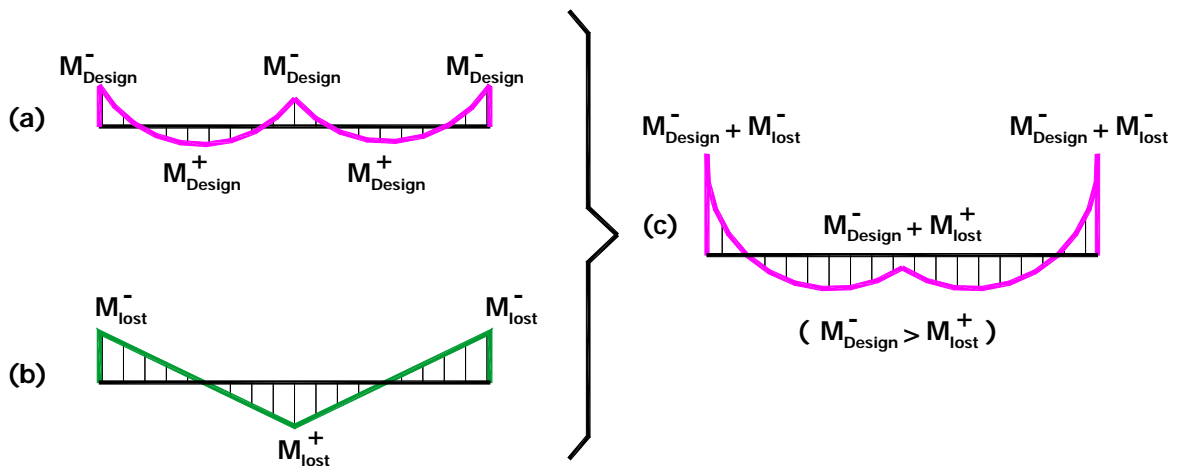


Figure 6.8. Bending moment diagram of equivalent beam in Phase 2

- (a) Initial state; (b) Additional state;
- (c) Bending moment of the equivalent beam within the elastic range.

6.2.2.b. The axial force in the beams

After point (2), axial forces appear in the directly affected beams. Those beams are pulled or pushed according to the deformation of the adjacent columns on both sides.

Compression appears in the top beam while tension acts on the bottom beam. Figure 6.9 presents the distribution of these axial forces along the height of the directly affected part.

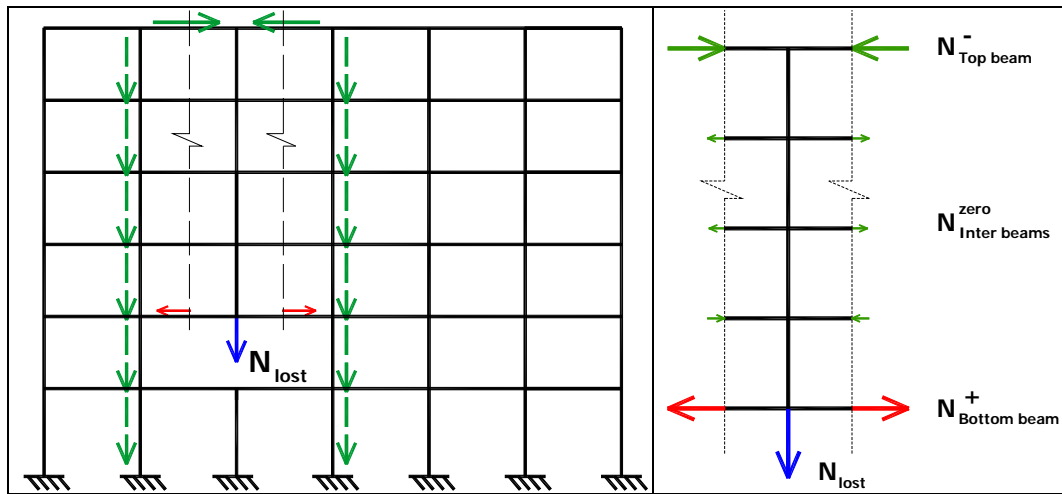


Figure 6.9. Axial forces in the directly affected beams

Thus, even though the bending moments, which appear in the beams, are similar, the bottom and top beams support a different level of loading. This internal force distribution is described as an arch effect. As mentioned above, this type of behavior will be explained more in Chapter 7.

Another consequence is the activation of the catenary effect in the directly affected part. In Figure 5.7, point (4) corresponds to the total yielding of this part. The equivalent beam's end sections are at their limit state at that point. After point (4), the top and intermediate beams still keep their initial states, with the axial force being negative or nearly zero. *Only* the bottom beam, with its initial level of tension, could activate a catenary action.

### 6.2.2.c. Middle columns

The last members to be checked were the columns which connect the middle points of equivalent beams. In the initial state, these columns support the design load.

After point (2) of the load-carrying curve, the additional load is applied progressively to the frame. Physically, the middle point of the equivalent beam sinks due to this load. Without its support at that point, the column undergoes a decrease in its axial forces. To illustrate this development, Figure 6.10 presents the axial force distribution in the middle columns.

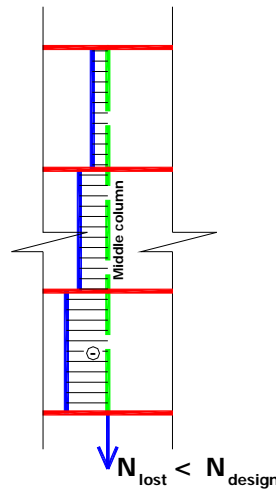
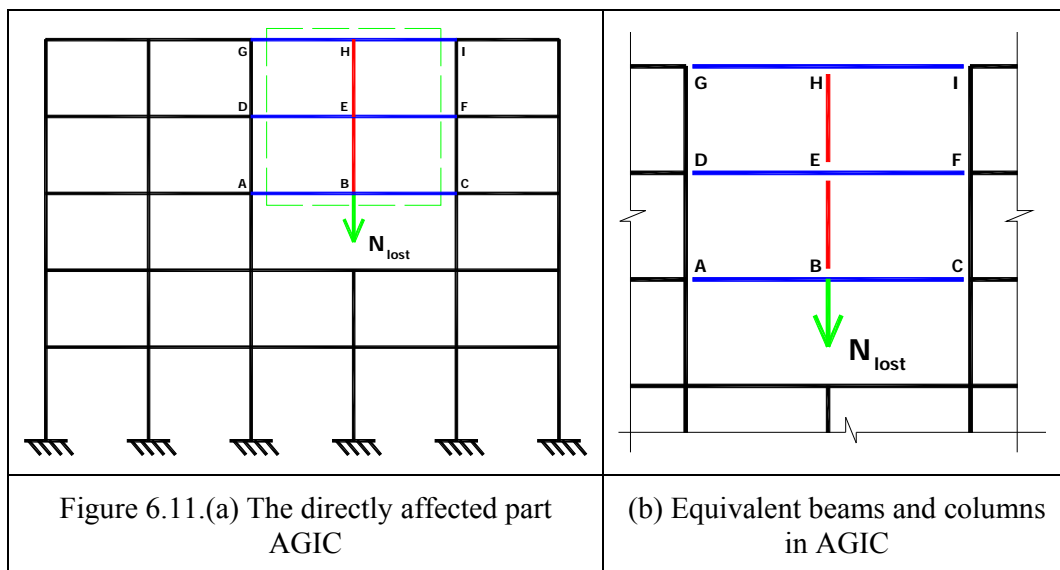


Figure 6.10: Axial forces of the middle columns (Phase 2)

### 6.3. SUB-MODEL SUBSTITUTED FOR THE WHOLE DIRECTLY AFFECTED PART

The present section examines Level 2 in Figure 6.1 in order to develop the substructure model of the directly affected part. To begin with, Figure 6.11.a presents the frame in which the area *AGIC* borders the directly affected part; Figure 6.11.b takes a closer view of *AGIC*. The equivalent beams and columns are broken down by colors. Three equivalent beams are in blue, while the two middle columns are in red.



In this section, the simulation of the directly affected part is explained in the additional state only. Later, the principle will be extended to the residual state, as presented in Figure 5.2.

### 6.3.1. Equivalent beam model

On each floor, the equivalent beam is composed of two beams to the left and right of the damaged column. Due to the loss of the column, the additional load  $N_{lost}$  is applied to point **B**. That force is then transferred to points **E** and **H** through the middle columns **BE** and **EH**.

This section aims to develop a model representing the behavior of an individual equivalent beam. As in Figure 6.1, this simulation corresponds to step 4 of Level 2, the substructure level.

Before going further, the continuity of the individual members' isolation has to be well defined, i.e., using appropriate boundary conditions. This is step 3 of Level 2. There are three conditions to mention. The first condition is in the continuity of the beam's end to the adjacent part through rotation and displacement. The second condition requires a semi-rigid beam-to-column connection on the beam. The last condition is to simulate the attachment of the middle column to the beam. In this way, the real working conditions of the individual equivalent beam are accurately simulated.

#### 6.3.1.a. Partially restrained ends

The first parameter studied was the beam ends' conditions. At points **A**, **D**, **G** or **C**, **F**, **I**, the directly affected part is connected to the frame. When the beam is deformed, the bending moment is transferred to the adjacent part of the frame. This bends the members connected to the same point: columns on the floor above, column on the floor below and the adjacent span beam.

For the equivalent beam, the boundary conditions for each end are represented by partial rotational stiffness  $K_{S1}$  and  $K_{S2}$ , respectively. This is called the partially restrained coefficient, which is drawn by blue springs at both points **A** and **B**. The end points' horizontal movement is also restricted by the frame. The restriction is represented by the horizontal straight springs  $K_1$  and  $K_2$ . The method for predicting their value will be presented in Section 6.4.



6.3.1.b. Restraint at beam middle point

The middle point of each equivalent beam is connected to the middle columns. In this case, the column mainly supports a tensile force. However, when the beam is deformed, the connected section rotates. Its rotation will nevertheless be restrained by the column's stiffness. In general, when the bending moments appearing on the left and right of point **B** differ, section **B** will rotate. In other cases, when both sides' bending moments are equal, section **B**'s rotation is zero.

In the equivalent beam model, such a restraining capacity in a column is represented by the rotation spring  $K_{S3}$ . Due to the loss of a column, the middle point of the beam loses its support. Therefore, in the model, that point is released in the vertical direction.

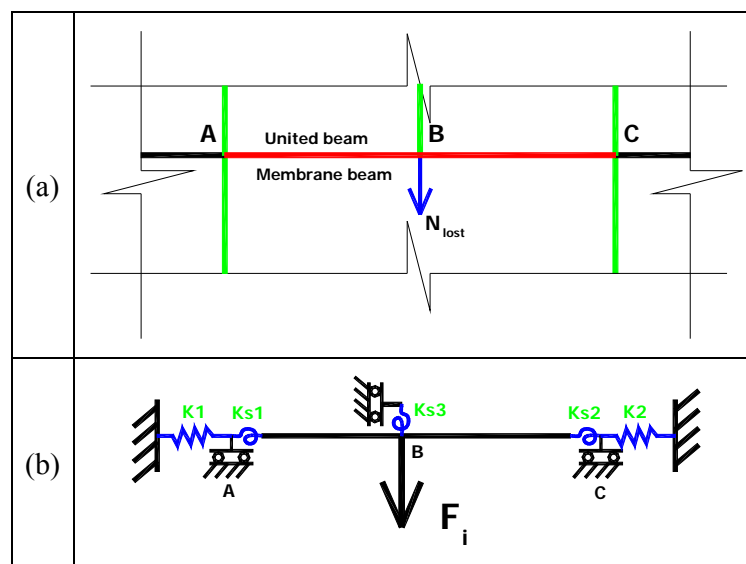


Figure 6.12.(a) The equivalent beam ABC (b) Analytical model

6.3.1.c. Semi-rigid beam-to-column connection

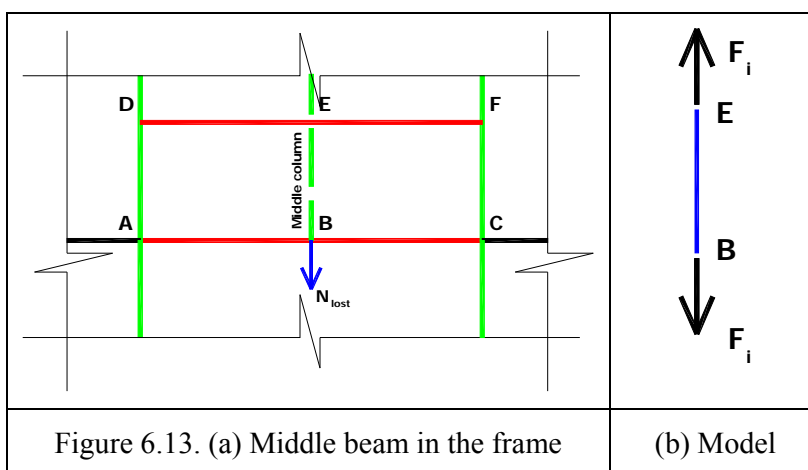
In the frame, the beam is connected to the column at its midpoint. According to EC3 and EC4 the connection is considered semi-rigid if its initial stiffness is between  $[1/2, 8]$  times the beam's bending stiffness.

If there is a semi-rigid joint in the frame, its initial stiffness is described in  $K_{S1}$  and  $K_{S2}$  by the serial connection between overall  $K_S$  and initial stiffness  $S_i$ . For example, the value of  $K_{S1}$  becomes:

$$K_{S1} = \frac{S_i K_S^{global}}{S_i + K_S^{global}} \quad (6.1)$$

### 6.3.2. Column under tension

The second directly affected component is the middle columns. In the additional state, each middle column supports positive axial forces and is connected to the equivalent beam, forming a hanging system. It has been decided to model this structure with the vertical member in pure tension.



### 6.3.3. Substructure model

From the individual member models, the substructure of the directly affected part is presented in Figure 6.14. Its stiffness is defined by combining the individual members' stiffness. They are connected by serial or parallel connections according to the position of the member. The idea of connection was first presented by Wong (2005) when predicting the influence of fire on a frame and it has been developed by the author to verify this particular simulation.

With the 3-story model, illustrated in Figure 6.15, the substructure's stiffness is described as:

$$K_{Model} = S_{B1} + \frac{1}{\frac{1}{S_{C2}} + \frac{1}{S_{B3} + \frac{1}{\frac{1}{S_{C4}} + \frac{1}{S_{B5}}}}} \quad (6.2)$$

where  $K_{Model}$  is the directly affected part model's stiffness under  $N_{lost}$ , and  $S_{Bi}$ ,  $S_{Ci}$  are the individual members' stiffness.

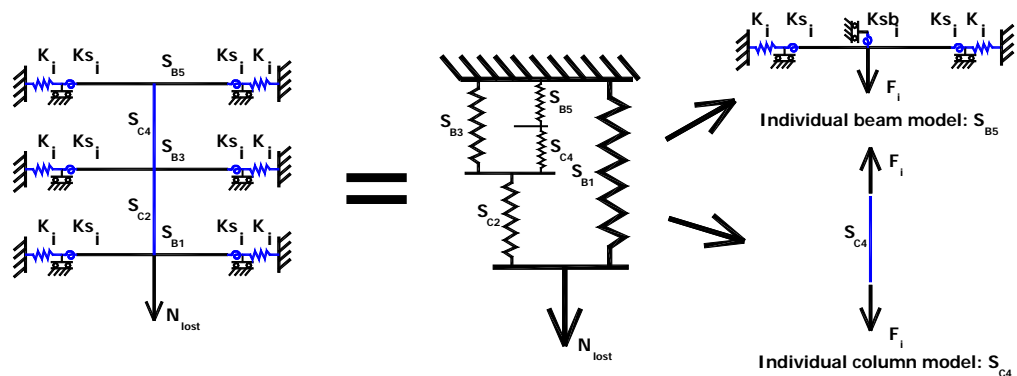


Figure 6.14. The analytical substructure model

In other words, the bending stiffness of equivalent beams and the elongation stiffness of the middle columns are connected to form  $K_{Model}$ . Normally, the column's level stiffness is elevated, owing to the capacity of the section and its tensile state. Through numerous investigations, it has been proved that when the column's stiffness is 20 times greater than that of the beam's stiffness or higher, the substructure's stiffness totals the sum of the beams' stiffness:

$$K_{Model} = S_{B1} + S_{B3} + S_{B5} \cdot \quad (6.3)$$

### 6.3.4. Conclusion

In this section, the directly affected part was extracted from the building in two steps. The first step was to denote the boundary conditions of the part. The second step consisted in explaining the individual analytical model of the equivalent beam and middle column. Afterwards, the assembly that connects the individual members to create the substructure model was presented.

It should be noted that these models were presented in their most simplified forms. The next section will provide the calculations to estimate  $K_S$ , the equivalent beam's stiffness and the column's stiffness.

## 6.4. PARTIAL RESTRAINT COEFFICIENT $K_S$

According to the procedure defined in Figure 6.1, this section will describe step 3 of Level 2 to create the boundary conditions of the individual members. Figure 6.13.b illustrates the individual analytical model of the equivalent beam in which the  $K_{S1}$  and  $K_{S2}$  simulate the frame's influence on restricting the rotation of the beam's end sections.

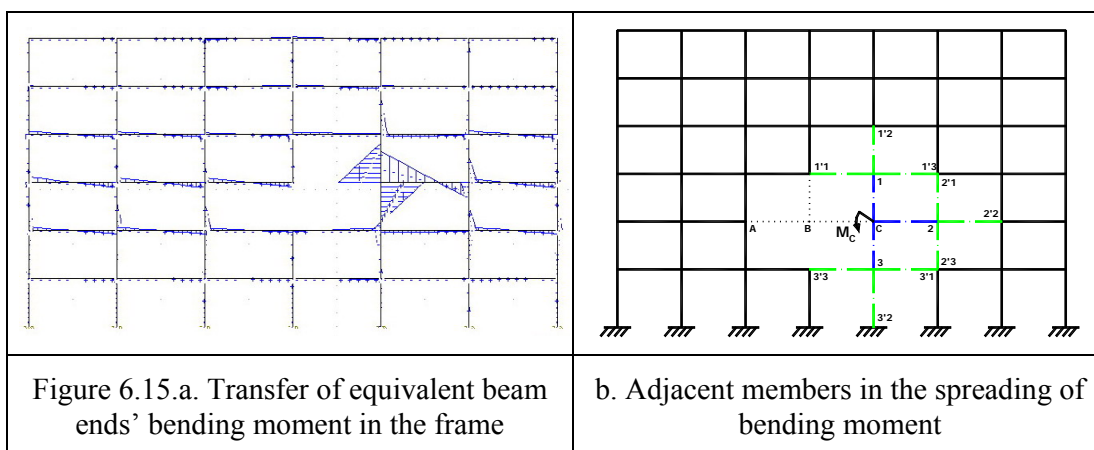
To develop the analytical formula for predicting these values, the investigation focused on the local behavior of the equivalent beam's end sections. This step was done to provide a parameter associated with the individual equivalent beam. Only one floor's behavior was studied.

#### 6.4.1. Adjacent members and continuity

To investigate the continuity of the equivalent beam ABC toward the adjacent members, the beam was physically replaced by a concentrated bending moment which appears at the beam end. Figure 6.15.a demonstrates the residual frame with a single bending moment applied to point C. The bending moment spreads out from point C and is distributed around the frame. As a result, the surrounding members are deformed.

Figure 6.15.b shows the members numbered in the order of the transferred rotations. From the beginning, point C is rotated due to the equivalent beam end's bending moment. Thus, the rotation reflects three adjacent members: C-1, C-2, and C-3. Likewise, the rotation of point 1 will produce the deformation of three adjacent components: 1'1, 1'2, and 1'3. The same types of behavior appear at points 2 and 3 to transfer to 2'1, 2'2, 2'3, then 3'1, 3'2, and 3'3, respectively.

Continuously, the deformation travels through these secondary points to the adjacent structural members, spreading more and more until the process extends throughout the frame.



#### 6.4.2. Influence of the position of the impacted column on $K_S$

As illustrated above, the bending moment at point C spreads widely within the frame, level

by level. However, this transfer could not go on indefinitely as the chain of influences depends on the geometrical position of the structural members. For example, in Figure 6.15.b, the deformation stops at the clamp of point 3'2.

Figure 6.16 shows the positions of the equivalent beam end divided into categories depending on the number of members or the number of transformation levels. In the example, four instances of  $K_S$  were predicted, as in Figure 6.16.

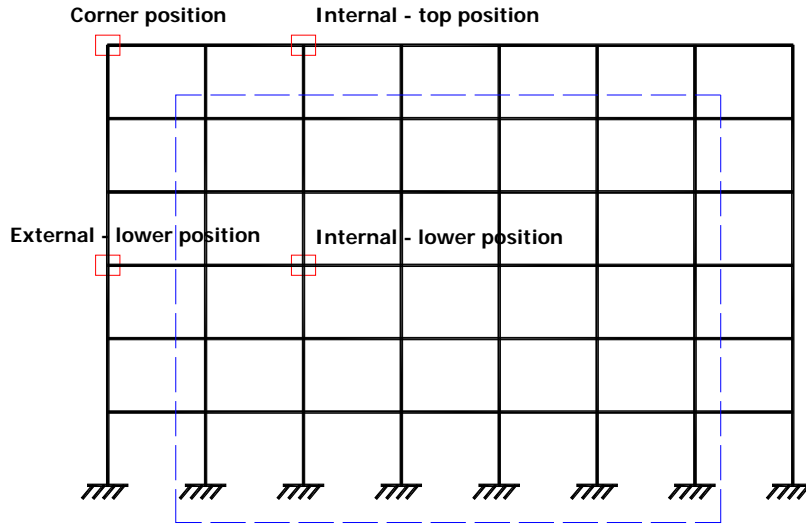


Figure 6.16. Different equivalent beam end positions

The next paragraph presents the development of the analytical formula for  $K_S$ .

### 6.4.3. Simplified model

From the earlier investigations, a model predicting the moment–rotation relation of the equivalent beam’s end point was developed. This partially restrained coefficient was predicted by calculating the stiffness of the related members.

After limiting the model to 2 transferred levels (in blue and green in Figure 6.16.b), the model was developed as in Figure 6.18. The stiffness of a single beam undergoing a unit rotation at the beam end is  $S_B$ . The column’s stiffness under the unit rotation at the column’s end is likewise  $S_C$ .

$$S_C = \frac{4E_C I_C}{L_C}$$

$$S_B = \frac{4E_B I_B}{L_B}$$
(6.4)

where  $E_B, E_C$  are the elastic moduli of the beam and column,

$I_B, I_C$  are the inertia of the beam and column sections, and  
 $L_B, L_C$  are the beam and column lengths.

The rotational capacity  $k_C$  of point 1 is equal to the sum of three sources of bending stiffness: beams 1-1'1 and 1-1'3 and column 1-1'2. Called  $k_C$  because of its nature, this term represents the rotational stiffness of the end point for column C-1. This method is applied to point 2 to obtain the rotational stiffness  $k_B$ .

Continuing to the next level, the end condition of point 1 is applied to member C-1 by the end spring  $k_C$ . The bending stiffness of a member with an end spring condition is calculated below in Equation 6.6.

$$\begin{aligned} k_C &= S_B + S_B + S_C \\ k_B &= S_C + S_B + S_C \end{aligned} \quad (6.5)$$

where  $k_C$  is the end rotational stiffness of columns C-1 and C-3, and  
 $k_B$  is the end rotational stiffness of beam C-2.

The rotational capacity of point C – the partially restrained coefficient – was defined in the previous step. Its stiffness is the sum of the bending stiffness of 2 columns, C-1 and C-3, and the bending stiffness of the beam C-2. The columns' stiffness is  $S_{C1}$  and the beam's stiffness is  $S_{B1}$ .

$$S_{C1} = \frac{4E_C I_C}{L_C} \frac{L_C k_C + 3E_C I_C}{L_C k_C + 4E_C I_C} \quad (6.6)$$

$$S_{B1} = \frac{4E_B I_B}{L_B} \frac{L_B k_B + 3E_B I_B}{L_B k_B + 4E_B I_B}$$

$$K_S = S_{B1} + S_{C1} + S_{C1} \quad (6.7)$$

where  $S_{C1}, S_{B1}$  are the bending stiffness of the column, beam with end's rotation spring, and  
 $K_S$  is the partially restrained coefficient of point C.

Obviously, the final value of  $K_S$  could be more accurate if more transferred levels are taken into account, i.e., by going to point 1'2'1. However, looking at Figure 6.17, it is easy to see that points 3'1 and 2'3 are overlapping. If the rotation transfers to the next level, it will lead to excess stiffness. In the end, the analytical model was limited to 2 transferred levels.

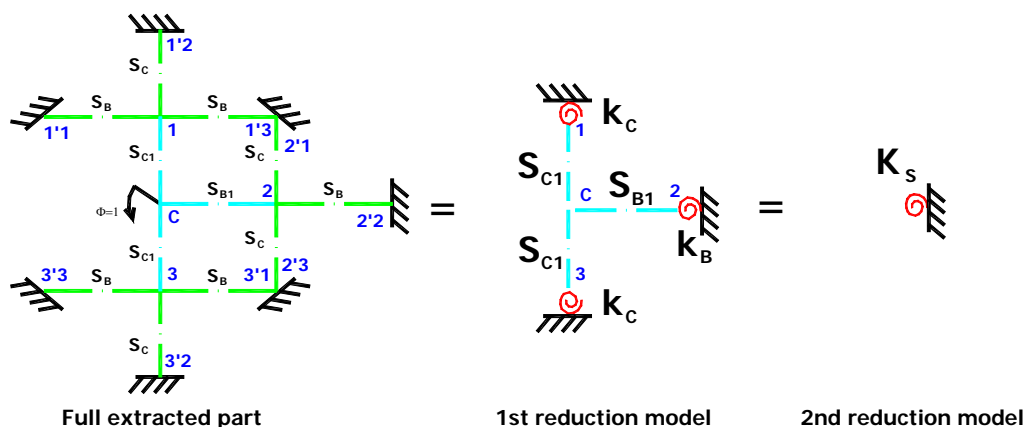


Figure 6.17. Three levels development of  $K_S$  at point C

Figure 6.18 presents the members included in the  $K_S$  formula in two cases: within the frame and at the top floor.

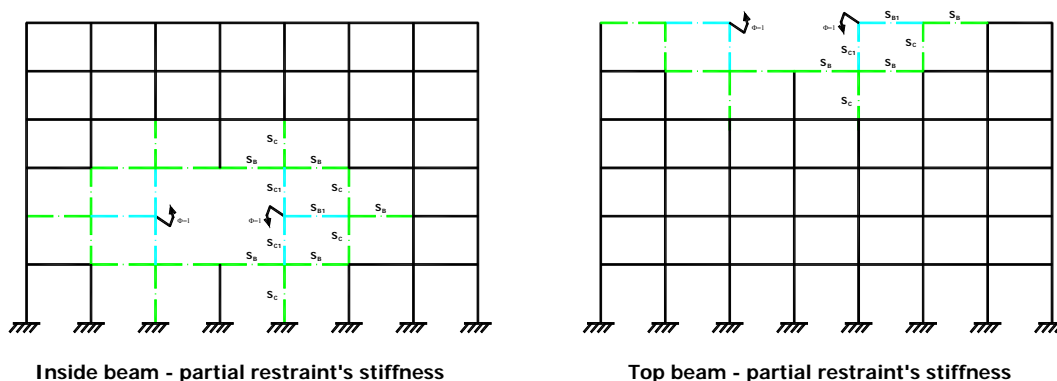


Figure 6.18. The  $K_S$  in different positions within the frame

#### 6.4.4. Semi-rigid connections

The analytical model in Section 6.4.3 concerns a typical frame with fully rigid connections. In general, the joints have semi-rigid connections. The rotation, which comes from the beam's end section, was not fully transferred to the columns.

So, the generally partially restrained coefficient was modified taking into account the connection's stiffness. There are two parts in the models and formulae which conclude the semi-rigid connection. The first part is the model of the beam in which both ends compose a semi-rigid connection.

Figure 6.19 (Degertekin, Hayalioglu 2004) presents beam segment **AB** with 2 semi-rigid joints which have an initial stiffness of  $S_{jA}$ ,  $S_{jA}$ . They are represented by a rotational spring. The rotations  $\theta_{rA}$ ,  $\theta_{rB}$  are the relative rotations of 2 springs.

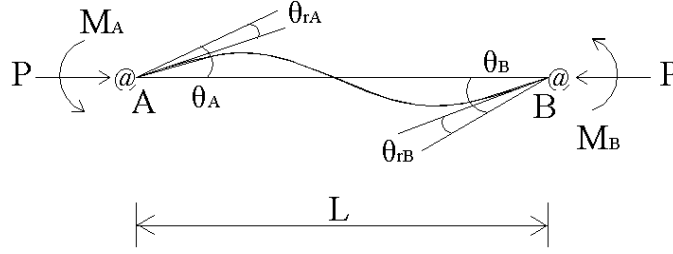


Figure 6.19: Semi-rigid beam segment.

So

$$S_{jA} = \frac{M_A}{\theta_{rA}}; \quad S_{jB} = \frac{M_B}{\theta_{rB}}. \quad (6.8)$$

Also the bending moment of both beam ends could be written as

$$M_A = \frac{E_B I_B}{L_B} \left[ 4 \left( \theta_A - \frac{M_A}{\theta_{rA}} \right) + 2 \left( \theta_B - \frac{M_B}{\theta_{rB}} \right) \right] \quad (6.9)$$

$$M_B = \frac{E_B I_B}{L_B} \left[ 2 \left( \theta_A - \frac{M_A}{\theta_{rA}} \right) + 4 \left( \theta_B - \frac{M_B}{\theta_{rB}} \right) \right]. \quad (6.10)$$

By taking  $M_A$ ;  $M_B$  out of the statement, we obtain

$$M_A = \frac{E_B I_B}{L_B} [r_{ii} \theta_A + r_{ij} \theta_B]; \quad (6.11)$$

$$M_B = \frac{E_B I_B}{L_B} [r_{ij} \theta_A + r_{jj} \theta_B]; \quad (6.12)$$

where

$$r_{ii} = \frac{1}{k_R} \left( 4 + \frac{12 E_B I_B}{L_B S_{jB}} \right),$$

$$r_{jj} = \frac{1}{k_R} \left( 4 + \frac{12 E_B I_B}{L_B S_{jA}} \right),$$

$$r_{ij} = \frac{2}{k_R},$$

$$k_R = \left( 1 + \frac{4 E_B I_B}{L_B S_{jA}} \right) \left( 1 + \frac{4 E_B I_B}{L_B S_{jB}} \right) - \left( \frac{E_B I_B}{L_B} \right)^2 \left( \frac{4}{S_{jA} S_{jB}} \right).$$

In shorter form, the bending stiffness at point A of the semi-rigid member is

$$S_B^{semi} = \frac{E_B I_B}{L_B} r_{ii} = \frac{E_B I_B}{L_B} \frac{1}{k_R} \left( 4 + \frac{12 E_B I_B}{L_B S_{jB}} \right) = \frac{4 E_B I_B S_{jB} (L_B S_{jA} + 3 E_B I_B)}{L_B^2 S_{jA} S_{jB} + 4 E_B I_B L_B (S_{jA} + S_{jB}) + 12 (E_B I_B)^2} \quad (0.1)$$

If two joints stiffness are equal ( $S_{jA} = S_{jB} = S_j$ ), the stiffness is



$$S_B^{semi} = \frac{4S_j E_B I_B (S_j L_B + 3E_B I_B)}{(S_j L_B + 2E_B I_B)(S_j L_B + 6E_B I_B)} \quad (6.14)$$

where  $S_{jA}, S_{jB}$  are the initial stiffness of the joints at points **A** and **B**.

Then the first level reduced formulae are

$$\begin{aligned} k_C^{semi} &= S_B^{semi} + S_B^{semi} + S_C \\ k_B^{semi} &= \frac{S_j (S_C + S_B^{semi} + S_C)}{S_j + S_C + S_B^{semi} + S_C} \end{aligned} \quad (6.15)$$

The second level is related to the second bending stiffness of the beam with a semi-rigid connection and the rotational springs  $k_C^{semi}$  and  $k_B^{semi}$  at the beam ends.

$$S_{C1}^{semi} = \frac{4E_C I_C L_C k_C^{semi} + 3E_C I_C}{L_C L_C k_C^{semi} + 4E_C I_C} \quad (6.16)$$

$$S_{B1}^{semi} = \frac{4E_B I_B k_B^{semi} (L_B S_j + 3E_B I_B)}{L_B^2 S_j k_B^{semi} + 4E_B I_B L_B (S_j + k_B^{semi}) + 12(E_B I_B)^2}$$

$$K_S^{semi} = S_{B1}^{semi} + S_{C1}^{semi} + S_{C1}^{semi} \quad (6.17)$$

where  $S_{C1}^{semi}, S_{B1}^{semi}$  are the levels of bending stiffness of the column and beam with rotational spring end taking into account the semi-rigid connection, and

$K_S^{semi}$  is the new semi-rigid partially restrained coefficient of point **C**.

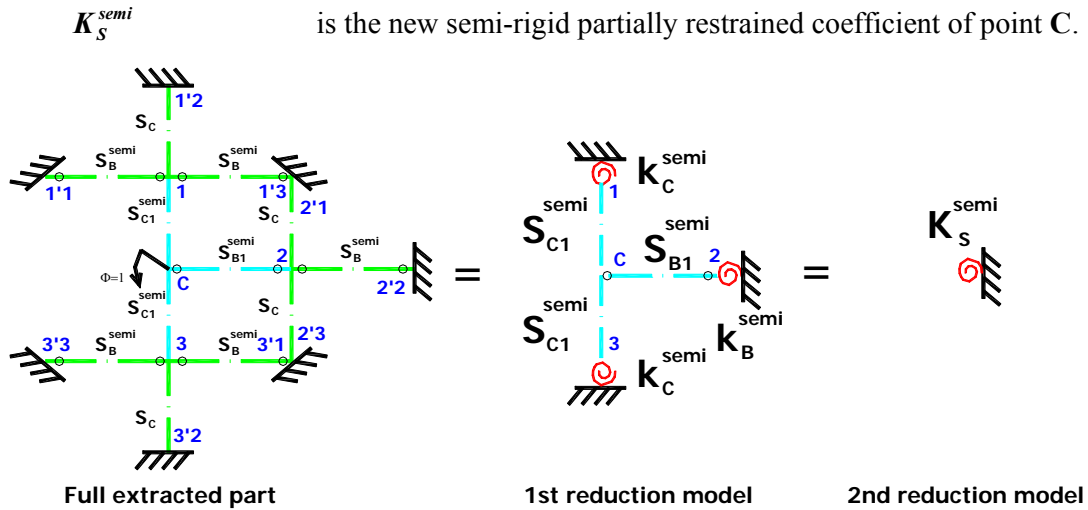


Figure 6.20. The partially restrained stiffness of point **C** with semi-rigid connections

### 6.4.5. Validation

In order to validate the analytical model of the restrained rotational stiffness  $K_S$ , a wide range of simulations were performed.

Three column sections were selected from the HEA table: HE 140A, HE 300A and HE

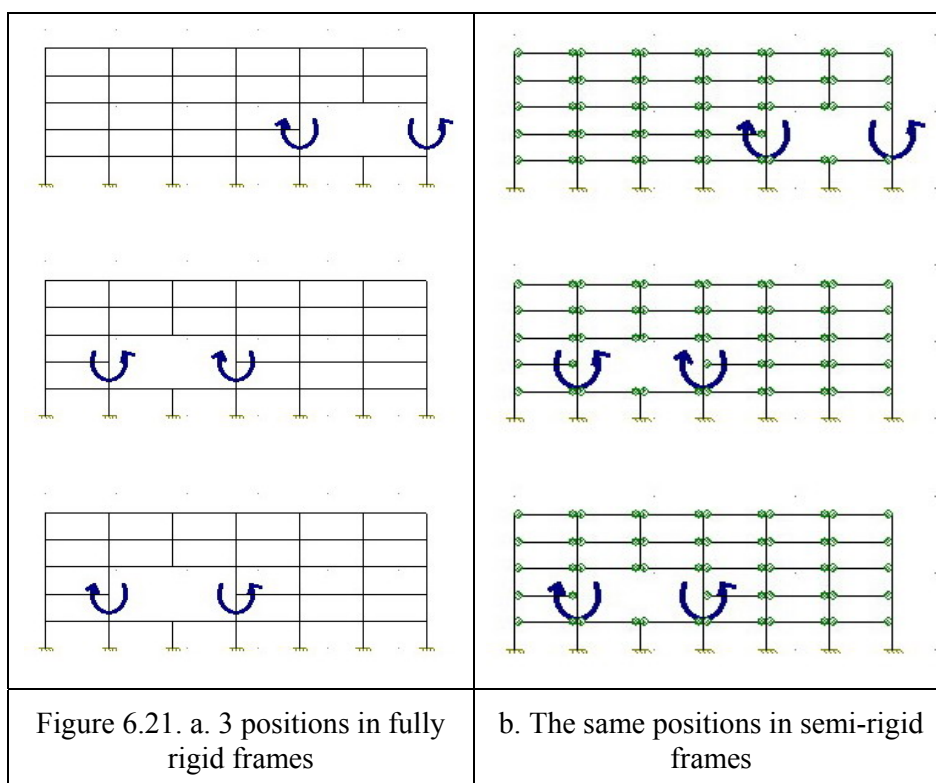
600A. Equivalently, three beam sections were chosen from the IPE table: IPE 160, IPE 270 and IPE 550. The properties of steel grade S355 were used. The frame was composed of 5 floors of 6 spans with a constant column height of 3.5 m and 4 beams of length 5 m, 7 m, 9 m and 11 m.

To validate not only the fully rigid frame but also the frames with semi-rigid connections, three elastic connections with an initial stiffness of 5000 kNm/rad, 50000 kNm/rad and 100000 kNm/rad were applied to the frame individually.

In each frame's configuration, three equivalent beam positions were selected. The investigation was performed by replacing the equivalent beam by a pair of bending moments equal to 10 kNm each applied to the beam ends. These are presented in Figure 6.21.

The analytical formulae were validated in 2 situations: for braced and unbraced frames. So, the total number of validations performed were

$$3 \text{ column sections} \times 3 \text{ beam sections} \times 4 \text{ beam lengths} \times 4 \text{ frame configurations} \times 3 \text{ positions} \times 2 \text{ boundary conditions} = 864$$



The results and the error percentages compared to the OSSA2D results are demonstrated in Table 6.1 for unbraced frames. The braced frame results were distributed similarly.

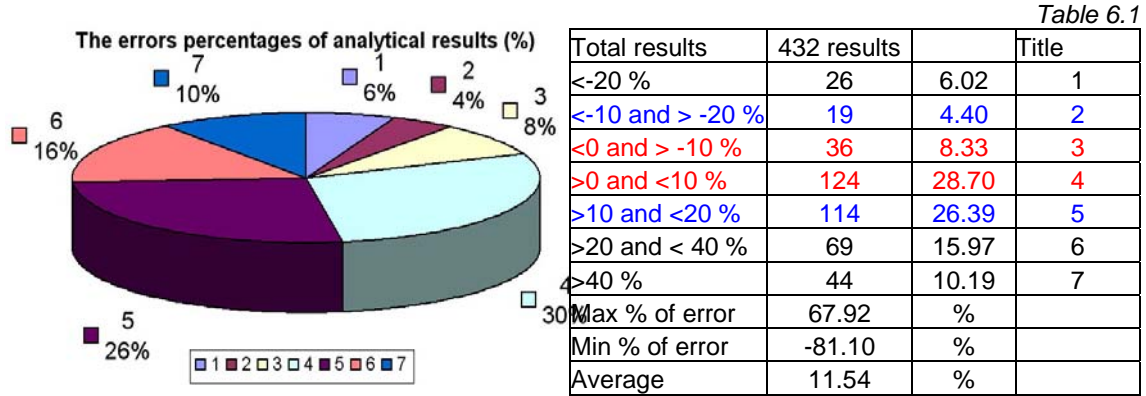


Chart 6.1. The error percentages of analytical results

In Chart 6.1 and Table 6.1, the results from 432 analyses are presented. The results were divided into 7 levels according to their percentage of errors in comparison with OSSA2D’s results. The 7 levels are as follows: less than -20%, greater than -20% and less than -10%, greater than -10% and less than 0%, greater than 0% and less than 10%, greater than 10% and less than 20%, greater than 20% and less than 40% and greater than 40%. They are also labeled from 1 to 7.

In particular, the number of analytical results which had absolute errors less than 10% and 20% was 160/432 and 293/432 respectively. Unfortunately, there still remain results with high errors, i.e., greater than 20%: 139/432.

Chart 6.2 presents the percentage of errors in the ratio between the column’s bending stiffness  $S_C$  and beam’s bending stiffness  $S_B$  in order to highlight the sensitivity of this ratio in the results. It can be concluded that, because the classic analysis method is applied, the accuracy of these results lessens when the column or the beam is very slender.

However, in the adjacent section with respect to  $K$ ,  $K$  is far less sensitive than  $K_S$ . Thus, the results are acceptable with an error of about 20%.

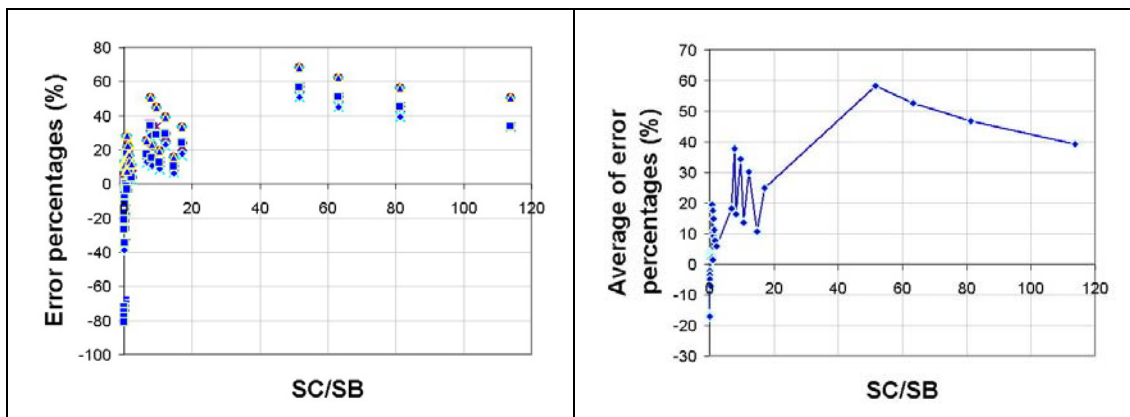


Chart 6.2. Error distribution for  $S_C/S_B$

### 6.4.6. Conclusion

Based on requirements established in the previous section, the partially restrained coefficient is introduced and obtained. The more practical formula for  $K_S$  is presented in Section 6.6.4, which includes semi-rigid frame properties. The formulae in Section 6.4.3 are modified by taking into account the initial stiffness of beam-to-column connections. A classic model of the beam segment with 2 semi-rigid joints is analyzed showing where the modifications are applied. The section finished on the  $K_S$  validations results.

Afterwards, the validation was carried out by comparing the analytical results and OSSA2D's results. 864 simulations were performed to carry out this wide-ranging validation. Based on the  $K$  formula's requirement, the formula of  $K_S$  is successfully validated.

The next section introduces the simulations performed to develop the equivalent beam model.

### 6.5. ANALYTICAL MODEL OF EQUIVALENT BEAM: 3-SPRING MODEL

The equivalent beam is investigated in this section. In Section 6.3, this structural member was identified as the main component of the directly affected part. In order to isolate its behavior in simulations, relevant assumptions need to be defined first.

The partially restrained coefficient  $K_S$  represents the continuity of the equivalent beam with respect to the surrounding members. Neglecting the axial deformation of the frame's members, the end sections could be assumed to be restrained in the vertical direction. In terms of the horizontal direction, the equivalent beam ends could move due to the bracing system of the frame. Figure 6.22 presents a simplified model of the individual equivalent beam.

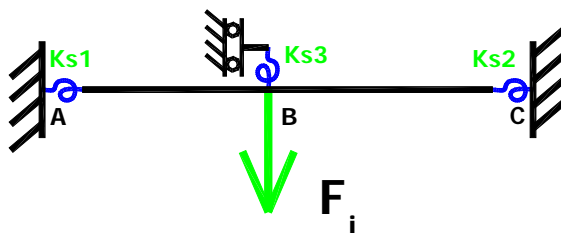


Figure 6.22. The simplified analytical model of the equivalent beam

The middle anti-rotational stiffness  $K_{S3}$  in Figure 6.22 represents the connection between

the middle column and the equivalent beam ABC. As presented in Section 6.3.1.b, the value of  $K_{S3}$  can be found by

$$K_{S3} = S_C = \frac{4E_c I_c}{L_c}. \quad (6.18)$$

### 6.5.1. Evaluation of the equivalent beam's stiffness

#### 6.5.1.a. Damage to the internal column

Using the model presented in Figure 6.21, the stiffness of the equivalent beam supporting the concentrated load  $N_{lost}$  was calculated with the finite element method in Figure 6.22. It includes 4 nodes and 3 beam elements which were presented in Section 6.4. The lengths of the elements are  $L_1$ ,  $L_2$  and  $L_3$ . Each element has an elastic modulus  $E_i$  and inertia  $I_i$ . The end springs  $K_{S1}$ ,  $K_{S2}$  and  $K_{S3}$  are predicted as in the previous sections.

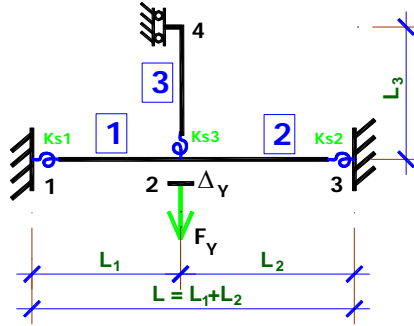


Figure 6.23. The FEM model to develop the analytical formula for the equivalent beam. Let  $K_B$  be the stiffness of the equivalent beam. The value of  $K_B$  is thus defined as

$$K_B = \frac{F_Y}{\Delta_Y}. \quad (6.19)$$

By calculating the value of  $\Delta_Y$  associated with  $F_Y$  using finite elements, then finding the limit value when length  $L_3$  tends to zero, the result is

$$K_B = \frac{3E_{B1}I_{B1}}{\alpha^2(\alpha-1)^2 L^3 \left[ 1 + \alpha(\gamma-1) - \frac{CD}{4H} \right]} \quad (6.20)$$

$$C = C_0 + C_1\beta_3; \quad D = D_0 + D_1\beta_3; \quad H = H_0 + H_1\beta_3 + H_2\beta_3^2; \quad (6.21)$$

where scalars  $C_i$ ;  $D_i$ ;  $H_i$  are functions of  $\beta_1, \beta_2, \alpha, \gamma$ . The formula is too complex to be solved by hand. The full version of the formula is presented in the Appendix.

$$\alpha = \frac{L_1}{L}; \quad \beta_1 = \frac{K_{S1}L}{E_{B1}I_{B1}}; \quad \beta_2 = \frac{K_{S2}L}{E_{B1}I_{B1}}; \quad \beta_3 = \frac{K_{S3}L}{E_{B1}I_{C1}}; \quad \gamma = \frac{E_{B2}I_{B2}}{E_{B1}I_{B1}} \quad (6.22)$$

where

$L_1, L_2$  are the lengths of the left and right parts of the beam,  
 $L$  is the whole equivalent beam length,  
 $E_{B1}, E_{B2}$  are the elastic moduli of the left and right parts of the beam,

and

$I_{B1}, I_{B2}$  are the inertia moments of the left and right parts of the beam.

### 6.5.1.b. Damage to the external column

Figure 6.24 demonstrates the isolated beam when the external column is destroyed. Unlike in the internal case, the beam's length is the same as before the accident. The model is of a one-beam element with two semi-rigid springs at both ends. The first spring  $K_S$  represents the influence of the adjacent part on the beam's behavior. The second spring  $K_{SC}$  shows the anti-rotational stiffness coming from the external column.

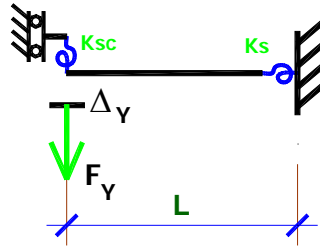


Figure 6.24. The analytical model of the side beam

So, the stiffness of the beam is given by

$$K_B = \frac{12(\beta_1 + \beta_2 + \beta_1\beta_2) E_B I_B}{L_B^3 (4\beta_1 + 4\beta_2 + \beta_1\beta_2 + 12)} \quad (6.22)$$

where

$$\beta_1 = \frac{K_{SC} L_B}{E_B I_B}; \quad \beta_2 = \frac{K_S L_B}{E_B I_B}; \quad (6.23)$$

$L_B$  is the side span beam's length,  
 $E_B$  is the elastic modulus of the beam, and  
 $I_B$  is the inertia of the beam.

## 6.5.2. Simplification of the equivalent beam's stiffness for practical use

### 6.5.2.a. The case of constancy EI

When  $E_{B1} I_{B1} = E_{B2} I_{B2} = \text{const}$  throughout the column's height, the formula for  $K_B$  can be simplified:

$$K_B = \frac{3E_B I_B}{\alpha^2 (\alpha - 1)^2 L^3 \left[ 1 - \frac{A}{4B} \right]} \quad (6.25)$$

$$\begin{aligned} A &= A_0 + A_1 \beta_3 & B &= B_0 + B_1 \beta_3 \\ A_0 &= a_{0,0} + a_{0,1} \alpha + a_{0,2} \alpha^2 & B_0 &= b_{0,0} \\ A_1 &= a_{1,0} + a_{1,1} \alpha + a_{1,2} \alpha^2 + a_{1,3} \alpha^3 + a_{1,4} \alpha^4 & B_1 &= b_{1,0} + b_{1,1} \alpha + b_{1,2} \alpha^2 + b_{1,3} \alpha^3 + b_{1,4} \alpha^4 \\ a_{0,0} &= -16\beta_1 - 4\beta_2 - 4\beta_1 \beta_2 & b_{0,0} &= -12 - 4\beta_1 - 4\beta_2 - \beta_1 \beta_2 \\ a_{0,1} &= 16\beta_1 - 8\beta_2 + 4\beta_1 \beta_2 & & \\ a_{0,2} &= -4\beta_1 - 4\beta_2 - 4\beta_1 \beta_2 & & \\ a_{1,0} &= -16 - 4\beta_2 & b_{1,0} &= -4 - \beta_2 \\ a_{1,1} &= 64 - 16\beta_1 + 20\beta_2 - 4\beta_1 \beta_2 & b_{1,1} &= 12 - 4\beta_1 + 4\beta_2 - \beta_1 \beta_2 \\ a_{1,2} &= -64 + 52\beta_1 - 32\beta_2 + 17\beta_1 \beta_2 & b_{1,2} &= -12 + 12\beta_1 - 6\beta_2 + 4\beta_1 \beta_2 \\ a_{1,3} &= -52\beta_1 + 4\beta_2 - 26\beta_1 \beta_2 & b_{1,3} &= -12\beta_1 - 6\beta_1 \beta_2 \\ a_{1,4} &= 12\beta_1 + 12\beta_2 + 13\beta_1 \beta_2 & b_{1,4} &= 3\beta_1 + 3\beta_2 + 3\beta_1 \beta_2 \end{aligned}$$

where

$$\alpha = L_1 / L; \quad \beta_1 = \frac{K_{S1} L}{E_B I_B}; \quad \beta_2 = \frac{K_{S2} L}{E_B I_B}; \quad \beta_3 = \frac{K_{S3} L}{E_B I_B}.$$

#### 6.5.2.b. Using $\alpha=0.5$

In general, in a typical building, beam lengths are uniform, so it can be assumed that  $\alpha = 0.5$ . In this case, the general formula for  $K_B$  could be simplified as:

$$K_B = \frac{192E_B I_B (\beta_1 \beta_2 \beta_3 + 16\beta_1 \beta_2 + 5\beta_2 \beta_3 + 5\beta_1 \beta_3 + 64\beta_1 + 64\beta_2 + 16\beta_3 + 192)}{L^3 (\beta_1 \beta_2 \beta_3 + 16\beta_1 \beta_2 + 8\beta_2 \beta_3 + 8\beta_1 \beta_3 + 112\beta_1 + 112\beta_2 + 64\beta_3 + 768)}. \quad (6.26)$$

#### 6.5.2.c. Using the same $K_S$ for both ends' rotational stiffness

As discussed in Sections 6.4.2 and 6.4.3, the value of  $K_S$  depends on the position of the investigated point within the frame. At an internal position,  $K_S$  on both sides of the equivalent beam could be considered to have the same value as  $\beta_1 = \beta_2$ .

In addition, the influence of the middle column, which is connected to the equivalent beam, would act only when there is rotation in the middle section. So the equivalent beam's stiffness could be calculated in the case  $\alpha = 0.5$  as follows:

$$\mathbf{K}_B = \frac{192E_B I_B (\beta_1 + 2)}{L^3 (\beta_1 + 8)}. \quad (6.27)$$

### 6.5.3. Validation

The following validations were performed according to the procedure presented in Section 4.5.1.

#### 6.5.3.a. Validation of the model and the substructure

##### *\*) The model with real $\mathbf{K}_S$ taken from the actual frame*

Before beginning the analytical calculation of  $\mathbf{K}$ , the validations of the equivalent beam's extraction were performed. With the 3-spring model described above, if  $\mathbf{K}_S$ , which is measured on the real frame, is applied, the analytical results are expected to be equal to the FEM results.

##### *\*\*\*) Validation of analytical $\mathbf{K}$*

The analytical substructure's validations were organized while the 3-spring model was built.

#### 6.5.3.b. Testing methods

##### *\*) Validation of the 3-spring model*

Six groups of models were calculated to compare the analytical results to the numerical results. There were 8 sections in one group (HEA 140, HEA 180, HEA 220, HEA 240, HEA 260, HEA 300, HEA 320, HEA 340), with the parameters listed in Table 1. The parameter  $\alpha$  and the partially restrained stiffness  $\mathbf{K}_S$  were varied. In total, 64 tests were carried out.

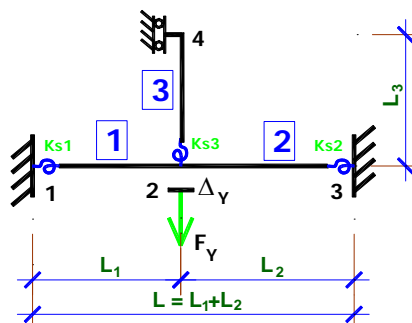


Figure 6.25. The 3-spring model



**\*\*\*) Validation of the simplified model**

To validate the substructure model, 3 groups of frames with 5 different beam lengths, 3 different collapsed column positions and 3 different sections were analyzed.

The displacements were taken from OSSA2D and compared to the analytical substructure's results. The input data for the analytical formula came from the numerical  $K_S$  which was measured for each column. The percentage of error is presented in Tables 6.2 and 6.3.

**\*\*\*) The  $K$  formula validation**

Figure 6.26 presents the frame configurations which were investigated using OSSA2D and simulated using analytical substructures. Here, the circles mark the positions of damaged columns and the squares represent the position of points where  $K_S$  was measured.

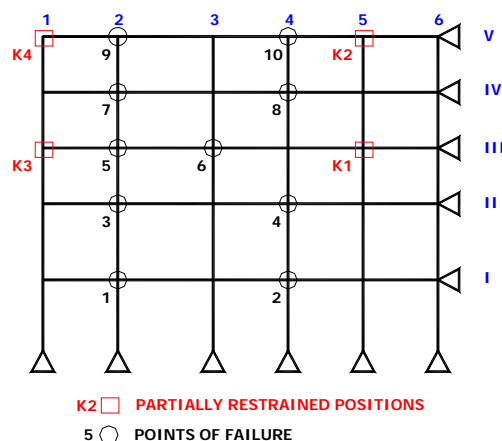


Figure 6.26. Tested frame configuration

For steel frames as well as composite frames, the 4 sections of columns (steel: HEA 140, HEA 220, HEA 450, HEA 600) and the 8 sections of beams (steel: IPE 160, IPE 270, IPE 400, IPE 550; composite: IPE 160 + Slab 150, IPE 270 + Slab 200, IPE 400 + Slab 200, IPE 550 + Slab 250) included in these tests are listed below with their associated results. These sections' dimensions cover most of the steel profile catalogue. Next, a typical 5-floor, 5-span frame's geometry was investigated. 10 positions of the damaged column were simulated, one by one. After that, 4 beam lengths were applied to this frame's geometry. Included were different boundary conditions such as the braced frame and unbraced frame, as well as different types of frames (i.e., steel and composite) and different connections (i.e., fully rigid and semi rigid). In total, 3840 frames were simulated.

6.5.3.d. Results

Table 6.2: The result of individual column model

| No | Section | L | Alpha | k1   | k2   | k3   | Disp    | F   | Kanalysis | Kossad  | %        |
|----|---------|---|-------|------|------|------|---------|-----|-----------|---------|----------|
| 1  | HE140A  | 7 | 0.500 | 2000 | 4000 | 5000 | 0.12926 | 100 | 773.66    | 773.64  | -0.00216 |
| 2  | HE180A  | 7 | 0.500 | 2000 | 4000 | 5000 | 0.06997 | 100 | 1429.11   | 1429.08 | -0.00200 |
| 3  | HE220A  | 7 | 0.500 | 2000 | 4000 | 5000 | 0.04125 | 100 | 2423.95   | 2424.50 | 0.02290  |
| 4  | HE240A  | 7 | 0.500 | 2000 | 4000 | 5000 | 0.03167 | 100 | 3157.32   | 3157.31 | -0.00045 |
| 5  | HE260A  | 7 | 0.500 | 2000 | 4000 | 5000 | 0.02520 | 100 | 3967.81   | 3967.80 | -0.00026 |
| 6  | HE300A  | 7 | 0.500 | 2000 | 4000 | 5000 | 0.01597 | 100 | 6260.28   | 6260.28 | -0.00009 |
| 7  | HE320A  | 7 | 0.500 | 2000 | 4000 | 5000 | 0.01313 | 100 | 7614.00   | 7614.00 | -0.00006 |
| 8  | HE340A  | 7 | 0.500 | 2000 | 4000 | 5000 | 0.01112 | 100 | 8991.53   | 8991.52 | -0.00005 |

Table 6.3: Comparing the results with real  $K_S$  from an actual frame

HEA 160 - IPE 140 - L = 7

Group 1 - position II-2-3

| No | L  | k1ossad  | k2ossad  | DisOssS      | DisAnaS     | %        | Dis in frame | %ossad   | %ana     |
|----|----|----------|----------|--------------|-------------|----------|--------------|----------|----------|
| 1  | 5  | 4819.473 | 4455.111 | 0.0793706860 | 0.079370766 | -0.00010 | 0.0793705796 | -0.00013 | -0.00024 |
| 2  | 7  | 4231.423 | 3915.380 | 0.0824127009 | 0.082412783 | -0.00010 | 0.0824059943 | -0.00814 | -0.00824 |
| 3  | 9  | 3877.266 | 3595.758 | 0.0845762321 | 0.084576318 | -0.00010 | 0.0845728410 | -0.00401 | -0.00411 |
| 4  | 11 | 3634.101 | 3374.862 | 0.0862555420 | 0.086255626 | -0.00010 | 0.0862541286 | -0.00164 | -0.00174 |
| 5  | 12 | 3537.630 | 3286.934 | 0.0869721114 | 0.086972195 | -0.00010 | 0.0869704662 | -0.00189 | -0.00199 |

Table 6.4 presents an overview on the percentage of error for analytical  $K$  values compared to the numerical results. The results show a higher accuracy for  $K$  than for the result for  $K_S$  before. Also, it proves that the analytical  $K$  value tends to be higher than the real results. Therefore, it can be concluded that the analytical result obtained in this way is somewhat unsafe.

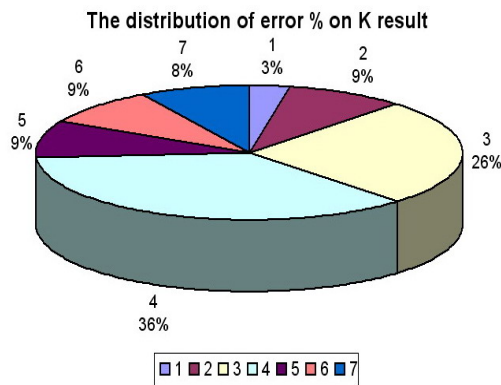


Chart 6.3. Distribution of  $K$  errors

Table 6.4

| Total results    | 640 results |       | Title |
|------------------|-------------|-------|-------|
| <-20 %           | 19          | 2.97  | 1     |
| <-10 and > -20 % | 58          | 9.06  | 2     |
| <0 and > -10 %   | 165         | 25.78 | 3     |
| >0 and <10 %     | 230         | 35.94 | 4     |
| >10 and <20 %    | 57          | 8.91  | 5     |
| >20 and < 40 %   | 57          | 8.91  | 6     |
| >40 %            | 54          | 8.44  | 7     |
| Max % of error   | 89.74       | %     |       |
| Min % of error   | -94.37      | %     |       |
| Average          | 6.76        | %     |       |

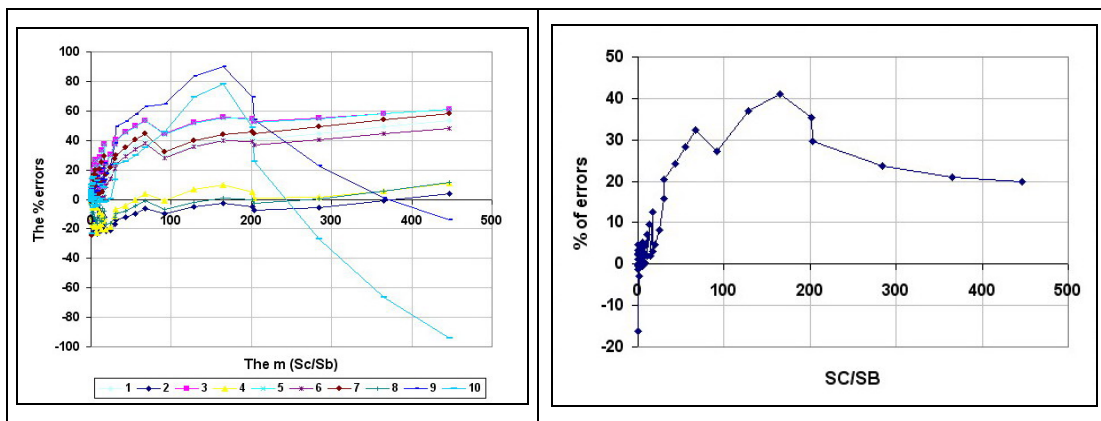


Chart 6.4.  $K$  Error distribution for  $S_C/S_B$

### 6.5.4. Conclusion

The current section has concentrated on the calculation of the equivalent beam's stiffness. Before going into detail, the equivalent beam's analytical model – called the 3-spring model – has been defined by simplifying the proposal given in Section 6.4.2. There are 2 models associated with the specific positions of the destroyed columns: external and internal damaged columns.

Throughout, this section has described the procedure for developing the FEM model to simulate the equivalent beam and a means of obtaining analytical stiffness. The full stiffness formula is presented here only in its abridged form due to its complexity. Using the properties of a typical building frame, simplified formulae have been proved step by step. Finally, the formula was also verified by hand.

## 6.6. RESISTANCE OF THE DIRECTLY AFFECTED PART

### 6.6.1. Simple example and collapse scenarios

To demonstrate the behavior and resistance of the directly affected part, a short example will now be investigated. The sub-structure has been extracted from the normal frame as shown in Figure 1. There are  $n$  equivalent beams and  $n-1$  middle columns. Because a typical frame was used, only one section has been applied to all of the beams. The beam's spans on both sides are equivalent. The influence of the surrounding members is also neglected to keep this example as simple as possible. All of the beams' ends are assumed to have fully rigid connections.

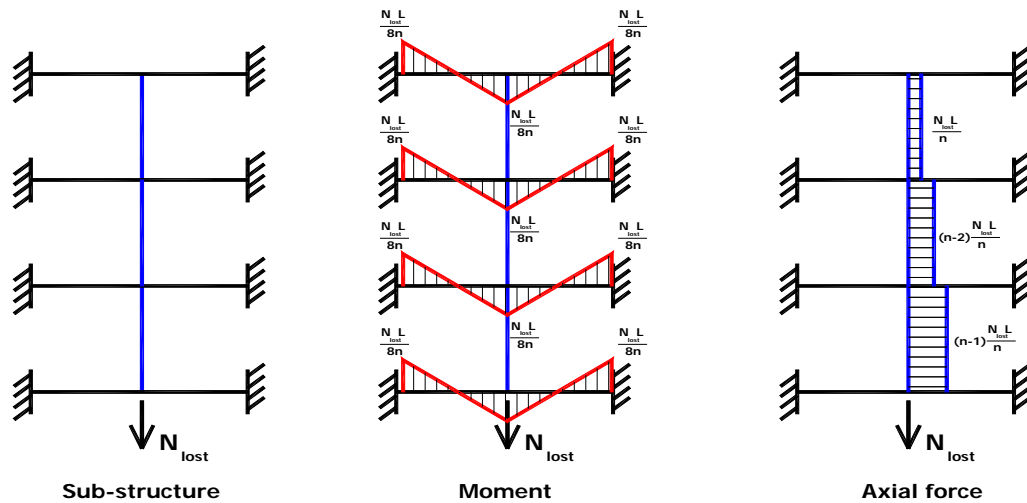


Figure 6.27. Substructure and the internal force distribution

To calculate the critical resistance  $N_{lost}^{Pl.Rd}$ , the additional load  $N_{lost}$  was applied progressively to the damaged column's top point. The limit plastic moment of the beam section is uniform and equals  $M_p^B$ . The plastic limit of the axial force in the middle column section is  $N_p$ .

The catenary load  $N_{lost}$  acting on the structure produced the bending moment on the beam with the highest value at both ends and at the midpoint of the column. Figure 6.27 shows the axial forces in the middle columns. The axial force in the column, where the force  $N_{lost}$  was directly applied, reaches the highest value. The maximum values are

$$M_{max} = \frac{N_{lost} L}{8n}; \quad N_{max} = \frac{(n-1) N_{lost}}{n} \quad (6.28)$$

where  $M_{max}; N_{max}$  are the maximum internal forces,

$n$  is the number of floors within the directly affected part, and  
 $L$  is the equivalent beam's full length.

Because the load  $N_{lost}$  increases progressively, three scenarios may come about depending on the relation between the values of  $N_P$  and  $M_P^B$ . An elastic—perfectly plastic material is applied.

There are three separate critical plastic resistances to be defined before calculating the whole part's resistance. The first plastic limit to be considered is the resistance of a single equivalent beam:

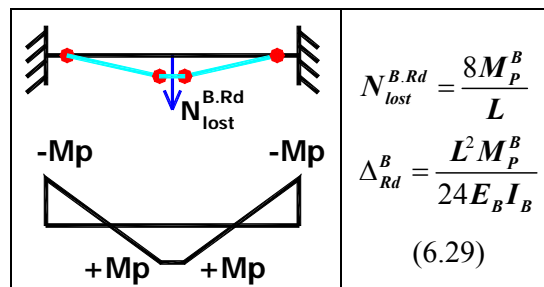


Figure 6.28. Resistance of the single equivalent beam

The second plastic limit is obtained in the case where all of the beams yield.

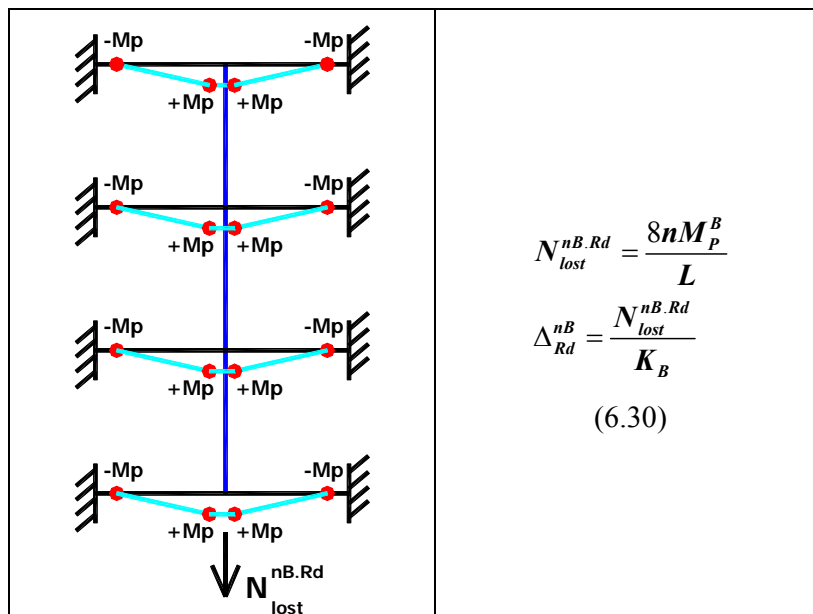


Figure 6.29. Resistance of the fully yielded beams

Finally, the last resistance value is the fully plastic yield of the middle column under tension:

$$\begin{aligned}
 N_{max} &= \frac{(n-1)N_{lost}^{C.Rd}}{n} = N_p \\
 N_{lost}^{C.Rd} &= \frac{nN_p}{(n-1)} \\
 \Delta_{Rd}^C &= \frac{N_{lost}^{C.Rd}}{K_{nB}}
 \end{aligned} \tag{6.31}$$

where

$N_{max}$  is the maximum axial force value,  
 $n$  is the number of columns within the structure,  
 $N_{lost}^{C.Rd}$  is the individual middle column resistance, and  
 $K_{nB}$  is the directly affected part's stiffness end  $n$  beams.

As discussed previously, the behavior of this structure depends on the relationship between the three resistances described above.

6.6.1.a. First scenario:  $N_{lost}^{C.Rd} > N_{lost}^{nB.Rd}$

In this simulation, the load was distributed within the structure as shown in Figure 6.27. Following the increase in load  $N_{lost}$ , the bending moment at the beam ends and the axial force acting on the middle both increase. Because  $N_{lost}^{C.Rd} > N_{lost}^{nB.Rd}$  when the bending moment in beam sections reaches the plastic limit, the axial force in the column is still less than its resistance:

$$\begin{aligned}
 N_{lost}^{C.Rd} > N_{lost}^{nB.Rd} &\rightarrow \frac{nN_p}{(n-1)} > \frac{8nM_p^B}{L} \\
 N_p &> \frac{8(n-1)M_p^B}{L}
 \end{aligned} \tag{6.32}$$

When the beam sections reach their plastic limit, the bending moment equals  $M_p$ . The force  $N_{lost}$  takes on the value

$$N_{lost}^{nB.Rd} = \frac{8nM_p^B}{L} \tag{6.33}$$

The displacement of the loaded point is

$$\Delta_1 = \frac{N_{lost}}{K_{nB}} = \frac{N_{lost}^{nB.Rd}}{K_{nB}} = \frac{8nM_p^B}{K_{nB}L} \tag{6.34}$$

where

$n$  is the number of floors within the directly affected part,  
 $N_{lost}^{nB.Rd}$  is the whole  $n$  equivalent beam's resistance,

$\Delta_1$  is the displacement of the loaded point, and  
 $M_p^B$  is the plastic bending moment of the beam section.

Due to the elastic—perfectly plastic behavior of the beam section, when the bending moment reaches that limit, the section fully yields. None of the beams can withstand the additional load anymore; as a result, the structure totally collapses.

The load-deflection relation in this case can be represented as seen below.

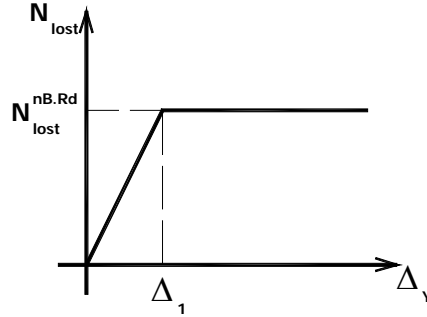


Figure 6.30. Loading process in the first scenario

6.6.1.b. *Second scenario:*  $N_{lost}^{B.Rd} < N_{lost}^{C.Rd} < N_{lost}^{nB.Rd}$

The structure's behavior is entirely different if the column's resistance  $N_{lost}^{C.Rd}$  is less than the whole equivalent beam's resistance  $N_{lost}^{nB.Rd}$ . Because the column's resistance was less than the resistance of all beams put together, the internal forces would crush the column while the bending moment of the beam remained within the elastic range. The failed column was the directly loaded one – the bottom segment. The load at that moment was obtained from the value of the third resistance above (6.31) and repeated here for clarity's sake.

$$N_{lost}^{C.Rd} = \frac{nN_p}{(n-1)}$$

$$\Delta_2 = \frac{N_{lost}}{K_{nB}} = \frac{N_{lost}^{C.Rd}}{K_{nB}} = \frac{nN_p}{(n-1)K_{nB}} \quad (6.35)$$

where  $\Delta_2$  is the displacement of the loaded point.

The same elastic—perfectly plastic behavior was applied to the column; as a result, the column yielded. The beam which directly supported the load as separated from the other parts of the structure.

Then, because the force was equal to the column's resistance, but higher than the

individual beams' resistance, the bottom beam yielded immediately. This collapse is easily recognizable in the figure below, showing the load-displacement curve recorded.

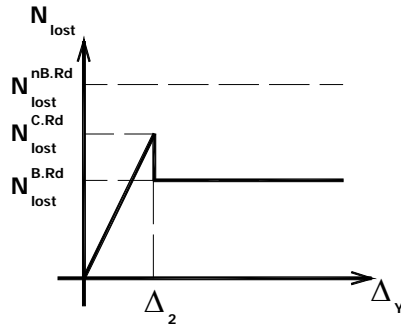


Figure 6.31. Loading process in the second scenario

6.6.1.c. Last scenario:  $N_{lost}^{C.Rd} < N_{lost}^{B.Rd}$

In the last scenario, the substructure was loaded in the same way. For the first part of the loading process, the structure behaved as in the second scenario. The load increase led to the first column yielding at the same moment.

$$N_{lost}^{C.Rd} = \frac{nN_p}{(n-1)}$$

$$\Delta_2 = \frac{N_{lost}}{K_{nB}} = \frac{N_{lost}^{C.Rd}}{K_{nB}} = \frac{nN_p}{(n-1)K_{nB}}$$

When the column fully yielded and could not transfer the additional load, the bottom equivalent beam was separated from the structure. But in this case, the single beams' resistance was higher than the column's resistance, so the remaining structure still functioned. More loading could be applied to the residual structure until the bottom beam reaches its limit.

The final displacement at the moment of collapse is described as

$$\Delta_3 = \Delta_2 + \frac{N_{lost}}{K_B} = \Delta_2 + \frac{N_{lost}^{B.Rd}}{K_B} = \Delta_2 + \frac{N_{lost}^{B.Rd} L^3}{192E_B I_B} \quad (6.36)$$

where

- $K_B$  is the single equivalent beam's stiffness,
- $N_{lost}^{B.Rd}$  is the single column's resistance, and
- $E_B I_B$  is the elastic modulus and inertia moment of the beam.



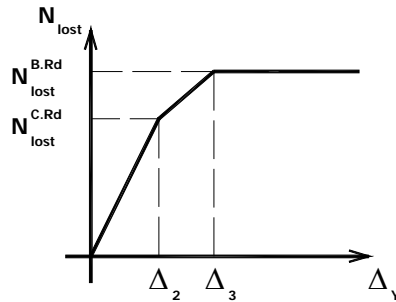


Figure 6.32: Loading process in the third scenario

### 6.6.2. Individual equivalent beam's load carrying curve – 1<sup>st</sup> order plastic hinge-by-hinge analysis

With the 3-spring model in Figure 6.22 and the semi-rigid beam element in Figure 6.19, the first-order plastic simplified analysis was carried out with 2 other basic assumptions:

- the structure was made of ductile material that could undergo large deformations beyond the elastic limit without fracturing or buckling;
- the deflections of the structure under loading were small enough that second-order effects could be ignored.

Hinge-by-hinge analysis, which was used in this calculation, determines the order of plastic hinge formation using the load factor associated with each plastic-hinge formation and member forces in the frame following each successive hinge formation. The procedure is as follows:

- 1) In the beginning, the model was solved by first-order analysis. Each member's internal forces and each node displacement were predicted.
- 2) Next, the maximum bending moment section was estimated. That section is the first section at which the plastic hinge formed. Because of the first-order elastic state of the frame, the critical load and the consequent displacement were calculated by a scalar multiplication of the initial load factor.

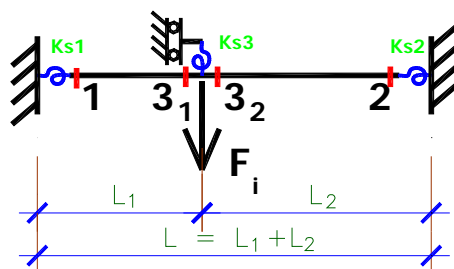
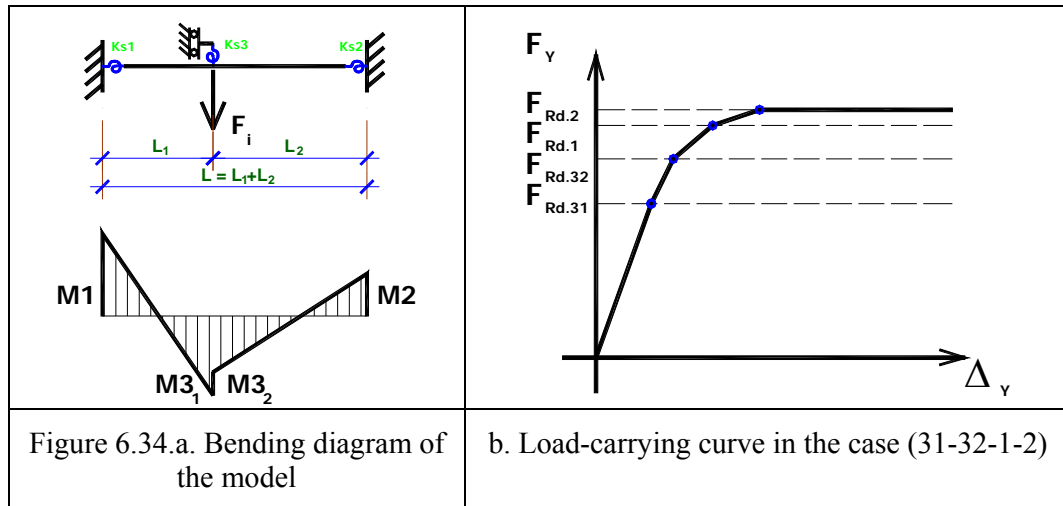


Figure 6.33. Critical sections on the model

Thus, the section which had yielded first was replaced by a perfect hinge, and the plasticity bending moment  $M_p^B$  was applied to that section. In the algorithm, the semi-rigid end for that section took on an exceptionally small stiffness value ( $10^{-7}$ ). The applied load increased continuously, while the bending moment increased in the remaining critical sections. The highest value of the three remaining sections was used to identify the second plastic hinge.

These steps were repeated until all four sections yielded. A full analytical calculation is given in the Appendix. Figure 6.34 presents a diagram of the bending moment of the general equivalent beam model and the load-carrying curve of that beam in the case where a plastic hinge appeared in the order 3<sub>1</sub>-3<sub>2</sub>-1-2.

The values of  $M_1$ ,  $M_2$ ,  $M_{3_1}$ , and  $M_{3_2}$  depend on the physical parameters of the directly affected part such as the floor heights  $L_1$  and  $L_2$  or the rotational stiffness  $K_{s1}$ ,  $K_{s2}$ , and  $K_{s3}$ . While the additional load was applied, the bending moment appeared with high values at these 4 critical sections. The column collapsed when all four critical sections yielded. The highest bending moment could be at any of these sections depending on the relationship between the stiffness of the equivalent beam segments and the three springs' stiffness. After the first then all four sections had yielded, the beam stiffness decreased. Also, with the 3-spring model, the expected behavior of the beam in the case of the elastic—perfectly plastic material was a tri-linear or quadri-linear diagram. The stiffness  $K_B$  had 3 or 4 values when the applied load changed.



### 6.6.3. Assembling the components' curves

In a real frame, the directly affected part's behavior is more complex than the simple case given previously in Section 6.6.1. In that example, the substructure's behavioral curve had 2 or 3 segments only, depending on whether the order of the members reached its limit. That simple characteristic came from the simple elastic—perfectly plastic behavior of each column or beam. However, the extracted member of the real frame has a more complex behavior. As illustrated in Section 6.5, there are 3 individual rotational springs and 2 beam segments in the model. The expected beam's behavior should be represented by 3 or 4 linear curves.

Moreover, a real frame beam also includes two beam—column connections at both ends. In a more detailed analysis, the elastic—plastic behavior of the beam would change according to the resistance of the connection.

The substructure's resistance included all of the members' resistance, according to compatibility and equilibrium rules. Then the simplified method from EC4 was used. Next, each basic member's resistance was obtained. After that, each member's resistance curve was added step by step into the substructure's behavioral curve. The method of assembly is reviewed below:

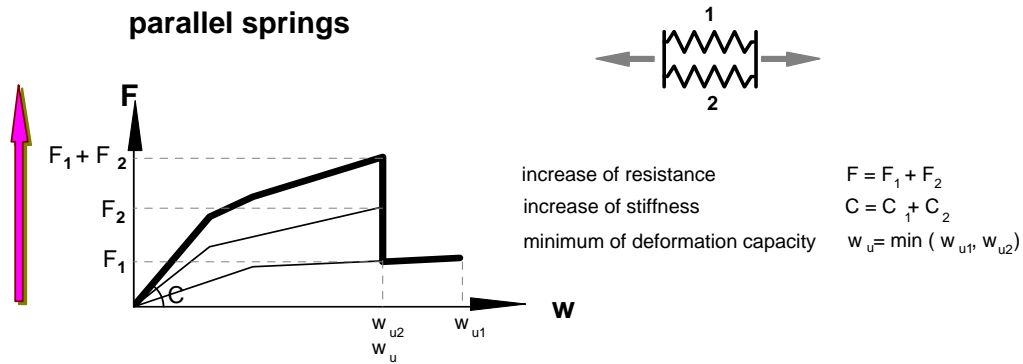


Figure 6.35. Assembly of parallel spring groups [SSEDTA, 2000]

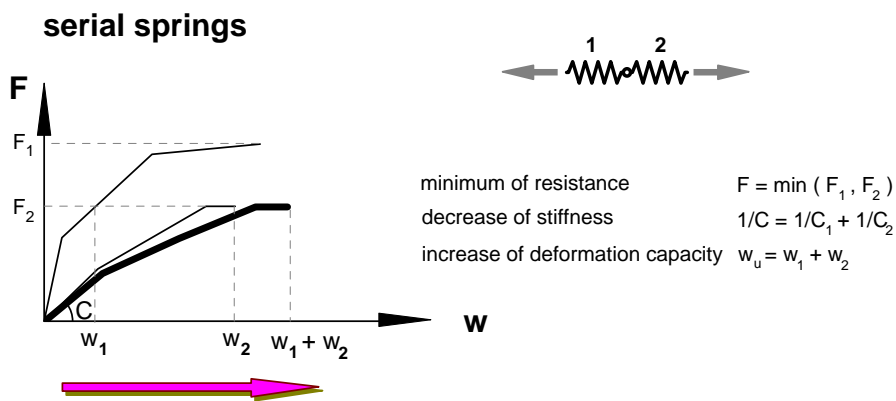


Figure 6.36. Assembly of serial spring groups [SSEDTA, 2000]

#### 6.6.4. Quick-estimation method for $N_{lost}^{Pl.Rd}$

Sections 6.6.2 and 6.6.3 present the method for developing the detailed elastic perfectly plastic behavior of the directly affected part. The load-displacement curve was derived from a combination of the behavioral curves of beams and columns within it.

In addition, the capacity of the column under tension was usually higher than the capacity of the equivalent beam under bending. The additional load led to a plastic yield in the beam before the column failed. In most cases, the directly affected part failed when all the equivalent beam's end sections yielded.

Since the source of failure is known, with the simple elastic—perfectly plastic calculation, the critical value  $N_{lost}^{Pl.Rd}$  was easily obtained. Figure 6.37 presents the two plastic limit states of the individual internal and external beams. Since the columns did not reach their plastic limit, the plastic limit of the directly affected part's model is equal to the sum of the beams' limits.

The general individual beam's plastic limit is

$$N_{lost}^{B.Rd} = \frac{M_P^{B.1} + M_P^{B.31} + \frac{\alpha}{1-\alpha} (M_P^{B.2} + M_P^{B.32})}{\alpha L_B} \quad (6.37)$$

where

$$\alpha = \frac{L_1}{L_B} \quad \text{is the ratio of the left span to whole equivalent beam length.}$$

In the case of plastic bending moments if all four sections are similar and equal  $M_P^B$  then

$$N_{lost}^{B.Rd} = \frac{2M_P^B}{\alpha(1-\alpha)L_B}. \quad (6.38)$$

Similarly, when an external column is destroyed,

$$N_{lost}^{B.Rd} = \frac{M_P^{B.1} + M_P^{B.2}}{L_B} \quad (6.39)$$

where the constant section bending moment of  $M_P^B$  the beam limit is

$$N_{lost}^{B.Rd} = \frac{2M_P^B}{L_B}. \quad (6.40)$$

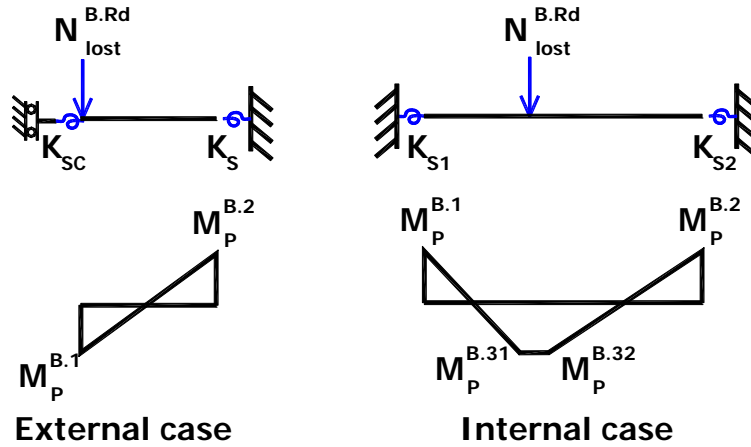


Figure 6.37. The individual beam's resistance

Then the directly affected part's resistance is easily estimated by

$$N_{lost}^{Rd} = \sum_{i=1}^n N_{lost.i}^{B.Rd} \quad (6.41)$$

where

$$N_{lost.i}^{B.Rd} \quad \text{is the resistance of beam number } i, \text{ and}$$

$$n \quad \text{is the number of floors within the directly affected part.}$$

### 6.6.3. Validation

Because the quick estimation method used to predict the directly affected part's resistance was based on a well-known plastic limit analysis, the validation performed in this section will consider only the validation of the extracted resistance in comparison to the real frame.

The validations were performed on the frame illustrated in Figure 6.38. This frame configuration was the object of investigation for the FRCS project "Robust structure by ductile joint" [RFSCR-04046, 2006]. The behavior of the frame was numerically simulated and calibrated by ABAQUS and FINELG in the same project thanks to PSP and Demonceau.

The frame had 7 spans and 6 floors. The span length and the floor height are uniform. The column material was HE 360A and the beam sections were IPE400v. The loads applied are listed below:

| Load No | Meaning                     | Position                   | Magnitude  |
|---------|-----------------------------|----------------------------|------------|
| 1       | Column self weight          | All columns                | 1.099 kN/m |
| 2       | Beam self weight            | All beams                  | 0.849 kN/m |
| 3       | Permanent load of all beams | All beams except top floor | 22.05 kN/m |
| 4       | Permanent load on the top   | On the roof                | 18.60 kN/m |
| 5       | Snow load                   | On the roof                | 3.25 kN/m  |
| 6       | Live load                   | All beams except top floor | 21.00 kN/m |

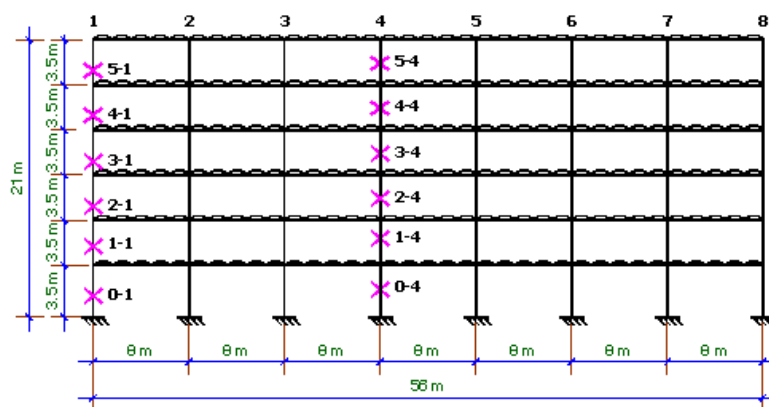


Figure 6.38. The frame configuration under investigation

According to the presentation in the previous section, the stiffness and the resistance of the directly affected part depend on the equivalent beams. Chart 6.3 presents the load-carrying curves for the damaged column's top points in 7 situations. The horizontal dashed lines represent the analytical values of the resistance which came from quick estimations. As demonstrated in the chart, the analytical results calculated by the first-order elastic—

perfectly plastic limit analysis did not describe the nonlinear behavior of the frame well. The idealistic assumptions on the boundary conditions of the model also neglected the influence of surrounding members, so the analytical results were lower than in reality. However, due to safety reasons, these inaccuracies were accepted.

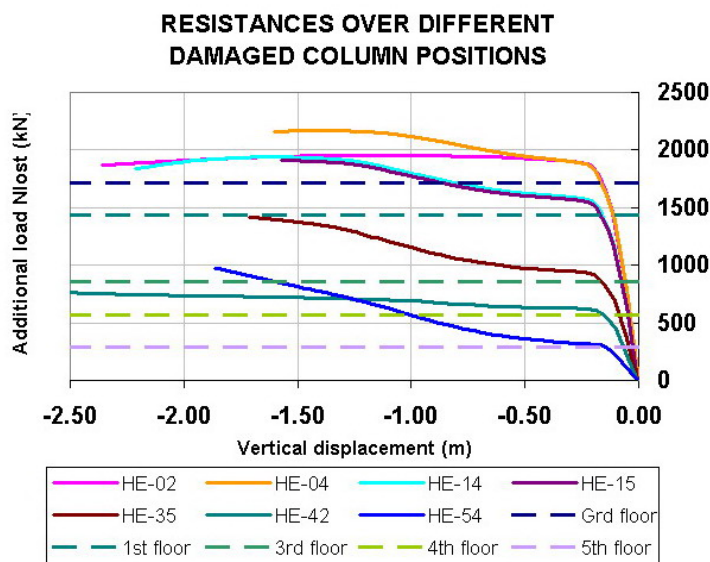


Chart 6.5. The resistances of the directly affected part for different damaged column positions

#### 6.6.4. Conclusion

The critical value  $N_{lost}^{Pl.Rd}$  represents an important state of the directly affected part when the behavior of the frame becomes fully non-linear. Figure 5.7 is repeated below to demonstrate these difference in behavior exhibited by the directly affected part.

In the figure, Load Phase 2 is limited from point (2) to point (4). It demonstrates the progressive disappearance of the column. From point (2) to (3), given certain assumptions for other parts of the frame, e.g. that adjacent columns are still stable, the directly affected part works within the elastic range. Point (3) shows the position of the first plastic hinge when it appears in the equivalent beam. As presented in Section 6.6, the directly affected part's behavior is very complex after that point. At this point, nonlinear and second-order effects play a role in the curve segment (3, 4). The full results for the directly affected part in Section 6.6 are shown in the approximate curve of Figure 5.7 from point (2) to point (4).

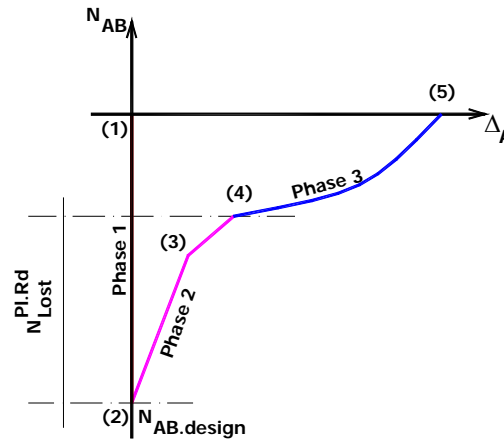


Figure 5.7. The axial force and deflection of top point of damaged column

Moreover, the more practical method for quickly estimating the value of  $N_{lost}^{Pl.Rd}$  was performed in the last part of Section 6.6. Based on the fact that the equivalent beam normally fails before the middle column and the other parts of the frame, a simple plastic limit calculation was carried out. Its validation demonstrated the advantage of this analytical method.

## 6.7. SUMMARY AND CONCLUSIONS

This chapter completed the full investigation of the directly affected part. This is one of three main subjects which are presented in the present thesis. In Chapter 3, the building frame's behavior was defined by the load-carrying curve of the damaged column's top point. Then, the behavior of the directly affected part, throughout the loading process, was investigated in this chapter, giving a better understanding of this concept.

However, as proved in this chapter, the directly affected part's behavior is a complex one which depends on many parameters, e.g. the structural configuration of the frame, the position of the damage and the material's properties. Given the boundary conditions and the compatibility of the members within the part, the substructure was developed. The substructure was analyzed in order to predict both stiffness and resistance in such a zone.

As illustrated in Sections 6.3 and 6.6, the main behavior and limits of the affected part are primarily linked to the behavior of the equivalent beam. To investigate this link, the beam's analytical model was developed as a 3-spring model. The substructure model requires that the adjacent column keep stable and be able to support to the transferred internal forces. Chapter 7 will explore this requirement.



The next chapter describes the integrity of the adjacent part, namely adjacent column zones and their effect on the behavior of the entire part. The investigation concentrates on the special behavior of the alternative load path forming the arch effect. The main parameters, which influence the axial forces appearing within the equivalent beams, are derived. With this knowledge, the conditions for the survival of the frame can finally be proposed.

**CHAPTER 7: ANALYTICAL MODEL TO INVESTIGATE THE  
ADJACENT COLUMNS AND ARCH EFFECT**

## 7.1. INTRODUCTION

As presented in Chapter 5, the alternative load path appears after point (2) of the load-carrying curve in Figure 5.7 and continues until the additional load  $N_{lost}$  reaches the value of design load  $N_{design}$ . The load path involves 2 zones: the directly affected part and its adjacent columns. Figure 5.5 is repeated here to recall the trajectory of the alternative load path and the zones involved in it.

Back to Chapter 4, the column placed at the end of the equivalent beam is called the *adjacent column* because of its position next to the damaged one. In addition, because that column is a side member of the directly affected part, it is also sometimes called the *column beside*.

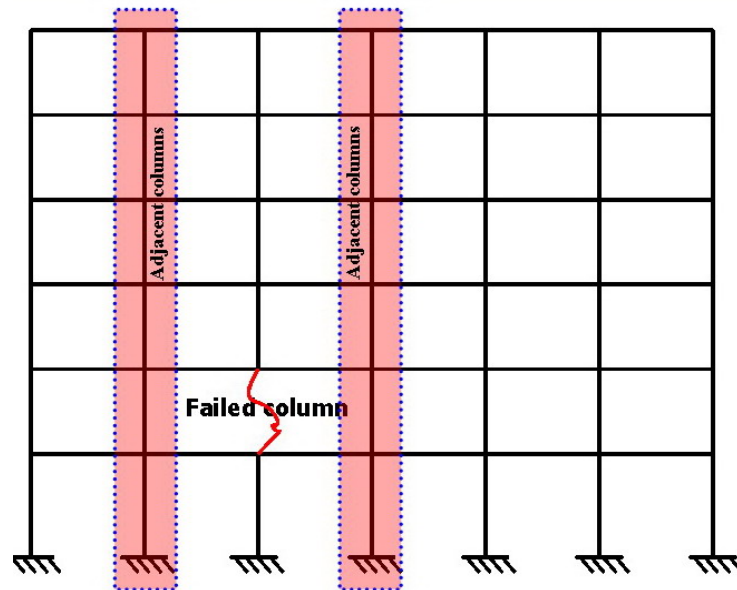


Figure 5.5. The alternative load path and the influenced zones

Previously, Chapter 6 described the directly affected part's behavior, especially in Load Phase 2, before catenary forces develop. The stiffness and the resistance of this part to the load path were investigated. Having ascertained certain assumptions, the substructure was then developed.

However, that substructure can only simulate the behavior of the directly affected part. As presented in Chapter 5, Load Phase 2 finishes at point (4). At that point, the directly affected part fully yields. Still, there is a possibility that the alternative load path might fail before this, due to other collapses, e.g., because of the instability of the adjacent columns or the instability of the beam on the top of the directly affected part. In that case, the

building collapses in Load Phase 2.

In fact, collapses in the frame which are not caused by the directly affected part's yielding are also important, critical situations. These cases are necessary for estimating the loading status of the adjacent columns or for investigating the load capacity of the top beam above the directly affected part. In light of this concern, this chapter describes the development of a more complex analytical model whose aim is to assess the essential characteristics of such a situation. Once again, the frame's behavior has been studied during Load Phase 2.

In the formation of an alternative load path, the additional load acting on the directly affected part is fully transferred to the adjacent columns. Specifically, the beam's bending moment is transferred to the columns through a beam-to-column connection. As a result, shear forces produce compression in the adjacent columns. Moreover, the arch effect is triggered by the deformation of the columns.

So, in order to obtain the loading state of the adjacent columns' zone, this chapter examines the continuity of all members within the load path in depth. First, the distribution of internal forces is studied in Section 7.2. Then, while maintaining continuity, a new substructure is developed in Section 7.3 as well as an analytical model. Following this development, Section 7.4 describes how the substructure was reduced for typical frames by simplification. Finally, Section 7.5 identifies this zone's critical members, namely the adjacent columns and the top beams. Because of their loading state, a stability check had to be performed on those members.

## **7.2. DISTRIBUTION OF INTERNAL FORCES AND DISPLACEMENT OF SPECIFIC POINTS**

This section describes the distribution of internal forces within the frame in its residual state. To illustrate the influence of the members adjacent to the column, the extended zone has been demonstrated in Figure 7.1. Instead of concentrating only on the adjacent columns zone, the investigated zone was extended by one column on each side.

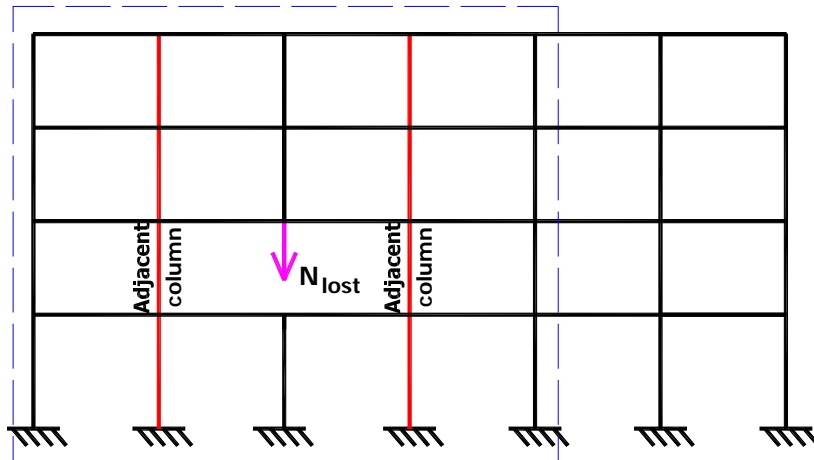


Figure 7.1. The investigated zone in the residual frame

A method of internal force analysis similar to that in Chapter 6 was applied to this extended section. The residual frame was then investigated in two separate loading states, i.e., the design and additional loading states.

### 7.2.1. Loading phases and the additional load

Figure 7.2 illustrates the distribution of bending moment and axial forces in the residual frame in Load Phase 2. As discussed in Chapter 5, the load was separated into two loading states. The first state in Load Phase 2 corresponds to the maximum state of Load Phase 1 at point (2). The second state is comprised of the additional load in which the residual frame supports the pair of concentrated forces representing the column's gradual disappearance. By analyzing how the residual frame supports this load, the nature of a frame's response following the loss of a column was revealed.

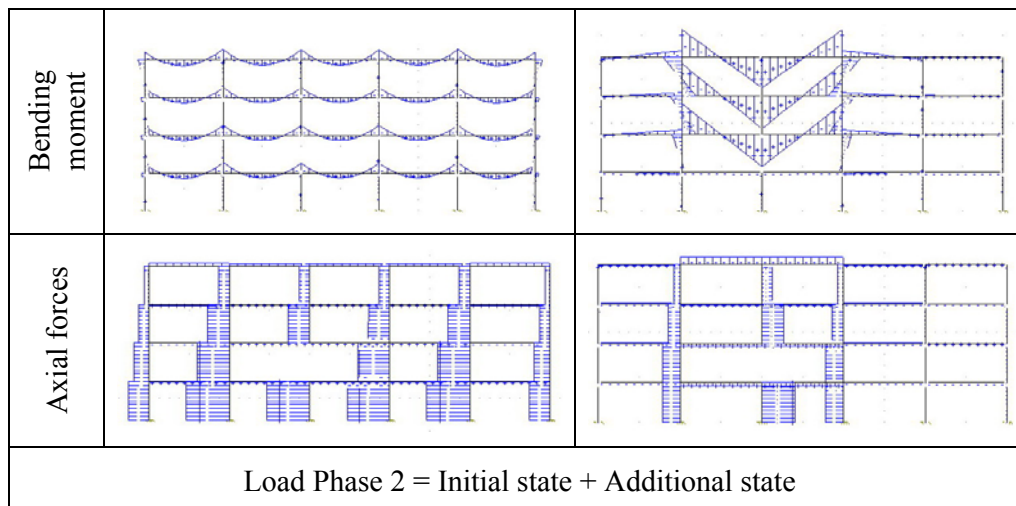


Figure 7.2. The distribution of internal forces in the residual frame in Load Phase 2

### 7.2.2. The arch effect and the axial force in the beams

In Chapter 6, the behavior of the directly affected part was investigated in order to calculate its critical resistance  $N_{lost}^{Pl,Rd}$ . The distribution of bending moment was illustrated to describe the development of the substructure visually, at which point the arrangement of axial forces in each beam was also briefly described. This chapter delves deeper into the latter phenomenon.

The “arch effect,” as it is called, is a phenomenon found in the residual frame, which must support the additional load, thereby forming an arch over the damaged position. The arch transfers the load to both sides of the damaged hole and produces horizontal compression on the members over the hole. The diagonal forces appearing in the wall above the lintel over a window is a telling example of this arch phenomenon, as in Figure 7.3.a.

In fact, when applying the additional load, above the directly affected part, axial forces appear in the equivalent beam due to the deformation of the adjacent columns.

The bending moment, which comes from the directly affected part, bends the adjacent columns. Depending on the capacity for horizontal movement on the left and right floors, the column deforms toward the center of the directly affected part. This deformation produces compression in the top equivalent beam and a smaller magnitude of tension in the bottom beam. According to the arrangement of the adjacent columns' and equivalent beam's stiffness, the axial forces within the equivalent beams varied. In particular, in a typical frame, the intermediate equivalent beam's axial force magnitude was very close to zero.

In fact, this phenomenon occurs only in the case where the adjacent column's end points can move horizontally. Therefore, if the frame is braced on both sides and the beam lengthens only slightly, the arch effect disappears.

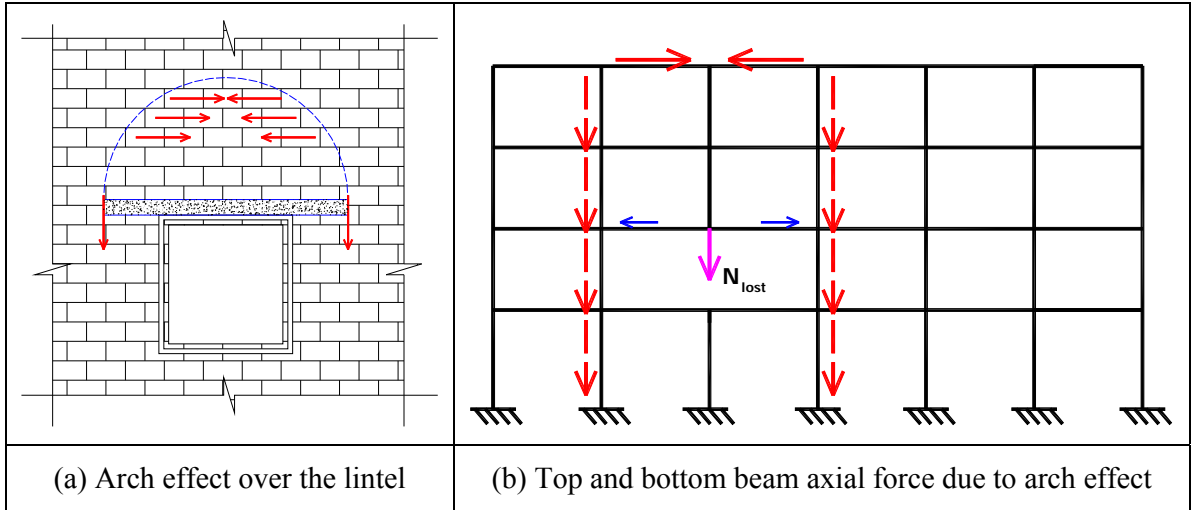


Figure 7.3. The distribution of axial forces in the equivalent beam due to the arch effect

### 7.2.3. Compression on the adjacent columns

Figure 7.4 demonstrates the distribution of axial forces and bending moment in the adjacent columns' zone during the additional loading state. On each floor, the equivalent beam receives pressure from the middle column and bends. Then the bending moment and shear forces are transferred to the adjacent column. From the top floor to the membrane beam, the adjacent columns' axial force increases floor by floor. On the floor under the damaged column, the axial forces are transferred from the columns above. Their magnitude remains unchanged from that of the columns on the damaged floor.

So, on each floor, the adjacent columns section must support a combined load of compression and bending moment. It is very clear that the column next to the damaged one must withstand the highest pair of  $(M, N)$ . Since Load Phase 2 consists of a combination of two loading states, the axial force and bending moment in the adjacent columns equals the sum of two values (in the elastic range):

$$\begin{aligned} N_{phase2} &= N_{design} + N_{add.load} \\ M_{phase2} &= M_{add.load} \end{aligned} \quad (7.1)$$

where  $N_{phase2}, M_{phase2}$  are the axial force and bending moment, respectively, in Load Phase 2,

$N_{design}$  is the axial force designated in the design, and

$N_{Add.load}, M_{Add.load}$  are the axial force and bending moment due to the additional load.

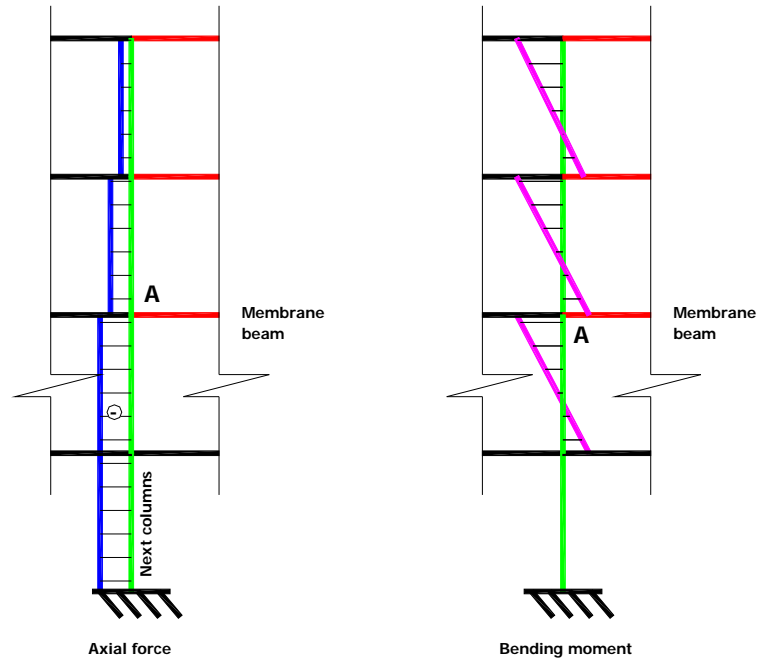


Figure 7.4. Adjacent column's internal forces

### 7.2.3. Conclusion

The response of the residual frame has been once again explained but this time in an extended zone in order to highlight the behavior of the adjacent columns. Moreover, the so-called “arch” effect has also been demonstrated. Next, the results proved the influence of the column's deformation on the arch effect. The most dangerous positions were estimated by understanding of the behavior of two specific parts. Finally, some remarks were made in order to show the member behavior in detail, a subject which is treated further in the next section.

### 7.3. DEVELOPMENT OF THE SUBSTRUCTURE MODEL

This section concentrates on the development of the extended substructure of the zone in Figure 7.1. The requirements of extraction were based on the results given in previous sections. Furthermore, the relation between the arch effect and column deformation will be analyzed in order to highlight the frame's role in triggering the development of the alternative load path.

Before moving on to details of this model's development, the two basic positions of the damaged column will be presented to highlight their differences. Figure 7.5 repeats the



diagram of the two alternative load paths corresponding to external and internal damage.

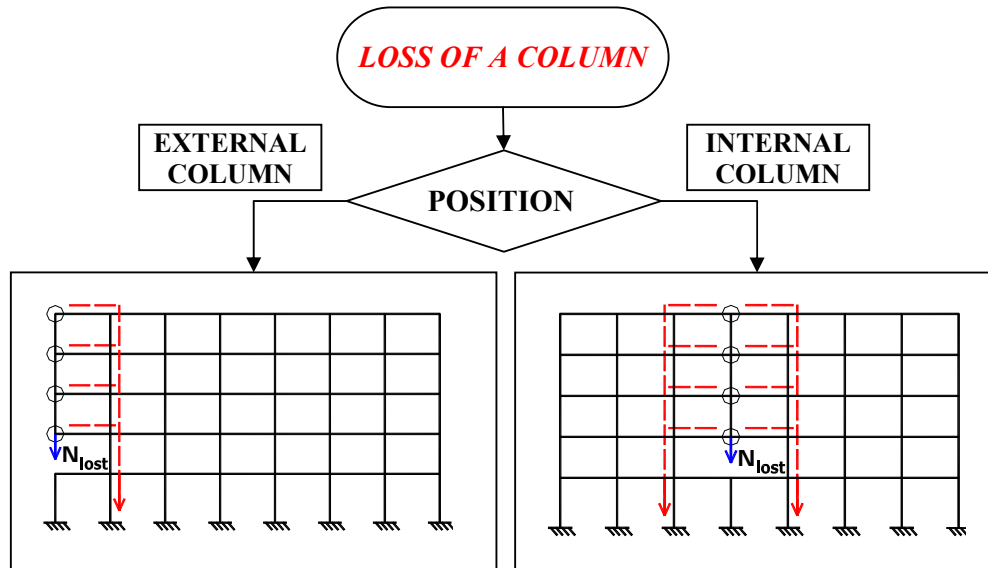


Figure 7.5. Two alternative load paths

### 7.3.1. Requirements for extraction

Section 7.2 mainly presented the alternative load path of the residual frame resulting from internal damage. As was explained in that section, the arch effect appears due to the deformation of the adjacent columns when they compress the top beam. However, in the case of external damage, the end points on one side of the beam are free. Hence, no arch effect occurs.

Figure 7.6 illustrates the full residual frame in which specific positions in the substructure are identified by colors. There are 3 requirements for ensuring an accurate damage model:

#### First requirement: Continuity

The adjacent column receives the bending moment transferred from the directly affected part as a function of the stiffness distribution. So, it is required that the adjacent columns, the equivalent beam and the beams on the adjacent span be connected as in a real frame. The full model has to cover the extended zone in Figure 7.1.

#### Second requirement: Compatibility

It has been shown that the bending moment distribution at the point where the equivalent beam, adjacent column and adjacent span beam connect depends on their bending stiffness. For example, when the adjacent span beam receives the bending moment, it distributes the

moment to the other end depending on the rotational capacity of its end points (the green zones numbered 1, 2, 3 and 5, 6, 7 in Figure 7.6). Another transfer point is the position with the same influence but on the column, which is presented by the red zone at the adjacent column's end point (zones 4 and 8).

Third requirement: Horizontal restraint

The arch effect may be triggered within the frame. This is represented by the axial forces that appear in the equivalent beams due to the deformation of the adjacent columns. However, that movement of the column's end points is influenced by the horizontal stiffness of the frame. In Figure 7.6, that part is defined by a blue rectangle on both sides (numbered 9 and 10).

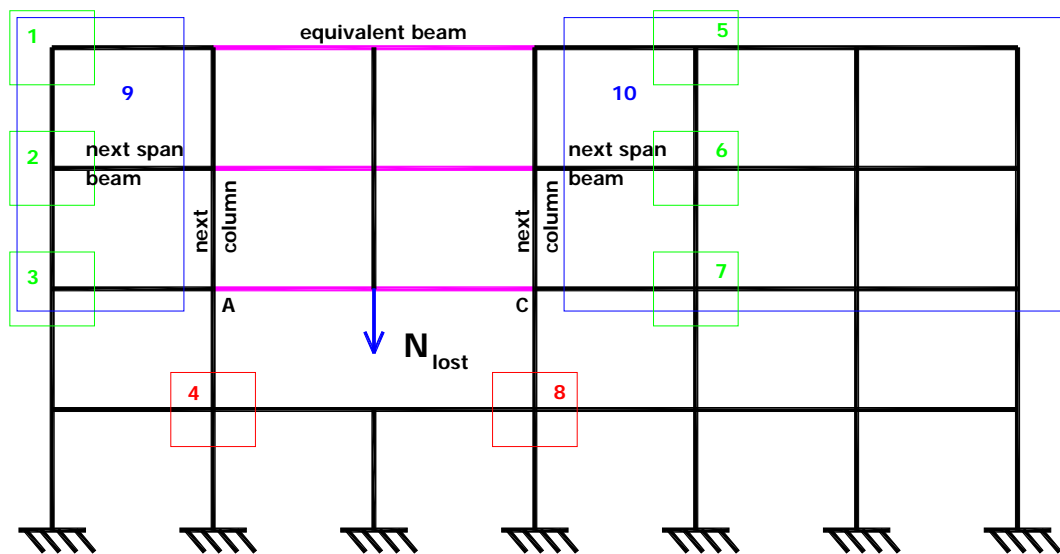


Figure 7.6. Specific identified zones

**7.3.2. Beam/column partial end restraints**

In order to keep the rotational capacity of the adjacent span beam's end point as it is in the real residual frame, the rotational stiffness  $K_S$  was defined in Section 6.4.3. It included the bending stiffness of all elements within the first and second levels expanding from the connection point. The calculation is repeated here in Figure 7.7.

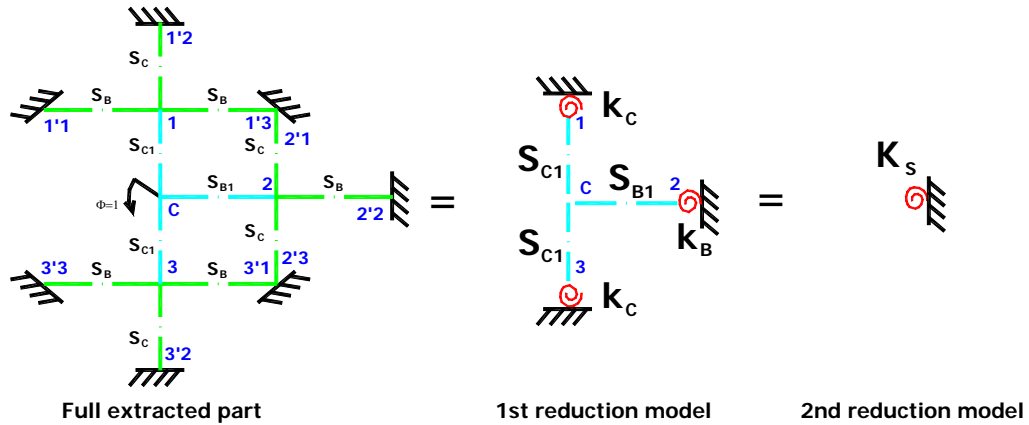


Figure 7.7. Repeat of the development of the formula for  $K_S$

### 7.3.3. Horizontal restraint

Figure 7.8 illustrates the method for predicting the horizontal restraint coefficient. In fact, the movement of point 7 in Figure 7.6, when supporting the axial force of the membrane beam, is limited by the stiffness of the members within the blue dashed rectangle. That stiffness is mainly bordered by two floors: the one below and the one above the loaded floor.

As a reminder, this coefficient was obtained in the concept defined in Section 6.3 – the directly affected part's substructure. So the same treatment can be applied. However, it is necessary to define the extended model for the braced part. Thus, in the following paragraphs, the term and concept are repeated for clarity's sake.

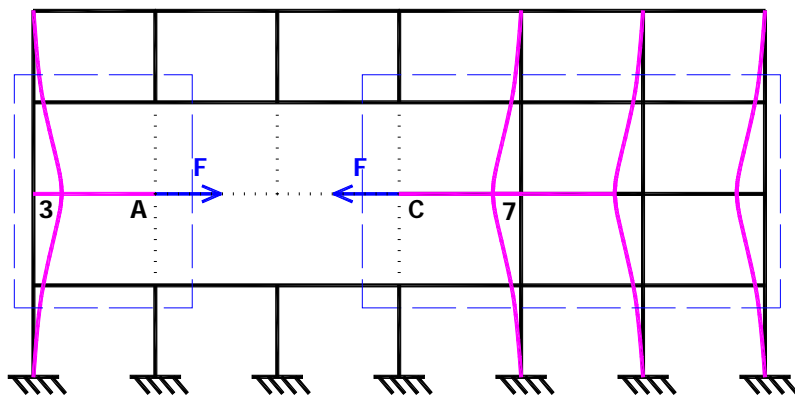


Figure 7.8. Horizontal restraint definition

#### 7.3.3.a. Unbraced part

This structural model with the perfect restraint system was presented first by Wong (2005),

who used this analysis to calculate the resistance of a frame in a fire. In particular, in the model, the column supports a lateral force. As a result, it behaves like a beam instead of a column. So, as a beam, it undergoes a tensile force at the end and is elongated. In this way, it works as a tensile member. In Figure 7.9, the model is extracted from the frame.

This thesis defines the partially restrained stiffness applied to the column end in order to simulate the continuity of the extracted model in relation to surrounding members.

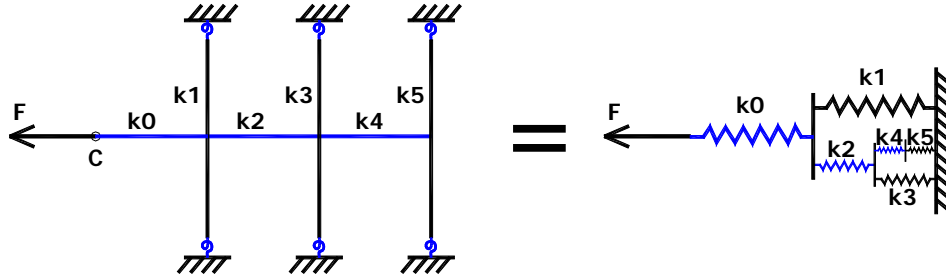


Figure 7.9. The development of the model and its stiffness

The model's stiffness was taken from the relation between the connected members. For example, the column's stiffness  $k_5$  connects to the beam's stiffness  $k_4$  at the loaded point, then the stiffness at equilibrium  $K_{eq}(4,5)$  was obtained by the serial connection rule. Next, the column's stiffness was connected to the group (4,5) at the end of beam 4, then  $K_{eq}(3,4,5)$  was treated as the group (4,5) parallel connected to column  $k_3$ . Consequently, the horizontal restraint coefficient  $K_{(3columns)}^{UnBraced}$  equals the total of group  $(k_0, k_1, k_2, k_3, k_4, k_5)$ .

$$\frac{1}{K_{(3columns)}^{UnBraced}} = \frac{1}{k_0} + \frac{1}{k_1 + \frac{1}{\frac{1}{k_2} + \frac{1}{k_3 + \frac{1}{\frac{1}{k_4} + \frac{1}{k_5}}}}} \quad (7.2)$$

where  $K_{(3columns)}^{UnBraced}$  is the horizontal restrained coefficient of point C, and  $k_i$  is the beam or column stiffness.

### 7.3.3.b. Braced part

The development of this model was simpler than for the unbraced case. Given the assembly rule, the displacement of the right loaded point was calculated like the unbraced part, but with a small change in configuration. Namely, the end of the beam is braced, so the member  $k_5$  is out of work. As a result the connection rule changes at the first connected member and the stiffness of the whole group mainly comes from the axial stiffness of the

beam.

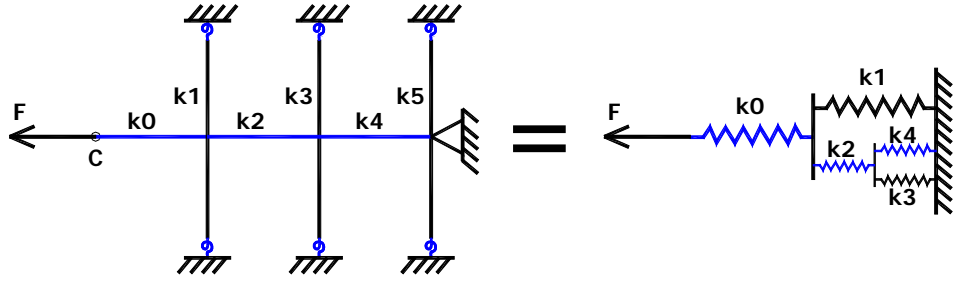


Figure 7.10. The braced part

So, the displacement of the braced side's loaded point equals

$$\frac{1}{K_{(3columns)}^{Braced}} = \frac{1}{k_0} + \frac{1}{k_1 + \frac{1}{\frac{1}{k_2} + \frac{1}{k_3 + k_4}}} \quad (7.3)$$

where  $K_{(3columns)}^{Braced}$  is the horizontal restrained coefficient of point C in the braced frame.

### 7.3.3.c. Equivalent adjacent span beam

The previous horizontal restraint coefficient was applied to the extended model to define a new concept: *equivalent adjacent span beam*. This term replaces the original adjacent span beam by the beam with the same bending ability but a new lengthening capacity. For example, the equivalent beam on the right side at the level 3 (level of membrane beam) has the value

$$A_{equ3.right} = \frac{K_{(3columns)}^{Un-braced} L_B}{E_B} \quad (7.4)$$

where  $A_{equ3.right}$  is the equivalent adjacent span beam's cross section area on the right,  
 $L_B$  is the adjacent span beam length, and  
 $E_B$  is the elastic modulus of the beam.

### 7.3.4. Extended substructure

Figure 7.11 demonstrates the substructure which resulted from the extraction process. The full residual frame with colored borders is presented in Figure 7.11.a. On the right side, the extracted substructure uses the same colors in order to represent the model and its included members.

This model takes the directly affected part, in magenta, as the core cause of the

deformation of the adjacent columns. The additional load  $N_{lost}$  is placed at the midpoint of the membrane beam **AC**. The adjacent columns zones, targeted in the study of this substructure, are connected to the end of the equivalent beam. Due to the distribution of internal forces within the column, the adjacent columns zone is limited to points 4 and 8. The columns below the damaged column are neglected in this model. To maintain the continuity of this column section with respect to the lower part, the column's bottom end point is defined by the partially restrained coefficient in Section 6.4.

As defined earlier, the arch effect represents the phenomenon of axial forces appearing in the equivalent beam due to the deformation of the adjacent columns. Those deformations are influenced by the distribution of bending stiffness of the members connected to the column's end. So, the adjacent span beams are also included in this model with the necessary modifications, i.e., in the equivalent adjacent span beam.

The first modification involves the partially restrained beam end's conditions. Once again, as demonstrated in the same problem in Chapter 6, the beam end's condition maintains the continuity of the model with respect to the whole frame. It is calculated as the bending capacity of the beam's end point according to the bending stiffness of the connected members.

The last but most important modification applied to the adjacent span beam is the equivalent lengthening stiffness. That concept is represented analytically by the horizontal movement capacity of the column's end points. It includes the capacity of one floor on one side of a beam axial stiffness.

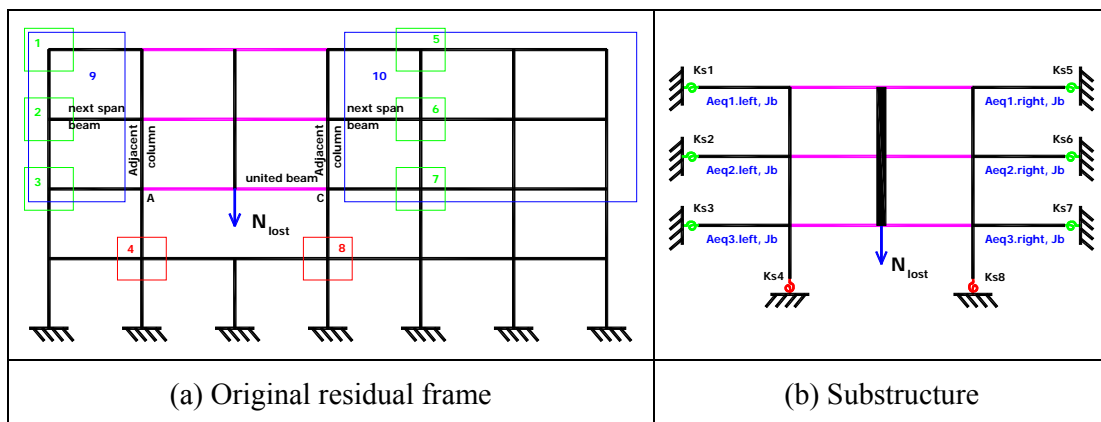


Figure 7.11. The original residual frame and the full model (internal damage)

The same process is applied to extract the model from the frame in the case of an external damaged column. Figure 7.12 illustrates the same process as in Figure 7.11 for external

damage.

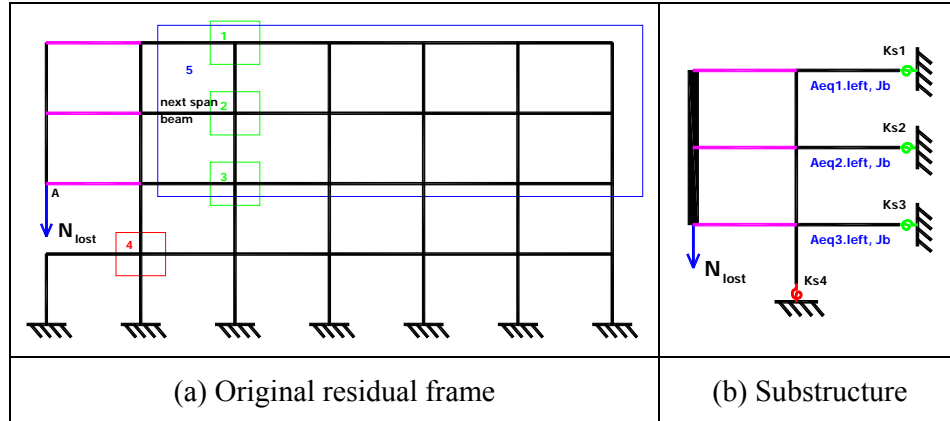


Figure 7.12. The original residual frame and the full model (external damage)

### 7.3.5. Conclusion

This section finished the analytical model in order to estimate the behavior of the second part in the alternative load path – the adjacent column zone. This investigation also presents two critical positions in the alternative load path: the top equivalent beam supporting compression and the adjacent column supporting the pair (M,N). They are the dangerous points which could cause the collapse of the frame even if the directly affected part manages to support the additional load.

Three parameters were calculated to ensure an accurate portrayal of the full substructure. The first parameter was the partial restraint coefficients. As in Chapter 6, in one frame, there are only 4 values of  $K_S$ . The column end's restraint coefficient was calculated using the same method. The last parameter was the equivalent cross section of the adjacent span beam. For each floor, it is necessary to estimate at least one value.

With the requirements demonstrated in Section 7.3.1, the substructure's parameters were defined as intricately as was necessary. So, more simplification was needed for practical purposes.

### 7.4. SIMPLIFICATION OF THE MODEL FOR TYPICAL BUILDING FRAMES

The substructure presented in the previous section was developed to investigate the behavior of the frame overall. As mentioned in the previous conclusion, that model is not simple enough for practical usage. In fact, building structures are normally typical forms with uniform columns and beam sections. The floor heights and beam spans are also

uniform. Those properties made the simplification of this model feasible, a process which will be presented in this section.

#### 7.4.1. Major properties of the model for typical frames

The 2D structural frame was analyzed assuming the axial deformation of the members to be neglected. That classic method is called the *rotation analysis*. If this assumption is applied to the model, the equivalent cross section parameter is neglected. The simple displacement method is used instead, in which the unknowns are node rotations.

In the typical frame, considering the middle columns as the border, the model was divided into two parts. These two parts have the same properties, i.e., the adjacent span beam lengths on each side, the two adjacent column zones and symmetrical equivalent beams. Except for the adjacent span beams' and bottom columns' end conditions, the second part of this model could be seen as a symmetrical structure.

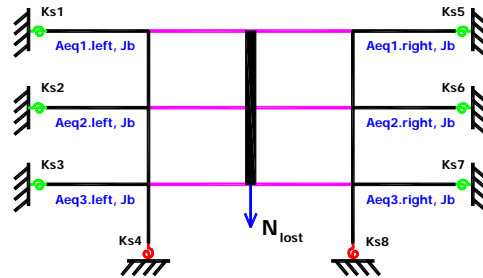


Figure 7.13. Resembling a symmetrical geometrical substructure

Figure 7.14 presents the bending stiffness of the beam members with different end conditions. The stiffness of the partially restrained member varies from the smallest value of a hinge end beam to the value of the fixed end beam. In this case, the highest stiffness difference is 25% between two limits ( $0 \leq K_S \leq \infty$ ).

In fact,  $K_S$  for the typical frame does not change as much as presented in Chapter 6.4.2. The values of  $K_S$  on both sides of the equivalent beam can be quite similar. This source of simplification is acceptable due to the small influence on the final distribution of bending moment in the model.



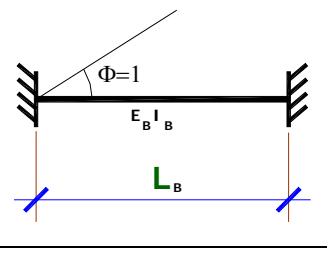
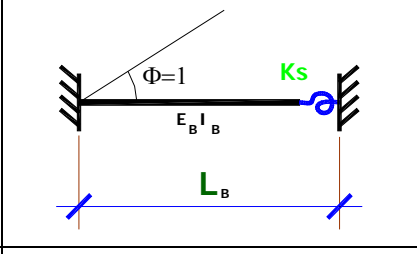
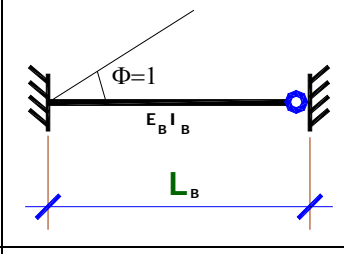
|   |  |   |
|---|--|---|
|  |  |  |
| $S_B^{Fixed} = \frac{4E_B I_B}{L_B}$  | $S_B^{K_S} = \frac{4E_B I_B (L_B K_S + 3E_B I_B)}{L_B (L_B K_S + 4E_B I_B)}$       | $S_B^{Hinge} = \frac{3E_B I_B}{L_B}$  |
| (a) Fixed end   | (b) Partially fixed end  | (c) Hinge end   |

Figure 7.14. The bending stiffness of different beam units

So, the substructure could be seen as a symmetrical system for the bending moment distribution. This property makes it possible to reduce the model by half following the classic principle that a symmetrical structure supports a symmetrical load.

One characteristic that should be clarified at this point is the middle column's behavior. The parameterized work presented in Chapter 6 proved that the middle column mainly works as a tensile member. So, the assumption of only vertical movement can be applied to the model. If the flexural and elongation of the middle columns are neglected, they could be replaced by the infinite stiff members as presented in Figure 7.15.

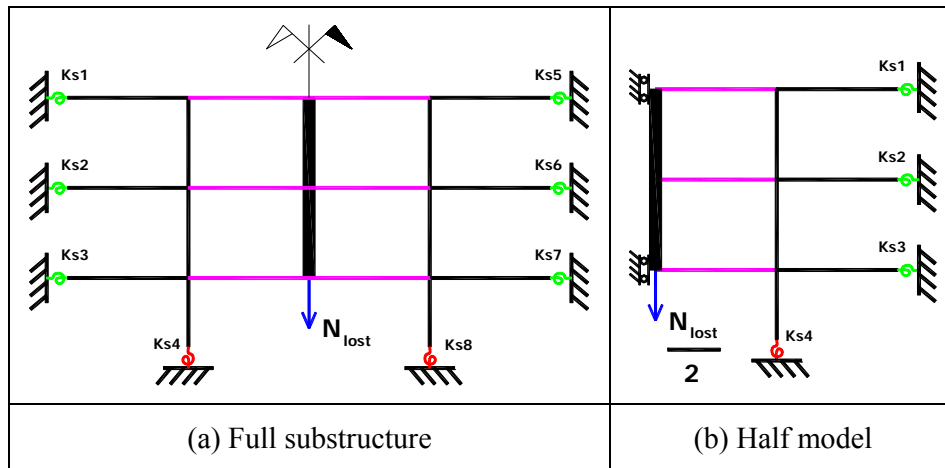


Figure 7.15. The simplified half model

#### 7.4.2. Half-model and the definition of the “weaker half”

According to the simplification in Section 7.5.1, the substructure was analyzed by the classic displacement method, which considers only the rotations of the nodes. In the typical building frame, the model is reduced to a half model as in Figure 7.15.

In order to estimate the axial force values in the adjacent columns, the nodes' equilibrium was investigated. From the bending moment diagram, the shear force distribution was obtained: at each frame node, the sum of shear forces in one direction equals the sum of axial forces in the orthogonal members. Figure 7.16 presents an example of a frame node, with 4 elements (1, 2, 3 and 4) connected together. The axial force and shear force of each element is  $N_i$  and  $T_i$  (with i from 1 to 4).

$$\begin{aligned} N_1 + N_3 &= T_2 + T_4 \\ N_2 + N_4 &= T_1 + T_3 \end{aligned} \quad (7.5)$$

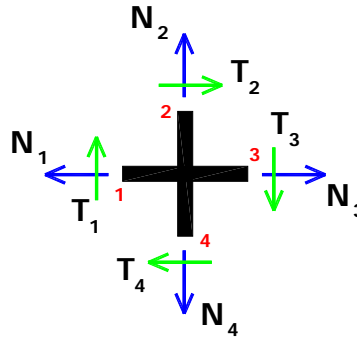


Figure 7.16. Equilibrium at a node

Applied to the extended substructure on one floor, the axial force in the equivalent beam  $N_{UB}$  was estimated by the equilibrium of shear forces on the upper column  $T_{UC}$  and lower column  $T_{LC}$  and distributed between the equivalent beam and adjacent span beam according to the distribution of their stiffness.

$$\frac{N_{UB}}{N_{NB}} = \frac{\frac{E_B A_{UB}}{L_B}}{\frac{E_B A_{NB}}{L_B}} = \frac{A_{UB}}{A_{NB}} = \frac{A_{UB}}{A_{Equivalent}} \quad (7.6)$$

Likewise, the axial forces in the equivalent beam equal

$$N_{UB} = (T_{UC} + T_{LC}) \frac{A_{UB}}{A_{Equivalent} + A_{UB}}. \quad (7.7)$$

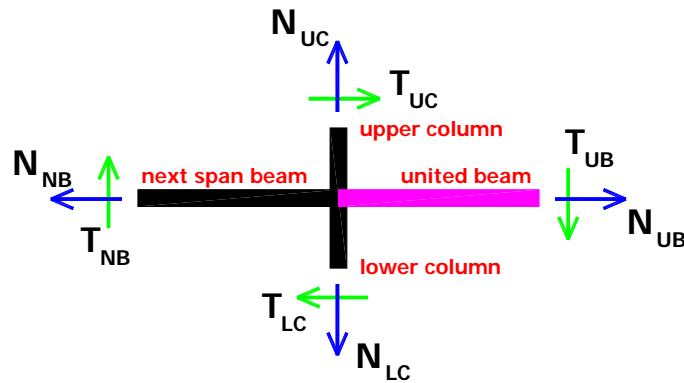


Figure 7.17. Calculating the axial forces in the equivalent beam (arch effect)

As presented before, the bending moment diagram was obtained from the “half” model. Based on the bending moment distribution, the axial forces were acquired. In fact, the left and right halves differed in the values of the equivalent cross sections applied to the adjacent span beams. That equivalent value comes from the horizontal restraint coefficient which includes the  $K$  value on each side.

By (7.6) and (7.7), it was proved that the smaller the equivalent cross section, the larger the value of equivalent beam axial forces. So between the two halves of the model, the part which includes the smaller equivalent cross section will show the safest axial force in the top equivalent beam.

According to the conclusion above, a new concept is presented as follows:

The application of a half model in order to estimate the axial forces in the equivalent beam has been applied to the “weaker half”. The *weaker half* is defined as the side where the number of outside spans is smaller. Through many simulations, it has been proved that the “weaker part’s” results are closer to the real frame than those of the “stronger” side.

By separating the applied load  $N_{lost}$  from each equivalent beam by the stiffness comparison, the final half model became

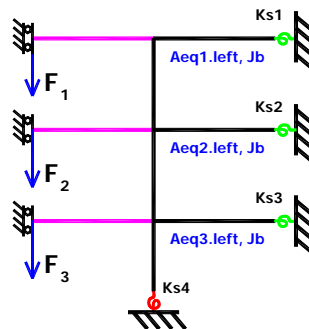


Figure 7.18. Simplified half model

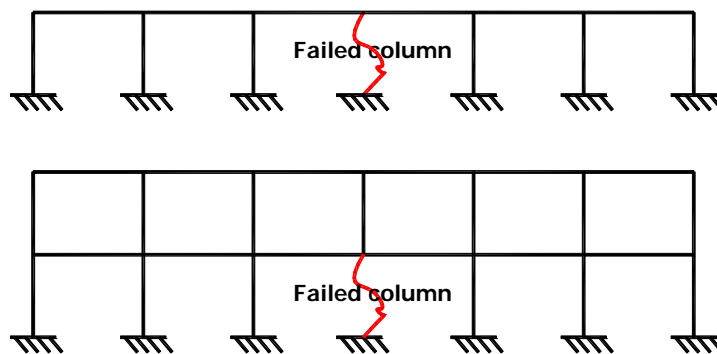
$$F_i = \frac{N_{lost}}{2} \frac{K_B^i}{\sum_{i=1}^n K_B^i} \quad (7.8)$$

where  $K_B^i$  is the equivalent beam number  $i$  calculated in Section 6.3,  
 $n$  is the number of floors within the model, and  
 $F_i$  is the vertical force applied to the equivalent beam number  $i$ .

### 7.4.3. Validation

The validations performed on the typical frame substructures have been organized into 5 frame types. Figure 7.19 presents the first and second frame types used for the validations. The first frame type was 6 spans x 1 floor. The beam length was 8m and column height was 3.5m. The beam sections were IPE400V. The columns sections ranged from 10 sections: HE 100A, 160A, 200A, 240A, 300A, 340A, 360A, 400A, 450A and 500A. The beam length and column height remained constant.

Three types of half models were carried out. They were the half model with the equivalent adjacent span beam, the half model with fixed beam ends and the model simulating the situation when the first hinge appears at the midsection. Figure 7.19.b, c, and d demonstrate these models. There is a model for the first hinge situation but with fixed beam ends.



(a) Full investigated frame

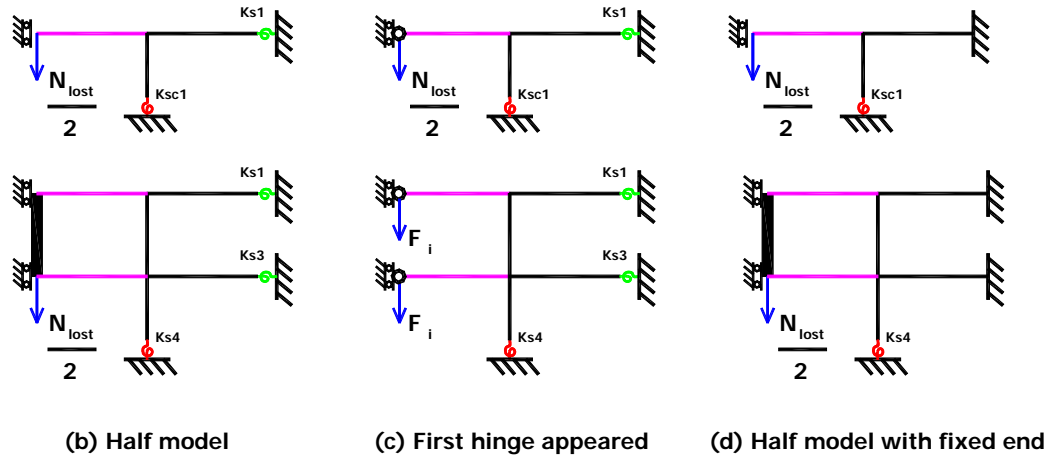


Figure 7.19. The first and second frames and models for validation

The other types of frames were modeled like the two previous frames. However, the third, fourth and fifth frames were 11 spans x 4 floors, 11 spans x 15 floors and 4 spans x 20 floors, respectively. They are drawn in Figure 7.20.

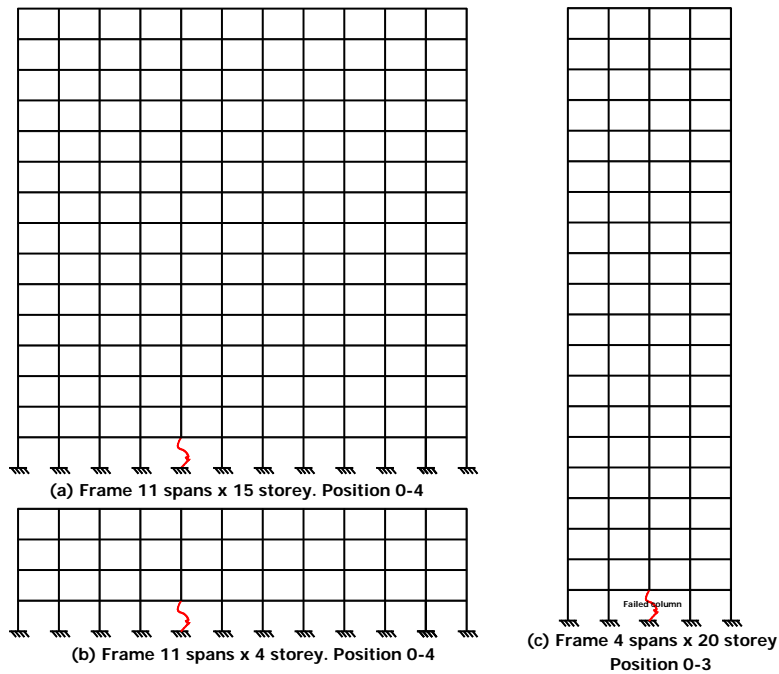


Figure 7.20. The third, fourth and fifth frames

Table 7.1 illustrates the results for error percentages of the 4-storey frame in the two major beam axial forces considered: the top and bottom equivalent beams (the arch effect). Briefly, these results showed that this analytical method provides acceptable results for simulating the behavior of a typical frame with the half models.

Table 7.1. The error percentages of the 20-storey frame

| Elastic                    |          |          |           |         |         |             |        |           |         |         |
|----------------------------|----------|----------|-----------|---------|---------|-------------|--------|-----------|---------|---------|
| Frame: 4 storey x 11 spans |          |          |           |         |         |             |        |           |         |         |
| Position: 0-4              |          |          |           |         |         |             |        |           |         |         |
| IPE400V                    |          |          |           |         |         |             |        |           |         |         |
| Section                    | Top beam |          |           |         |         | Bottom beam |        |           |         |         |
|                            | OSSAD    | Model    | Fixed mod | % model | % fixed | OSSAD       | Model  | Fixed mod | % model | % fixed |
| HE 100A                    | -8.91    | -10.270  | -9.620    | -15.26  | -7.97   | 4.44        | 5.170  | 4.830     | -16.44  | -8.78   |
| HE 160A                    | -33.34   | -39.200  | -36.910   | -17.58  | -10.71  | 15.92       | 18.680 | 17.600    | -17.34  | -10.55  |
| HE 200A                    | -58.09   | -67.750  | -64.670   | -16.63  | -11.33  | 26.26       | 30.280 | 29.030    | -15.31  | -10.55  |
| HE 240A                    | -87.85   | -100.420 | -97.400   | -14.31  | -10.87  | 36.31       | 40.670 | 39.710    | -12.01  | -9.36   |
| HE 300A                    | -123.37  | -136.410 | -134.370  | -10.57  | -8.92   | 43.62       | 46.710 | 46.300    | -7.08   | -6.14   |
| HE 340A                    | -138.46  | -150.460 | -148.990  | -8.67   | -7.61   | 44.58       | 46.500 | 45.640    | -4.31   | -2.38   |
| HE 360A                    | -144.17  | -155.490 | -154.250  | -7.85   | -6.99   | 44.46       | 45.810 | 45.640    | -3.04   | -2.65   |
| HE 400A                    | -152.86  | -162.660 | -161.770  | -6.41   | -5.83   | 43.58       | 43.860 | 43.770    | -0.64   | -0.44   |
| HE 450A                    | -160.61  | -168.190 | -167.610  | -4.72   | -4.36   | 41.7        | 40.760 | 40.720    | 2.25    | 2.35    |
| HE 500A                    | -165.72  | -170.790 | -170.420  | -3.06   | -2.84   | 39.36       | 37.410 | 37.390    | 4.95    | 5.01    |
| 1st hinge                  |          |          |           |         |         |             |        |           |         |         |
| Frame: 4 storey x 11 spans |          |          |           |         |         |             |        |           |         |         |
| Position: 0-4              |          |          |           |         |         |             |        |           |         |         |
| IPE400V                    |          |          |           |         |         |             |        |           |         |         |
| Section                    | Top beam |          |           |         |         | Bottom beam |        |           |         |         |
|                            | OSSAD    | Model    | Fixed mod | % model | % fixed | OSSAD       | Model  | Fixed mod | % model | % fixed |
| HE 100A                    | -22.280  | -25.960  | -23.570   | -16.52  | -5.79   | 10.840      | 12.780 | 11.560    | -17.90  | -6.64   |
| HE 160A                    | -79.720  | -94.770  | -87.430   | -18.88  | -9.67   | 37.300      | 44.290 | 40.960    | -18.74  | -9.81   |
| HE 200A                    | -133.430 | -157.250 | -148.230  | -17.85  | -11.09  | 59.040      | 68.830 | 65.290    | -16.58  | -10.59  |
| HE 240A                    | -193.740 | -223.590 | -215.410  | -15.41  | -11.19  | 78.300      | 88.500 | 85.990    | -13.03  | -9.82   |
| HE 300A                    | -261.450 | -291.540 | -286.380  | -11.51  | -9.54   | 90.570      | 97.600 | 96.580    | -7.76   | -6.64   |
| HE 340A                    | -289.120 | -316.660 | -313.040  | -9.53   | -8.27   | 91.410      | 95.830 | 95.280    | -4.84   | -4.23   |
| HE 360A                    | -299.430 | -325.400 | -322.360  | -8.67   | -7.66   | 90.780      | 93.960 | 93.550    | -3.50   | -3.05   |
| HE 400A                    | -314.900 | -337.490 | -335.330  | -7.17   | -6.49   | 88.450      | 89.350 | 89.120    | -1.02   | -0.76   |
| HE 450A                    | -328.410 | -316.190 | -344.790  | 3.72    | -4.99   | 84.200      | 82.540 | 82.430    | 1.97    | 2.10    |
| HE 500A                    | -337.060 | -349.510 | -348.600  | -3.69   | -3.42   | 79.200      | 75.420 | 75.370    | 4.77    | 4.84    |

In Table 7.1, the errors decreased following the increase in the number of column sections. However, with the applied load’s magnitude being 500 kN, which represented a 1000 kN additional load, the error in the value of the top beam’s compression is not so significant.

There is another interesting conclusion to be drawn from the results: the actual model’s and the fixed end model’s results showed the less detailed model to be more accurate. In Chapter 10, a proposal to perform more investigations related to this aspect will be made.

#### 7.4.4. Conclusion

From the extended substructure, the simplification process was applied with the aim of obtaining a more useful model. Due to the necessity of a more practical building frame, the analysis concentrated on normal buildings usually constructed with a uniform design, i.e., uniform bays, spans and section. Using repeated geometrical and stiffness parameters, the substructure was reduced to the “weaker half”.

In fact, the reduction was divided into two steps. The first step was to reduce the model with respect to the bending moment analysis which decided the model was symmetrical. With this decision, the general model of a typical frame can be converted to a half model.

The second step defined a way to predict the axial forces within the equivalent beams approximately. That method was based on the distribution of internal forces as a function of stiffness arrangement. Only during this step, a new term “weaker part” was defined.

The next section goes further in explaining why the dangerous position calculation is the most important part of the building frame’s robustness assessment. With Chapters 6 and 7, the fully detailed calculation will be completed for the alternative load path in a frame losing one column.

### 7.5. ADJACENT COLUMNS’ KEY ELEMENT AND RESISTANCE

The content of this section concentrates on the key elements of the alternative load path. Those elements are the critical elements which are present in certain dangerous conditions due to the loss of a column. Using the definition of *progressive collapse* in Chapter 5, Section 5.2.2, the frame collapse is identified when a second member is damaged.

This section points out the most dangerous positions in the investigated zone of the frame. Their critical resistances are discussed in order to apply the robustness assessment afterwards. Figure 7.21 presents the behavioral load-carrying curve with a remark on possibilities for instability.

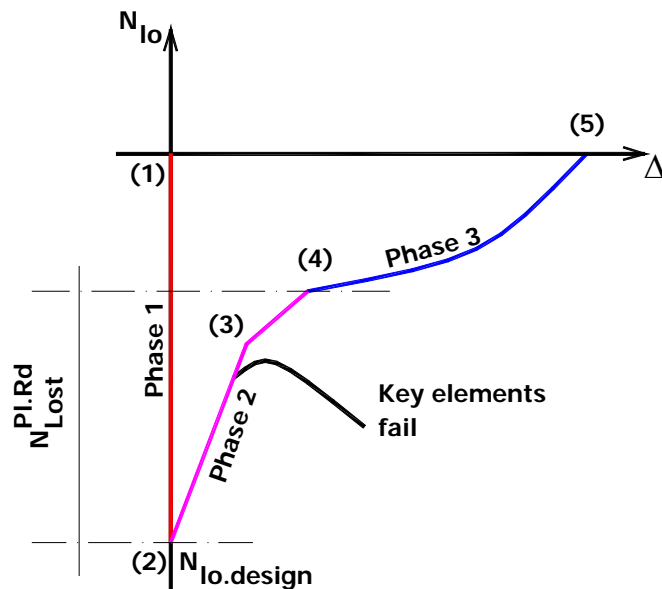


Figure 7.21. Moment where frame could collapse due to the loss of second key element

#### 7.5.1. Key elements and the loading status

In the extended substructure, the most dangerous positions are the equivalent beam end section in pair ( $M$ ,  $+N/-N$ ), the adjacent column in ( $M$ ,  $N$ ) and the middle beam under tension. If one of these members fails, the frame will collapse before point (2). The internal force magnitudes were estimated for the specific point on the load-carrying curve in Figure 7.22.

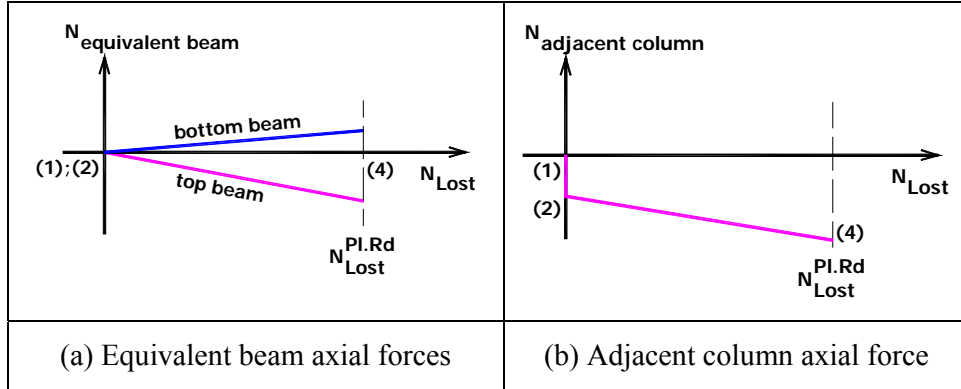


Figure 7.22. Axial forces in the key elements

Figure 7.23 repeats the substructure in which the key members are illustrated. Those key members' survival will ultimately determine the frame's robustness in Load Phase 2.

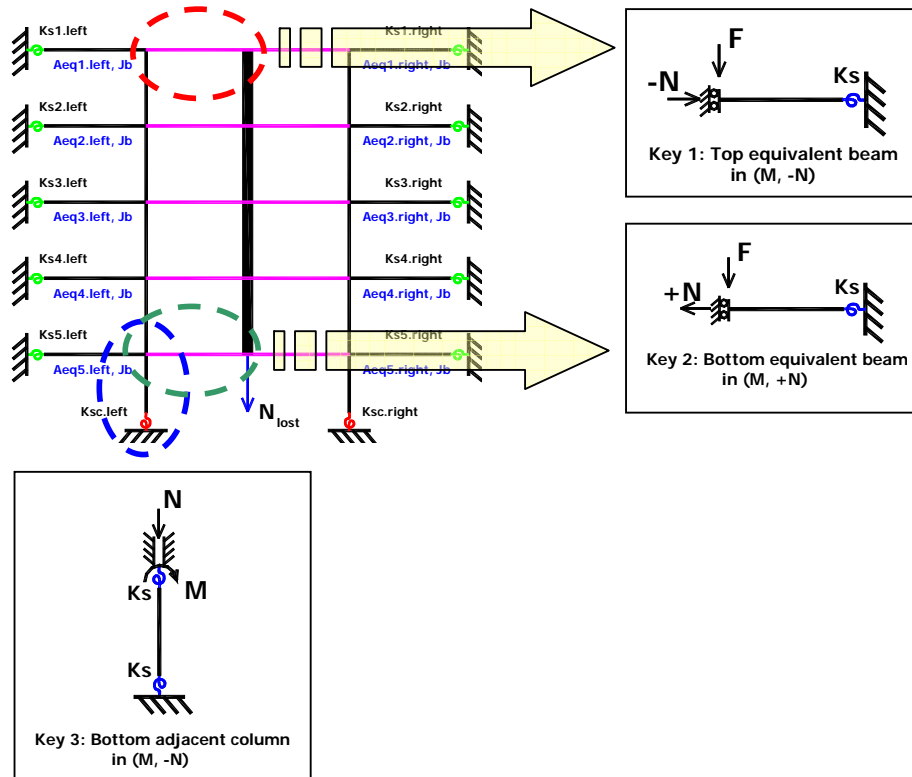


Figure 7.23. General model and the key elements



### 7.5.2. Element stability check

From the results, two dangerous positions have been identified: the equivalent beam in compression and bending simultaneously, and the adjacent column in compression and bending.

With the special load-carrying curve applied to these key elements, each element must be checked not only for plastic resistance but also for stability. The next paragraph demonstrates the stability test for the bottom adjacent column. In the typical frame, it is the most dangerous member.

In the Phase 2, the top point of the column does not move. The bending moment and the axial force increase in the adjacent column. Due to  $N_{lost}$ , the compression force increases linearly in the adjacent column, as does the bending moment. The  $N$  and  $M$  applied to the column are the result of the vertical load  $N_{lost}$ . They are a linear function of  $N_{lost}$ . In other words,  $N$  is the linear function of  $M$  and vice versa. With that  $M, N$  pair, the check is done by the following formula:

$$\Rightarrow 0 \leq \frac{N_{Sd}}{N_{pl.Rd}} \leq \frac{A_w}{A}$$

$$M_{N.y.Rd} = M_{pl.y.Rd} \left[ 1 - \left( \frac{N_{Sd}}{N_{pl.Rd}} \right)^2 \frac{1}{2 \left( \frac{h-t_f}{h-2t_f} \right) \left( 1 - \frac{A_w}{A} \right) \frac{A_w}{A} + \left( \frac{A_w}{A} \right)^2} \right] \quad (7.9)$$

$$\Rightarrow \frac{A_w}{A} \leq \frac{N_{Sd}}{N_{pl.Rd}} \leq 1$$

$$M_{N.y.Rd} = bt_f (h-t_f) f_y - \frac{1}{2} (N_{Sd} - A_w f_y) \left[ (h-2t_f) + \frac{N_{Sd} - A_w f_y}{2bf_y} \right] \quad (7.10)$$

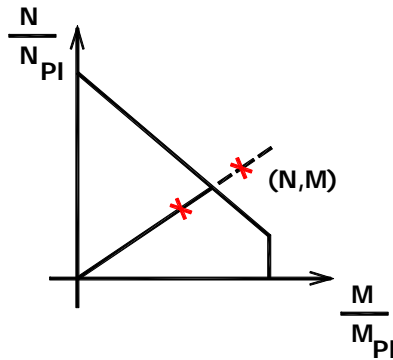


Figure 7.24. Frame member section stability check

#### 7.5.4. Conclusion

The extended substructure in Section 7.5 was developed to calculate the distribution of internal forces in the whole frame. On a specific point of the load-carrying curve in Figure 5.7, the internal forces of each member on the load path were predicted. Based on that knowledge of the individual members' loading status, the design check procedure was carried out.

Chapter 9 systematizes all of the special key elements associated with the load-carrying curve and their resistance. In Chapter 8, the full robustness assessment method will be finalized.

#### 7.6. SUMMARY AND CONCLUSIONS

In these two chapters, 6 and 7, the alternative load path's members' behavior was presented not only overall but also individually. The results provide a major critical value  $N_{lost}^{Pl.Rd}$  which decides the scenario of the load path. Until now, the frame's behavior was mostly investigated within the elastic range.

Two major zones were included in the alternative load path. The first zone was the directly affected part, presented in Chapter 6. That zone's behavior is representative of the main action in the frame. Its plastic limit  $N_{lost}^{Pl.Rd}$  is the critical point which decides the frame's behavior.

However, it is possible that the alternative load path could not survive due to the secondary collapse of a member included in the path. In fact, the alternative load path transfers the load through the chain of the members. Each member within the chain has the ability to bridge the load to the next member. The individual behavior of each member along the path was investigated. Their specific behavior in supporting the additional load was highlighted.

Two substructures were built in order to simulate the frame's behavior. This chapter concentrates particularly on the analytical simulation of the arch effect and the adjacent column actions. The model was developed based on the parametrical study earlier. The specific continuity of the adjacent column with respect to neighboring members was implemented in the analytical formula.

The typical building frame's properties were simplified for more practical applications. The "weaker half model" was finally completed. With this type of model, the distribution of internal forces within the frame was estimated in an analytically simplified way.

The last paragraph of this section identified the members which are in the most dangerous positions on the alternative load path. The internal forces resulting from the frame analysis were used as input for the capacity assessment of individual members.

The next chapter will describe the special behavior of the damaged level which influences the so-called catenary action.

**CHAPTER 8: PARAMETERS INFLUENCING THE DEVELOPMENT  
OF CATENARY ACTION AFTER THE LOSS OF A COLUMN**

## 8.1. INTRODUCTION

The previous chapters described Load Phase 2 where the directly affected part's behavior changes from elastic to fully non-linear behavior. Load Phase 2 finishes when the equivalent beams yield. As an illustration of this development, the load-carrying curve presented in Chapter 5 is repeated below to introduce this chapter's contents.

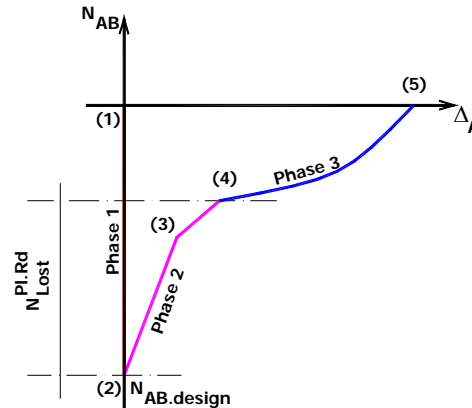


Figure 8.1. The full loading process where the catenary action take effect

This chapter concentrates on the third loading phase, where the membrane phenomenon is triggered. This phenomenon has an advantage in that it extends the alternative load path and increases the frame's load capacity. Together with Demonceau, the results of the investigation allowed the author to better understand the global behavior of the frame in Load Phase 3.

In the first section, a general explanation of the nature and parameters of the catenary effect will be given thanks to Demonceau's work. More specifically, the conditions necessary to activate the effect will be briefly discussed. As mentioned earlier, the membrane phenomenon represents the local behavior of the bottom beams when the directly affected part fully yields. There are three important parameters influencing this phenomenon, as it is influenced by the surrounding members. Each parameter's calculation will thus be explained in one section and the reciprocal relation between them will be presented.

In the same section, the assumption on the internal force distribution, especially in Load Phase 3, is discussed to identify the parameters necessary for calculating catenary behavior. More precisely, it involves the assumption on the evolution of applied load  $Q$  associated with the axial force of the middle column just above the damaged column. It is also referred to in Section III.3.3 of Demonceau's thesis.

The next section will describe the behavior of the members in the damaged level on both the left and right sides. In fact, Load Phase 3 encompasses the non-linear behavior of the membrane beams which is associated with the adjacent parts' behavior.

The third section describes the author's method for simulating the *damaged level's* behavior. An analytical model was constructed using a similar process to the one used in Chapters 6 and 7. The process includes three steps, as presented in Chapter 4: boundary condition simulation, individual member modeling, assembling the stiffness and finalizing the substructure.

Next, Section 8.5 investigates the substructure's model by defining the analytical formula to predict this part's stiffness. After a parametrical investigation, the method for simplification by taking into account the individual columns' stiffness will be developed.

The last section solves the problem of the damaged level's resistance. With the answer of this problem, the ability of catenary action to be maintained was proved according to the surrounding influences. This is also the last step in the theory proposed for assessing the full frame's robustness.

## 8.2. CATENARY ACTION IN BEAMS AND INFLUENCING PARAMETERS

As presented in Chapter 5, when the directly affected part reaches its plastic limit at point (4), the additional load  $N_{lost}$  attains the critical value of  $N_{lost}^{Pl.Rd}$ . It is possible, however, that the additional load will never reach the plastic limit. This happens when

$$N_{design} < N_{lost}^{Pl.Rd}. \quad (8.1)$$

Then, when all three conditions, i.e., if the appropriate value of  $N_{lost}^{Pl.Rd}$ , the surrounding part stability and the full yielding of the directly affected part are fulfilled, the special non-linear behavior called "catenary action" is activated in the bottom equivalent beam. Before introducing any other concepts, these statements will be proved using the previous chapter's results.

### 8.2.1. Why only the bottom equivalent beam undergoes catenary action

Chapter 7 illustrates the distribution of axial forces in the directly affected part as the result of the adjacent columns' deformations. The top equivalent beam is under compression,

while the bottom beam is under tension. Other intermediate beams have very small normal forces.

At the limit point, all of the beam's end sections yield. As a result, all the equivalent beams become mechanisms. Indeed, not every mechanism can withstand the load. Right after that point, the distribution of internal forces within the directly affected part maintains its value at the limit point. For example, the equivalent beam's end sections maintain their plastic bending moment's value  $M_p$ . Discontinuity between equivalent beams also results from this plastic yield.

Then, the additional load increases, eventually reaching the final value of  $N_{design}$ . When continuity is disrupted, the additional load acts only on the bottom beam. The upper equivalent beam mechanisms then are free to follow without constraint. If the beam's end points are tied to the outside part of the frame (i.e., when  $K \neq 0$ ), then catenary action may be triggered.

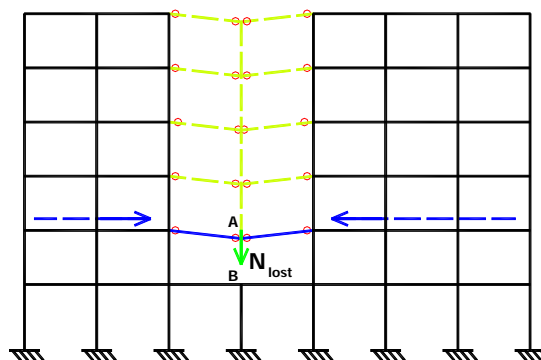


Figure 8.2. Only the bottom equivalent beam undergoes catenary action

### 8.2.2. Load-carrying behavior of the bottom equivalent beam

As discussed in the previous paragraphs, catenary action occurs in the frame during Load Phase 3 (Figure 8.1). In fact, if the building frame fulfills the three conditions laid out in Section 8.2.1, the membrane effect may be triggered. The directly affected part remains stable after it reaches its plastic limit, and the extended alternative load path forms.

Considering the bottom equivalent beam in Figure 8.2, after the beam's end sections yield, this beam becomes a mechanism. Due to the additional load applied to the beam, the vertical displacement of point A rapidly increases. The second order effect appears within the beam, and then the beam's axial forces build up. The upper equivalent beam is still under compression or undergoing small normal forces at this point, as at the end of Load

Phase 2.

Figure 8.3.a represents the membrane beam which is extracted from the frame. Figure 8.3.b shows the load carrying curve of this beam. Both figures come from Jean-Francois Demonceau's thesis. Thanks to the closely linked research on these two theses, it was possible to formulate the building frame's full behavior.

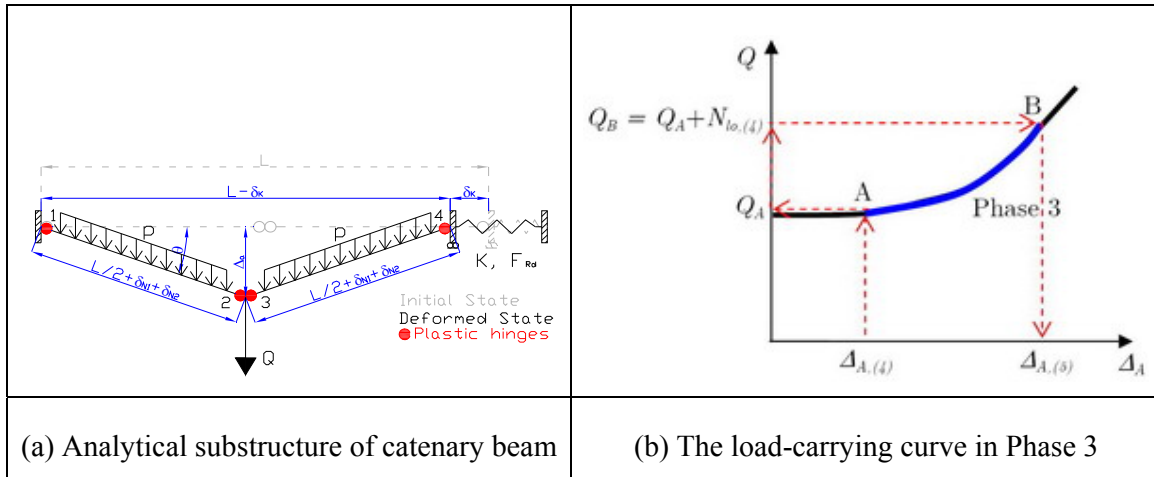


Figure 8.3. Simplified substructure simulating the behavior of the frame during Phase 3 [Demonceau, 2008]

### 8.2.3. Lateral translation stiffness $K$

Based on hundreds of parametrical analyses performed by Demonceau, it can be concluded that the behavior of the catenary beam is influenced by the tying restraints at the beam's ends. As the value of lateral stiffness coefficient  $K$  varies, it will change the form of the load carrying curves, as presented in Figure 8.4. This has been briefly summarized for three scenarios in that figure.

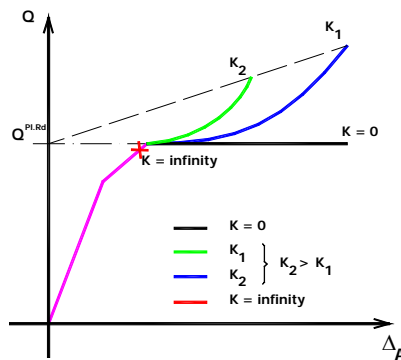


Figure 8.4. Different scenarios of the bottom beam depending on  $K$  values.

When the tying restraint coefficient is very high, such as when it is fixed or in a fully



braced frame, the load carrying evolution stops when close to the plastic limit. Thus, no catenary action occurs.

If the beam end can freely move in the horizontal direction, or if  $K = 0$ , the vertical displacement at point **A** rapidly increases without any normal force appearing in the beam. In this case, there is no catenary action either.

The third situation involves the case of the appropriate value for  $K$  where the load—displacement relation appears as in Figure 8.3.b. Figure 8.4 illustrates the four load-carrying curves with infinite, zero and two different values for  $K$ .

#### 8.2.4. Limit of the restraint at the end of catenary beam - $F_{Rd}$

The lateral restraint stiffness  $K$  represents the influences of the remaining frame's part on the catenary action. This stiffness comes from the surrounding frame elements such as beams, columns, and connections. If one of them fails due to instability or reaches its limit,  $K$  becomes zero. In graphic terms, the behavior curve falls to the horizontal line as in Figure 8.5.

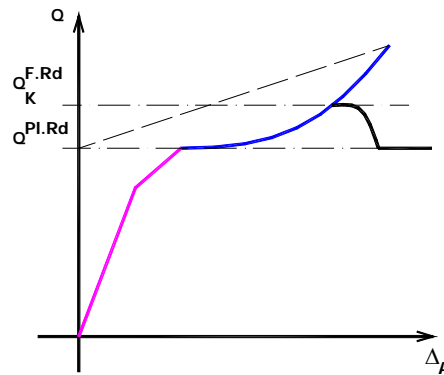


Figure 8.5. Behavior when  $Q$  reaches  $Q_K^{F.Rd}$ .

#### 8.2.5. Hanging force and $Q$

For both theses,  $Q$  in Figure 8.3 defines the load applied only to an individual catenary beam. That force is the resultant force of two forces: the additional forces applied to the residual frame  $N_{lost}$  and the axial force of the upper column  $N_{up}$ . Figure 8.6 presents the position of the forces on point **A** at top of the the damaged column.

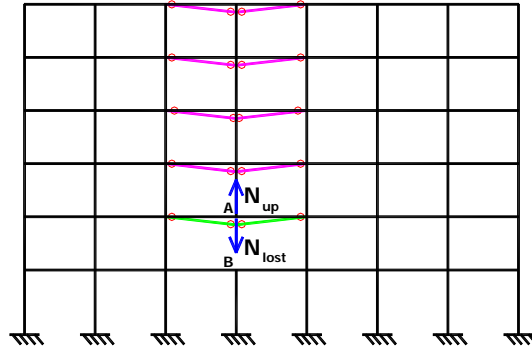


Figure 8.6. The hanging force  $N_{up}$  and the additional load  $N_{lost}$

As in Chapter 6, in the additional load case how the axial forces are distributed along the middle column in Load Phase 2 depends on the arrangement of the equivalent beam's stiffness. Then the hanging force takes on the value

$$N_{up} = N_{up.design} - N_{lost} \left( 1 - \frac{K_{bottom.beam}}{\sum_{i=1}^n K_{Bi}} \right) \quad (8.2)$$

where  $K_{bottom.beam}$  is the single bottom beam's stiffness calculated in Section 6.5,

$K_{Bi}$  is the single equivalent beam's stiffness included in the bottom beam, and

$N_{up.design}$  is the design value of axial force in the upper column.

Then, when the loading process reaches point (4),  $N_{lost} = N_{lost}^{Pl.Rd}$  and it continues to remain constant.

$$N_{up}^{(4)} = N_{up.design} - N_{lost}^{Pl.Rd} \left( 1 - \frac{K_{bottom.beam}}{\sum_{i=1}^n K_{Bi}} \right) \quad (8.3)$$

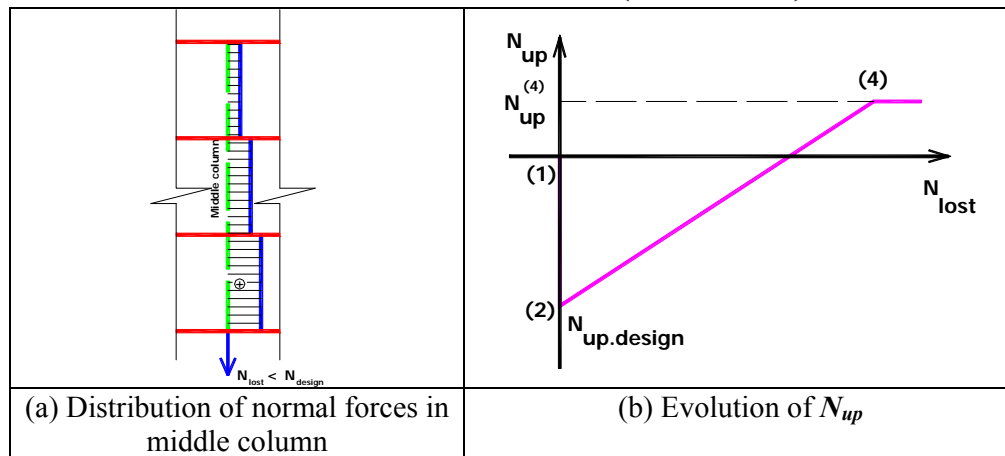


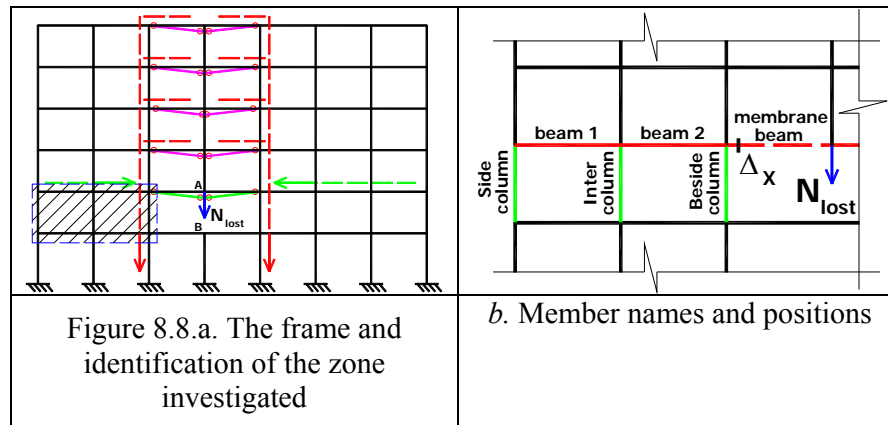
Figure 8.7. Axial forces of the middle columns and evolution of  $N_{up}$

### 8.2.6. Conclusion

As presented in the previous paragraphs, the objectives of this chapter were fulfilled by Demonceau's thesis. The terms and values presented in this chapter were needed for his theory and formulae on the catenary action of the bottom beams, which represents the behavior of the frame in Load Phase 3. In particular, with his analyses of the influence of each parameter on catenary action, the full behavior of the frame in the accidental loss of a column was predicted.

### 8.3. BEHAVIOR OF THE MEMBERS ADJACENT TO THE DAMAGED COLUMN

In the present section, the members on the damaged level (which are placed within the blue rectangle in Figure 8.8.a), i.e., the columns on the same floor as the lost column, are under consideration.



#### 8.3.1. Extra compression and bending in the columns

##### 8.3.1.a. Initial loading phase

During the first phase, each type of column undergoes a different type of force depending on its position. The loads which were applied to the frame induce compression on the columns, whereas normally the external column has to support significant bending moments. The axial forces in the internal columns are larger than the value appearing in the external column. The bending moment and axial force values are called  $N_{design}$ ,  $M_{design}$  respectively at the end of Phase 1. During this phase, it is reasonable to

assume that the horizontal displacement at the top of the investigated columns is equal to 0 ( $\Delta_x \approx 0$ ).

$$\begin{aligned} N &= 0 \nearrow N_{design}; \\ M &= 0 \nearrow M_{design}; \\ \Delta_x &\approx 0. \end{aligned} \tag{8.4}$$

where  $M_{design}; N_{design}$  are respectively the initial bending moment and axial force within the columns at the end of Phase 1, and  $\Delta_x$  is the horizontal displacement of the top of the columns investigated.

### 8.3.1.b. Load Phase 2

During Phase 2, the column progressively disappears. The column loss induces an increase in the bending moments at the beam's extremities within the directly affected part. Within the damaged level, the remaining columns which are affected by the loss of the column are on either side of the damaged one. In particular, an increase in the bending moments applied and axial compression load was observed in the adjacent columns. The other remaining columns are not significantly affected, as shown in Figure 8.9. At the end of Phase 2, the internal forces within the columns ( $M_{Elastic}^{Max}$ ) were calculated as the sum of the design value at the end of Phase 1 plus the value associated with the column loss at the end of Phase 2 (i.e., at point (4) in Figure 8.1). Also, during this phase, the variation in the internal loads within the columns investigated is proportional to the variation in the load within the lost column, as in Formula 8.5.

During Phase 2, it was assumed that the horizontal displacement at the top point of the investigated columns was not significant and, accordingly, could be neglected.

$$\begin{aligned} N &= N_{design} \nearrow N_{Elastic}^{Max} = N_{design} + \Delta N_2; \\ \Delta N_2 &= n_1 N_{lost}^{Pl.Rd} \\ M &= M_{design} \nearrow M_{Elastic}^{Max} = M_{design} + \alpha \Delta N_2; \\ \Delta_x &\approx 0. \end{aligned} \tag{8.5}$$

where  $M_{Elastic}^{Max}; N_{Elastic}^{Max}$  are the maximum internal force values within the columns studied at the end of Phase 2,

$\alpha$  is the coefficient linking the bending moment and the axial load within the columns studied during Phase 2 ( $\Delta N_2$ ), and

$n_1$  is the coefficient linking  $\Delta N_2$  and  $N_{lost}^{Pl.Rd}$ .

8.3.1.c. Load Phase 3

During Phase 3, when a plastic mechanism forms within the directly affected part, significant membrane forces develop within the bottom beams. This influenced the value of the internal loads within the columns studied. It was determined that the additional compression within the columns is linearly proportional to the membrane forces developing in the directly affected part as detailed in Formula 8.6. Also, the bending moments within these columns were evaluated according to the horizontal forces applied. During this phase, significant horizontal displacements at the top of the investigated columns were observed.

$$\begin{aligned}
 N &= N_{Elastic}^{Max} \nearrow N_{Failure} = N_{Elastic}^{Max} + \Delta N_3; \\
 \Delta N_3 &= n_2 H_{memb} \\
 M &= M_{design} \searrow 0 \searrow M_{Failure}; \quad M = M_{design} + M_{Elastic}^{Max} - \beta H_{memb} \\
 \Delta_x &\neq 0.
 \end{aligned}
 \tag{8.6}$$

where  $M_{Failure}, N_{Failure}$  are the maximum internal forces values resulting from the collapse of the damaged level,

$\beta$  is the coefficient linking the bending moment and the horizontal load due to the membrane forces, and

$n_2$  is the coefficient linking  $\Delta N_3$  and the membrane forces  $H_{memb}$ .

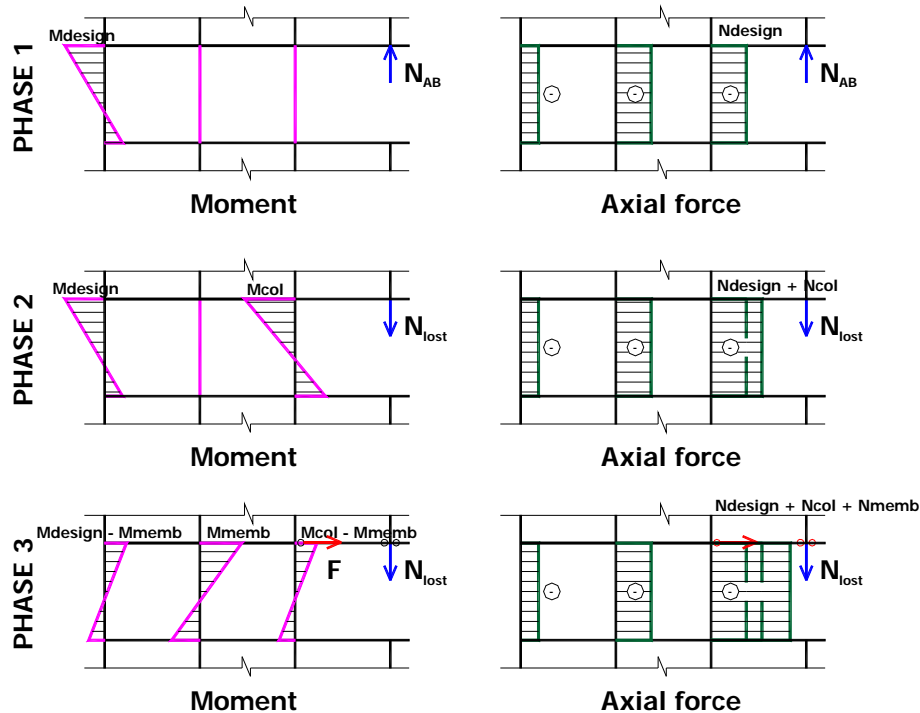


Figure 8.9. Evolution of the bending moment  $M$  and axial force  $N$  within the columns of the damaged level at the collapsed floor level

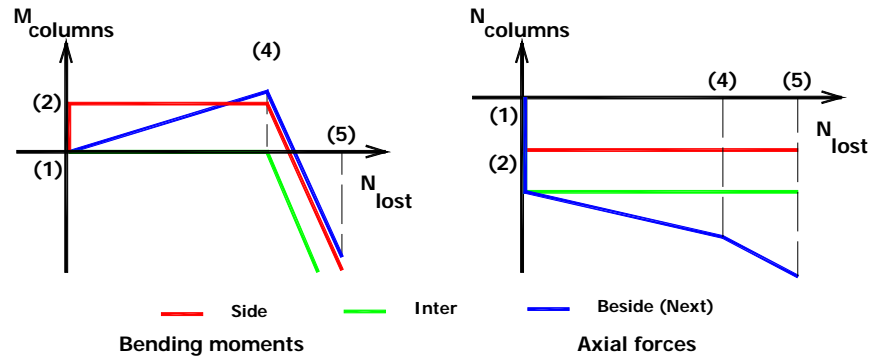


Figure 8.10. Diagrams of the bending moment  $M$  and axial force  $N$  within the columns

### 8.3.2. Axial forces in the beams

Beams 1 and 2 will be investigated in this section. When the frame supports an additional load, the force is transferred to the beam in a special way.

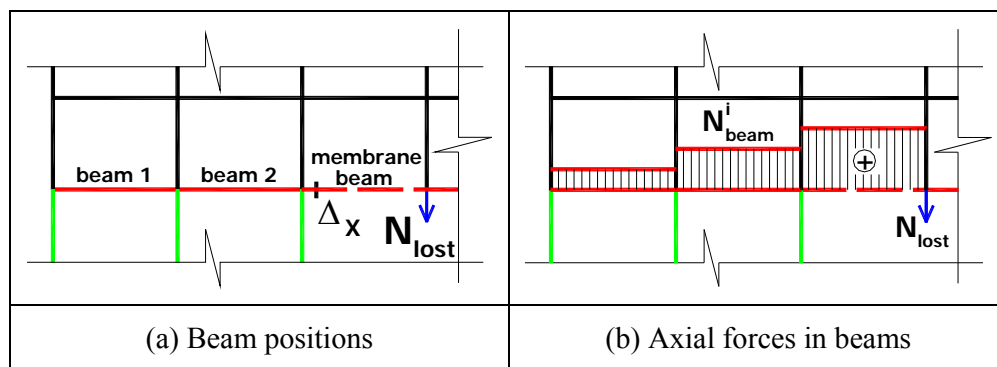


Figure 8.11: The beams at column top

Beginning with the first phase, the frame has to support the normal initial load. The beam supports the vertical loads, which are a combination of the distributed loads such as self weight, service load or permanent load. The beam's axial force is so small it can be considered zero. The bending moment diagram is displayed in Figure 8.11.

In the second phase, the additional load produces an axial force in the membrane beam due to the equilibrium of forces at the column's top point. From right to left, the beams' normal forces decline proportionally. The distribution of internal forces among these beams results from a combination of three effects. They comprise the elongation of the beam, the load transfer to the bended beam and the influence of the adjacent members on this part. It is difficult to calculate this distribution without performing a full-scale frame analysis.

In developing a simplified formula to predict the axial forces, the stiffness distribution is investigated to calculate more quickly. If one considers the axial force distribution, which

follows the concentration of stiffness, these forces take on the value

$$N_{beam}^i \approx H_{memb} \frac{\sum_{i=1}^{m-i} S_{Ci}}{\sum_{i=1}^m S_{Ci}}, \quad (8.7)$$

where  $S_{Ci}$  is the stiffness of column number  $i$ , and  $m$  is the number of columns in the zone investigated.

Continuing now to the third phase, when the catenary action occurs, the membrane force increases in the beam over the destroyed column. That axial force acts on the top of the adjacent column just as in the previous phase and continues to increase until the frame collapses.

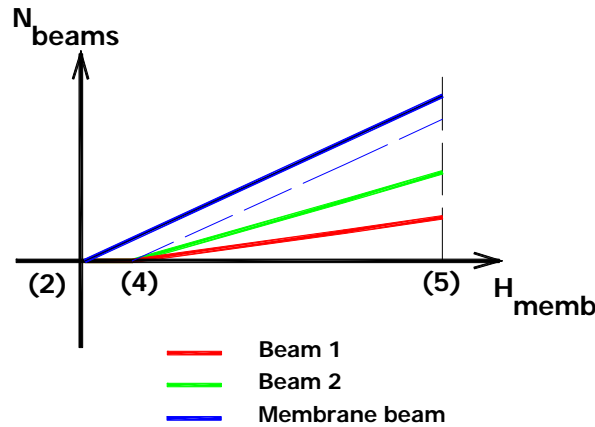


Figure 8.12: Distribution of axial forces in the beams as a function of the membrane force

### 8.3.3. Conclusion

This section concentrates on the behavior of the left side of the damaged level. The distribution of internal forces among its members was described. Based on the particular behavior of those members, the next section will develop the individual member analytical model.

Because the second order effect takes on an important role in Load Phase 3, the surrounding frame elements are directly influenced by that non-linear behavior. However, using the investigation of each member's internal forces, the linearized behavior of the columns and beams in the investigated zone was defined, illustrated in Figures 8.10 and 8.12. They provide the possibility of simplifying the analytical calculation of those members. A more detailed development of these analytical models is discussed in the next section.

## 8.4. ANALYTICAL MODEL TO SIMULATE THE DAMAGED LEVEL

As presented in Section 8.2, in Load Phase 3, the directly affected part goes over its plastic limit. All equivalent beam ends yield, then the catenary action is triggered on only the bottom equivalent beam. Recall that the outside blocks move freely in accordance with the membrane force. The only part which supports that load is the damaged level.

Continuing with the discussions begun in Chapter 6, this section focuses on the simulation process for developing an analytical model of the damaged level. For simplicity's sake, the damaged level was simulated by the model of only the left side, as in Figure 8.1.3. The objective of this extracting process was to obtain the analytical model which is used in predicting the lateral stiffness  $K$  and the damaged level's resistance  $F_{Rd}$ .

The analytical model extraction was performed on the left part of damaged level in Figure 8.13. A colored separation is used within the zone for the three columns: the side/external column AD, the intermediate column BE and the adjacent column CF are in green while the two top beams AB and BC are in red. In reality, the membrane force  $H_{memb}$  applied to the part was transferred to the lower level and compressed beams DE and EF through the column's bottom points. That reaction was neglected in the analytical model in order to keep the model simple.

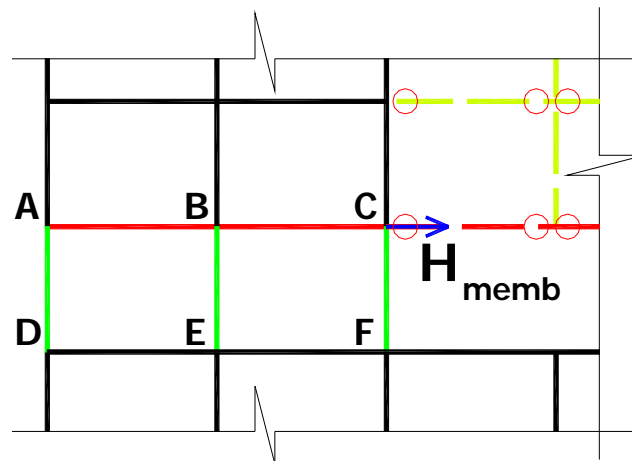


Figure 8.13: Left part of damaged level

### 8.4.1. Individual columns

In the damaged level, the columns are connected by the beams at the top and bottom. When extracting an individual column from the frame, its relation to the surrounding frame



members was first identified. At this time, two parameters needed to be considered. The first parameter was the partially restrained coefficient of the column's end points. The second was the column's top boundary condition dependent on the working condition of the column in Load Phase 3 only.

*8.4.1.a. Partial restraint at the columns' ends*

Once more, the rotational capacity of structural members' end points needs to be considered. This coefficient represents the partial restraints at the column's end points. Usually, the top and bottom points of the columns are neither hinges nor fixed. They are restrained by the adjacent members.

A similar coefficient has already been developed in Section 6.4. The only difference here is the direction of the expansion order, presented in Figure 8.14 when the bending moment  $M_C$  was applied to the top point of column FC. This illustrates the members' expansion order to account for their bending ability in the partial restraint coefficient.

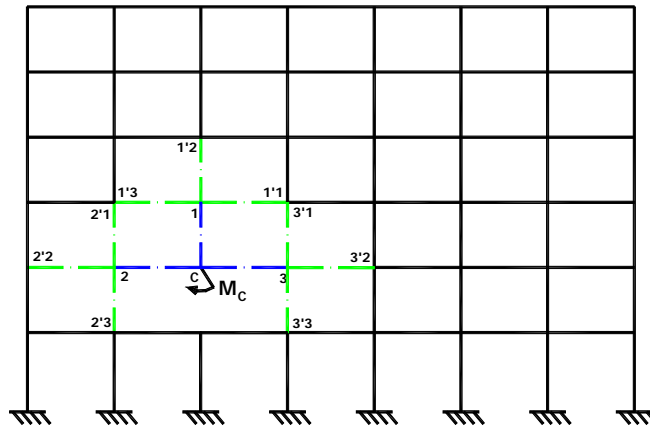


Figure 8.14: The members' influence on the column's restrained end rotation

*8.4.1.b. Boundary condition at the top of column*

Only in Load Phase 3, where beams AB and BC connected three columns and the left side was designated the free side, the three columns' top points could move horizontally.

Another property concerns the second-order behavior of the column in this part. According to this behavior, the boundary condition applied to the model was the rotating block end. Then the final individual column model was obtained, as illustrated in Figure 8.15.

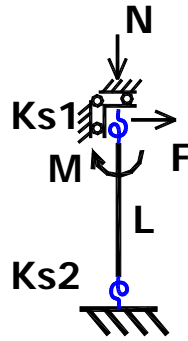


Figure 8.15. Analytical individual model

### 8.4.2. Beam under tension

Due to the deflection of the bottom equivalent beam, the membrane force acts as shown in Figure 8.16. This force is divided into two components, namely, the additional compression on the adjacent column CF and the horizontal force applied to point C.

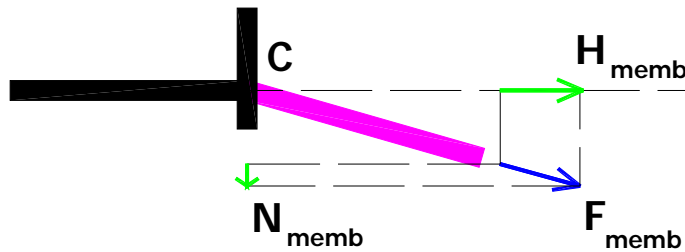


Figure 8.16. Horizontal and vertical components of the membrane force

The top beams AB and BC transfer the horizontal force to the column's top points. In order to estimate the lateral stiffness  $K$ , the bending stiffness of these beams was neglected in the model. They were considered tension only members.

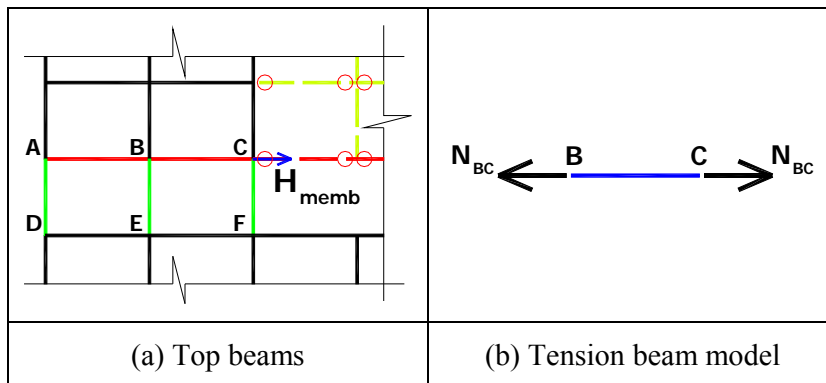


Figure 8.17. Top beams and their analytical models

### 8.4.3. Assembly of the members

Figure 8.18 presents the model of the left side of the damaged level substituting the real members by their models. The beam is considered a tension only member. The 2-spring model is applied to the column with all outer influences being replaced by the springs. In Phase 3, the top of the column was considered to be clamped, so a rotational restraint was applied to that point. Other degrees of freedom were released.

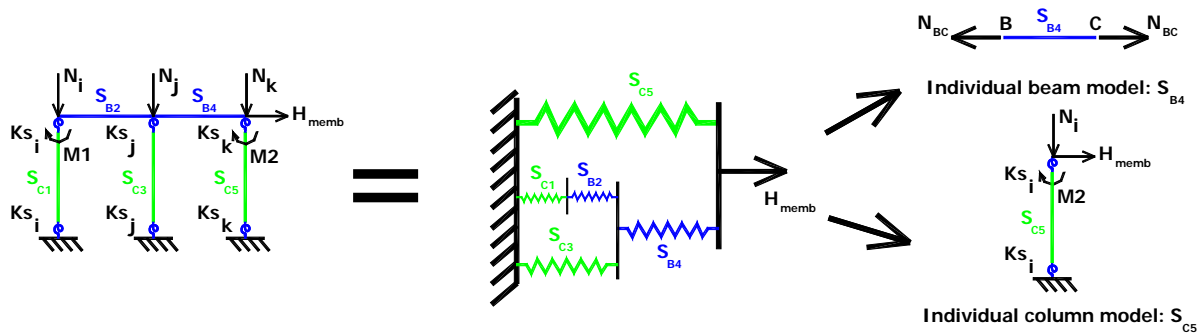


Figure 8.18. The left side damaged level model

### 8.4.4. Conclusion

The process used in Chapter 6 has been repeated to develop the analytical model of the damaged level. For this, the individual members were connected in the substructure by serial or parallel connections according to their relations.

However, in Load Phase 3, the second-order effect takes on an important role. Each individual column must support its own level of compression from the upper floor loads. For example, the adjacent column has to support additional compression due to the loss of the column. So, the stiffness and resistance formula of each individual member is not treated in the same way. The details involved in each of the calculations are illustrated in their respective sections below.

## 8.5. LATERAL STIFFNESS COEFFICIENT $K$

Chapter 5 presented the alternative load path in Phase 2 and also the extension of that load path due to the activation of catenary action. Afterwards, Section 8.2 demonstrated the distribution of internal forces within the damaged level by concentrating on its major second-order behavior. Then, the three load phases were illustrated.

Unlike in Chapter 6, where the directly affected part was investigated within the elastic range, the damaged level was simulated here by an analytical model working under high compression. The first paragraph of this section describes the analytical frame members which were applied to simulate the column's behavior under the complex loading state. The displacement method was used with the full stiffness matrix and a modification to its shear component to obtain the second order effect's influence.

The previous stiffness matrix was applied to the column model with two partial restraint coefficients, as in Section 8.4. The shear component of the stiffness matrix was extracted in order to obtain the column's stiffness. The two formulae were described according to the constant or inconstant compression forces loaded on the columns.

The next paragraph recalls the simplification of the substructure's stiffness thanks to the very high stiffness of the top beams compared to the column's stiffness.

### 8.5.1. Column model and stiffness matrix with 2<sup>nd</sup> order effects

#### 8.5.1.a. First-order full stiffness matrix

The model and formula in Section 6.4.4 are repeated below to help develop the stiffness matrix of a member of the frame.

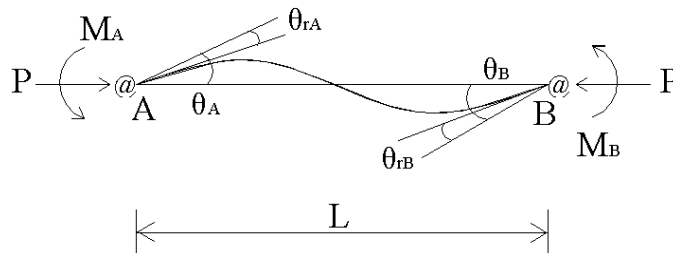


Figure 8.19. Semi-rigid frame member.

So

$$k_A = \frac{M_A}{\theta_{rA}}; \quad k_B = \frac{M_B}{\theta_{rB}}. \quad (8.8)$$

Then, the bending moment of both beam ends could be written as:

$$M_A = \frac{E_C I_C}{L_C} \left[ 4 \left( \theta_A - \frac{M_A}{\theta_{rA}} \right) + 2 \left( \theta_B - \frac{M_B}{\theta_{rB}} \right) \right]; \quad (8.9)$$

$$\mathbf{M}_B = \frac{E_C I_C}{L_C} \left[ 2 \left( \theta_A - \frac{M_A}{\theta_{rA}} \right) + 4 \left( \theta_B - \frac{M_B}{\theta_{rB}} \right) \right]. \quad (8.10)$$

Taking  $M_A; M_B$  out of the statement, one obtains

$$M_A = \frac{E_C I_C}{L_C} [r_{ii} \theta_A + r_{ij} \theta_B] \quad (8.9a)$$

$$M_B = \frac{E_C I_C}{L_C} [r_{ij} \theta_A + r_{jj} \theta_B] \quad (8.10a)$$

where

$$r_{ii} = \frac{1}{k_R} \left( 4 + \frac{12 E_C I_C}{L_C k_B} \right)$$

$$r_{jj} = \frac{1}{k_R} \left( 4 + \frac{12 E_C I_C}{L_C k_A} \right)$$

$$r_{ij} = \frac{2}{k_R}$$

$$k_R = \left( 1 + \frac{4 E_C I_C}{L_C k_A} \right) \left( 1 + \frac{4 E_C I_C}{L_C k_B} \right) - \left( \frac{E_C I_C}{L_C} \right)^2 \left( \frac{4}{k_A k_B} \right).$$

Finally, the classic full element stiffness matrix becomes

$$k_e^{1st} = \begin{bmatrix} \frac{A_C E_C}{L_C} & 0 & 0 & -\frac{A_C E_C}{L_C} & 0 & 0 \\ 0 & (r_{ii} + 2r_{ij} + r_{jj}) \frac{E_C I_C}{L_C^3} & (r_{ii} + r_{ij}) \frac{E_C I_C}{L_C^2} & 0 & -(r_{ii} + 2r_{ij} + r_{jj}) \frac{E_C I_C}{L_C^3} & (r_{ij} + r_{jj}) \frac{E_C I_C}{L_C^2} \\ 0 & (r_{ii} + r_{ij}) \frac{E_C I_C}{L_C^2} & r_{ii} \frac{E_C I_C}{L_C} & 0 & -(r_{ii} + r_{ij}) \frac{E_C I_C}{L_C^2} & r_{ij} \frac{E_C I_C}{L_C} \\ -\frac{A_C E_C}{L_C} & 0 & 0 & \frac{A_C E_C}{L_C} & 0 & 0 \\ 0 & -(r_{ii} + 2r_{ij} + r_{jj}) \frac{E_C I_C}{L_C^3} & -(r_{ii} + r_{ij}) \frac{E_C I_C}{L_C^2} & 0 & (r_{ii} + 2r_{ij} + r_{jj}) \frac{E_C I_C}{L_C^3} & -(r_{ij} + r_{jj}) \frac{E_C I_C}{L_C^2} \\ 0 & (r_{ij} + r_{jj}) \frac{E_C I_C}{L_C^2} & r_{ij} \frac{E_C I_C}{L_C} & 0 & -(r_{ij} + r_{jj}) \frac{E_C I_C}{L_C^2} & r_{jj} \frac{E_C I_C}{L_C} \end{bmatrix}. \quad (8.11)$$

The first order stiffness of a column supporting a horizontal force applied to the column's top point is

$$\begin{aligned} K_C^{1st} &= (r_{ii} + 2r_{ij} + r_{jj}) \frac{E_C I_C}{L_C^3} = \\ &= \frac{12 E_C I_C}{L_C^2} \frac{L_C k_{s1} k_{s2} + (k_{s1} + k_{s2}) E_C I_C}{L_C^2 k_{s1} k_{s2} + (k_{s1} + k_{s2}) 4 E_C I_C L_C + 12 E^2 I_C^2} \end{aligned} \quad (8.12)$$

Then, taking into account initial rotation, such as the initial bending, the formula becomes

$$\mathbf{K}_C^{1st} = \frac{\left[ L_C^3 k_{s1} k_{s2} + 4E_C I_C L_C^2 (k_{s1} + k_{s2}) + 12(E_C I_C)^2 \right]}{12E_C I_C \left[ L_C k_{s1} k_{s2} + E_C I_C (k_{s1} + k_{s2}) \right]} - \frac{12(E_C I_C)^2 \alpha \left\{ \left[ k_{s1} + \gamma(k_{s1} + k_{s2}) \right] + L_C k_{s1} k_{s2} E_C I_C (6 + 8\gamma) \right\}}{12E_C I_C \left[ L_C k_{s1} k_{s2} + E_C I_C (k_{s1} + k_{s2}) \right]} \quad (8.13)$$

where  $\mathbf{K}_C^{1st}$  is the shear stiffness of column included the second order effect and the initial rotation at the column's ends,

$k_{s1}, k_{s2}$  is the semi-rigid rotational stiffness of both column ends,

$E_C I_C$  is the elastic modulus and inertia moment of the column section,

$\alpha$  is the linear coefficient of end rotation from the horizontal force  $H_{memb}$ , and

$\gamma$  is the ratio between two initial rotations of both column ends (normally,  $\gamma = 2$ ).

#### 8.5.1.b. Second-order effect

According to the stability function approach from the slope—deflection differential equation, the horizontal stiffness of the beam—column member is written as

$$\mathbf{k}_e^{2nd} = \mathbf{k}_e^{1st} + \begin{bmatrix} 0 & 0 & 0 & 0 & 0 & 0 \\ 0 & -\left( L \sqrt{\frac{P_i}{E_C I_C}} \right)^2 \frac{E_C I_C}{L_C^3} & 0 & 0 & \left( L \sqrt{\frac{P_i}{E_C I_C}} \right)^2 \frac{E_C I_C}{L_C^3} & 0 \\ 0 & 0 & 0 & 0 & 0 & 0 \\ 0 & 0 & 0 & 0 & 0 & 0 \\ 0 & \left( L \sqrt{\frac{P_i}{E_C I_C}} \right)^2 \frac{E_C I_C}{L_C^3} & 0 & 0 & -\left( L \sqrt{\frac{P_i}{E_C I_C}} \right)^2 \frac{E_C I_C}{L_C^3} & 0 \\ 0 & 0 & 0 & 0 & 0 & 0 \end{bmatrix} \quad (8.14)$$

Regarding the horizontal stiffness of the beam—column with the force acting on the column's top, it is obtained from the shear stiffness of the column, which takes on the value of member [2, 2] in the stiffness matrix. If one takes the initial bending of the beam—column into account, the members [2, 3] and [2, 6] appear as in Formula 8.14.

The second-order stiffness of the column supporting horizontal forces simultaneously with constant vertical load  $N$  is described by

$$\mathbf{K}_C^{2nd} = \mathbf{K}_C^{1st} - \frac{N}{L_C}, \quad (8.15)$$

where  $\mathbf{K}_C^{2nd}$  is the shear stiffness of the column including the second order effect and the initial rotation at the column's ends.

### 8.5.2. Individual columns' shear stiffness with 2<sup>nd</sup> order effects

There are specific stiffness formulae for three types of columns: the external column, the intermediate column and the adjacent column. According to the forces applied to each of them individually, the stiffness due to horizontal displacement was calculated.

Figure 8.20 presents the evolution of the axial forces of the three column positions due to the horizontal component of the membrane force.

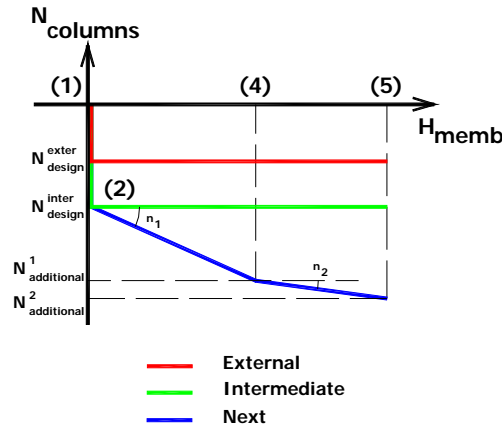


Figure 8.20. Axial forces in the three column positions

#### 8.5.2.a. External column

The external (or *outside*) column undergoes constant compression during the three loading phases, as presented in Section 8.2. Here, the compression force applied takes on the value of the initial axial force of this position. So, the external column's stiffness in Load Phase 3 is

$$K_C^{side} = K_{C.1st}^{side} - \frac{N_{design}^{exter}}{L_C}, \quad (8.16)$$

where  $K_C^{side}$  is the shear stiffness of the outside column involved in the second order effect,

$K_{C.1st}^{side}$  is the first order shear stiffness of the outside column,

$N_{design}^{exter}$  is the compression force applied to the column's top, and

$L_C$  is the column's length.

#### 8.5.2.b. Intermediate column

Figure 8.20 illustrates the similarity in behavior between the intermediate column and the

external column. Unlike the bending moment, the compressed force applied to this position keeps the same value as the initial axial force, which reaches its maximum in Load Phase 1. So,

$$\mathbf{K}_C^{Inter} = \mathbf{K}_{C.1st}^{Inter} - \frac{N_{design}^{inter}}{L_C}, \quad (8.16)$$

where  $\mathbf{K}_C^{Inter}$  is the shear stiffness of the intermediate column involved in the second order effect,

$\mathbf{K}_{C.1st}^{Inter}$  is the first order shear stiffness of the intermediate column,

$N_{design}^{inter}$  is the compression force applied to the top of the column, and

$L_C$  is the column's length.

### 8.5.2.c. Adjacent column

Due to its particular role on both the first and extended alternative load paths, the adjacent column must support high and complex transferred forces. From Formula 8.12, the second order stiffness of the adjacent column is defined as

$$\mathbf{K}_C^{Beside} = \mathbf{K}_{C.1st}^{Beside} - \frac{N^{Beside}}{L_C}, \quad (8.17)$$

where  $N^{Beside}$  is the full axial force applied to the adjacent column in Load Phase 3, and  $\mathbf{K}_{C.1st}^{Beside}$  is the first order shear stiffness of the adjacent column.

However, in Load Phase 3, the column's axial force varies. Its magnitude takes on the initial value of the intermediate column plus the additional axial force in Load Phase 2. In Load Phase 3, it varies according to the horizontal component of the membrane force:

$$\begin{aligned} N^{Beside} &= N_{(H_{memb})}^{Beside} = N_{design}^{inter} + N_{additional}^1 + N_{additional}^2 = \\ &= N_{design}^{inter} + N_{additional}^1 + n_2 H_{memb} \end{aligned} \quad (8.18)$$

where  $N_{additional}^1$  is the additional axial force applied to the adjacent column at point (4), calculated in Section 7.6,

$N_{additional}^2$  is the additional axial force applied to the adjacent column after point (4), and

$H_{memb}$  is the horizontal component of the membrane force.

Returning to the load—displacement relation, it is written as



$$\begin{aligned} H_{memb} &= K_C^{Beside} \Delta_X = \left( K_{C.1st}^{Beside} - \frac{N^{Beside}}{L_C} \right) \Delta_X = \\ &= \left( K_{C.1st}^{Beside} - \frac{N_{design}^{inter} + N_{additional}^1 + n_2 H_{memb}}{L_C} \right) \Delta_X \end{aligned} \quad (8.19)$$

where  $\Delta_X$  is the horizontal displacement of the adjacent column's top point.

Taking  $H_{memb}$  out of Formula 8.19 and bringing it to the left, one obtains

$$H_{memb} = \left( \frac{K_{C.1st}^{Beside} L_C - N_{design}^{inter} - N_{additional}^1}{L_C + n_2 \Delta_X} \right) \Delta_X \quad (8.20)$$

where  $n_2$  is the scalar of the secondary additional axial force due to the horizontal component of the membrane force.

Because the displacement  $\Delta_X$  is very small, the column's second-order stiffness becomes

$$K_C^{Beside} \approx \frac{K_{C.1st}^{Beside} L_C - N_{design}^{inter} - N_{additional}^1}{L_C + n_2} \quad (8.21)$$

where  $K_C^{Beside}$  is the shear stiffness of the adjacent column involved in the second order effect and the initial rotation at the column's ends.

### 8.5.3. Stiffness assembly principle

The previous paragraph explained how to obtain the stiffness of individual columns according to their positions within the frame. It also proved that, for external and intermediate columns, due to their constant compression state, their stiffness is constant. The particular position of the adjacent column's stiffness has already been simulated by the linearization of the second-order behavior of the column. The result is that the column's stiffness is approximately constant also.

According to the assembly rule in Section 6.3.3, the full part's stiffness in Figure 8.18 is obtained by the simplified connection method:

$$K_{Damage.Level}^{Left} = S_{C5} + \frac{1}{\frac{1}{S_{B4}} + \frac{1}{S_{C3} + \frac{1}{\frac{1}{S_{C1}} + \frac{1}{S_{B2}}}}} \quad (8.22)$$

#### 8.5.4. Simplifying the $K$ formula by summing the individual columns

Furthermore, as proved in Section 6.3 when the beam's elongation stiffness is higher than 20 times the bending stiffness of the individual column, the connection law is reduced to the simple sum of the columns' stiffness, so:

$$K_{DamageLevel}^{Left} = S_{C1} + S_{C3} + S_{C5} = K_C^{Side} + K_C^{Inter} + K_C^{Beside}, \quad (8.23)$$

and  $K$ , when taking into account the left and right sides' behavior, is equal to

$$K = \frac{K_{DamageLevel}^{Left} K_{DamageLevel}^{Right}}{K_{DamageLevel}^{Left} + K_{DamageLevel}^{Right}}. \quad (8.24)$$

#### 8.5.5. Validation

The validity of the analytical procedures proposed was verified by comparisons with the numerical results. An example of one of the frames analyzed is presented here below.

The frame has 7 spans and 6 floors, where the span length and the floor height are uniform. The column sections are HE360A and the beam sections are IPE400v. For this building, twelve positions of the lost column were investigated as presented in Figure 8.21.

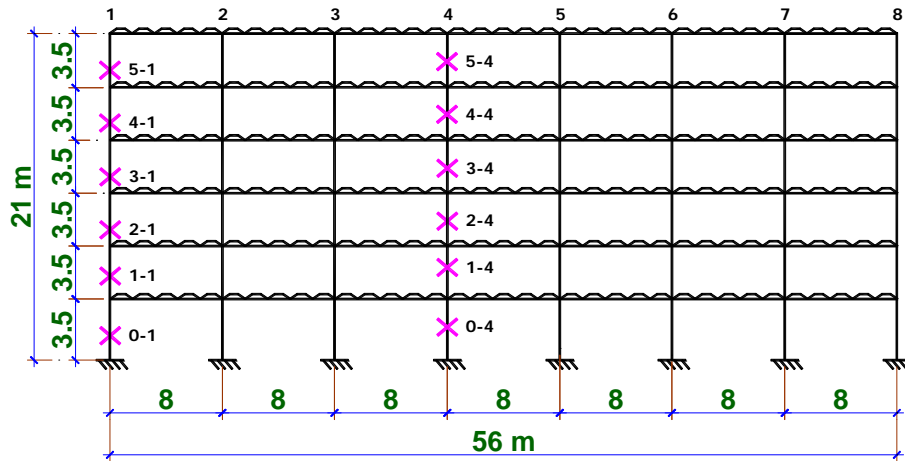


Figure 8.21. Frame investigated.

Figure 8.22 demonstrates the first validation step, where a single, 6-meter high HE180A column supported a compressed load of 510 kN. The two end points of the column were connected to springs of 15,000 and 25,000 kNm/rad. The analytical results of the first- and second-order stiffness are included here with a comparison to data from FINELG.

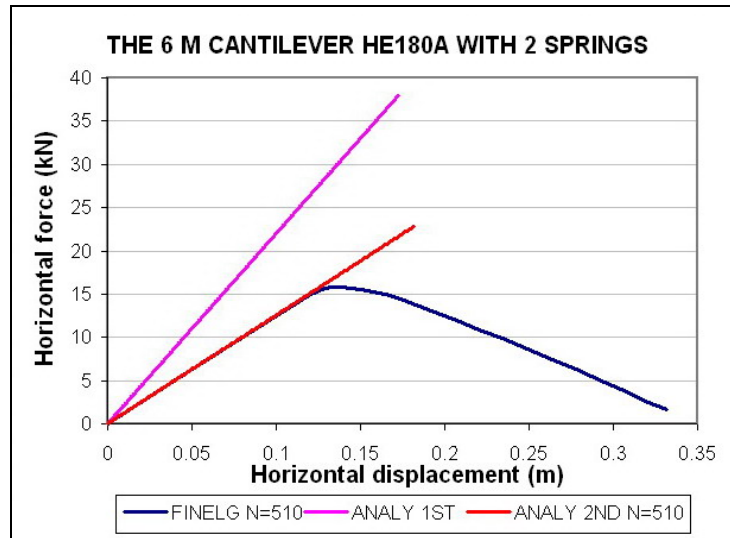


Figure 8.22. Single analytical model validation

Next, the frame in Figure 8.21 with full loads being applied was investigated. Figure 8.23 shows the column extracted next to position 1-4 and its analytical results. The partial restraint coefficients were taken out of the frame configuration and applied to the simulated model.

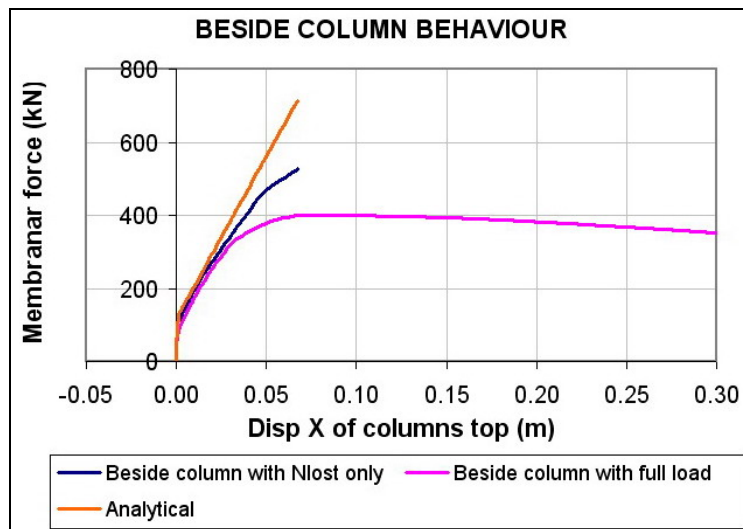


Figure 8.23. Individual column in frame and model result

An example for comparison is given in Figure 8.24. In it, the analytical prediction obtained through the proposed procedures has been compared to the response obtained through a fully non-linear numerical analysis.

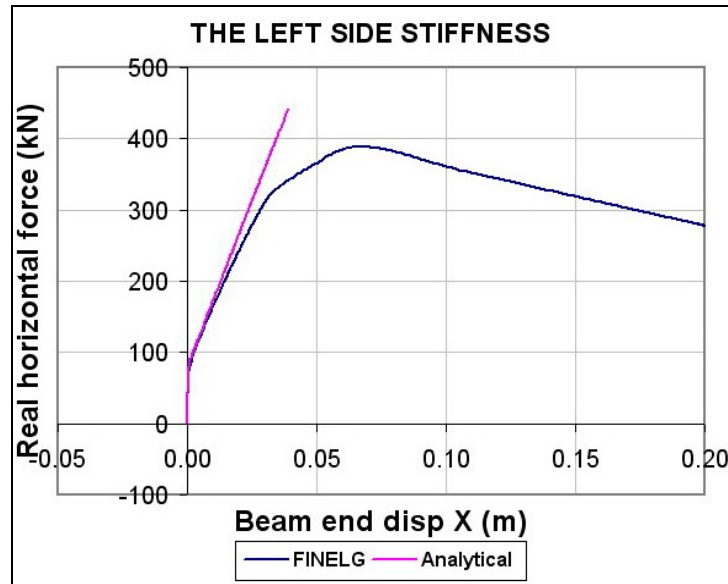


Figure 8.24. Left side of damaged level behavior and analytical results

### 8.5.6. Conclusion

This section has demonstrated the analytical method for simulating the behavior of the damaged level by influencing the behavior of the catenary action. The tying action on the membrane beam was explained by the particular behavior of the columns within the damaged level. The assumptions and analytical calculations were developed in order to simplify the complex behavior of the full residual frame.

The validation proved how practical this method actually is. Obviously, the rough assumptions, e.g., applying second-order linearization to the frame when extracting the substructure, produced relatively approximate results. However, as proved by Demonceau,  $\mathbf{K}$  stiffness is useful because of its constant value during Load Phase 3. His other conclusion was that the 10% tolerance of  $\mathbf{K}$  does not influence the behavior of the catenary action. This assumption was also validated by the analysis and simulation of the frame by PSP and the ULg in [Demonceau, 2008].

## 8.6. LATERAL RESISTANCE OF THE DAMAGED LEVEL

In the previous section, the method for analytically calculating lateral stiffness  $\mathbf{K}$  was described. Based on the behavior of the damaged level under the complex loading state during Load Phase 3, the individual columns' stiffness is taken into the part's stiffness,  $\mathbf{K}$ .

This section presents the response of the column in such a loading state. Once again, the hinge-by-hinge, elastic—perfectly plastic limit analysis was applied. The resulting full behavioral curve of the column is presented. First, though, the next paragraph points out the necessity of an individual column stability test, especially on the damaged level in Load Phase 3.

### 8.6.1. Column instability

#### 8.6.1.a. Plastic resistance of the individual column

At point (4) on the load-carrying curve, depending on the column's position, the column may or may not support the initial bending. After the catenary action occurs, its horizontal force produces the opposite bending moment at each column section. That bending moment rises until the frame collapses due to the catenary beam's collapse or because the beam's end joints reach their rotational limits. The other possible failure could stem from the instability of the column.

Figure 8.25 presents the column model and its behavior when such a load was applied. In the very beginning, the column supported the initial bending moment, the horizontal force and compression. When the top section reached its plastic limit, the hinge appeared. The model then corresponds to the second one, in Figure 8.25. Due to the boundary condition and compression, the column may even collapse before it reaches its plastic limit because of this instability.

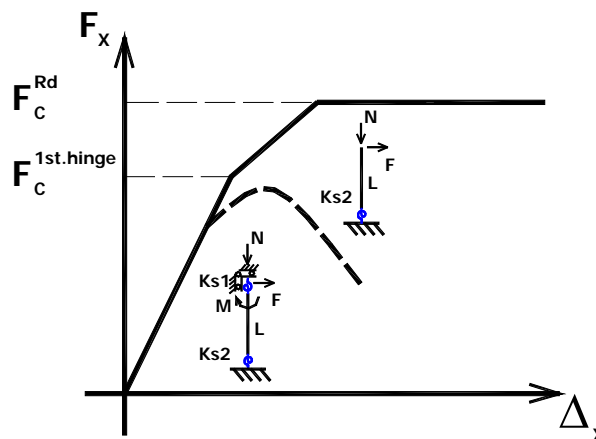


Figure 8.25: The resistance of the first floor column

With the elastic—perfectly plastic behavior, the column on one floor behaves as shown in the figure above. At each segment, the column's stiffness is defined by

$$\begin{aligned} K_C^1 &= \frac{12EI_C}{L_C^2} \frac{L_C k_{s1} k_{s2} + (k_{s1} + k_{s2}) EI_C}{L_C k_{s1} k_{s2} + (k_{s1} + k_{s2}) 4EI_C L_C + 12E^2 I_C^2} - \frac{N}{L_C}; \\ K_C^2 &= \frac{3EI_C}{L_C^2} \frac{k_{s2}}{L_C k_{s2} + 3EI_C} - \frac{N}{L_C}; \end{aligned} \quad (8.25)$$

and the critical value of horizontal force being applied is

$$F_{Rd} = \frac{(M_p^{C.1} + M_p^{C.2}) K_C^{2nd}}{K_C^{2nd} L_C + N} \quad (8.26)$$

where  $M_p^{C.1}, M_p^{C.2}$  are the plastic moments of the column section at two end points.

In a standard case, the column is placed within the frame, so  $k_{s1} = k_{s2}$ , thereby giving the column's stiffness by

$$\begin{aligned} K_C^1 &= \frac{12EI_C}{L_C^2} \frac{k_{s2}}{L_C k_{s2} + 6EI_C} - \frac{N}{L_C}; \\ K_C^2 &= \frac{3EI_C}{L_C^2} \frac{k_{s2}}{L_C k_{s2} + 3EI_C} - \frac{N}{L_C}; \end{aligned} \quad (8.27)$$

$$F_{Rd} = \frac{2M_p^C K_C^{2nd}}{K_C^{2nd} L_C + N}. \quad (8.28)$$

#### 8.6.1.b. Columns' instability

The columns in the damaged level always support the vertical load coming from the floor above during the whole loading process, even after the loss of the column. It follows that checking the stability of these columns is essential. In the second and third phases, the applied load increases first through bending moment and then on the paired forces of compression and bending moment. For each phase, therefore, on the column next to the destroyed column, both section and global stability must be checked.

#### 8.6.2. Weakest column and the simplification of the resistance formula

Section 8.3.2 demonstrates the distribution of axial forces within the top beams. Then, the horizontal force applied to the column top equals

$$F^i \approx H_{memb} \frac{K_C^i}{\sum_{i=1}^m K_C^i}. \quad (8.29)$$

The column supporting the most dangerous force has the stiffness  $K_C^{dangerous}$  and so

$$\frac{F^i}{F^{dangerous}} = \frac{K_C^i}{K_C^{dangerous}} \Rightarrow F^i = F^{dangerous} \frac{K_C^i}{K_C^{dangerous}} \quad (8.30)$$

where  $F_C^{dangerous}$  is the dangerous applied force,  
 $F_C^i$  is the force applied to column number  $i$ , and  
 $K_C^{dangerous}, K_C^i$  are the respective columns' stiffness.

$$H_{memb} = \sum_{i=1}^m F^i = F^{dangerous} \frac{\sum_{i=1}^m K_C^i}{K_C^{dangerous}} \quad (8.31)$$

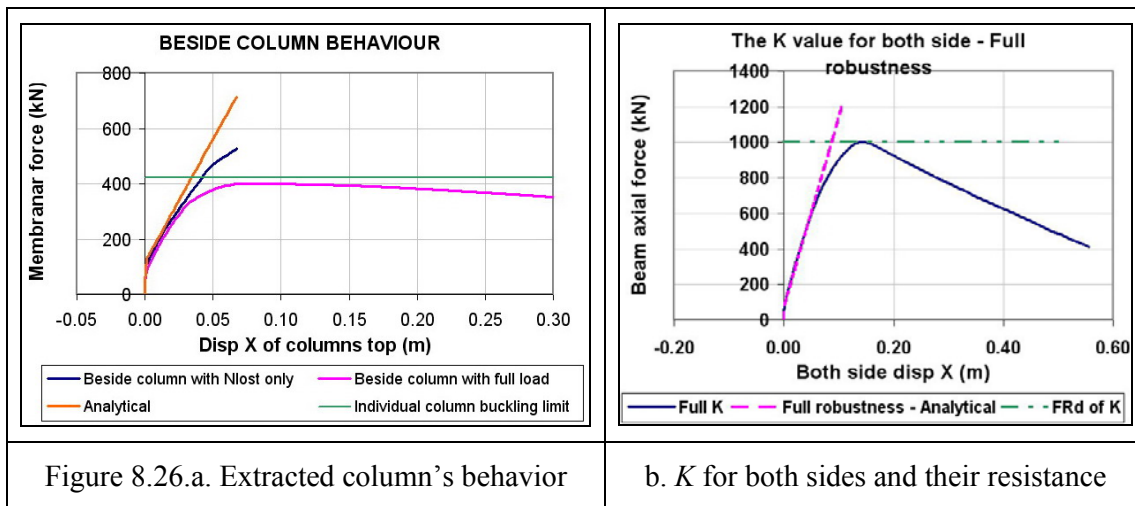
The resistance  $F_{Rd}$  is reached when one of the columns in the damaged level fails. The resistance of the damaged level can be predicted through Formula 8.27 where the distribution of the internal loads according to the column's stiffness is taken into account. In fact, the weakest column in a typical frame normally is the side column. So the full part's resistance is

$$F_{Rd} = F_C^{Rd} \frac{\sum_{i=1}^m K_C^i}{K_C^{max}} \quad (8.32)$$

where  $F_C^{Rd}$  is the weakest column resistance.

### 8.6.3. Validation

Figure 8.26 demonstrates the validity results from the frame investigated in Figure 8.21 using the application of the analytical resistance calculation method.



#### 8.6.4. Conclusion

As proved in this section, the resistance of the damaged level depends on the capacity of the individual columns within this part. In Load Phase 3, the column supports a complex loading state due to a pair of bending moment and axial force or even the varying additional axial force.

The plastic resistance and the formula to estimate the stability of individual columns were developed. With the distribution of pulling force transferred through the top beams, the horizontal forces acting on the column top were quickly calculated and then the resistance of the whole part was derived from that of the most dangerous one. As a result, it can be concluded that the first/weakest column failure leads to the whole part's collapsing.

#### 8.7. SUMMARY AND CONCLUSIONS

Through Chapters 6, 7, and 8, the full account of the alternative load path appearing in the frame after the impact of the loss of a column has been demonstrated. First, Chapter 6 presented the directly affected part's behavior. Then, Chapter 7 continued by describing the second part, the adjacent columns, in order to investigate the behavior of the members along the first alternative load path. Last but not least, Chapter 8 explained the extension of the alternative load path by the activation of catenary action.

In this chapter, the first section concentrated on the work of Jean-Francois Demonceau, with whose complementary thesis, the present work aimed to provide the full description of a frame's response to the loss of a column. To demonstrate the nonlinear behavior of the catenary action, the influential nature of surrounding members has been predicted. The requirements for predicting this are fulfilled by three parameters:  $K$ , its resistance  $F_{Rd}$  and the hanging force  $Q$ .

Then, the multilevel analytical simulation described in Chapter 4 was used to simulate the damaged level's behavior. Only the left side of this area was dealt with, but the method was applied similarly to both sides of the frame. Then the final  $K$  was estimated by taking into account both sides' stiffness and that of the internal beams under compression.

The individual column's stiffness in Load Phase 3 was defined. Its calculation included not only the second-order effect but also the position of the formation of plastic hinges. Then, the full and simplified substructure of the part was built by assembling the members



within. Moreover, this simplification using the individual columns provides the most practical application. That simple model gives the user the opportunity to predict the full part's resistance quickly.

To conclude, Chapter 8 finalizes the complete theoretical and methodological discussion of this thesis. The next chapter demonstrates the systematized process representing the practical application of these theories to a real building problem.

**CHAPTER 9: MULTILEVEL ROBUSTNESS ASSESSMENT  
OF A BUILDING FRAME**

## 9.1. INTRODUCTION

The frame's response following the exceptional loss of a column was thoroughly examined in the previous eight chapters. From the assumptions made on the loss of a column, on the residual frame state and on the additional load, the theoretical analytical method was built. However, it is difficult to gather the numerous details necessary in order to calculate such a problem systematically. From the user's point of view, there needs to be a clear methodology to follow for the analysis and for the measurement of the frame's load capacity. Indeed, explanations on the alternative load paths and their key elements' behavior alone are not enough.

In this light, this chapter systematizes the calculations which have been presented in earlier sections. The conclusions and formulae of the previous chapters have been gathered together and enumerated in an object-oriented list. According to the frame's load capacity, conveyed by the residual frame and the alternative load paths, the assessment method of this work was developed through three phases of the loading process, in the aim of identifying the critical points regarding the key elements. For the sake of clarity, the frame's zones and the members' names have not been listed; furthermore, only the shortest analytical formulae are presented.

Thus, this chapter's principal content comprises two key components. The first assembles the analytical formulae which have been developed in this thesis. The second presents a thorough example of the calculation of an existing frame.

In more detail, the first major division of this chapter concentrates on the formulae and methodology used. It consists of a flowchart regrouping the concepts and formulae arranged in order of users' needs. These elements have been separated into four steps which cover the whole loading process. The steps were defined by the requirements of the assessment procedure, each of them containing the list of events in order and a set of guidelines. After each step, the results related to continuity and the decisions to be taken for that step have been summarized. After reading the first division of this chapter, the user will have obtained the full assessment procedure for the entire frame. Any exceptional loading situation and the different damaged column positions can then be better understood.

The second part repeats the first part's concepts, this time applying actual detailed mathematical calculations. To accomplish this, the previous step-by-step assessment was

illustrated in an existing building frame where a single column was destroyed. The process of applying the additional state to the residual frame and the response of the real frame to the loss of a single column were simulated.

The second part presents a number of descriptions and figures, some of which are repeated from previous chapters in order to aid readability and to bring together a global view of the problem.

## 9.2. MULTI-LEVEL ROBUSTNESS ASSESSMENT FRAMEWORK

Through the presentation of the progressive loss of a column in Chapter 3, the evolution of the damaged column's axial forces was explained in detail. That global concept is defined with remarks on separating the additional and residual states. For the discussions within the chapters, normally the additional state was used. However, in the total real frame calculation, the residual state was used more often.

To clarify the method used in robustness assessment, a complete flowchart describing the alternative load path and including the critical points is repeated in Figure 9.1.

At the beginning of the flowchart, a brief description of the frame with the detailed parameters, provided for the assessment, is entered first. The exceptional loss of a column has been illustrated together with Chart 5.7 to demonstrate the evolution of the load and of the loading phases. A small figure illustrating the difference between the residual state and additional state applied to the residual frame is also attached.

The next step is the conditional block that defines the different outcomes for the frame's response according to the destroyed column's position. Here, the chart was separated into two scenarios: internal vs. external damage.

The first and most complex situation results from the internal column being damaged. The first critical value  $N_{lost}^{Pl.Rd}$  was defined and placed within a conditional block. If the value  $N_{lost}^{Pl.Rd}$  is smaller than the limit of  $N_{design}$ , the residual frame may undergo to the catenary action. On the contrary, when the limit load is smaller than the plastic resistance of the directly affected part, the membrane effect never arises. Calculation step *I* refers to the estimate for  $N_{lost}^{Pl.Rd}$ .

Normally, the directly affected part works within the elastic range. However, if the adjacent column zone is overloaded or unstable, the alternative load path fails. The other

phenomenon that should be considered is the arch effect. For these considerations, the conditional block labeled “*Integrity and continuity*” has been introduced in order to make this assessment.

In the second situation, an external column is destroyed. As for the internal damage, the same condition is applied: if  $N_{design}$  is smaller than  $N_{lost}^{Pl.Rd}$ , which has been obtained in step *1'*, the frame survives. However, the frame can fail due to the adjacent columns' failure. Then the same calculation for *2* is performed to reach the same conditional block, “*Integrity and continuity*”.

The critical value just mentioned,  $N_{lost}^{Pl.Rd}$ , defines the end of Load Phase 2. Only the situation resulting from a damaged internal column leads to Load Phase 3, due to the catenary action. The condition necessary for triggering the catenary action is demonstrated by the conditional block labeled “*Integrity and ductility*”. The ductility condition depends on a structural parameter, namely, having ductile joints or a class 1 or 2 beam section. As for the integrity requirement, it is used to determine whether the surrounding frame members can remain stable enough to maintain the extended alternative load path. These conditions are solved by calculation step *3*.

When this last condition is fulfilled and the membrane phenomenon occurs, the two parameters which influence the catenary effect are estimated in step *4*. Using these parameters, Jean-Francois Demonceau aims to give the final solution regarding the catenary action's behavior.

In the following table, the first three calculation steps are defined in order:

| STEP NAME    | DESCRIPTION  |
|--------------|--|
| <i>1; 1'</i> | Quick estimate of $N_{lost}^{Pl.Rd}$                   |
| <i>2</i>     | First alternative load path's integrity and continuity |
| <i>3</i>     | Obtaining the values of $K$ and $F_{Rd}$               |

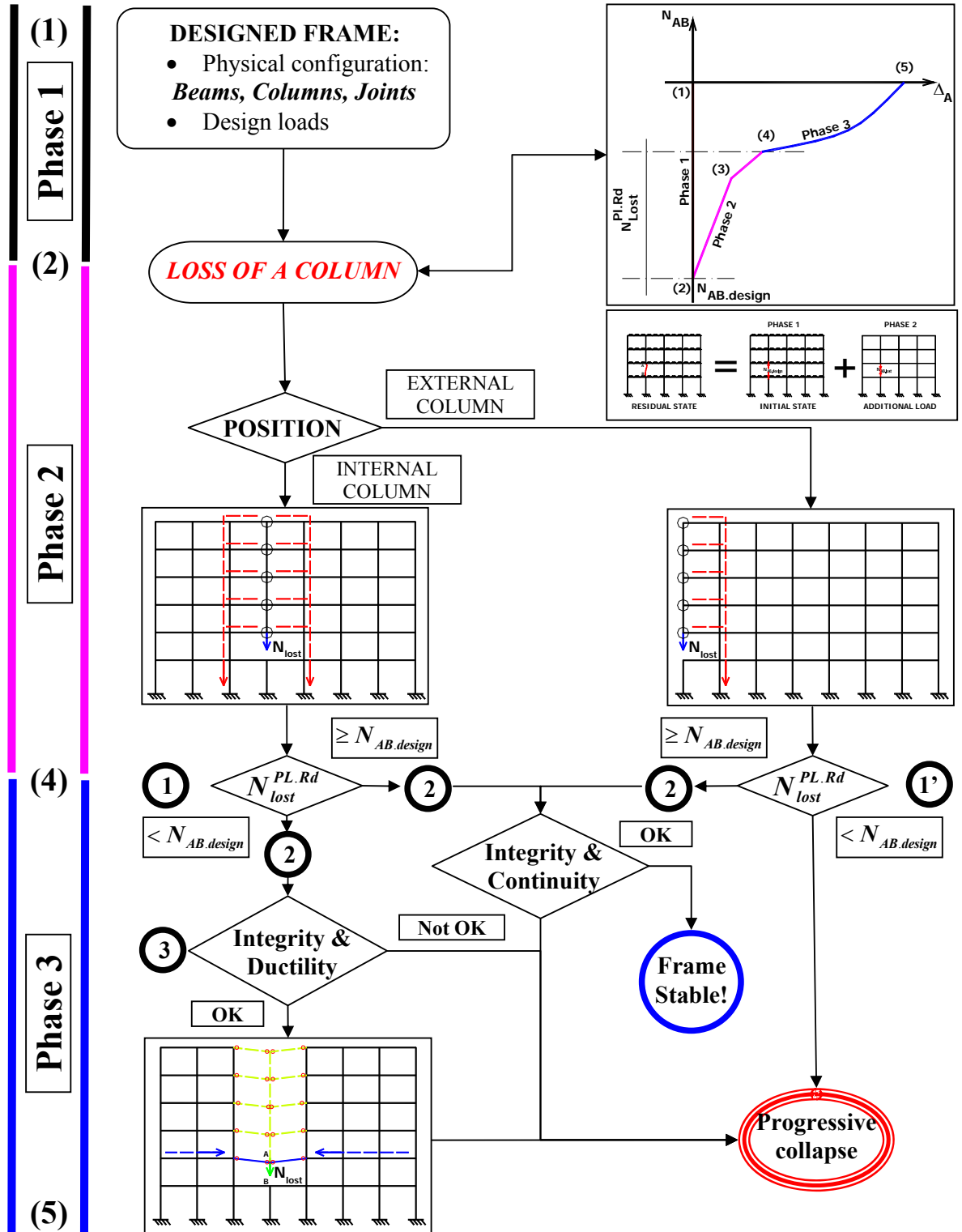


Figure 9.1. The multi-level frame robustness assessment

### 9.2.1. Critical value $N_{lost}^{Pl.Rd}$

#### 9.2.1.a. Objective

As presented in the introduction, the objective of this calculation is the critical value  $N_{lost}^{Pl.Rd}$  – the plastic resistance of the directly affected part.

#### 9.2.1.b. Input data

The input data are defined by the figure below. They consist of the beams' lengths on both sides of the damaged column,  $L_B^{left}$ ;  $L_B^{right}$ ; the number of floors in the directly affected part,  $n$ ; the columns' heights on each floor,  $H_C^i (i=1..n)$ ; the beam and column sections,  $I_B$ ;  $I_C$ ;  $M_P^B$ ;  $N_P^C$ ; and the beam and column material,  $E_B$ ;  $E_C$ . Finally, the internal forces in the equivalent beam and adjacent columns are also required.

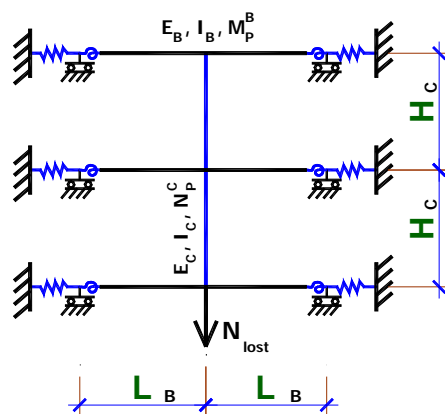


Figure 9.2. The model and required data

#### 9.2.1.c. Methodology

In the quick estimation method used, the model of the directly affected part is put in a plastic limit state to achieve the load applied at that point. For general cases, the two values of resistance for the equivalent beam and the elongation limit of the middle column are compared to get the part's smallest resistance value.

#### 9.2.1.d. Formulae

The general individual beam plastic limit is

$$N_{lost}^{B.Rd} = \frac{M_P^{B.1} + M_P^{B.31} + \frac{\alpha}{1-\alpha} (M_P^{B.2} + M_P^{B.32})}{\alpha L_B} \quad (9.1)$$

where  $\alpha = \frac{L_1}{L_B}$  is the ratio of the left span to the whole equivalent beam's length, and

$M_P^{B.i}$  is the plastic moment of the beam section, taking into account the original design's bending moment.

In the case where plastic bending moments of all four sections are similar and equal  $M_P^B$  then

$$N_{lost}^{B.Rd} = \frac{2M_P^B}{\alpha(1-\alpha)L_B}, \quad (9.2)$$

and when the external column is destroyed

$$N_{lost}^{B.Rd} = \frac{M_P^{B.1} + M_P^{B.2}}{L_B}, \quad (9.3)$$

where the section bending moment of  $M_P^B$  is constant, the beam limit is defined by

$$N_{lost}^{B.Rd} = \frac{2M_P^B}{L_B}. \quad (9.4)$$

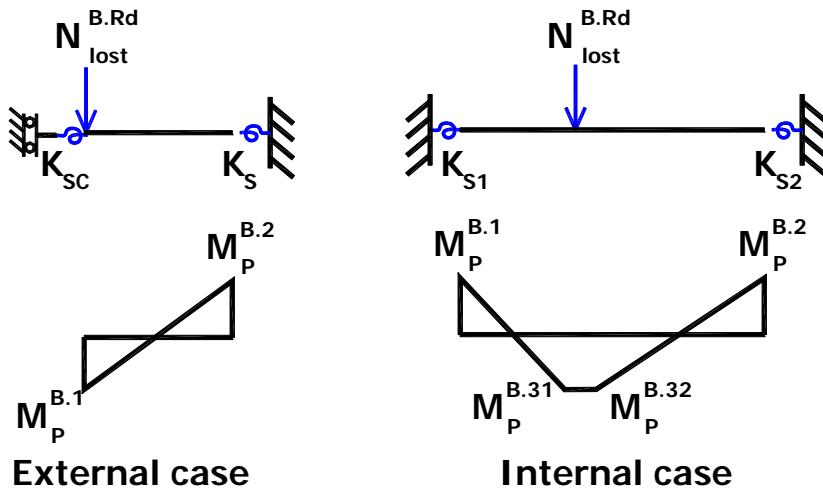


Figure 9.3. The individual beam's resistance

Once these are obtained, the directly affected part's resistance is easily estimated by

$$N_{lost}^{Rd} = \text{MIN} \left( \sum_{i=1}^n N_{lost.i}^{B.Rd}, \frac{|N_{design}^d - N_P^d| \sum_{k=1}^n K_B^k}{\sum_{k=1}^{n-d} K_B^k} \right), \quad (9.5)$$

where  $N_{lost.i}^{B.Rd}$  is the resistance of beam number  $i$ ,



$n$  is the number of floors within the directly affected part, and  
 $d$  is the number of the weakest column.

Normally, the column rarely fails since it works mostly under compression, so

$$N_{lost}^{Rd} = \sum_{i=1}^n N_{lost.i}^{B.Rd} \quad (9.6)$$

#### 9.2.1.e. Expected results

The target value sought in this step is the critical value of  $N_{lost}^{Pl.Rd}$ .

#### 9.2.1.f. Remarks – Decisions

There are two possible outcomes when performing this step.

If  $N_{lost}^{Pl.Rd}$  is derived from the beam's resistance, the residual frame continues to function as discussed earlier. On the contrary, when the value of  $N_{lost}^{Pl.Rd}$  is obtained from the damaged column, the situation becomes extremely complex, as described in Section 6.6.1.

### 9.2.2. First alternative load path: integrity and continuity

#### 9.2.2.a. Objective

This analysis requires an understanding of how the alternative load path is maintained. To this end, the adjacent columns' performance, integral to the overall performance of the alternative load path, is investigated in this section.

#### 9.2.2.b. Input data

The general data required are the same as those employed in the previous step. The critical value of  $N_{lost}^{Pl.Rd}$  obtained from the previous step is also used.

#### 9.2.2.c. Methodology

In order to identify the key elements in the loading states, the distribution of internal forces within the first alternative load path had to be determined. From that distribution, the number of key elements was identified. The procedure below describes the estimation of all critical load states of those key elements.

Finally, each key element was checked using stability and resistance tests.

However, the temporary parameters of the frame's stiffness should also be obtained at this time, i.e.,  $K_S$  and  $K$  and the equivalent adjacent span's beam sections.

9.2.2.d. Formulae

Firstly, the individual equivalent beam was checked to obtain the complete behavioral curve of the directly affected part.

The calculation began by estimating a value for  $K_S$ . These formulae as well as graphic descriptions of the process are given below.

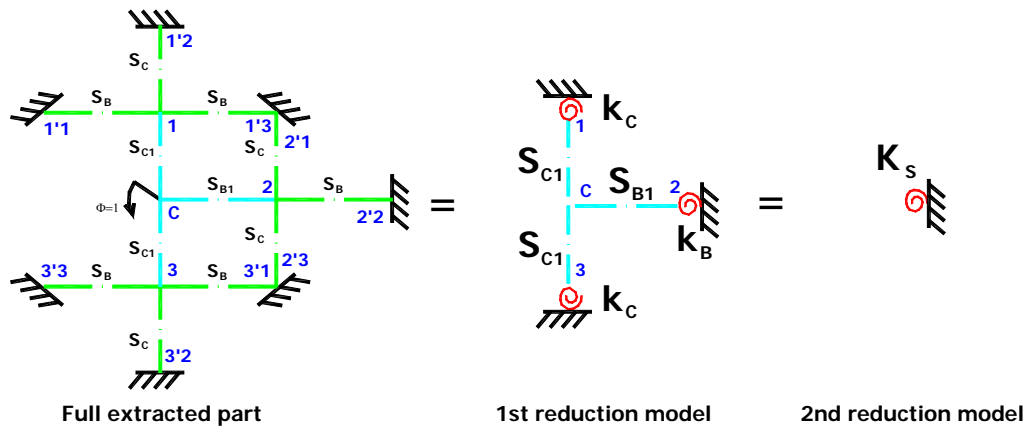


Figure 9.4. The reduction process to simulate the partially restrained stiffness of point C

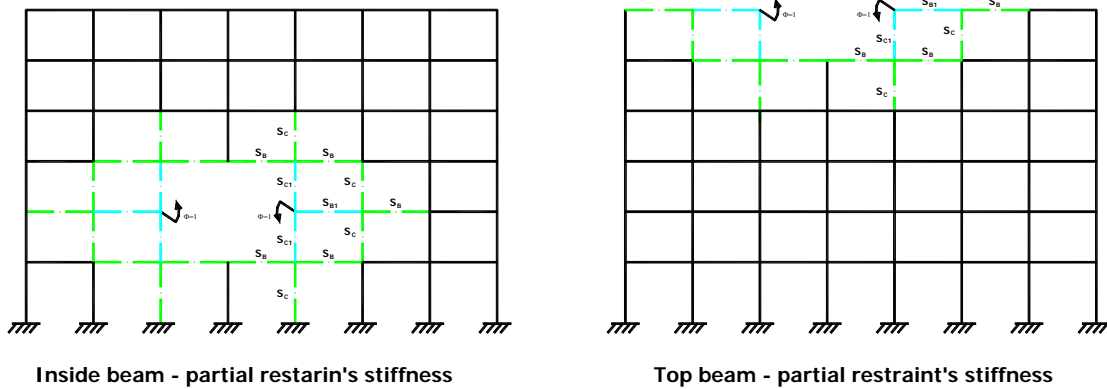


Figure 9.5.  $K_S$  in different positions within the frame

$$S_C = \frac{4E_C I_C}{L_C} \tag{9.7}$$

$$S_B = \frac{4E_B I_B}{L_B}$$

where  $E_B, E_C$  are the elastic moduli of the beam and column,  
 $I_B, I_C$  are the inertia of the beam and column sections, and  
 $L_B, L_C$  are the beam's and column's lengths.

$$\begin{aligned} k_C &= S_B + S_B + S_C \\ k_B &= S_C + S_B + S_C \end{aligned} \quad (9.8)$$

where  $k_C$  is the rotational stiffness of the ends of columns C-1 and C-3, and  
 $k_B$  is the rotational stiffness of the end of beam C-2.

$$S_{C1} = \frac{4E_C I_C}{L_C} \frac{L_C k_C + 3E_C I_C}{L_C k_C + 4E_C I_C} \quad (9.9)$$

$$S_{B1} = \frac{4E_B I_B}{L_B} \frac{L_B k_B + 3E_B I_B}{L_B k_B + 4E_B I_B}$$

$$K_S = S_{B1} + S_{C1} + S_{C1} \quad (9.10)$$

where  $S_{C1}, S_{B1}$  are the bending stiffness of the column and beam with rotational spring ends, and

$K_S$  is the partial restraint coefficient of point C.

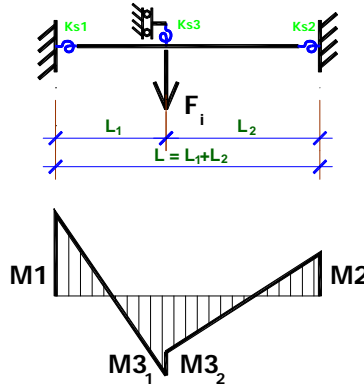


Figure 9.6. Bending diagram on the model

Secondly, the stiffness and resistance values of the individual equivalent beam are given by

$$K_B = \frac{3E_B I_B}{\alpha^2 (\alpha - 1)^2 L^3 \left[ 1 - \frac{A}{4B} \right]} \quad (9.11)$$

$$A = A_0 + A_1 \beta_3$$

$$A_0 = a_{0,0} + a_{0,1} \alpha + a_{0,2} \alpha^2$$

$$A_1 = a_{1,0} + a_{1,1} \alpha + a_{1,2} \alpha^2 + a_{1,3} \alpha^3 + a_{1,4} \alpha^4$$

$$a_{0,0} = -16\beta_1 - 4\beta_2 - 4\beta_1 \beta_2$$

$$a_{0,1} = 16\beta_1 - 8\beta_2 + 4\beta_1 \beta_2$$

$$a_{0,2} = -4\beta_1 - 4\beta_2 - 4\beta_1 \beta_2$$

$$B = B_0 + B_1 \beta_3$$

$$B_0 = b_{0,0}$$

$$B_1 = b_{1,0} + b_{1,1} \alpha + b_{1,2} \alpha^2 + b_{1,3} \alpha^3 + b_{1,4} \alpha^4$$

$$b_{0,0} = -12 - 4\beta_1 - 4\beta_2 - \beta_1 \beta_2$$

$$a_{1,0} = -16 - 4\beta_2$$

$$a_{1,1} = 64 - 16\beta_1 + 20\beta_2 - 4\beta_1\beta_2$$

$$a_{1,2} = -64 + 52\beta_1 - 32\beta_2 + 17\beta_1\beta_2$$

$$a_{1,3} = -52\beta_1 + 4\beta_2 - 26\beta_1\beta_2$$

$$a_{1,4} = 12\beta_1 + 12\beta_2 + 13\beta_1\beta_2$$

$$b_{1,0} = -4 - \beta_2$$

$$b_{1,1} = 12 - 4\beta_1 + 4\beta_2 - \beta_1\beta_2$$

$$b_{1,2} = -12 + 12\beta_1 - 6\beta_2 + 4\beta_1\beta_2$$

$$b_{1,3} = -12\beta_1 - 6\beta_1\beta_2$$

$$b_{1,4} = 3\beta_1 + 3\beta_2 + 3\beta_1\beta_2$$

where  $\alpha = L_1 / L$ ;  $\beta_1 = \frac{K_{S1}L}{E_B I_B}$ ;  $\beta_2 = \frac{K_{S2}L}{E_B I_B}$ ;  $\beta_3 = \frac{K_{S3}L}{E_B I_B}$ .

The results of the previous calculation were used to identify the critical point of the applied load, which in turn was used to build the intermediate analytical model.

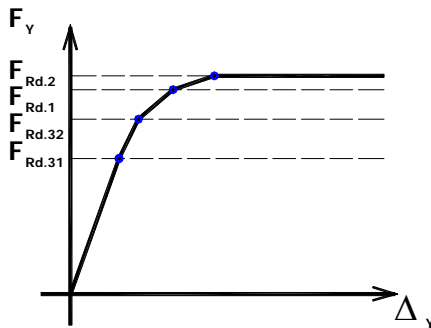


Figure 9.7. Load-carrying curve in the case where hinges appear in order (31-32-1-2) Thirdly, from the order of plastic hinges' appearance, the model used to calculate the adjacent column's internal forces was modified in the calculation procedure.

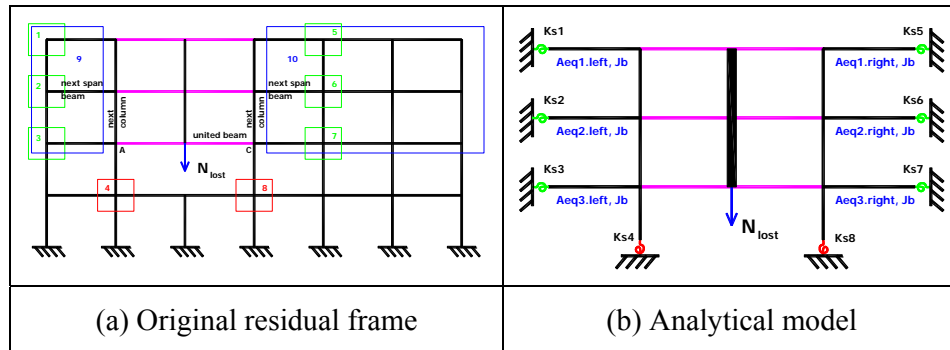


Figure 9.8. The original residual frame and the full model

Normally, the full model above can even be reduced to the half model as developed in Section 7.5.1.

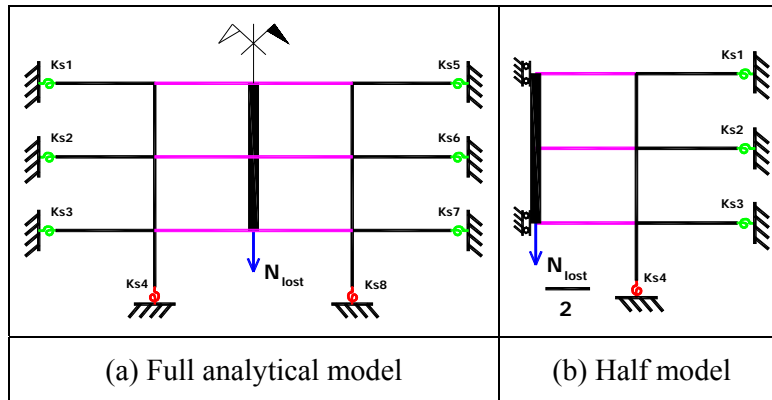


Figure 9.9. The simplified half model

Finally, after the distribution of bending moment was obtained, the bending model above was modified to convey the arch effect. The axial forces in the equivalent beams were calculated based on the horizontal restraint coefficient, as shown in Figures 9.10 and 9.11.

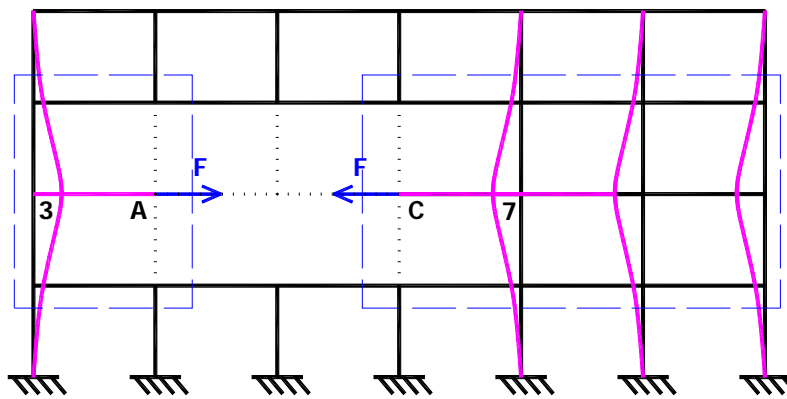


Figure 9.10. Horizontal restraint definition

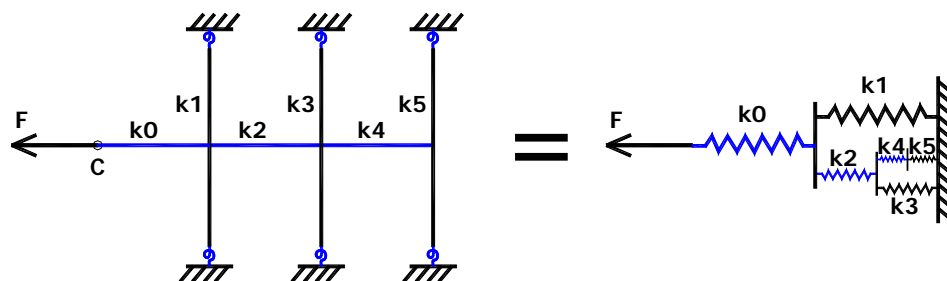


Figure 9.11. The relation between members in the group

Next, the final axial forces were predicted by the equilibrium of the horizontal forces distributed along the column's top point:

$$N_{UB} = (T_{UC} + T_{LC}) \frac{A_{UB}}{A_{Equivalent} + A_{UB}} \tag{9.12}$$

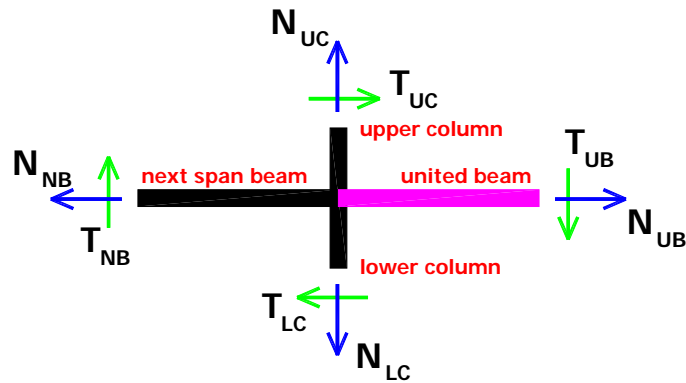


Figure 9.12. Calculating the axial forces in the equivalent beam (arch effect)

9.2.2.e. Expected results

The calculations illustrated above were used to predict the internal force distribution within the alternative load path. They clearly identified three particular dangerous positions, namely the three pairs of  $(M, N)$ :  $(M_1, -N_1)$  for key element 1,  $(M_2, +N_2)$  for key element 2 and  $(M_3, -N_3)$  for key element 3.

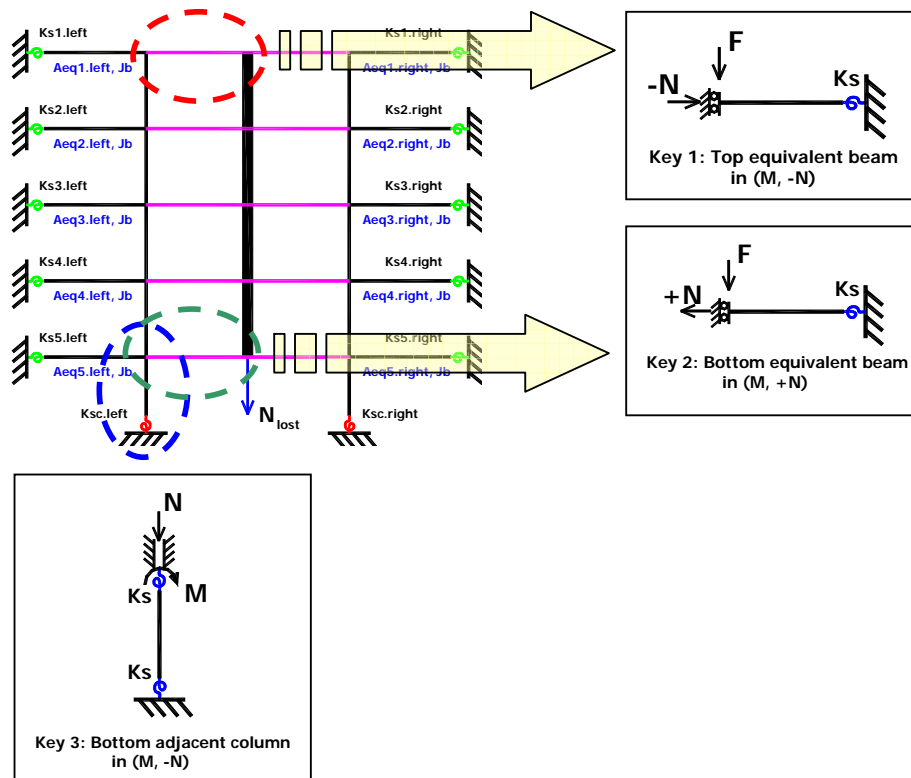


Figure 9.13. General model and the key elements

9.2.2.f. Remarks – Decisions

When the stability and resistance tests were finished, the answer to whether the alternative

load path can be maintained was determined. This internal force distribution may also be used to judge the load capacity of the frame.

### 9.2.3. Obtaining the values of $K$ , $F_{Rd}$

#### 9.2.3.a. Objective

When the catenary action happens, the secondary additional state is applied to the damaged level. This section's objective was to obtain the two parameters,  $K$  and  $F_{Rd}$ , provided for Demonceau's calculation, and to test the remaining part's survival.

#### 9.2.3.b. Input data

The input data were the results for the three pairs of  $(M, N)$  given in the previous chapter. The critical value  $N_{lost}^{Pl.Rd}$  was also used again.

#### 9.2.3.c. Methodology

With the initial loading state at the end of Load Phase 2, the secondary additional state applied to the adjacent column and all the columns in the damaged level were organized in the analytical model. The second-order stiffness and the final state of each column were incorporated into the total value of  $K$  and  $F_{Rd}$ . This process was developed in detail in Chapter 8.

#### 9.2.3.d. Formulae

To calculate the damaged level's total stiffness, the individual column's stiffness was first predicted.

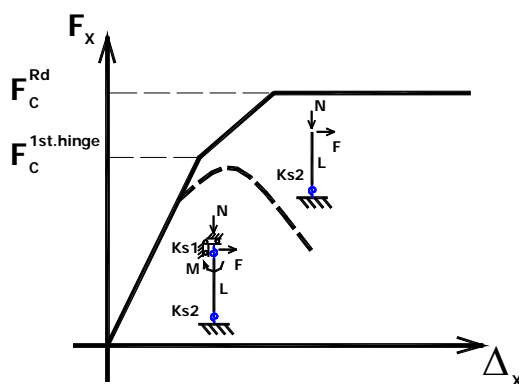


Figure 9.14: The resistance of the one floor column

The first-order stiffness of a column supporting the horizontal force applied to the column's top point is

$$\begin{aligned} \mathbf{K}_C^{1st} &= (r_{ii} + 2r_{ij} + r_{jj}) \frac{E_C I_C}{L_C^3} = \\ &= \frac{12E_C I_C}{L_C^2} \frac{L_C k_{s1} k_{s2} + (k_{s1} + k_{s2}) E_C I_C}{L_C^2 k_{s1} k_{s2} + (k_{s1} + k_{s2}) 4E_C I_C L_C + 12E^2 I_C^2} \end{aligned} \quad (9.13)$$

Then, taking into account the initial rotation (such as the initial bending) the formula becomes

$$\begin{aligned} \mathbf{K}_C^{1st} &= \frac{\left[ L_C^3 k_{s1} k_{s2} + 4E_C I_C L_C^2 (k_{s1} + k_{s2}) + 12(E_C I_C)^2 \right]}{12E_C I_C \left[ L_C k_{s1} k_{s2} + E_C I_C (k_{s1} + k_{s2}) \right]} - \\ &\quad \frac{12(E_C I_C)^2 \alpha \left\{ \left[ k_{s1} + \gamma(k_{s1} + k_{s2}) \right] + L_C k_{s1} k_{s2} E_C I_C (6 + 8\gamma) \right\}}{12E_C I_C \left[ L_C k_{s1} k_{s2} + E_C I_C (k_{s1} + k_{s2}) \right]} \end{aligned} \quad (9.14)$$

where  $\mathbf{K}_C^{1st}$  is the shear stiffness of the column including the second order effect and the initial rotation at the column's ends,

- $k_{s1}, k_{s2}$  is semi-rigid rotational stiffness of both column ends,
- $E_C I_C$  is the elastic modulus and inertia moment of column section,
- $\alpha$  is linear coefficient of end rotation to the horizontal force  $H_{memb}$ , and
- $\gamma$  is ratio between 2 initial rotation of both column ends (normal case,  $\gamma = 2$ ).

The columns' stiffness according to their position is examined below.

*The external column:*

$$\mathbf{K}_C^{side} = \mathbf{K}_{C.1st}^{side} - \frac{N_{design}^{exter}}{L_C} \quad (9.15)$$

where  $\mathbf{K}_C^{side}$  is the shear stiffness of the outside column including the second-order effect,

- $\mathbf{K}_{C.1st}^{side}$  is the first-order shear stiffness of the outside column,
- $N_{design}^{exter}$  is the compression force applied to the column's top, and
- $L_C$  is the column's length.

*The intermediate column:*

$$\mathbf{K}_C^{Inter} = \mathbf{K}_{C.1st}^{Inter} - \frac{N_{design}^{inter}}{L_C} \quad (9.16)$$

where  $\mathbf{K}_C^{Inter}$  is the shear stiffness of the intermediate column including the second-order effect,

- $\mathbf{K}_{C.1st}^{Inter}$  is the first-order shear stiffness of the intermediate column,



$N_{design}^{inter}$  is the compression force applied to the column's top, and  
 $L_C$  is the column's length.

Finally, for the most dangerous column, *the adjacent column*:

$$K_C^{Beside} \approx \frac{K_{C.1st}^{Beside} L_C - N_{design}^{inter} - N_{additional}^1}{L_C + n_2} \quad (9.17)$$

where  $K_C^{Beside}$  is the shear stiffness of the adjacent column including the second-order effect and the initial rotation at the column's ends.

Depending on the stiffness of each column, the resistance of an individual column is given by

$$F_{Rd} = \frac{M_P^{C.1} + M_P^{C.2}}{L_C}, \quad (9.18)$$

where  $M_P^{C.1}, M_P^{C.2}$  are the plastic moments of the column section at two end points.

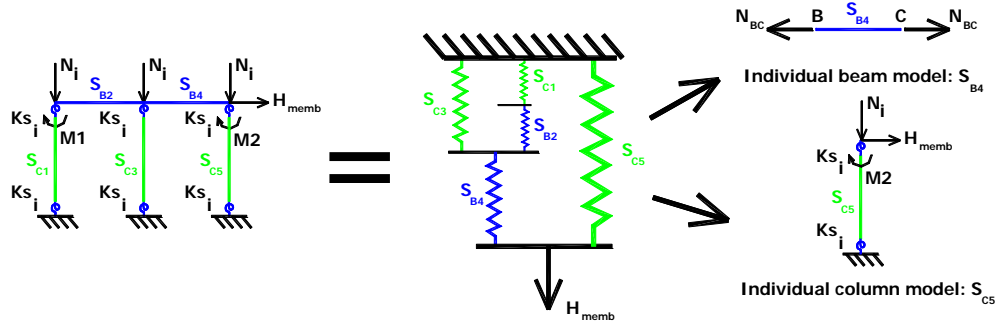


Figure 9.15. Model of the left side of the damaged level

Then, the stiffness of the damaged level on one side is defined by

$$K_{DamageLevel}^{Left} = S_{C1} + S_{C3} + S_{C5} = K_C^{Side} + K_C^{Inter} + K_C^{Beside}, \quad (9.19)$$

and the value of  $K$  taking into account the left and right sides' behavior is

$$K = \frac{K_{DamageLevel}^{Left} K_{DamageLevel}^{Right}}{K_{DamageLevel}^{Left} + K_{DamageLevel}^{Right}}. \quad (9.20)$$

The resistance of the damaged level is finally estimated by

$$F_{Rd} = F_C^{Rd} \frac{\sum_{i=1}^m K_C^i}{K_C^{\max}}, \quad (9.21)$$

where  $F_C^{Rd}$  is the weakest column resistance.

### 9.2.3.e. Expected results

The damaged level might or might not pass the stability and resistance test.

The values of  $K$  and  $F_{Rd}$  were obtained.

*9.2.3.f. Remarks – Decisions*

The final conclusion reached is a description of the frame's behavior in the accidental loss of a column.

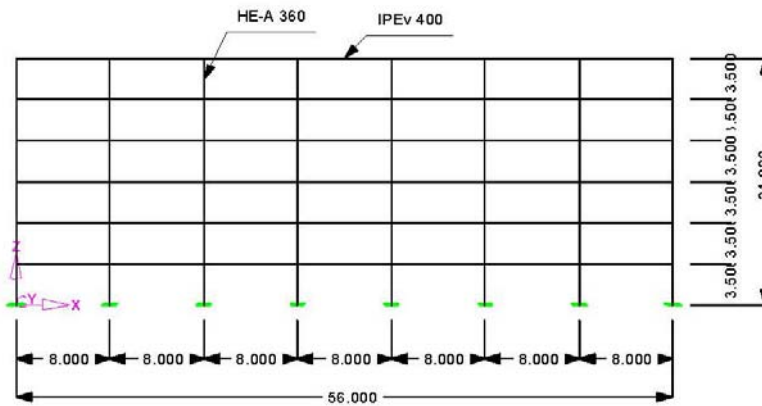
### 9.3. EXAMPLE

#### 9.3.1. Input data

## ROBUSTNESS ASSESSMENT OF THE REGULAR FRAME

#### The investigated frame

The frame has 7 spans and 6 floors. The span length and the floor height are uniform on whole the frame. Only one HE 360A column section and one IPE400v beam section are applied. All sections were on the S355 grade. The bellow figure shows out the structure.



| Load No | Meaning                    | Postion                   | Magnitude  |
|---------|----------------------------|---------------------------|------------|
| 1       | Column self weight         | All columns               | 1.099 kN/m |
| 2       | Beam self weight           | All beams                 | 0.849 kN/m |
| 3       | Permanent load of all beam | All beam except top floor | 22.05 kN/m |
| 4       | Permanent load on the top  | On the roof               | 18.60 kN/m |
| 5       | Snow load                  | On the roof               | 3.25 kN/m  |
| 6       | Live load                  | All beam except top floor | 21.00 kN/m |

#### PARAMETERS:

(UNIT: m, kN)

#### FRAME: 6 STOREY - 7 SPANS.

|                |                                 |                       |
|----------------|---------------------------------|-----------------------|
| Column HE 360A | $J_c = 0.000330898 \text{ m}^4$ | $H_c = 3.5 \text{ m}$ |
| Beam IPEv 400  | $J_b = 0.000301363 \text{ m}^4$ | $L_b = 8.0 \text{ m}$ |

#### PARAMETERS

|          |                        |                         |                            |
|----------|------------------------|-------------------------|----------------------------|
| Material | $E := 2.05 \cdot 10^8$ | $f_y := 355 \cdot 10^3$ | $G_c := 8.0770 \cdot 10^7$ |
| Sections | $J_c := 0.000330898$   | $F_c := 0.01427578$     |                            |
|          | $J_b := 0.000301363$   | $F_b := 0.01070236$     |                            |

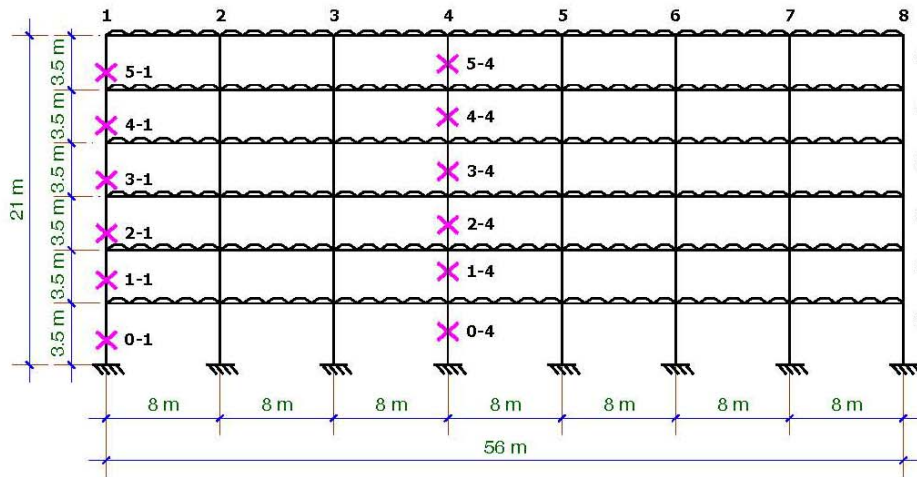
$$M_{P,B} := \left[ 0.182 - 0.0175 \cdot \frac{0.408 - 0.0175}{2} + \frac{(0.408 - 2 \cdot 0.0175)^2 \cdot 0.0106}{8} \right] \cdot 2 \cdot M_{P,B} = 572.414$$

|                |              |            |
|----------------|--------------|------------|
| Frame Geometry | $L_c := 3.5$ | $L_b := 8$ |
|----------------|--------------|------------|

#### DESIGN LOADS

|                                   |                    |      |
|-----------------------------------|--------------------|------|
| $q_{top} := 0.849 + 18.60 + 3.25$ | $q_{top} = 22.699$ | kN/m |
| $q_{in} := 0.849 + 22.05 + 21$    | $q_{in} = 43.899$  | kN/m |

9.3.2. Internal forces



**CALCULATE THE COLUMN AXIAL FORCES N.lo.design**

**OUTSIDE POSITIONS:**

|               |   |              |
|---------------|---|--------------|
| Ground floor: | $N_{lo.des.out.0} := 983.78 \text{ kN}$ | Position 0-1 |
| 1st floor:    | $N_{lo.des.out.1} := 801.66 \text{ kN}$ | Position 1-1 |
| 2nd floor:    | $N_{lo.des.out.2} := 624.63 \text{ kN}$ | Position 2-1 |
| 3rd floor:    | $N_{lo.des.out.3} := 446.54 \text{ kN}$ | Position 3-1 |
| 4rt floor:    | $N_{lo.des.out.4} := 267.84 \text{ kN}$ | Position 4-1 |
| 5ft floor:    | $N_{lo.des.out.5} := 89.62 \text{ kN}$  | Position 5-1 |

**INSIDE POSITIONS:**

|               |   |              |
|---------------|---|--------------|
| Ground floor: | $N_{lo.des.in.0} := 1967.56 \text{ kN}$ | Position 0-4 |
| 1st floor:    | $N_{lo.des.in.1} := 1603.21 \text{ kN}$ | Position 1-4 |
| 2nd floor:    | $N_{lo.des.in.2} := 1248.09 \text{ kN}$ | Position 2-4 |
| 3rd floor:    | $N_{lo.des.in.3} := 893.05 \text{ kN}$  | Position 3-4 |
| 4rt floor:    | $N_{lo.des.in.4} := 537.99 \text{ kN}$  | Position 4-4 |
| 5ft floor:    | $N_{lo.des.in.5} := 182.68 \text{ kN}$  | Position 5-4 |

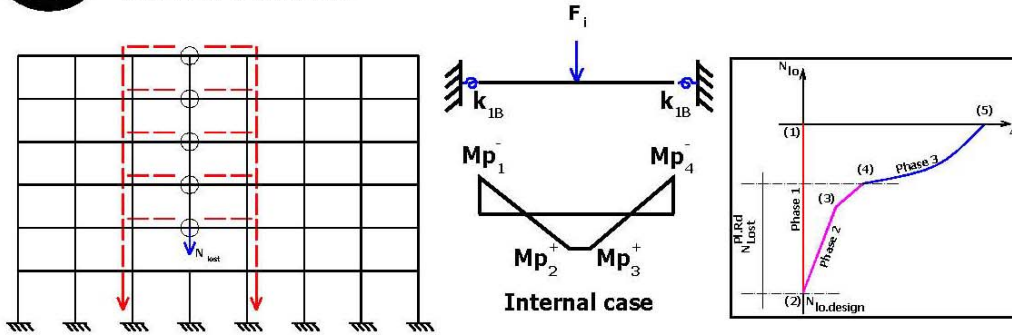


9.3.4. Step 1.

**1**

**CALCULATE THE PLASTIC RESISTANCE OF THE BEAMS**

**INSIDE POSITIONS:**



Individual floor:

$$N_{Pl.lost.in} := \frac{8 \cdot M_{P.B}}{2 \cdot L_b}$$

$$N_{Pl.lost.in} = 286.207 \quad \text{kN}$$

Inside position - each floor

$$N_{Pl.lost.0.4} := 6 \cdot N_{Pl.lost.in}$$

$$N_{Pl.lost.0.4} = 1.717 \times 10^3 \quad \text{kN}$$

$$N_{Pl.lost.1.4} := 5 \cdot N_{Pl.lost.in}$$

$$N_{Pl.lost.1.4} = 1.431 \times 10^3 \quad \text{kN}$$

$$N_{Pl.lost.2.4} := 4 \cdot N_{Pl.lost.in}$$

$$N_{Pl.lost.2.4} = 1.145 \times 10^3 \quad \text{kN}$$

$$N_{Pl.lost.3.4} := 3 \cdot N_{Pl.lost.in}$$

$$N_{Pl.lost.3.4} = 858.621 \quad \text{kN}$$

$$N_{Pl.lost.4.4} := 2 \cdot N_{Pl.lost.in}$$

$$N_{Pl.lost.4.4} = 572.414 \quad \text{kN}$$

$$N_{Pl.lost.5.4} := 1 \cdot N_{Pl.lost.in}$$

$$N_{Pl.lost.5.4} = 286.207 \quad \text{kN}$$

**COMPARE IF  $N_{lo.design} > N_{lost.PI}$**

**INSIDE POSITIONS:**

Ground floor:  $N_{lo.des.in.0} = 1.968 \times 10^3 \quad \text{kN}$

$N_{Pl.lost.0.4} = 1.717 \times 10^3 \quad \text{kN}$

1st floor:  $N_{lo.des.in.1} = 1.603 \times 10^3 \quad \text{kN}$

$N_{Pl.lost.1.4} = 1.431 \times 10^3 \quad \text{kN}$

2nd floor:  $N_{lo.des.in.2} = 1.248 \times 10^3 \quad \text{kN}$

$N_{Pl.lost.2.4} = 1.145 \times 10^3 \quad \text{kN}$

3rd floor:  $N_{lo.des.in.3} = 893.05 \quad \text{kN}$

$N_{Pl.lost.3.4} = 858.621 \quad \text{kN}$

4th floor:  $N_{lo.des.in.4} = 537.99 \quad \text{kN}$

$N_{Pl.lost.4.4} = 572.414 \quad \text{kN}$

5th floor:  $N_{lo.des.in.5} = 182.68 \quad \text{kN}$

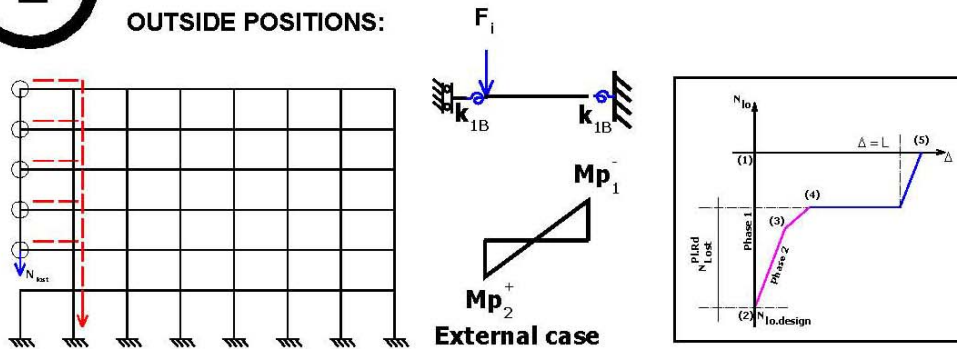
$N_{Pl.lost.5.4} = 286.207 \quad \text{kN}$

**Conclusion for this step:** The same as the outside positions, if the frame integrity and ductility is fulfilled, the position 4.1 and 5.1 will not collapse. The other 4 positions 0.1, 1.1, 2.1, 3.1 will pass the plastic limit when the column is fully removed. The catenary phenomenon could happen.

**1'**

**CALCULATE THE PLASTIC RESISTANCE OF THE BEAMS**

OUTSIDE POSITIONS:



Individual floor:

$$N_{Pl,lost.out} := \frac{2 \cdot M_{P,B}}{L_b}$$

$$N_{Pl,lost.out} = 143.104 \quad \text{kN}$$

Outside position - each floor

$$N_{Pl,lost.0.1} := 6 \cdot N_{Pl,lost.out}$$

$$N_{Pl,lost.0.1} = 858.621 \quad \text{kN}$$

$$N_{Pl,lost.1.1} := 5 \cdot N_{Pl,lost.out}$$

$$N_{Pl,lost.1.1} = 715.518 \quad \text{kN}$$

$$N_{Pl,lost.2.1} := 4 \cdot N_{Pl,lost.out}$$

$$N_{Pl,lost.2.1} = 572.414 \quad \text{kN}$$

$$N_{Pl,lost.3.1} := 3 \cdot N_{Pl,lost.out}$$

$$N_{Pl,lost.3.1} = 429.311 \quad \text{kN}$$

$$N_{Pl,lost.4.1} := 2 \cdot N_{Pl,lost.out}$$

$$N_{Pl,lost.4.1} = 286.207 \quad \text{kN}$$

$$N_{Pl,lost.5.1} := 1 \cdot N_{Pl,lost.out}$$

$$N_{Pl,lost.5.1} = 143.104 \quad \text{kN}$$

**COMPARE IF  $N_{lo,design} > N_{lost,Pl}$**

OUTSIDE POSITIONS:

|               |                             |    |                             |    |
|---------------|-----------------------------|----|-----------------------------|----|
| Ground floor: | $N_{lo,des.out.0} = 983.78$ | kN | $N_{Pl,lost.0.1} = 858.621$ | kN |
| 1st floor:    | $N_{lo,des.out.1} = 801.66$ | kN | $N_{Pl,lost.1.1} = 715.518$ | kN |
| 2nd floor:    | $N_{lo,des.out.2} = 624.63$ | kN | $N_{Pl,lost.2.1} = 572.414$ | kN |
| 3rd floor:    | $N_{lo,des.out.3} = 446.54$ | kN | $N_{Pl,lost.3.1} = 429.311$ | kN |
| 4rt floor:    | $N_{lo,des.out.4} = 267.84$ | kN | $N_{Pl,lost.4.1} = 286.207$ | kN |
| 5ft floor:    | $N_{lo,des.out.5} = 89.62$  | kN | $N_{Pl,lost.5.1} = 143.104$ | kN |

**Conclusion for this step:** If the frame integrity and ductility is fulfill, the position 4.1 and 5.1 will not collapse. The other 4 position 0.1, 1.1, 2.1, 3.1 will reach the plastic limit when the column is fully removed.



9.3.5. Step 2

**2**

**DISTRIBUTION OF INTERNAL FORCES IN THE FRAME**  
***(Only for specific position 1-4)***

**PARTIALLY RESTRAINED STIFFNESS FOR BEAM ENDS POINT:**

Beam and column flexural stiffness:

$$S_B := \frac{4 \cdot E \cdot J_b}{L_b} \quad S_C := \frac{4 \cdot E \cdot J_c}{L_c} \quad S_B = 3.089 \times 10^4 \quad \text{kNm/Rad}$$

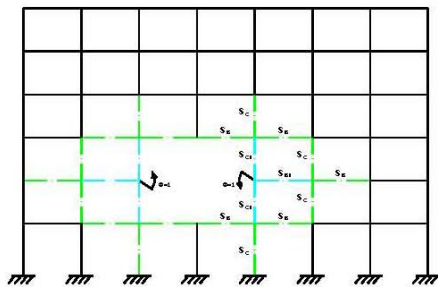
$$\text{Intermediate value:} \quad S_C = 7.752 \times 10^4 \quad \text{kNm/Rad}$$

$$k_C := 2 \cdot S_B + S_C \quad k_C = 1.393 \times 10^5 \quad \text{kNm/Rad}$$

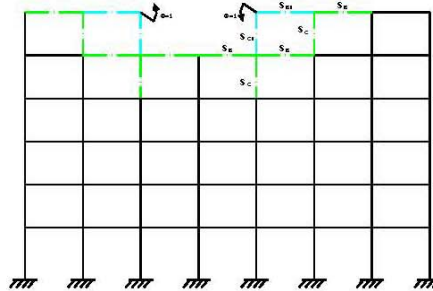
$$k_B := 2 \cdot S_C + S_B \quad k_B = 1.859 \times 10^5 \quad \text{kNm/Rad}$$

$$S_{B1} := \frac{4E \cdot J_b}{L_b} \cdot \frac{L_b \cdot k_B + 3 \cdot E \cdot J_b}{L_b \cdot k_B + 4 \cdot E \cdot J_b} \quad S_{B1} = 2.979 \times 10^4 \quad \text{kNm/Rad}$$

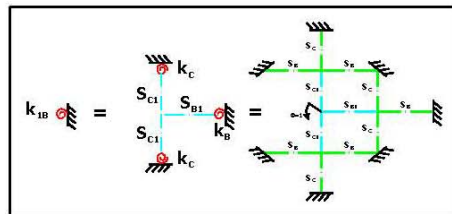
$$S_{C1} := \frac{4E \cdot J_c}{L_c} \cdot \frac{L_c \cdot k_C + 3 \cdot E \cdot J_c}{L_c \cdot k_C + 4 \cdot E \cdot J_c} \quad S_{C1} = 7.06 \times 10^4 \quad \text{kNm/Rad}$$



Inside beam - partial restraint's stiffness



Top beam - partial restraint's stiffness

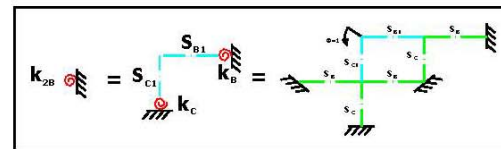


**INSIDE BEAMS - 2 COLUMNS**

$$k_{1B} := 2S_{C1} + S_{B1} \quad k_{1B} = 1.71 \times 10^5 \quad \text{kNm/Rad}$$

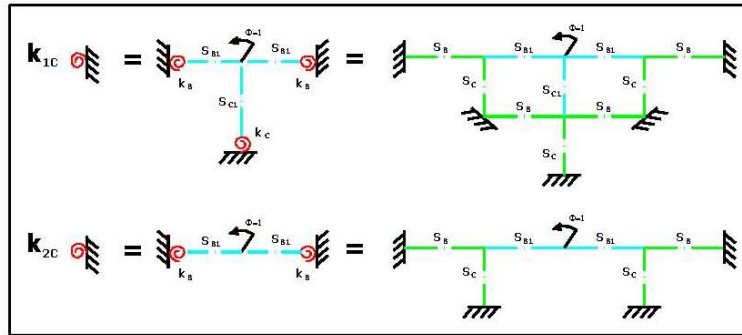
**TOP BEAMS - 1 COLUMN**

$$k_{2B} := S_{C1} + S_{B1} \quad k_{2B} = 1.004 \times 10^5 \quad \text{kNm/Rad}$$





**PARTIALLY RESTRAINED STIFFNESS FOR COLUMNS:**



Intermediate value:

$$k_{C1} := S_B + S_C \quad k_{C1} = 1.084 \times 10^5$$

$$S_{B11} := \frac{4E \cdot J_b}{L_b} \cdot \frac{L_b \cdot k_{C1} + 3 \cdot E \cdot J_b}{L_b \cdot k_{C1} + 4 \cdot E \cdot J_b} \quad S_{B11} = 2.918 \times 10^4$$

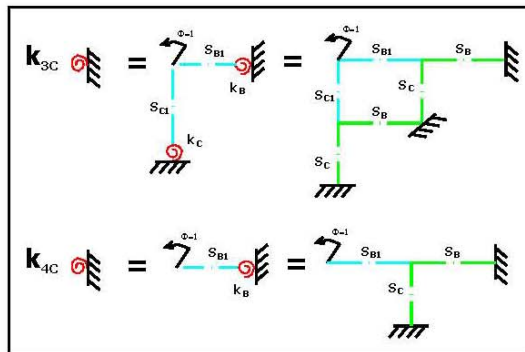
$$S_{C11} := \frac{4E \cdot J_c}{L_c} \cdot \frac{L_c \cdot k_{C1} + 3 \cdot E \cdot J_c}{L_c \cdot k_{C1} + 4 \cdot E \cdot J_c} \quad S_{C11} = 6.944 \times 10^4$$

**INSIDE COLUMNS - 2 BEAMS - WITHIN THE FRAME**

$$k_{1C} := S_{C1} + 2S_{B11} \quad k_{1C} = 1.289 \times 10^5 \quad \text{kNm/Rad}$$

**INSIDE COLUMNS - 2 BEAMS - TOP FLOOR**

$$k_{2C} := 2S_{B11} \quad k_{2C} = 5.835 \times 10^4 \quad \text{kNm/Rad}$$



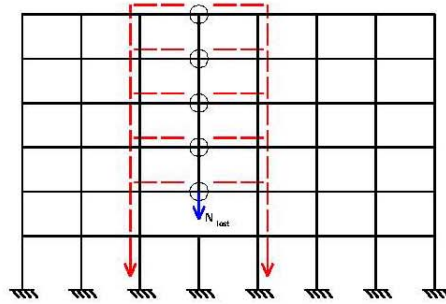
**OUTSIDE COLUMNS - 1 BEAM**

$$k_{3C} := S_{C11} + S_{B11} \quad k_{3C} = 9.862 \times 10^4 \quad \text{kNm/Rad}$$

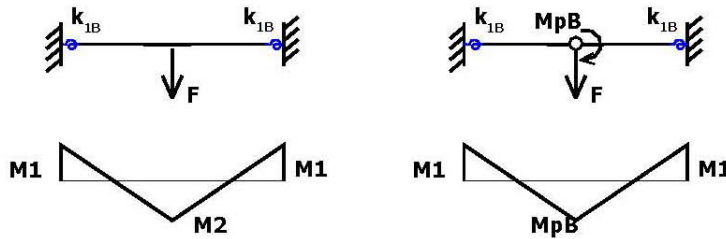
**OUTSIDE COLUMNS - 1 BEAM - TOP FLOOR**

$$k_{4C} := S_{B11} \quad k_{4C} = 2.918 \times 10^4 \quad \text{kNm/Rad}$$

**CALCULATE THE 1ST ORDER ELASTIC - PERFECTLY PLASTIC BEHAVIOUR OF BEAMS IN THE CASE 1- 4**



**INSIDE POSITIONS:**



Because the partially restrained ratio is equal at both beam ends inside the frame then the 3 spring model become the symmetric one, two bending value of M should be checked.

$$\beta_{1,b} := \frac{k_{1B} \cdot 2 \cdot L_b}{E \cdot J_b}$$

$$N_{in.Pl.1} := \frac{M_{P,B}}{\frac{2 \cdot L_b \cdot (\beta_{1,b} + 4)}{8 \cdot (\beta_{1,b} + 2)}} \quad N_{in.Pl.1} = 274.351 \quad \text{kN}$$

$$N_{in.Pl.2} := \frac{M_{P,B}}{\frac{2 \cdot L_b \cdot \beta_{1,b}}{8 \cdot (\beta_{1,b} + 2)}} \quad N_{in.Pl.2} = 299.134 \quad \text{kN}$$

$$\text{PositionMp} := \begin{cases} \text{"Mid Hinge"} & \text{if } N_{in.Pl.1} < N_{in.Pl.2} \\ \text{"End Hinge"} & \text{otherwise} \end{cases} \quad \text{PositionMp} = \text{"Mid Hinge"}$$

$$N_{in.1sthinge} := N_{in.Pl.1} \quad N_{in.1sthinge} = 274.351 \quad \text{kN}$$

The hinge appear first at the mid point of the double spans beam is as presented in the figure below, then the new model is as present at the figure bellow, the force is taken from the value of final state - as calculated for the N.lost PL:

$$N_{in.2ndhinge} := N_{Pl.lost.in} \quad N_{in.2ndhinge} = 286.207 \quad \text{kN}$$



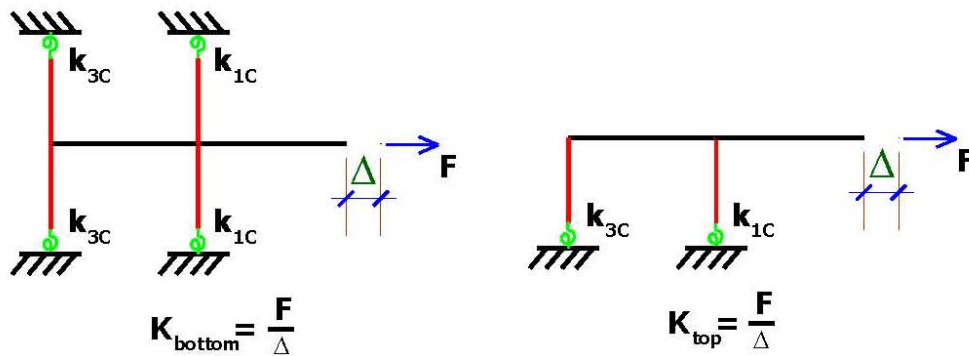
**3 - Calculate the axial forces in the top and bottom beams:**

The axial force in each beam is calculated through the equilibrium of shear force and its distribution concentrates on the higher stiffness part

$$Q_{\text{top}} := Q_0 + Q_{1_0} \quad Q_{\text{top}} = -208.965 \quad \text{KN}$$

$$Q_{\text{bottom}} := Q_{n-2} - Q_{n-1} + Q_{1_{n-2}} - Q_{1_{n-1}} \quad Q_{\text{bottom}} = -77.795 \quad \text{KN}$$

Calculate the K - lateral stiffness of each beam end:



The bottom beam:

The top beam:

The bottom beam:

$$\beta_1 := \frac{k_{1C}}{E \cdot J_c} \cdot 2L_c \quad \beta_2 := \frac{k_{3C}}{E \cdot J_c} \cdot 2L_c$$

$$K_{\text{bottom}} := \frac{192 \cdot E \cdot J_c}{(2L_c)^3} \cdot \left( \frac{\beta_1 + 2}{\beta_1 + 8} + \frac{\beta_2 + 2}{\beta_2 + 8} \right)$$

$$K_{\text{bottom}} = 5.272 \times 10^4 \quad \text{kN/m}$$

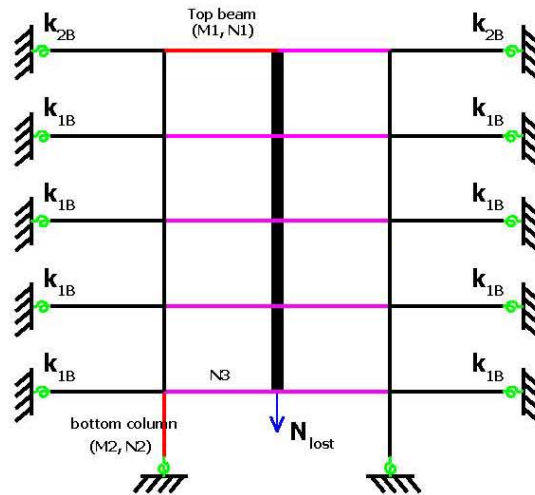
The top beam:

$$\beta_{1t} := \frac{S_B}{E \cdot J_c} \cdot L_c \quad \beta_{2t} := \frac{k_{1C}}{E \cdot J_c} \cdot 2L_c \quad \beta_{3t} := \frac{k_{3C}}{E \cdot J_c} \cdot 2L_c$$

$$K_{\text{top}} := \frac{12 \cdot E \cdot J_c}{L_c^3} \cdot \left( \frac{\beta_{1t} + \beta_{2t} + \beta_{1t} \cdot \beta_{2t}}{4\beta_{1t} + 4\beta_{2t} + \beta_{1t} \cdot \beta_{2t} + 12} + \frac{\beta_{1t} + \beta_{3t} + \beta_{1t} \cdot \beta_{3t}}{4\beta_{1t} + 4\beta_{3t} + \beta_{1t} \cdot \beta_{3t} + 12} \right)$$

$$K_{\text{top}} = 1.444 \times 10^4 \quad \text{kN/m}$$

**4 - The three couples of (M, N) should be checked:**



**The first couple of (M1, N1):**

$$N_1 := \left| Q_{\text{top}} \right| \cdot \frac{\frac{E \cdot F_b}{L_b}}{\frac{E \cdot F_b}{L_b} + K_{\text{top}}}$$

$$M_1 := M_{P,B}$$

$$N_1 = 198.51 \quad \text{kN}$$

$$M_1 = 572.414 \quad \text{kNm}$$

**The second couple of (M2, N2):**

$$N_2 := \left| N_{\text{col}_{n-1}} \right| + \left| N_{\text{coll}_{n-1}} \right| + \left| N_{\text{lo.des.in.1}} \right|$$

$$M_2 := \left| M_{\text{col}_{n-1,0}} \right| + \left| M_{\text{coll}_{n-1,0}} \right|$$

$$N_2 = 2.414 \times 10^3 \quad \text{kN}$$

$$M_2 = 197.209 \quad \text{kNm}$$

**The bottom beam axial force before the catenary action happens:**

$$N_3 := \left| Q_{\text{bottom}} \right| \cdot \frac{\frac{E \cdot F_b}{L_b}}{\frac{E \cdot F_b}{L_b} + K_{\text{bottom}}}$$

$$N_3 = 65.253 \quad \text{kN}$$

**2**

**CHECKING THE FRAME INTEGRITY AND DUCTILITY**

**5 - Check the 2 dangerous internal forces couples (M1, N1) & (M2, N2)**

**BEAM CROSS SECTION CHARACTERISTIC**

**SECTION: IPE 400V**

|  |   |                     |                |
|--|---|---------------------|----------------|
| Flexural buckling length:                | $L_B := L_b$                            |                     |                |
| Flange and web dimension:                | $b_{f,b} := 0.182$                      | $t_{f,b} := 0.0175$ | $r_b := 0.021$ |
|  | $h_{w,b} := 0.408$                      | $t_{w,b} := 0.0106$ |                |
| Cross section area:                      | $A_b := 10.701 \cdot 10^{-3}$           |                     |                |
| Inertia:                                 | $I_{y,b} := 301.249 \cdot 10^{-6}$      |                     |                |
|  | $I_{z,b} := 17.66 \cdot 10^{-6}$        |                     |                |
| Section plastic modulus:                 | $M_{ply,Rk,b} := 572.41419$             |                     |                |
| Radius of gyration:                      | $i_{y,b} := 91.7 \cdot 10^{-3}$         |                     |                |
|  | $i_{z,b} := 55.1 \cdot 10^{-3}$         |                     |                |
| St Venant torsional and warping inertia: | $I_{t,b} := 284600 \cdot 10^{-12}$      |                     |                |
|  | $I_{\omega,b} := 193300 \cdot 10^{-12}$ |                     |                |
| Partial safety factors:                  | $\gamma_{M0} := 1.0$                    |                     |                |
|  | $\gamma_{M1} := 1.0$                    |                     |                |

**BUCKLING CURVE DEFINITION**

Imperfection factors for strong axis buckling:  $\alpha_y := 0.21$

**BEAM CROSS SECTION CLASSIFICATION**

Web in compression:

|                 |   |
|-----------------|---|
| BeamWebClass := | "Class 1" if $\frac{h_{w,b}}{t_{w,b}} < 33 \cdot \varepsilon$   |
|                 | "Class 2" if $\frac{h_{w,b}}{t_{w,b}} < 38 \cdot \varepsilon \wedge \frac{h_{w,b}}{t_{w,b}} > 33 \cdot \varepsilon$ |
|                 | "Class 3 and 4" otherwise   |

$$\varepsilon := \sqrt{\frac{f_y}{235 \cdot 10^3}}$$

BeamWebClass = "Class 1"

Outstand part of flange in compression:

|              |  |
|--------------|--|
| BeamClass := | "Class 1" if $\frac{0.5 \cdot (b_{f,b} - t_{w,b} - 2 \cdot r_b)}{t_{f,b}} < 9 \cdot \varepsilon$                   |
|              | "Class 2" if $\frac{h_{w,b}}{t_{w,b}} < 10 \cdot \varepsilon \wedge \frac{h_{w,b}}{t_{w,b}} > 9 \cdot \varepsilon$ |
|              | "Class 3 and 4" otherwise  |

BeamClass = "Class 1"

**CHECK COUPLE (M1, N1) ON BEAM**

At the end of phase 2, both beam end section is fully yield then it is not necessary check the section stability

**THE BEAM GLOBAL STABILITY**

$$N_{b,Rk} := A_b \cdot f_y \qquad N_{b,Rk} = 3.799 \times 10^3 \text{ kN}$$

Reduction factor for compression buckling:

$$N_{cr1,y} := \frac{\pi^2 \cdot E \cdot I_{y,b}}{L_b^2} \qquad N_{cr1,y} = 9.524 \times 10^3 \text{ kN}$$

$$\lambda_{-y1} := \sqrt{\frac{A_b \cdot f_y}{N_{cr1,y}}} \qquad \lambda_{-y1} = 0.632$$

$$\Phi_{y1} := 0.5 \cdot \left[ 1 + \alpha_y \cdot (\lambda_{-y1} - 0.2) + \lambda_{-y1}^2 \right] \qquad \Phi_{y1} = 0.745$$

$$\chi_{y1} := \frac{1}{\Phi_{y1} + \sqrt{\Phi_{y1}^2 - \lambda_{-y1}^2}} \qquad \chi_{y1} = 0.878$$

$$\text{Check}\chi_{y1} := \begin{cases} \text{"OK"} & \text{if } \chi_{y1} \leq 1 \\ \text{"Warning"} & \text{otherwise} \end{cases} \qquad \text{Check}\chi_{y1} = \text{"OK"}$$

$$\Psi_{y1} := -0.917 \qquad \Psi_{y1} = -0.917$$

Equivalent uniform moment factor Cm:

$$C_{my1} := \max(0.6 + 0.4 \cdot \Psi_{y1}, 0.4) \qquad C_{my1} = 0.4$$

$$\text{Check}C_{m1} := \begin{cases} \text{"OK"} & \text{if } C_{my1} \geq 0.4 \\ \text{"Not OK"} & \text{otherwise} \end{cases} \qquad \text{Check}C_{m1} = \text{"OK"}$$

Interaction factor:

$$n_{y1} := \frac{N_1}{\chi_{y1} \cdot \frac{N_{b,Rk}}{\gamma_{M1}}} \qquad n_{y1} = 0.06$$

Because  $\lambda_{-y} < 1$  then

$$k_{yy1} := \min \left[ C_{my1} \cdot \left[ 1 + (\lambda_{-y1} - 0.2) \cdot n_{y1} \right], C_{my1} \cdot (1 + 0.8 \cdot n_{y1}) \right] \qquad k_{yy1} = 0.41$$

$$M_{Ed1} := \frac{1 - \frac{N_1}{\chi_{y1} \cdot \frac{N_{b,Rk}}{\gamma_{M1}}}}{\frac{k_{yy1} \cdot C_{my1}}{\frac{M_{ply,Rk,b}}{\gamma_{M1}}}} \qquad M_{Ed1} = 3.28 \times 10^3 \text{ kNm}$$



BeamPhase2Global :=  $\begin{cases} \text{"The beam is OK in phase 2!"} & \text{if } M_{Ed1} > M_1 \\ \text{"The beam is unstable!"} & \text{otherwise} \end{cases}$       $M_1 = 572.414$

BeamPhase2Global = "The beam is OK in phase 2!"

**COLUMNS CROSS SECTION CHARACTERISTIC**

**SECTION: HE 360 A**

Flexural buckling length:  $L_C := L_c$

Flange and web dimension:  $b_{f,c} := 0.30$       $t_{f,c} := 0.0175$       $r_c := 0.027$   
 $h_{w,c} := 0.35$       $t_{w,c} := 0.01$

Cross section area:  $A_c := F_c$

Inertia:  $I_{y,c} := 330.9 \cdot 10^{-6}$   
 $I_{z,c} := 78.87 \cdot 10^{-6}$

Section plastic modulus:  $W_{Pl,y,c} := 2088 \cdot 10^{-6}$   
 $W_{Pl,z,c} := 802.3 \cdot 10^{-6}$

Section elastic modulus:  $W_{El,y,c} := 1891 \cdot 10^{-6}$   
 $W_{El,z,c} := 525.8 \cdot 10^{-6}$

Radius of gyration:  $i_{y,c} := 152.2 \cdot 10^{-3}$   
 $i_{z,c} := 74.3 \cdot 10^{-3}$

St Venant torsional and warping inertia:  $I_{t,c} := 1488000 \cdot 10^{-12}$   
 $I_{\omega,c} := 2177000 \cdot 10^{-12}$

Partial safety factors:  $\gamma_{M0} := 1.0$   
 $\gamma_{M1} := 1.0$

**BUCKLING CURVE DEFINITION**

Imperfection factors for strong axis buckling:  $\alpha_{sw} := 0.21$



**COLUMN CROSS SECTION CLASSIFICATION**

Web in compression:

$$\text{ColWebClass} := \begin{cases} \text{"Class 1"} & \text{if } \frac{h_{w,c}}{t_{w,c}} < 33 \cdot \varepsilon \\ \text{"Class 2"} & \text{if } \frac{h_{w,c}}{t_{w,c}} < 38 \cdot \varepsilon \wedge \frac{h_{w,c}}{t_{w,c}} > 33 \cdot \varepsilon \\ \text{"Class 3 and 4"} & \text{otherwise} \end{cases} \quad \text{ColWebClass} = \text{"Class 1"}$$

Outstand part of flange  
in compression:

$$\text{ColumnClass} := \begin{cases} \text{"Class 1"} & \text{if } \frac{0.5 \cdot (b_{f,c} - t_{w,c} - 2 \cdot r_c)}{t_{f,c}} < 9 \cdot \varepsilon \\ \text{"Class 2"} & \text{if } \frac{h_{w,c}}{t_{w,c}} < 10 \cdot \varepsilon \wedge \frac{h_{w,c}}{t_{w,c}} > 9 \cdot \varepsilon \\ \text{"Class 3 and 4"} & \text{otherwise} \end{cases} \quad \text{ColumnClass} = \text{"Class 1"}$$

**CHECK COUPLE (M2, N2)**

**THE SECTION OF COLUMNS**

The interaction curve between M,N:

$$\begin{aligned}
 N_{c,Rk} &:= A_c \cdot f_y & N_{c,Rk} &= 5.068 \times 10^3 \text{ kN} \\
 M_{pl,y,Rk,c} &:= W_{pl,y,c} \cdot f_y & M_{pl,y,Rk,c} &= 741.24 \text{ kNm} \\
 n_c &:= \frac{N_2}{N_{c,Rk}} & n_c &= 0.476 \\
 a_c &:= \min\left(\frac{A_c - 2 \cdot b_{f,c} \cdot t_{f,c}}{A_c}, 0.5\right) & a_c &= 0.264 \\
 M_{Ny,c} &:= M_{pl,y,Rk,c} \cdot \frac{1 - n_c}{1 - 0.5 \cdot a_c} & M_{Ny,c} &= 447.328 \text{ kNm}
 \end{aligned}$$

$$\text{ColPhase2Sect} := \begin{cases} \text{"The column section is OK in phase 2!"} & \text{if } M_{Ny,c} > |M_2| \\ \text{"The column is unstable!"} & \text{otherwise} \end{cases}$$

$$\text{ColPhase2Sect} = \text{"The column section is OK in phase 2!"}$$

**THE COLUMN GLOBAL STABILITY**

Calculate the equivalent buckling length:

In the phase 2, the column's end points do not move, so the column had been treated as if in a non-swaying situation:

$$\begin{aligned}
 \eta_{t,c} &:= \frac{S_C}{S_C + 2 \cdot S_{B1}} & \eta_{b,c} &:= \frac{S_C}{S_C + 2 \cdot S_{B1}} \\
 K_{buck,c} &:= \frac{1 + 0.145 \cdot (\eta_{b,c} + \eta_{t,c}) - 0.265 \cdot \eta_{t,c} \cdot \eta_{b,c}}{2 - 0.364 \cdot (\eta_{b,c} + \eta_{t,c}) - 0.247 \cdot \eta_{t,c} \cdot \eta_{b,c}} & K_{buck,c} &= 0.715
 \end{aligned}$$

Reduction factor for compression buckling:

$$\begin{aligned}
 N_{cr2,y} &:= K_{buck,c}^2 \cdot E \cdot I_{y,c} & N_{cr2,y} &= 3.468 \times 10^4 \text{ kN} \\
 \lambda_{-y2} &:= \sqrt{\frac{A_c \cdot f_y}{N_{cr2,y}}} & \lambda_{-y2} &= 0.382 \\
 \Phi_{y2} &:= 0.5 \cdot \left[ 1 + \alpha_y \cdot (\lambda_{-y2} - 0.2) + \lambda_{-y2}^2 \right] & \Phi_{y2} &= 0.592 \\
 \chi_{y2} &:= \frac{1}{\Phi_{y2} + \sqrt{\Phi_{y2}^2 - \lambda_{-y2}^2}} & \chi_{y2} &= 0.957 \\
 \text{Check}\chi_{y2} &:= \begin{cases} \text{"OK"} & \text{if } \chi_{y2} \leq 1 \\ \text{"Warning"} & \text{otherwise} \end{cases} & \text{Check}\chi_{y2} &= \text{"OK"}
 \end{aligned}$$

$$\Psi_{y2} := -2$$

$$\Psi_{y2} = -2$$

Equivalent uniform moment factor Cm:

$$C_{my2} := \max(0.6 + 0.4 \cdot \Psi_{y2}, 0.4)$$

$$C_{my2} = 0.4$$

$$\text{Check}C_{m2} := \begin{cases} \text{"OK"} & \text{if } C_{my2} \geq 0.4 \\ \text{"Not OK"} & \text{otherwise} \end{cases}$$

$$\text{Check}C_{m2} = \text{"OK"}$$

Interaction factor:

$$n_{y2} := \frac{N_2}{\chi_{y2} \cdot \frac{N_{c.Rk}}{\gamma_{M1}}}$$

$$n_{y2} = 0.498$$

Because  $\lambda_y < 1$  then

$$k_{yy2} := \min[C_{my2} \cdot [1 + (\lambda_{y2} - 0.2) \cdot n_{y2}], C_{my2} \cdot (1 + 0.8 \cdot n_{y2})]$$

$$k_{yy2} = 0.436$$

$$M_{Ed2} := \frac{1 - \frac{N_2}{\chi_{y2} \cdot \frac{N_{c.Rk}}{\gamma_{M1}}}}{\frac{k_{yy2} \cdot C_{my2}}{\frac{M_{pl.y.Rk.c}}{\gamma_{M1}}}}$$

$$M_{Ed2} = 2.134 \times 10^3 \text{ kNm}$$

$$\text{ColPhase2Global} := \begin{cases} \text{"The column is OK in phase 2!"} & \text{if } M_{Ed2} > |M_2| \\ \text{"The column is unstable!"} & \text{otherwise} \end{cases}$$

$$\text{ColPhase2Global} = \text{"The column is OK in phase 2!"}$$

9.3.6. Step 3

**3**

**CALCULATE THE LATERAL STIFFNESS K**

**6 - The stiffness of each column in the damaged floor**

Force parameter:  $P_1 := N_{lo.des.out.1}$   $F_1 := N_3$

$P_2 := N_{lo.des.in.1}$

The ratio of F to column axial force - by Finelg

$n := \frac{2691.5 - N_2}{970.6 - 159.9}$   $n = 0.342$

**THE COLUMN STIFFNESS**

The column beside and inside the frame: 1st order elastic stiffness

$K_{c.1st} := \frac{12 \cdot E \cdot J_c}{L_c^2} \cdot \frac{k_{1C}}{L_c \cdot k_{1C} + 6 \cdot E \cdot J_c}$   $K_{c.1st} = 9.98298 \times 10^3$  kN/m

The external column:

$K_{cs.1st} := \frac{12 \cdot E \cdot J_c}{L_c^2} \cdot \frac{k_{3C}}{L_c \cdot k_{3C} + 6 \cdot E \cdot J_c}$   $K_{cs.1st} = 8.712 \times 10^3$  kN/m

The second order stiffness of the column - neglecting the initial bending moment:

$K_{c.2nd.inter} := K_{c.1st} - \frac{P_2}{L_c}$   $K_{c.2nd.inter} = 9.525 \times 10^3$  kN/m

$K_{c.2nd.out} := K_{cs.1st} - \frac{P_1}{L_c}$   $K_{c.2nd.out} = 8.483 \times 10^3$  kN/m

Especially in the case of beside column the column 2nd order stiffness linearised is:

$K_{c.2nd.beside} := \frac{K_{c.1st} \cdot L_c - N_2 - P_2}{L_c + n}$   $K_{c.2nd.beside} = 8.048 \times 10^3$  kN/m

**The lateral stiffness on the left and right side:**

$K_{left} := K_{c.2nd.inter} + K_{c.2nd.beside} + K_{c.2nd.out}$   $K_{left} = 2.606 \times 10^4$  kN/m

$K_{right} := 2K_{c.2nd.inter} + K_{c.2nd.beside} + K_{c.2nd.out}$   $K_{right} = 3.558 \times 10^4$  kN/m

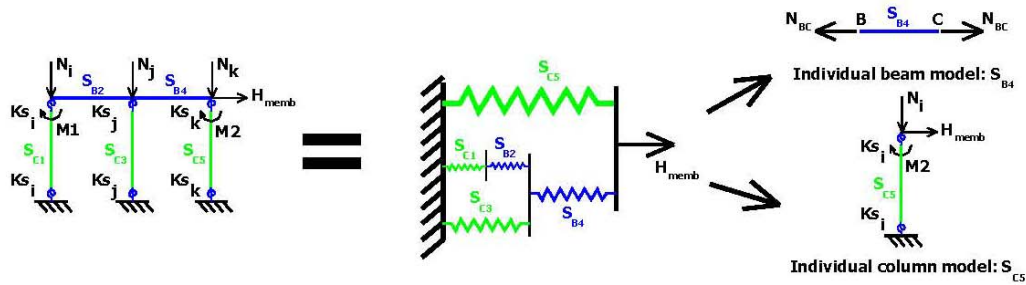
**The beams elongation stiffness of the bottom beams is:**

$K_{beams} := \frac{E \cdot F_b}{2 \cdot L_b}$   $K_{beams} = 1.37124 \times 10^5$  kN/m

**The lateral stiffness taking into account both sides:**

$K_{both} := \frac{K_{left} \cdot K_{right} \cdot K_{beams}}{K_{left} \cdot K_{beams} + K_{right} \cdot K_{beams} + K_{left} \cdot K_{right}}$   $K_{both} = 1.35546 \times 10^4$  kN/m

**THE RESISTANCE OF LATERAL STIFFNESS K**



**7 - The resistance of each column in the damaged floor is presented by the weakest column - the intermediate column.**

$$F_{Pl.Rd.col} := \frac{2 \cdot W_{Pl.y.c} \cdot f_y \cdot K_{c.2nd.inter}}{K_{c.2nd.inter} \cdot L_c + P_2} \quad F_{Pl.Rd.col} = 404.131 \quad \text{KN}$$

The horizontal plastic resistance of the lateral stiffness is on the left side:

$$F_{K.Rd} := F_{Pl.Rd.col} \cdot \left( \frac{K_{c.2nd.out} + K_{c.2nd.beside} + K_{c.2nd.inter}}{K_{c.2nd.inter}} \right)$$

$F_{K.Rd} = 1.10554 \times 10^3$

KN

The maximum axial force applied to the beside column is equal to half of the difference between

the  $N_{lo.design}$  and  $N_{Pl.lost}$  - the  $M$  of each column take by  $F_{ineIg}$  - at that point,  
 $F = 368.813 \text{ kN}$

$$N_{beside.3} := P_2 + N_2 + \frac{N_{lo.design.in.1} - N_{Pl.lost.1.4}}{2} \quad N_{beside.3} = 4.10325 \times 10^3 \quad \text{KN}$$

$$M_{beside.3} := 12 \quad \text{kNm}$$

$$N_{inter.3} := P_2 \quad N_{inter.3} = 1.60321 \times 10^3 \quad \text{KN}$$

$$M_{inter.3} := 173 \quad \text{kNm}$$

**CHECK COUPLE (Mbeside3, Nbeside3)**

**THE SECTION OF COLUMNS**

The interaction curve between M,N:

$$n_{c1} := \frac{N_{\text{beside.3}}}{N_{\text{c.Rk}}} \quad n_{c1} = 0.81$$

$$M_{N_{y.c1}} := M_{\text{pl.y.Rk.c}} \cdot \frac{1 - n_{c1}}{1 - 0.5 \cdot a_c} \quad M_{N_{y.c1}} = 162.594 \quad \text{kNm}$$

$$\text{ColPhase3Sect} := \begin{cases} \text{"The column section is OK in phase 3!"} & \text{if } M_{N_{y.c1}} > M_{\text{beside.3}} \\ \text{"The column is unstable!"} & \text{otherwise} \end{cases}$$

ColPhase3Sect = "The column section is OK in phase 3!"

**THE COLUMN GLOBAL STABILITY**

Because all the parameters are estimated for column in the Step 3 then the column is directly checked by M, N

Interaction factor:

$$n_{y3} := \frac{N_{\text{beside.3}}}{\chi_{y2} \cdot \frac{N_{\text{c.Rk}}}{\gamma_{M1}}} \quad n_{y3} = 0.846$$

Because  $\lambda_y < 1$  then

$$k_{yy3} := \min[C_{my2} [1 + (\lambda_{y2} - 0.2) \cdot n_{y3}], C_{my2} (1 + 0.8 \cdot n_{y3})]$$

$$k_{yy3} = 0.462$$

$$M_{\text{Ed3}} := \frac{1 - \frac{N_{\text{beside.3}}}{N_{\text{c.Rk}}}}{\chi_{y2} \cdot \frac{\gamma_{M1}}{k_{yy3} \cdot C_{my2}}} \cdot \frac{M_{\text{pl.y.Rk.c}}}{\gamma_{M1}} \quad M_{\text{Ed3}} = 619.422 \quad \text{kNm}$$

$$\text{ColPhase3Global} := \begin{cases} \text{"The column is OK in phase 3!"} & \text{if } M_{\text{Ed3}} > M_{\text{beside.3}} \\ \text{"The column is unstable!"} & \text{otherwise} \end{cases}$$

ColPhase3Global = "The column is OK in phase 3!"

**CHECK COUPLE (Minter3, Ninter3)**

**THE SECTION OF COLUMNS**

The interaction curve between M,N:

$$n_{c2} := \frac{N_{inter.3}}{N_{c.Rk}} \quad n_{c2} = 0.316$$

$$M_{Ny.c2} := M_{ply.Rk.c} \cdot \frac{1 - n_{c2}}{1 - 0.5 \cdot a_c} \quad M_{Ny.c2} = 583.98 \quad \text{kNm}$$

$$\text{ColIntPhase3Sect} := \begin{cases} \text{"The inter column section is OK in phase 3!"} & \text{if } M_{Ny.c2} > M_{inter.3} \\ \text{"The column is unstable!"} & \text{otherwise} \end{cases}$$

$$\text{ColIntPhase3Sect} = \text{"The inter column section is OK in phase 3!"}$$

**THE COLUMN GLOBAL STABILITY**

Because all the parameters are estimated for column in the Step 3 then the column is directly checked by M, N

Interaction factor:

$$n_{y4} := \frac{N_{inter.3}}{\chi_{y2} \cdot \frac{N_{c.Rk}}{\gamma_{M1}}} \quad n_{y4} = 0.33$$

Because  $\lambda_y < 1$  then

$$k_{yy4} := \min \left[ C_{my2} \cdot \left[ 1 + (\lambda_{-y2} - 0.2) \cdot n_{y4} \right], C_{my2} \cdot (1 + 0.8 \cdot n_{y4}) \right] \quad k_{yy4} = 0.424$$

$$M_{Ed4} := \frac{1 - \frac{N_{inter.3}}{N_{c.Rk}}}{\chi_{y2} \cdot \frac{\gamma_{M1}}{k_{yy4} \cdot C_{my2}}} \cdot \frac{M_{ply.Rk.c}}{\gamma_{M1}} \quad M_{Ed4} = 2.926 \times 10^3 \quad \text{kNm}$$

$$\text{ColIntPhase3Global} := \begin{cases} \text{"The inter column is OK in phase 3!"} & \text{if } M_{Ed4} > |M_{inter.3}| \\ \text{"The column is unstable!"} & \text{otherwise} \end{cases}$$

$$\text{ColIntPhase3Global} = \text{"The inter column is OK in phase 3!"}$$

**Conclusion:** The frame's integrity fulfils the necessity of lateral stiffness and influences the formation of the catenary action. When the Nlost reaches the N.lo.design, the frame is still stable.



#### 9.4. CONCLUSION

The objective of the robustness assessment was to predict the load capacity of the frame after it undergoes an exceptional event. In the present work, that accidental event was chosen to be the loss of a column. As presented in the chapter on the state of the art, the measurement method which was applied in this research was the direct design calculation.

The capacity of the frame has been illustrated by the list of the key elements which were presented in three chapters (6, 7, and 8). The key elements are defined as critical members of the different zones which have been designated within the frame. In fact, those zones are comprised in the two alternative load paths which appear in the structure. The critical value of  $N_{lost}^{Pl.Rd}$  in the additional state is the conditional key to deciding if the two alternative load paths could be produced. Step 1's objective was thus to predict that value by quick estimation formulae.

The first path moves along the hanging action of the directly affected part to transfer the additional loads to the adjacent columns. There are three key elements on that load path. The first key element is the top equivalent beam under compression from the arch effect. The adjacent column in the damaged level was identified as the second key element due to the high additional compression it had to support. The last element is the tension forces appearing in the catenary beam.

If the extended load path was activated in the frame, the new key elements were checked. They were key element number 2 in the previous load path under the new loading state and the intermediate column which received the highest bending moment combined with high compression. Those columns were located within the damaged level.

The frame under investigation with the damaged column at position 1-4 in the example of Section 9.3 was analyzed, for which the conclusion was reached that the frame could undergo the catenary action without any pre-failures. This frame's response trajectory provided the complete example for the calculation where the assessment formulae have been listed.

The formulae, which were applied to the example, in general, are simplified calculations. In fact, due to the simplifications and assumptions made by the author, the analytical model provided approximate results, as discussed in the previous chapter's validations. However, from a practical point of view, the simplified formulae used here, which have



produced acceptable results, were preferred.

**CHAPTER 10: DISCUSSIONS AND CONCLUSIONS**

### **10.1. INTRODUCTION**

In all of the preceding chapters, the state of the art, the problems encountered, the methods applied, the simulations performed and analytical formulae developed for this thesis have been presented and discussed. To illustrate the applications of this research, a detailed example was calculated and simulated, as provided in Chapter 9. In this example, all of the essential points were arranged in a more logical order in order to highlight the ideas and solutions related to the study of a building frame undergoing the exceptional loss of a column.

The present chapter proposes the discussion of and conclusions on the major results produced in this work. The next section (10.2) considers the main conclusions on the methodology employed and its calculation properties. The background and assumptions will be examined to highlight the tolerance of the calculations' results and the relationship of the result to the catenary action to cover the complete behavior of the frame up until its final collapse. The disadvantages of this approach, as well as the necessity for further development, will also be discussed.

The discussions are placed in Section 10.3 where the author will debate these methods' and solutions' bearing in practical applications. Due to the narrowed approach of the author, the discussions are limited to the purpose of this work and its scope.

Finally, the last section explores prospective research aimed at reaching the highest benefits in solving this problem. The extensions of the present work's conclusions can be followed in four directions: application to the composite steel—concrete structure, the applicability of the methodology in a 3D frame, coding the automatic assessment tool, and the comparison of the catenary action's energy absorption to the full frame's absorption, which is investigated to orient the local structural elements' development.

### **10.2. CONCLUSION OF THE THESIS**

The major goal of this thesis was to investigate the behavior of steel and steel—concrete composite frames following the accidental loss of a column. In Chapter 2, the literature on the most recent studies on progressive collapse prevention, especially regarding the specific problem of the loss of a column within a frame, was reviewed. That chapter

concluded by pointing out the lack of knowledge on the global behavior of the frame during such an event. Thus, the investigation on a residential and office building frame following their partial destruction by column loss was carried out in this thesis, to elucidate the little known aspects of their behavior.

### **10.2.1. Main achievements related to the global behavior of the frame following the loss of a column**

#### *10.2.1.a. Prediction of the two alternative load paths activated within the frame*

When a column is damaged within the frame, the frame goes from its initial state to a residual state. Due to the change in the frame's physical character, the forces flowing within the frame must change their path to reach the foundation. Thus, these paths appear in the frame because of the additional load. Influenced by the particular properties of different structures, the alternative load path is activated within the frame, a phenomenon represented by the redistribution of internal forces. The results obtained from the author's numerical investigations on the frames in such an accidental event proved the presence of these alternative load paths. Each alternative load path has been defined herein in order to identify the chain of structural members which must support the additional load.

In particular, the trajectory of the alternative load path changes according to the behavior of the members within it. When the directly affected part yields, for example, catenary action could be activated depending on the ductility of the structure and the additional load's amplitude. In fact, identifying the two alternative load paths and determining their initial conditions were the first achievements of this thesis. Determining the possibility of activating the alternative load path was made possible by comparing the critical value of

$$N_{Lost}^{Pl.Rd} \text{ and the initial load, } N_{design} .$$

#### *10.2.2.b. Investigation on the redistribution of the internal forces within the frame after the accidental event through the simplified analytical model*

In the process of investigating the alternative load path, the distribution of internal forces was obtained. Through the simulation of the directly affected part in the real frame by the simplified analytical model, the fundamental behavior of the part was portrayed. The

results obtained were then compared to the FEM analysis. In the end, the validation proved the substructure's ability to accurately represent the real frame's behavior at the specific point selected at the top of the damaged column.

A new model was extended from the previous analytical model in order to calculate how the forces act on each member within the alternative load path. Their loading states were used to measure the frame's ability to maintain the alternative load path after the accidental event. In turn, this ability determined the robustness of the frame. Also, the special distribution of the internal forces within the frame, called the "arch effect", was identified and estimated.

*10.2.2.c. Development of the analytical method to predict the behavior of the frame following the loss of a column*

As presented in Chapters 4 and 5, the survival of the frame is in reality influenced by the activation of an alternative load path. If the frame finds the right alternative load path, progressive collapse will be prevented. Thus, the two previous conclusions on the frame's global behavior following the loss of a column were systematized to determine the frame's robustness assessment. This procedure follows a series of critical values which correspond to the outcome scenarios for the frame's behavior. In this thesis, the development of the simplified analytical calculation, using these critical values, was carried out.

*10.2.2.d. Development of the analytical method to assess the influences of the surrounding structural member on the activation of the catenary action*

In Load Phase 3, the directly affected part fully yields. If certain parametrical conditions are fulfilled, however, catenary action is activated. Regarding these conditions, the activation and behavior of the membrane beam are influenced by the surrounding structural members. The last achievement of this thesis was to calculate the lateral stiffness,  $\mathbf{K}$ , of the damaged floor. Moreover, the resistance of the two sides against the membrane forces was predicted by the value of  $F_{Rd}$ . These two parameters were investigated to provide Demonceau with the means to develop the full frame's robustness assessment method.

**10.2.2. Accuracy and tolerance**

*10.2.2.a. Error in the analytical method*

The analytical approaches, which were applied to the structure in Load Phase 2, consist of elastic—perfectly plastic rules taking into account the second-order P-Delta effect. The final state was identified by the fully plastic mechanism of the directly affected part at point (4), when the additional load applied takes on the value of  $N_{lost}^{Pl.Rd}$ . The illustration of the evolution of load carrying on point A at the top of the damaged column is repeated below in Figure 10.2.

The green line in Figure 10.2 represents the actual behavior of point A as a function of the evolving load. The blue line defines the behavior of the catenary action, which was provided in Demonceau’s thesis. The magenta line represents the expected analytical result due to the elastic—perfectly plastic assumption with second-order elastic calculation applied. In this case, the point under investigation shifts to point (4’) instead of the right point (4) in the figure.

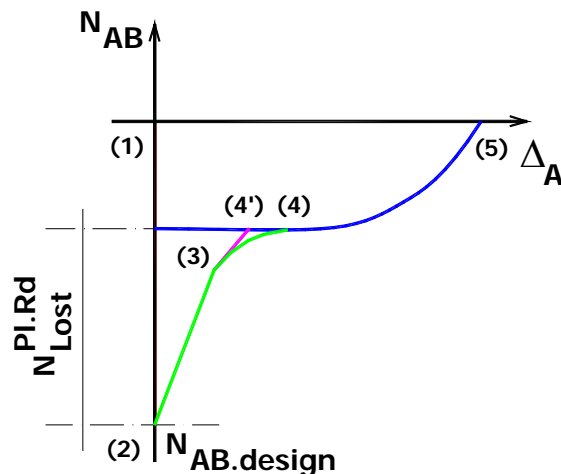


Figure 10.1. The tolerance of analytical results

*10.2.2.b. Error in the selected analytical model*

The model in Chapter 7 was first solved by the rotational method, and then the estimation of the axial forces within the equivalent beam was carried out using the distribution of axial stiffness. In other words, the first calculation neglected the elongation of the frame’s members. The second calculation step just obtained the axial forces based on the nodes’

equilibrium. This simplification is suitable for practical purpose but results in an associated error in the results. In the validation of these results in Chapter 7, the errors were reported in comparison to the numerical simulations' results; fortunately, the conclusion was that this simplified method reports an acceptable level of accuracy.

#### *10.2.2.c. Error in the values for $K$ and $F_{Rd}$*

During Load Phase 3, the catenary action appeared as the most recurrent behavior of the frame. The values for  $K$  and  $F_{Rd}$  were provided for Jean-François Demonceau for the fully constituted analytical model. However, for clarity's sake, the nonlinear  $K$  value was obtained by the linearized curve and was applied to the calculation as a constant. The influence of  $K$ 's value on the catenary action was then investigated by Demonceau in his thesis. In addition, the value of  $F_{Rd}$  was presented.

### **10.2.3. Necessity of development**

#### *10.2.3.a. Simplifying the practically oriented analytical method for typical and general buildings*

Chapter 7 demonstrated the expanded analytical model in order to simulate the behavior of the frame exhibiting the arch effect. These calculations required a high level of complexity in the simulated model. As a result, the rotational method applied in the example in Chapter 9 included too many steps to calculate all of the parameters and solve the entire system of linear algebraic equations. Indeed, the general building frame was too complex to solve by hand. Thus, it was necessary to develop a simpler, easier, and more efficient calculation method.

#### *10.2.3.b. Development of the expanded analytical model*

As illustrated in Chapter 7, Section 7.5, the analytical model provided the most accurate results regarding the bending moment and axial force diagrams by replacing the rotational stiffness  $K_S$  at the end of adjacent span beams by a fixed end. This unreasonable conclusion requires further parametrical analyses on such a phenomenon. If that conclusion is proved, the simplification of extracted analytical model can be developed to a higher degree.

### **10.3. DISCUSSIONS**

#### **10.3.1. Determining structural risks**

The first point to discuss relates to the determination of threats and acceptable structural risks. As in Chapter 2, the most popular idea of researchers and designers today is to consider the alternative load path with the “independence to threat” method. Uninfluenced by the cause of damage, this method considers only the damage’s result, as in this situation where a column is destroyed. Thus, this approach and the simplified alternative load path method in this thesis have made it possible to identify the acceptable risks which are caused by the loss of a column.

#### **10.3.2. Energy absorption**

In some documents and provisions, progressive collapse is considered to be a phenomenon whose nature is dynamic. To solve the problem in practical domains, the solution proposed was to analyze the structure under the combination of (100% DL+ 50% LL + 20% WL) multiplied by the dynamic load factor (also referred to as a Demand Capacity Ratio) of 2.

When the load is statically defined, using this method provides the frame’s capacity on the total energy absorption measurement. With the extended analytical model described in Chapter 7, plus the energy absorbed only by the catenary action in Chapter 8 and in Demonceau’s thesis, the total energy absorption of the frame was quickly obtained in only two models and using simplified analytical formulae.

Then, based on the behavioral curve in Figure 10.1, the dynamic loading rate-dependent robustness assessment method of Izzuddin, Vlassis (2007) could be applied.



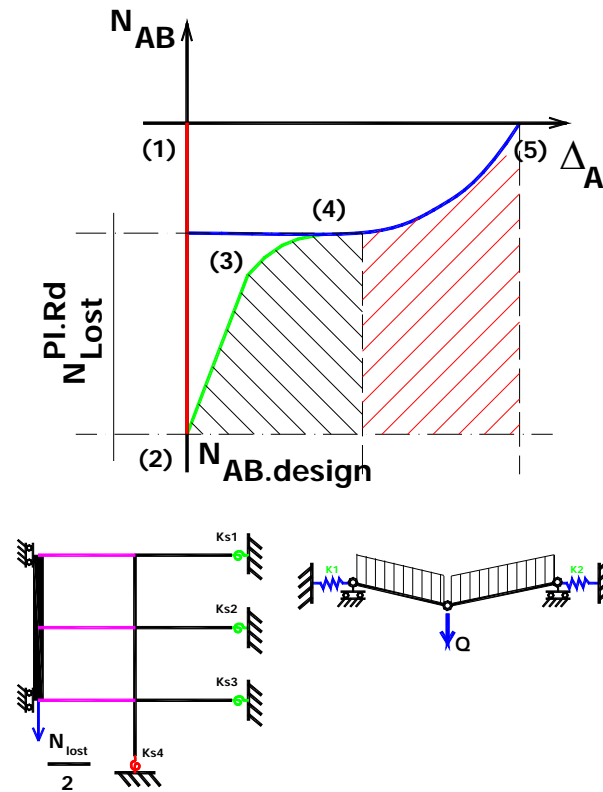


Figure 10.1. Total approximate frame energy absorption taking into account the second-order elastic and non-linear catenary action

### 10.3.3. Design process

In EUROCODE, BS and US provisions, the key elements must be identified in order to design the building with adequate robustness. The building frame's vulnerability analysis, in fact, is achieved by examining the failure fronts within the frame due to the abnormal situation. Thanks to the work in this thesis, the specific key elements, which were determined according to the trajectory of the alternative load path, have been identified as follows: the top equivalent beam, the bottom adjacent column and the intermediate column in the damaged level.

With this knowledge of the key structural elements' positions and their working conditions, the progressive collapse scenarios can be predicted and, more importantly, avoided.

### 10.3.4. Damage assessment

The other advantage of the knowledge of the failure fronts within the frame was being able

to perform an accurate simulation of the damaged level. From a practical angle, the damage assessment was already obtained in this alternative load path analysis and expressed in the final analysis report. Which key element was injured and whether the alternative load path could be maintained or not was reported as the detailed extent of the damage.

### **10.3.5. Monitoring and protection**

The need to determine threats, which was described above in Section 10.3.1, also highlights the benefit of monitoring the frame's vulnerability by converging many exceptional causes to one particular situation, namely, the loss of a column. With the identification of threats and key elements, the protection of existing buildings and those only in the design phase can be thoroughly examined. In other words, when imagining the threats which could attack a particular building, the most dangerous position of a column can be quickly and easily predicted by the method presented here.

The guidelines for providing frames capable of activating the catenary action and also for providing protection to the structures, such as the ductile joint, should be followed. By considering each key element as presented before, the user can predict the alternative load path. On that path, chief vulnerabilities are monitored and, thanks to that monitoring, the appropriate protection processes can be applied effectively to prevent possible progressive collapse.

## **10.4. FUTURE RESEARCH RECOMMENDATIONS**

### **10.4.1. Extend the analytical approaches to composite steel-concrete structure**

The present alternative load path method was described and validated in steel frame examples. The beams' and columns' behaviors at each calculation step were considered to be symmetric for **H** steel sections. For example, the sagging and hogging plastic bending moments were given the same value. Also, in  $K_S$  simulations, the beam sections on the left and right of the column worked under opposing bending moments but were treated with the same bending stiffness. Thus, the full investigation and analytical simulation presented in this thesis should be performed on a new type of structure: the composite steel—concrete structures.

#### **10.4.2. Extend the solution to the 3D problem**

As assumed in Chapter 5, the building structure which was dealt with throughout this thesis was reduced to a 2D frame. The 2D frame's behavior reflected most of the building's practical actions well but neglected the spatial phenomenon and connectivity. To provide a more accurate solution in progressive collapse prevention, an investigation on 3D frames will be crucial. However, the assessment method provided here does include the ability to be extended to cover the 3D problem after a small development.

#### **10.4.3. Automatic tool programmed for frame robustness assessment**

Even though the analytical method was built in order to achieve a practically orientated robustness assessment tool, the formulae and procedures performed were still too complex. In order to maximize this method's usefulness, a fully automatic, systematized tool could be developed. Based on an arrangement such as the one in Chapter 2, a simple worksheet to prevent errors due to inexperience and lack of practice can be constructed.

#### **10.4.4. Energy absorption comparison between the catenary action and the full alternative load path.**

By organizing the redundancy assessment and design guidelines associated with the method in this thesis, it has been proved that this method has the potential ability to distribute energy absorption within the structure. Presented in Figure 10.1, the energy absorbed in the frame was divided according to Load Phases 2 and 3. In particular, the energy along the alternative load path was absorbed by the load path's members. Regarding this distribution of energy absorption, the structural elements can be designed according to the necessary amount of energy to be absorbed. Finally, the other possibility in preventative building strategies would be to arrange and design the structural members along the alternative load path so as to increase the energy dissipated.

## References

- Adey, B.T.; Grondin, G.Y.; Cheng, J.J.R, Extended End Plate Moment Connections Under Cyclic Loading, *Journal of Constructional steel research*, vol. 46, no. 1/3, 1998.
- Agarwal, J.; Blockley, D.; Woodman, N, Vulnerability of structural systems, *Structural Safety* 25 (2003) 263–286.
- Ahmed, B.; Li, T. Q.; Nethercot, D. A, Design of Composite Finplate and Angle Cleated Connections, *Journal of Constructional Steel Research*, vol. 41, no. 1, pp. 1-29(29), 1997.
- Altmann, R.; Maquoi, R.; Jaspert, J. P, Experimental Study of the Non-Linear Behaviour of Beam-to- Column Composite Joints, *Proc. COST CI Conference on Semi Rigid Connections*, Strassbourg, October, 1992.
- American Society of Civil Engineers (AISC), Specifications for structural steel buildings: Part 1- Provisions, *ANSI/ AISC 360-05*, Edition March, 9, 2005.
- American Society of Civil Engineers (AISC), Specifications for structural steel buildings: Part 2- Commentary, *ANSI/ AISC 360-05*, Edition March, 9, 2005.
- Aribert, J.M.; Et, Lachal, A, Experimental investigation of Composite Connections and Global Interpretation, *Proc. COST CI*, France, Oct-92.
- Aristotle, K, Seismic Behaviour of Steel Frames with Semi-Rigid Joints, Experimental and Analytical Procedures, *Proc. COST CI Conference on Semi Rigid Connections*, Strassbourg, October, 1992.
- Azizinamini, A.; Bradburn, J. H.; Radziminski, J. B, Initial Stiffness of Semi-Rigid Steel Beam-to-Column Connections, *Journal of Constructional Steel Research*, vol. 8, pp. 71-90 (20), 1987.
- Bae, Sang-Wook; LaBoube, Roger A.; Belarbi, Abdeldjelil; Ayoub, Ashraf, Progressive collapse of cold-formed steel framed structures – *Journal of Thin-Walled Structures* – 2008.
- Bernuzzi, C.; Zandonini, R, Failure Assessment of Beam-to-Column Steel Joints via Low-Cycle Fatigue Approaches, *Proceedings of the 2nd International Conference in Advanced Steel Structures (ICASS'99)*, Hong Kong, 15-17 December, 1999.
- Bernuzzi, C.; Zandonini, R, Slim Floor Steel-Concrete Composite Systems, *Proceedings of the International Conference on Composite Structures III*, Irsee, Germany, June, 1996.
- Bloomberg, M. R. (Mayor), Abstract: Findings and Recommendations- The City of New York, New York City Department of Buildings, World Trade Centre Building Task Force, February, 2003.
- Braham, M.; Jaspert, J. P, Is it safe to design a building structure with simple joints, when they are known to exhibit a semi-rigid behaviour?, *Journal of Constructional Steel Research*, vol. 60, pp. 713-723 (11), 2004.
- British Standard Normative, BS 5950, Part 1: Structural use of steelwork in building. Code of practice for design. Rolled and welded sections, *BS 5950-1:2000*, 2000.
- British Standard Normative, BS 5950, Part 2: Structural use of steelwork in building. Specification for materials, fabrication and erection: Rolled and welded sections, *BS 5950-2:2001*, 2001.

- Brown, N. D.; Anderson, D.; Hughes, A. F, Wind Moment Steel Frames with Standard Ductile Connections, *Journal of Constructional Steel Research*, vol. 52, pp. 255-268(14), 1999.
- Building Seismic Safety Council for the Federal Emergency Management Agency, NEHRP Recommended Provisions for Seismic Regulations for New Buildings and other Structures, FEMA 302- Provisions, *FEMA-302, Building Seismic Safety Council, Washington D.C, First Edition*, 1997.
- Building Seismic Safety Council for the Federal Emergency Management Agency, NEHRP Recommended Provisions for Seismic Regulations for New Buildings and other Structures, FEMA 303- Commentary, *FEMA-303, Building Seismic Safety Council, Washington D.C, First Edition*, 1997.
- Building Seismic Safety Council for the Federal Emergency Management Agency, NEHRP Recommended Seismic Design Criteria for New Steel Moment-Frame Buildings, *FEMA-350, Building Seismic Safety Council, Washington D.C, First Edition*, June 2000.
- Building Seismic Safety Council for the Federal Emergency Management Agency, NEHRP Recommended Seismic Evaluation and Upgrade Criteria for Existing Welded Steel Moment-Frame Buildings, *FEMA-351, Building Seismic Safety Council, Washington D.C, First Edition*, 2000.
- Building Seismic Safety Council for the Federal Emergency Management Agency, NEHRP Recommended Post Earthquake Evaluation and Repair. Criteria for Welded Steel Moment-Frame Buildings, *FEMA-352, Building Seismic Safety Council, Washington D.C, First Edition*, 2000.
- Building Seismic Safety Council for the Federal Emergency Management Agency, NEHRP Recommended Specifications and Quality Assurance. Guidelines for Steel Moment-Frame Construction for Seismic Applications, *FEMA-353, Building Seismic Safety Council, Washington D.C, First Edition*, 2000.
- Building Seismic Safety Council for the Federal Emergency Management Agency, NEHRP Recommended Provisions for Seismic Regulations for new Buildings and other Structures, *FEMA-368, Building Seismic Safety Council, Washington D.C*, 2000.
- Building Seismic Safety Council for the Federal Emergency Management Agency, NEHRP Recommended Provisions for Seismic Regulations for new Buildings and other Structures, *FEMA-369, Building Seismic Safety Council, Washington D.C*, 2000.
- Bursi, O. S.; Colombo, A.; Lucchesi, D.; Savaltore, W, Improved Design and Modelling of Ductile Beam-to-Column Joints for Composite Moment Resisting Frame Structures, *Proceedings of the 4th European Conference on Steel and Composite Structures, Maastricht, The Netherlands*, June 8-10, 2005.
- Bursi, O. S.; Ferrario, F.; Fontanari, V, Non-Linear analysis of the low-cycle fracture behaviour of isolated T-stub Connections, *Computers and Structures*, vol. 80, pp. 2333-2360 (28), 2002.
- Bursi, O. S.; Gerstle, K. H, Analysis of Flexibly Connected Steel Frames, *Journal of Constructional Steel Research*, vol. 30, no. 1, pp. 61-83 (23), 1994.
- Bursi, O. S.; Gerstle, K. H, The Effect of Bracing Connection Deformations on the Behaviour of Braced Steel Frames, *Atti del XIII Congresso C.T.A. Giornate Italiane della Costruzione in Acciaio, Abano, Terme*, 27-30 October, 1991.
- Bursi, O. S.; Gerstle, K. H.; Shing, P. B, Analysis and Tests of a Partially Restrained

- Braced Frame subjected to Seismic Loadings, *Proc. of the Tenth World Conference on Earthquake Engineering, Madrid*, July 19-24, 1992.
- Bursi, O. S.; Gerstle, K. H.; Sigfusdottir, A.; Zitur, J. L., Behaviour and Analysis of Bracing Connections for Steel Frames, *Journal of Constructional Steel Research*, vol. 30, no. 1, pp. 39-60 (22), 1994.
- Bursi, O. S.; Jaspert, J. P., Basic issues in the finite element simulation of Extended End-Plate Connections, *Computers and Structures*, vol. 69, no. 1, pp. 361-382 (21), 1998.
- Bursi, O. S.; Piluso, V.; Rizzano, G.; Zandonini, R., Modelling of the Cyclic Behaviour of Bolted T-Stubs Subjected to Variable Amplitude Loading, *Atti del convegno XVIII Congresso C.T.A. Giornate Italiane della Costruzione in Acciaio, Venezia*, 26-28 September, 2001.
- Bursi, O. S.; Zandonini, R., Behaviour of Steel-Concrete Composite Substructures with Partial Shear Connection and Column Web Panel Yielding, *Proc. of the Fifth International Conference on Steel and Composite Structure, Pusan, Korea*, 14-16 June, 2001.
- Buschemi, N.; Marjanishvili, S., SDOF Model for Progressive Collapse Analysis, *Proc. of the 2005 Structures Congress and Forensic Engineering symposium, New York*, April, 2005.
- Calado, L.; Simoes da Silva, L.; Simoes, R., Cyclic Behaviour of Steel and Composite Beam-to-Column Joints, *AISC*.
- Cerfontaine, F.; Jaspert, J. P., Resistance of Joints submitted to Combined Axial force and Bending, *Proceedings of the 4th European Conference on Steel and Composite Structures, Maastricht, The Netherlands*, June 8-10.
- Chen, W. F.; Goto, Yoshiaki, Liew, J. Y. Richard, *Stability Design of Semi-Rigid frame, John Willey and son*, 1996.
- Choo, B. S.; Li, T. Q.; Nethercot, D. A.; Xiao, Y., Behaviour and Design of Composite Connections, *Proc. COST CI Conference on Semi Rigid Connections, Strasbourg*, October, 1992.
- Coelho, A.G.; Silva, L.S.; Bijlaard, F.S.K., Ductility Analysis of Bolted Extended End Plate Beam-to-Column Connections, *Third International Conference on Steel and Composite Structures, Seoul, Korea*, September 2-4, 2004.
- Commission of the European Committees, Directorate General for Science, Research and Development, Technical Research Steel (XII-C4):, *Frame Design including joint behaviour, Universit, de Liege, D,partement M.S.M, Liege; C.T.I.C.M. Saint-Remy-les-Chevreuse; TNO, Building and Construction Research, Delft; RWTH, Lehrstuhl für Stahlbau, Aachen; CRIF, D,partement Construction M,tallique, Liege, ECSC Contracts n° 7210/SA212 and 320*, January 1997.
- Corley, W. G., Applicability of Seismic Design in Mitigating Progressive Collapse, *Proc. of Workshop on Prevention of Progressive Collapse Multihazard Mitigation, Council of National Institute of Building Sciences, U.S.A*, 10-12 July, 2002.
- Corley, W. G., Lessons Learned on Improving Resistance of Buildings to Terrorists Attacks, *Journal of Performance of Constructed Facilities*, May, 2004, pp. 68-78(11).
- Corley, W. G.; Mlakar, P. F.; Sozen, M. A.; Thornton, C. H., The Oklahoma City Bombing: Summary and Recommendations for Multihazard Mitigation, *Journal of Performance of Constructed Facilities*, August 1998, pp. 100-112(13).

- Costa Borges L.A, Probabilistic evaluation of the rotation capacity of steel joints, *Facultade de Ci ncias e Tecnologia da Universidade de Coimbra*, 2003.
- Davison, J. B.; Kirby, P. A.; Nethercot, D. A, Rotational Stiffness Characteristics of Steel Beam to Column Connections, *Journal of Constructional Steel Research*, vol. 8, pp. 17-54 (38), 1987.
- Davison, J.B.; Lam, D.; Nethercot, D.A, Semi-Rigid action of Composite joints, *The Structural Engineer*, vol. 68, no. 24, December 1990.
- De Mita, L.; Piluso, V.; Rizzano, G, Ultimate Behaviour of Column Web in Compression: Theoretical and Experimental Analysis, *Proceedings of the 4th European Conference on Steel and Composite Structures*, Maastricht, The Netherlands, June 8-10.
- Degertekin, S. O.; Hayalioglu, M. S., Design of non-linear semi-rigid steel frames with semi-rigid column bases, *Electronic Journal of Structural Engineering*, 4 (2004)
- Demonceau J.F., Luu H.N.N. & Jaspart J.-P., Recent investigations on the behaviour of buildings after the loss of a column, *Proceedings of the International Conference in Metal Structures, Poiana Brasov, Romania*, 2006.
- Demonceau J.-F., Steel and composite building frames: sway response under conventional loading and development of membranar effects in beams further to an exceptional action, *PhD thesis presented at Li ge University*, 2008.
- Demonceau, J.F.; Jaspart, J.P., Experimental test simulating the loss of a column in a composite building – Li ge University. *Internal report for the RFCS project RFSCR-04046 “Robust structures by joint ductility”*, Li ge University, September 2006.
- Demonceau, J.-F.; Luu, H.N.N.; Jaspart, J.-P., Development of membranar effects in frame beams: Experimental and analytical investigations, *Eurosteel conference in Gratz*, 2008.
- Deng, C.; Bursi, O. S.; Zandonini, R, A Hysteretic Connection Element and its Applications, *Computers & Structures*, Vol. 78, n. 1-3, pp. 93-110, 2000.
- Department of Defense, Abstract: Interim Antiterrorism/Force Protection Construction Standards, *Progressive Collapse Design Guidance, Amendment No.2000*, 2000.
- Donald, O. D, Review of Existing Guidelines and Provisions Related to Progressive Collapse, *Proc. of Workshop on Prevention of Progressive Collapse Multihazard Mitigation, Council of National Institute of Building Sciences, U.S.A*, 10-12 July, 2002.
- Easterling, W. S, New Shear Stud Provisions for Composite Beam Design, *Proc. of the 2005 Structures Congress and Forensic Engineering symposium, New York*, 5-Apr.
- Edited by Baniotopoulos, C.C.; Wald, F, The Paramount Role of Joints into the Reliable Response of Structures, *Proceedings of the NATO Advanced Research Workshop, Kluwer Academic Publishers*, May 21-23, 2000.
- Edited by Jaspart J.P, Recent advances in the field of structural steel joints and their representation in the building frame analysis and design process, *COST C1*, Edited by Jaspart J.P, University of Liege, 1999.
- Edited by Schaur C, Mazzolani F, Huber G, de Matteis G, Improvement of buildings? *Structural quality by new technologies, COST C12 Final Conference Proceedings*, 2005.
- Ellingwood, B, Design and Construction Error Effects on Structural Reliability, *Journal of Structural Engineering*, vol. 113, no. 2, February, p. no. 409-422, 1987.
- Ellingwood, B. R.; Dusenberry, D. O, Building Design for Abnormal Loads and

- Progressive Collapse, *Computer-Aided Civil and Infrastructure Engineering*, Vol. 20, 2005.
- Ellingwood, B. R.; Smilowitz, R.; Dusenberry, D. O.; Duthinh, D.; Lew, H.S.; Carino, N. J, Best Practices for Reducing the Potential for Progressive Collapse in Buildings, National Institute of *Standards and Technology, Technology Administration, U.S. Department of Commerce*, February 2007.
- Ellingwood, B.; Leyendecker, V, Approaches for Design Against Progressive Collapse, *Journal of the Structural Division, March 1978*, pp. 413-423(11).
- Elvira; Ngo, T.; Lam, N, Development of a progressive collapse analysis procedure for concrete frame structure –*Development in Mechanics of structures and Materials – Deeks and How, London – 2005*.
- England, J.; Agarwal, J.; Blockley, D, The vulnerability of structures to unforeseen events, *Computers and Structures* 86 (2008) 1042–1051.
- Engstrom, B, Combined effects of Dowel Action and Friction in Bolted Connections, *Proc. COST CI Conference on Semi Rigid Connections, Strassbourg, October, 1992*.
- Erlicher, S.; Bursi, O. S.; Zandonini, R, Low-Cycle Fatigue Behaviour of Pull-Push Specimens with Headed Stud Shear Connectors, *Symposium on Connections between Steel and Concrete, Stuttgart, 10-12 Sept? 2001*.
- European Committee for Standardization, Eurocode 1:-Part 7. Accidental actions due to impact and explosions.
- European Committee for Standardization, Eurocode 3: Design of Steel Structures-part 1.1: General rules and rules for buildings, *Final Draft prEN 1993-1-1:2003 E*, December 2003.
- European Committee for Standardization, Eurocode 3: Design of Steel Structures-part 1.8: Design of Joints, *Final Draft prEN 1993-1-8:2003 E*, December 2003.
- Faella, C.; Piluso, V.; Rizzano, G., STRUCTURAL STEEL SEMIRIGID CONNECTION: Theory, Design and Software, *CRC press*, 1999.
- Feldmann, M.; Sedlacek, G.; Weynand, K, Safety Considerations of Annex J of Eurocode 3, *The 3rd Int. Workshop on Connections in Steel Structures, Trento, Italy, 1995*.
- Fenner, R. T, Mechanics of Solids, *Blackwell Scientific Publication*, 1989.
- Fertis, D.G., NONLINEAR MECHANICS, *CRC press*, 1993.
- FINELG user’s manual. Non-linear finite element analysis software. Version 8.2, July 1999.
- Gerardy, J. C.; Schliech, J. B, Semi-Rigid action in Steel Frame Structures, Commission of the European Communities: technical steel research, *Report EUR 14427 EN*, 1992.
- Ghobarah, A.; Osman, A.; Korol, R. M, Behaviour of Extended End Plate Connections under Cyclic Loading, *Engineering Structures*, vol. 12(1), pp. 15-27 (12), January 1990.
- Ghobarah, A; Korol, R. M. .; Osman, A, Cyclic Behaviour of Extended End-Plate Joints, *Journal of Structural Engineering*, vol. 118, no. 5, pp. 1333-1353 (20), May 1992.
- Girao Coelho, A. M.; da Silva, L. S.; Bijlaard, F. S. K, Ductility Analysis of End Plate Beam-to-Column Joints, *Proceedings of the 4th European Conference on Steel and Composite Structures, Maastricht, The Netherlands, June 8-10*.
- Gomes, F.C.T.; Kuhlmann, U.; De Matteis, G.; Mandara, A, Recent Developments on



- Classification of Joints, Document COST C1, *Proceedings of the international conference, Liege*, 17-19 Sept, 1999.
- Graham, J. D.; Sherbourne, A. N.; Khabbaz, R. N.; Jensen, C. D, Welded Interior Beam-to-Column Connections, *Welding Research Council Bulletin Nø63*, August, 1960.
- Gurney, T.R, Fatigue of Welded Structures, *Cambridge University Press, 2nd Edition*, 1979.
- Heyman, J., STRUCTURAL ANALYSIS: A historical approach, *Cambridge University Press*, 1998.
- Huber, G, Non-Linear Calculations of Composite Sections and Semi-Continuous Joints, *Ph D Thesis, Institute of Steel and Timber Construction, University of Innsbruck*, 1999.
- Huber, G.; Kronenberger, H. J.; Weynand, K, Representation of Joints in the Analysis of Structural Systems, *Proc. COST CI Conference on Semi Rigid Connections, Liege*, September, 1998.
- Iding, R.H, A Methodology to Evaluate Robustness in Steel Buildings-Surviving Extreme Fires or Terrorist Attack using a Robustness Index, *Proc. of the 2005 Structures Congress and Forensic Engineering symposium, New York*, April, 2005.
- International working group, Safety in tall buildings and other buildings with large occupancy, *The Institution of Structural Engineers*, July, 2002.
- Izzuddin, B.A.; Vlassis, A.G. Elghazouli, A.Y. & Nethercot, D.A., Progressive collapse of multi-storey buildings due to sudden column loss – Part I: Simplified assessment framework. *Engineering Structures*, 2007 (doi:10.1016/j.engstruct.2007.07.011).
- Izzuddin, B.A.; Vlassis, A.G. Elghazouli, A.Y. & Nethercot, D.A., Progressive collapse of multi-storey buildings due to sudden column loss – Part II: Application. *Engineering Structures*, 2007 (doi:10.1016/j.engstruct.2007.08.011).
- Izzuddin, B.A.; Vlassis, A.G. Elghazouli, A.Y. & Nethercot, D.A., Assessment of progressive collapse in multi-storey buildings. *Proceedings of the Institution of Civil Engineers – Structures & Buildings 160 – Issue SBI*, 2007.
- Janss, J.; Jaspert, J. P.; Maquoi, R, Experimental Study of the Non-Linear Behaviour of Beam to Column Bolted Joints, *Connections in steel structures, behaviour, strength and design, pp. 26-32 (7)*, 1988.
- Jaspert, J. P, Contributions to recent advances in the field of steel joints. Column bases and and further configurations for beam to column joints and beam splices, *These, Universite de Liege*, 1997.
- Jaspert, J. P.; Steenhuis, M.; Anderson, D, Characterisation of the Joint properties by means of the Component Method, *Proc. COST CI Conference on Semi Rigid Connections, Liege*, September, 1998.
- Jaspert, J.P.; Weynand, K.; Steenhuis, M, Plastic hinge idealization of structural joints. EC3 philosophy, *COST CI Document C1/WD2/96-02, Liege, Belgium*, 1996.
- Joint WRC and ASCE committee on plasticity related to design, Commentary on Plastic Design in Steel: Connections, *Progress Report 6, Journal Eng.Mech, Div, EM2*, April, 1960.
- Kaewkulchai, G.; Williamson, E. B, Dynamic behavior of planar frames during progressive collapse – *16th ASCE Engineering mechanics conference – 2003 – Seattle*.

- Khalil, H. S.; Ho, C. M, Black Bolts under Combined Tension and Shear, *The Structural Engineer*, vol. 57B, no. 4, pp. 69-76 (8), 1979.
- Khandelwal, K.; El-Tawil, S.; Sadek, F, Progressive collapse analysis of seismically designed steel braced frames, *Journal of Constructional Steel Research*, accepted 18 February 2008.
- Khandelwal, K.; Tawil, S, Progressive Collapse of Moment Resisting Steel Frame Buildings, *Proc. of the 2005 Structures Congress and Forensic Engineering symposium*, New York, April, 2005.
- Kim, S.; Kang, K.; Lee, D, Full-scale testing of space steel frame subjected to proportional Loads, *Engineering Structures* 25 (2003) 69–79.
- Kirby, B. R, The Behaviour of High-strength Grade 8.8 Bolts in Fire, *Journal of Constructional Steel Research*, vol. 33, pp. 3-38(36), 1995.
- Krauthammer, T.; Hall, R. L.; Woodson, S. C.; Baylot, J. T.; Hayes, J. R, Development of Progressive Collapse Analysis Procedure and Condition Assessment for Structures, *Proc. of Workshop on Prevention of Progressive Collapse Multihazard Mitigation*, Council of National Institute of Building Sciences, U.S.A, 10-12 July, 2002.
- Kuhlmann, U, Definition of Flange Slenderness Limits on the Basis of Rotation Capacity Values, *Journal of Constructional Steel Research*, vol. 14, pp. 21-40 (20), 1989.
- Kuhlmann, U.; Davison, J.B.; Kattner, M, Structural Systems and Rotation Capacity, Document COST C1, *Proceedings of the international conference*, Liege, 17-19 Sept, 1999.
- Kuhlmann, U.; Kuhnemund, F, Procedures to Verify Rotation Capacity- Part III, *University of Stuttgart*, Stuttgart, Germany.
- Kuhlmann, U.; Kuhnemund, F, Rotation Capacity of Steel Joints? Verification Procedure and Component Tests, The paramount role of joints into the reliable response of structures. From the classic pinned and rigid joint to the notation of semi-rigidity, *Kluwer Academic Publishers*.
- Leon, R.T, Semi Rigid Composite Construction, *Journal of Constructional steel research*, vol. 15, issue 1/2, 1990.
- Leon, R.T.; Ammerman, D.J.; Lin, J.; McCauley, R.D, Semi-Rigid Composite Steel Frames, American Institute of Steel Construction Engineering, *Journal fourth Quarter*, 1987.
- Li, T. Q.; Choo, B. S.; Nethercot, D. A, Connection Element Method for the Analysis of Semi-Rigid Frames, *Journal of Constructional Steel Research*, vol. 32, pp. 143-171 (29), 1995.
- Li, T. Q.; Nethercot, D. A.; Choo, B. S, Behaviour of Flush End-Plate Composite Connections with Unbalanced Moment and Variable Shear/ Moment Ratios-I. Experimental Behaviour, *Journal of Constructional Steel Research*, vol. 38, no. 2, pp. 125-164(39), 1996.
- Li, T.Q. ; Moore, D.B.; Nethercot, D.A.; Choo, B.S, The Experimental Behaviour of Full Scale, Semi-Rigidly Connected Composite Frame: Overall Consideration, *Journal of Constructional steel research*, vol. 39, no. 3, 1996.
- Li, T.Q. ; Moore, D.B.; Nethercot, D.A.; Choo, B.S, The Experimental Behaviour of Full Scale, Semi-Rigidly Connected Composite Frame: Detailed Appraisal, *Journal of*

- Constructional steel research*, vol. 39, no. 3, 1996.
- Li, T.Q. ; Nethercot, D.A.; Choo, B.S, Determination of Rotation Capacity Requirements for Steel and Composite Beams, *Journal of Constructional steel research*, vol. 32, 1995.
- Li, T.Q, The analysis and ductility requirements of semi-rigid composite connections, *Dept. of Civil Engineering, University of Nottingham*, 1994.
- Liew, J.Y. Richard; Shanmugam, N.W., and C.H. Yu. STRUCTURAL ANALYSIS, *Structural Engineering Handbook, Ed Chen Wai-Fah*. 1999.
- Lindberg, R.; Keronen, A, Semi-Rigid Behaviour of a RC Portal Frame, *Proc. COST CI Conference on Semi Rigid Connections, Strassbourg*, October, 1992.
- Liu, R. ; Davison, J. B. ; Tyas, A, A Study of progressive Collapse in a Multi-Storey Steel Frames, *Proc. of the 2005 Structures Congress and Forensic Engineering symposium*, April, 2005.
- Liu, R.; Davison, J. B.; Tyas, A, Is Catenary Action Sufficient to Resist Progressive Collapse in a Steel Framed Building ?, *Proceedings of the 4th European Conference on Steel and Composite Structures - Maastricht, The Netherlands*, June 8-10, 2005.
- Liu, T.C.H.; Fahad, M.K.; Davies, J.M, Experimental investigation of behaviour of axially restrained steel beams in fire, *Journal of Constructional Steel Research* 58 (2002) 1211–1230.
- Luu, N. N. H, Interaction between bending moment and axial force in the bolted steel joints, *Documents in the framework of the activities of the Inter-University Cooperation Program sponsored by Belgian Government and realized by University of Liege, Presented at Ho Ci Minh City University of Technology*.1999.
- Marchand, K. A.; Alfawakhiri, F., Facts for Steel Buildings: Blast and Progressive Collapse – *AISC* 2004.
- Mayer, U.; Eligehausen, R, Bond Behaviour of Ribbed Bars at Inelastic Steel Strains, *2nd International Ph.D Symposium in civil Engineering, 1998, Budapest*, 1998.
- Moore, D. B.; BRE, The UK and European Regulations for Accidental Actions, *Proc. of Workshop on Prevention of Progressive Collapse Multihazard Mitigation, Council of National Institute of Building Sciences, U.S.A*, 10-12 July, 2002.
- Mullers, I.; Vogel, T, Robustness of Reinforced Concrete Structures Subjected to Column Failure, *Proceedings of the 2nd FIB Congress, FIB Italy*, , Vol. 2, Naples, 2006, pp. 592-593.
- Munoz, E. G. ; Davison, J. B. ; Tyas, A, Analysis of the Response of Structural Bolts Subjected to Rapid Rates of Loading, *Proc. Of the 4th European Conference on Steel and Composite Structures- Maastricht, The Netherlands*, June 8-10, 2005.
- Munoz, E. G. ; Davison, J. B. ; Tyas, A, Structural Integrity of Steel Connections Subjected to Rapid Rates of Loadings, *Proc. of the 2005 Structures Congress and Forensic Engineering symposium*, April, 2005.
- Nemati, N.; Le Houedec, D.; Zandonini, R, Numerical Modelling of the Cyclic Behaviour of the Basic Components of the Steel End Plate Connections, *Advances in Engineering Software, Vol. 31*, pp. 837-849, 2000.
- Newmann, G. M.; Robinson, J. T.; Bailey, C. G, Fire Safe Design: A New Approach to Multi-Storey Steel-Framed Buildings, *Steel Construction Institute, Ascot Berkshire*, 2000.

- Osman, A.; Ghobarah, A.; Korol, R. M, Seismic Performance of Moment Resisting Frames with Flexible Joints, *Engineering Structures*, vol. 15, no. 2, pp. 117-134 (18), 1993.
- Outcome of the cooperative activities, improvement of buildings structural quality by new technologies, *COST C12 Final Conference Proceedings*, 2004.
- Owens, G. W.; Moore, D. B, The Robustness of Simple Connections, *The Structural Engineer*, vol. 70, no. 3 pp. 37-46(10), 1992.
- Piluso, V.; Rizzano, G.; Tolone, I, Rotation Behaviour of Composite Connections under Hogging and Sagging Moments: An Advanced Analytical Model, *Proceedings of the 4th European Conference on Steel and Composite Structures*, Maastricht, The Netherlands, June 8-10, 2005.
- Plumier, A, Behaviour of Connections, *Journal of Constructional steel research*, vol. 29, issue 1/3, 1994.
- Powell, G, Progressive Collapse: Case Studies Using Nonlinear Analysis, 2004 *SEAOC Annual Convention*, Monterey, August 2004.
- Powell, G., Progressive Collapse: Case Studies using Nonlinear Analysis, *Proc. of the 2005 Structures Congress and Forensic Engineering symposium*, New York, April, 2005.
- Puhali, R.; Smotlak, I.; Zandonini, R, Semi-Rigid Composite action: Experimental Analysis and a suitable model, *Journal of Constructional steel research*.
- Salmon, C. G.; Johnson. J. E., STEEL STRUCTURE: Design and Behaviour, Second Edition. *Harper & Row, Publisher, New York*,1980.
- Sasani, Mehrdad, Response of a reinforced concrete infilled-frame structure to removal of two adjacent columns – *Jour. Engineering Structures* , Jan 2008.
- Schafer, B.W.; Bajpai, P, Stability degradation and redundancy in damaged structures – *Jour. Engineering Structures* 27 (2005) 1642–1651.
- Schleich, J. B.; Chabrolin, B.; Espiga, F, Improved Classification of Steel and Composite Cross-Sections: New Rules for Local Buckling in Eurocodes 3 and 4, *Technical Steel Research, Final Report, ProfilARBED Recherches*, Luxembourg, 1998.
- Schleich, J.B.; Chantrain, Ph. Et Al, Promotion of plastic design for steel and composite cross sections: new required conditions in Eurocodes 3 and 4, practical tools for designers, *RPS Report No 123/96 and 124/96. ProfilARBED Recherches*, 1996.
- Scott, D, ARUP, Fire Induced Progressive Collapse, Proc. of Workshop on Prevention of Progressive Collapse Multihazard Mitigation, *Council of National Institute of Building Sciences, U.S.A*, 10-12 July, 2002.
- Smilowitz, R, Analytical tools for Progressive Collapse Analysis, Proc. of Workshop on Prevention of Progressive Collapse Multihazard Mitigation, *Council of National Institute of Building Sciences, U.S.A*, 10-12 July, 2002.
- Standards Australia, Standards New Zealand, Structural design actions, General principles, *AS/NZS 1170.0: 2002*, Edition 2002.
- Standards Australia, Standards New Zealand, Structural design actions, General principles, Commentary, *AS/NZS 1170.0 Supplement 1: 2002*, Edition 2002.
- Starossek, U, Progressive collapse of structures-Invited Lecture, *The 2006 Annual Conference of the Structural Engineering Committee of the Korean Society of Civil Engineers*, Seoul, Korea, May 25, 2006.

- Starossek, U, Typology of progressive collapse-*Engineering Structures* 29 (2007) 2302–2307.
- Starossek, U.; Progressive Collapse of Bridges, Aspects of Analysis and Design, *International Symposium on Sea-Crossing Long-Span Bridges, Mokpo, Korea, Feb. 15-17, 2006.*
- Steenhius, C. M.; Herwinjen, F. V.; Snijder, H. H, Safety Concepts for Ductility of Joints, *International AISC/ECCS Workshop on Connections in Steel Structures IV, Roanoke, October 22-25, 2000.*
- Steenhius, M.; Jaspart, J. P.; Gomes, F.; Leino, T, Application of the Component Method to Steel Joints, *Proc. COST CI Conference on Semi Rigid Connections, Liege, September, 1998.*
- Structural Steelwork Eurocodes Development of a Trans-National Approach, Course in ARGENCO – University of Liege.
- Sumner, E. A.; Mays, T. W.; Murray, T. M, End Plate Moment Connections: Test Results and Finite Element Validation Method, *AISC.*
- Swanson, J. A.; Kokan, D. S.; Leon, R. T, Advanced Finite Element Modelling of Bolted T-Stub Connection Component, *Journal of Constructional Steel Research, vol. 58, pp. 1015-1031 (17), 2002.*
- Swanson, J. A.; Leon, R. T, Bolted Steel Connections: Tests on T-Stub Components, *Journal of Structural Engineering, vol. 126, no. 1, pp. 51-56 (6), January, 2000.*
- Taylor, D. A, Progressive Collapse, *Canadian Journal of Civil Engineering, No. 4, Dec. 1975.*
- The Multihazard Mitigation Council of the National Institute of Building Council, Prevention of Progressive Collapse, *Report on the July 2002 national workshop and recommendations for future research, Washington, 2003.*
- Tschemmerneegg, F, Testing and Test Results of Composite Joints, *Proc. COST CI Conference on Semi Rigid Connections, Strassbourg, October, 1992.*
- Tschemmerneegg, F.; Rubin, D.; Pavlov, A, Application of the Component Method to Composite Joints, *Proc. COST CI Conference on Semi Rigid Connections, Liege, September, 1998.*
- Unified Facilities Criteria (UFC): Design of buildings to resist progressive collapse UFC 4-023-03 – *Department of Deffense (DoD) – US, 2005.*
- US General Services Administration (GSA). Progressive collapse analysis and design guidelines for new federal office buildings and major modernization projects. June 2003.
- Vlassis. A. G. Progressive collapse assessment of tall buildings. *Thesis submitted in fulfilment of the requirements for the degree of Doctor of Philosophy of the University of London and the Diploma of Imperial College London.* April 2007.
- Walda, F.; Simões da Silvab, L.; Moorec, D.B.; Lennond, T.; Chladna´ e, M.; Santiagob, A.; Benes´a, M.; Borgesf, L, Experimental behaviour of a steel structure under natural fire, *Fire Safety Journal 41 (2006) 509–522.*
- Wang, C.M.; Reddy, J. N.; Lee, K. H., Shear deformable beams and plates: Relationships with classical solutions, *ELSEVIER, 2000.*
- Weynand, K, COST C1: Column Bases in Steel Building Frames, *Semi Rigid Behaviour of*

- Civil Engineering Structural Connections, Brussels, 1999.*
- Weynand, K.; Jaspart, J. P.; Steenhuis, M, The Stiffness Model of revised Annex J of Eurocode 3, *The 3rd Int. Workshop on Connections in Steel Structures, Trento, Italy, 1995.*
- Weynand, K.; Jaspart, J. P.; Steenhuis, M, Economy Studies of Steel Building Frames with Semi-Rigid Joints, *Proceeding of the 2nd World Conference on Constructional Steel Design, Spain, 1998.*
- Wong, M.B, Modelling of axial restraints for limiting temperature calculation of steel members in fire, *Journal of Constructional Steel Research 61 (2005) 675–687.*
- Xiao, Y.; Choo, B. S.; Nethercot, D. A, Composite Connections in Steel and Concrete. Part 2-Moment Capacity of End Plate Beam to Column Connection, *Journal of Constructional Steel Research, vol. 37, no. 1, pp. 63-90(28), 1996.*
- Xiao, Y.; Choo, B. S.; Nethercot, D. A, Composite Connections in Steel and Concrete- I. Experimental Behaviour of Composite Beam-Column Connections, *Journal of Constructional Steel Research, vol. 31, no. 4, pp. 3-30 (28), 1994.*
- Yandzio, E.; Gough, M, Protection of Buildings against Explosions, The Steel Construction Institute, *Ascot Berkshire, P244, 1999.*
- Yin, Y.Z.; Wang, Y.C, A numerical study of large deflection behaviour of restrained steel beams at elevated temperatures, *Journal of Constructional Steel Research 60 (2004) 1029–1047.*
- Yin, Y.Z.; Wang, Y.C, Analysis of catenary action in steel beams using a simplified hand calculation method, Part 1: theory and validation for uniform temperature distribution, *Journal of Constructional Steel Research 61 (2005) 183–211.*
- Yin, Y.Z.; Wang, Y.C, Analysis of catenary action in steel beams using a simplified hand calculation method, Part 2: validation for non-uniform temperature distribution, *Journal of Constructional Steel Research 61 (2005) 213–234.*
- Yu, J.; Jones, N, Further Experimental Investigations on the Failure of Clamped Beams under Impact Loads, *International Journal on Solids and Structures , vol. 27, no. 9, pp. 1113-1137 (25), 1991.*
- Zandonini, R, Design of Beam-to-Column Connections- *The European Approach, Structural Steel Developing Africa- Conference, 1996.*
- Zandonini, R, Semi-Rigid Composite Joints, Strength and Stability Series, vol. 8, Connections, edited by R. Narayanan, *Elsevier Applied Science, London, 63-120.*
- Zandonini, R.; Bursi, O. S, Monotonic and Hysteretic Behaviour of Bolted Endplate Beam-to-Column Joints, *Atti del convegno ICASS'02, Hong Kong, 2002.*
- Zoetemeijer, P, Summary of the Research on Bolted Beam-to-Column Connections, Delft University of Technology, Faculty of Civil Engineering, *Stevin Laboratory, Report 6-90-02, 1990.*